National Library
of Canada

Acquisitions and
Bibliographic Services Branch

395 Wellington Street
Ottawa, Ontario
K1A 0N4

Bibliothèque nationale
du Canada

Direction des acquisitions et
des services bibliographiques

395, rue Wellington
Ottawa (Ontario)
K1A 0N4

Your file Votre référence

Our file Notre référence

NOTICE

The quality of this microform is heavily dependent upon the quality of the original thesis submitted for microfilming. Every effort has been made to ensure the highest quality of reproduction possible.

If pages are missing, contact the university which granted the degree.

Some pages may have indistinct print especially if the original pages were typed with a poor typewriter ribbon or if the university sent us an inferior photocopy.

Reproduction in full or in part of this microform is governed by the Canadian Copyright Act, R.S.C. 1970, c. C-30, and subsequent amendments.

AVIS

La qualité de cette microforme dépend grandement de la qualité de la thèse soumise au microfilmage. Nous avons tout fait pour assurer une qualité supérieure de reproduction.

S'il manque des pages, veuillez communiquer avec l'université qui a conféré le grade.

La qualité d'impression de certaines pages peut laisser à désirer, surtout si les pages originales ont été dactylographiées à l'aide d'un ruban usé ou si l'université nous a fait parvenir une photocopie de qualité inférieure.

La reproduction, même partielle, de cette microforme est soumise à la Loi canadienne sur le droit d'auteur, SRC 1970, c. C-30, et ses amendements subséquents.

Canada

UNIVERSITY OF ALBERTA

MINE WASTE GEOTECHNICS

BY

RICHARD FREDERICK DAWSON ©

A THESIS
SUBMITTED TO THE FACULTY OF GRADUATE STUDIES AND RESEARCH IN
PARTIAL FULFILLMENT OF THE REQUIREMENTS FOR THE DEGREE OF
DOCTOR OF PHILOSOPHY

IN

GEOTECHNICAL ENGINEERING

DEPARTMENT OF CIVIL ENGINEERING
EDMONTON, ALBERTA
FALL, 1994

National Library
of Canada

Acquisitions and
Bibliographic Services Branch

395 Wellington Street
Ottawa, Ontario
K1A 0N4

Bibliothèque nationale
du Canada

Direction des acquisitions et
des services bibliographiques

395, rue Wellington
Ottawa (Ontario)
K1A 0N4

Your file Votre référence

Our file Notre référence

The author has granted an irrevocable non-exclusive licence allowing the National Library of Canada to reproduce, loan, distribute or sell copies of his/her thesis by any means and in any form or format, making this thesis available to interested persons.

L'auteur a accordé une licence irrévocable et non exclusive permettant à la Bibliothèque nationale du Canada de reproduire, prêter, distribuer ou vendre des copies de sa thèse de quelque manière et sous quelque forme que ce soit pour mettre des exemplaires de cette thèse à la disposition des personnes intéressées.

The author retains ownership of the copyright in his/her thesis. Neither the thesis nor substantial extracts from it may be printed or otherwise reproduced without his/her permission.

L'auteur conserve la propriété du droit d'auteur qui protège sa thèse. Ni la thèse ni des extraits substantiels de celle-ci ne doivent être imprimés ou autrement reproduits sans son autorisation.

ISBN 0-315-95171-0

Canada

Name Mine Waste Geotechnics

Dissertation Abstracts International is arranged by broad, general subject categories. Please select the one subject which most nearly describes the content of your dissertation. Enter the corresponding four-digit code in the spaces provided.

Geotechnology
SUBJECT TERM

0 4 2 8
SUBJECT CODE

U·M·I

Subject Categories

THE HUMANITIES AND SOCIAL SCIENCES

COMMUNICATIONS AND THE ARTS

Architecture	0729
Art History	0377
Cinema	0900
Dance	0378
Fine Arts	0357
Information Science	0723
Journalism	0391
Library Science	0399
Mass Communications	0708
Music	0413
Speech Communication	0459
Theater	0465

EDUCATION

General	0515
Administration	0514
Adult and Continuing	0516
Agricultural	0517
Art	0273
Bilingual and Multicultural	0282
Business	0688
Community College	0275
Curriculum and Instruction	0727
Early Childhood	0518
Elementary	0524
Finance	0277
Guidance and Counseling	0519
Health	0680
Higher	0745
History of	0520
Home Economics	0278
Industrial	0521
Language and Literature	0279
Mathematics	0280
Music	0522
Philosophy of	0998
Physical	0523
Psychology	0525
Reading	0535
Religious	0527
Sciences	0714
Secondary	0533
Social Sciences	0534
Sociology of	0340
Special	0529
Teacher Training	0530
Technology	0710
Tests and Measurements	0288
Vocational	0747

LANGUAGE, LITERATURE AND LINGUISTICS

Language	
General	0679
Ancient	0289
Linguistics	0290
Modern	0291
Literature	
General	0401
Classical	0294
Comparative	0295
Medieval	0297
Modern	0298
African	0316
American	0591
Asian	0305
Canadian (English)	0352
Canadian (French)	0355
English	0593
Germanic	0311
Latin American	0312
Middle Eastern	0315
Romance	0313
Slavic and East European	0314

PHILOSOPHY, RELIGION AND THEOLOGY

Philosophy	0422
Religion	
General	0318
Biblical Studies	0321
Clergy	0319
History of	0320
Philosophy of	0322
Theology	0469

SOCIAL SCIENCES

American Studies	0323
Anthropology	
Archaeology	0324
Cultural	0326
Physical	0327
Business Administration	
General	0310
Accounting	0272
Banking	0770
Management	0454
Marketing	0338
Canadian Studies	0385
Economics	
General	0501
Agricultural	0503
Commerce-Business	0505
Finance	0508
History	0509
Labor	0510
Theory	0511
Folklore	0358
Geography	0366
Gerontology	0351
History	
General	0578
Ancient	0579
Medieval	0581
Modern	0582
Black	0328
African	0331
Asia, Australia and Oceania	0332
Canadian	0334
European	0335
Latin American	0336
Middle Eastern	0333
United States	0337
History of Science	0585
Law	0398
Political Science	
General	0615
International Law and Relations	0616
Public Administration	0617
Recreation	0814
Social Work	0452
Sociology	
General	0626
Criminology and Penology	0627
Demography	0938
Ethnic and Racial Studies	0631
Individual and Family Studies	0628
Industrial and Labor Relations	0629
Public and Social Welfare	0630
Social Structure and Development	0700
Theory and Methods	0344
Transportation	0709
Urban and Regional Planning	0999
Women's Studies	0453

THE SCIENCES AND ENGINEERING

BIOLOGICAL SCIENCES

Agriculture	
General	0473
Agronomy	0285
Animal Culture and Nutrition	0475
Animal Pathology	0476
Food Science and Technology	0359
Forestry and Wildlife	0478
Plant Culture	0479
Plant Pathology	0480
Plant Physiology	0817
Range Management	0777
Wood Technology	0746
Biology	
General	0306
Anatomy	0287
Biostatistics	0308
Botany	0309
Cell	0379
Ecology	0329
Entomology	0353
Genetics	0369
Limnology	0793
Microbiology	0410
Molecular	0307
Neuroscience	0317
Oceanography	0416
Physiology	0433
Radiation	0821
Veterinary Science	0778
Zoology	0472
Biophysics	
General	0786
Medical	0760

EARTH SCIENCES

Biogeochemistry	0425
Geochemistry	0996
Geodesy	0370
Geology	0372
Geophysics	0373
Hydrology	0388
Mineralogy	0411
Paleobotany	0345
Paleoecology	0426
Paleontology	0418
Paleozoology	0985
Palynology	0427
Physical Geography	0368
Physical Oceanography	0415

HEALTH AND ENVIRONMENTAL SCIENCES

Environmental Sciences	0768
Health Sciences	
General	0566
Audiology	0300
Chemotherapy	0992
Dentistry	0567
Education	0350
Hospital Management	0769
Human Development	0758
Immunology	0982
Medicine and Surgery	0564
Mental Health	0347
Nursing	0569
Nutrition	0570
Obstetrics and Gynecology	0380
Occupational Health and Therapy	0354
Ophthalmology	0381
Pathology	0571
Pharmacology	0419
Pharmacy	0572
Physical Therapy	0382
Public Health	0573
Radiology	0574
Recreation	0575
Speech Pathology	0460
Toxicology	0383
Home Economics	0386

PHYSICAL SCIENCES

Pure Sciences

Chemistry	
General	0485
Agricultural	0749
Analytical	0486
Biochemistry	0487
Inorganic	0488
Nuclear	0738
Organic	0490
Pharmaceutical	0491
Physical	0494
Polymer	0495
Radiation	0754
Mathematics	0405
Physics	
General	0605
Acoustics	0986
Astronomy and Astrophysics	0606
Atmospheric Science	0608
Atomic	0748
Electronics and Electricity	0607
Elementary Particles and High Energy	0798
Fluid and Plasma	0759
Molecular	0609
Nuclear	0610
Optics	0752
Radiation	0756
Solid State	0611
Statistics	0463

Applied Sciences

Applied Mechanics	0346
Computer Science	0984
Engineering	
General	0537
Aerospace	0538
Agricultural	0539
Automotive	0540
Biomedical	0541
Chemical	0542
Civil	0543
Electronics and Electrical	0544
Heat and Thermodynamics	0348
Hydraulic	0545
Industrial	0546
Marine	0547
Materials Science	0794
Mechanical	0548
Metallurgy	0743
Mining	0551
Nuclear	0552
Packaging	0549
Petroleum	0765
Sanitary and Municipal	0554
System Science	0790
Geotechnology	[✓ 0428]
Operations Research	0796
Plastics Technology	0795
Textile Technology	0994

PSYCHOLOGY

General	0621
Behavioral	0384
Clinical	0622
Developmental	0620
Experimental	0623
Industrial	0624
Personality	0625
Physiological	0989
Psychobiology	0349
Psychometrics	0632
Social	0451

UNIVERSITY OF ALBERTA

RELEASE FORM

NAME OF AUTHOR: Richard Frederick Dawson

TITLE OF THESIS: Mine Waste Geotechnics

DEGREE: Doctor of Philosophy in Geotechnical Engineering

YEAR THIS DEGREE GRANTED: Fall 1994

PERMISSION IS HEREBY GRANTED TO THE UNIVERSITY OF ALBERTA LIBRARY TO REPRODUCE SINGLE COPIES OF THIS THESIS AND TO LEND OR SELL SUCH COPIES FOR PRIVATE, SCHOLARLY OR SCIENTIFIC RESEARCH PURPOSES ONLY.

THE AUTHOR RESERVES ALL OTHER PUBLICATION AND OTHER RIGHTS IN ASSOCIATION WITH THE COPYRIGHT IN THE THESIS, AND EXCEPT AS HEREINBEFORE PROVIDED NEITHER THE THESIS NOR ANY SUBSTANTIAL PORTION THEREOF MAY BE PRINTED OR OTHERWISE REPRODUCED IN ANY MATERIAL FORM WHATEVER WITHOUT THE AUTHOR'S PRIOR WRITTEN PERMISSION.

RDawson

30 Sleigh Drive
Redwood Meadows, Alberta
T3Z 1A1

Date: October 5, 1994

UNIVERSITY OF ALBERTA

FACULTY OF GRADUATE STUDIES AND RESEARCH

THE UNDERSIGNED CERTIFY THAT THEY HAVE READ, AND RECOMMEND TO THE FACULTY OF GRADUATE STUDIES AND RESEARCH FOR ACCEPTANCE, A THESIS ENTITLED **MINE WASTE GEOTECHNICS** SUBMITTED BY **RICHARD FREDERICK DAWSON** IN PARTIAL FULFILLMENT FOR THE DEGREE OF **DOCTOR OF PHILOSOPHY IN GEOTECHNICAL ENGINEERING**.

Dr. N.R. Morgenstern

Dr. D.C. Sego

Dr. P.K. Robertson

Dr. P. M. Steffler

Dr. Ken Barron

Mr. C.O. Brawner

Date: September 30, 1994

ABSTRACT

Mine waste management is dominated by issues related to the handling and storage of large volumes of relatively loose materials. The management of these materials involves special consideration for engineered containment strategies that are sensitive to both economic and environmental matters.

In order to ensure that mine wastes are being managed in a manner that minimizes the present and future threat to human health and the environment mine operators must ensure that their practices are continually calibrated with the best available technologies. This thesis presents the results of research activities that demonstrate the role that geotechnical engineering plays in identifying and developing the best available mine waste management technologies. In this context, detailed studies are carried out on the management of tailings (wet stream mine wastes) in cold climates, and the containment of waste rock (dry stream mine wastes) in mine waste dumps.

Much of Canada's mineral wealth is located in cold regions. Mines in these areas can take advantage of the cold climate to manage their tailings by utilizing freezing for providing physical and chemical containment or thawing for dewatering. It is shown that maximum benefits are attained when the hydraulically placed tailings are frozen in thin layers. Thaw dewatering is a particularly attractive strategy for increasing the solids content of high moisture content fine tailings. The results of laboratory tests and design calculations for oil sands fine tailings are presented that illustrate the benefits that could be attained.

There have been a large number of high runout flowslides in British Columbian mountain coal mine waste dumps. An understanding of the mechanisms responsible for these events has been lacking. Detailed study of three of these events demonstrates that static liquefaction was likely the cause for the failures and the ensuing highly mobile runouts. An evaluation of potential mitigation strategies shows that the risk of a liquefaction flowslides could be reduced by selective management and placement of liquefaction susceptible sandy gravel materials. Furthermore the current practice of re-sloping from angle-of-repose to a 2:1 reclaimed slope is sufficient to virtually eliminate the hazard.

ACKNOWLEDGEMENTS

I wish to express my sincerest gratitude to Dr. N.R. Morgenstern and Dr. D.C. Sego for their continual support and special contributions both to the thesis itself and the experiences that accompanied it's preparation and eventual completion. Dr. Morgenstern's overall guidance allowed me to explore many different facets of the thesis topic without losing site of the overall objective. Dr. Sego's encouragement, enthusiasm and constant flow of ideas were a welcome contribution to the experience.

Special thanks are also extended to Dr. P.K. Robertson, Dr. D. Scott, and the other members of the geotechnical group for finding the time to discuss topics at various stages along the way.

The work would not have been possible without financial support from the oil sands industry (mainly Esso Resources OSLO group), CANMET, and the British Columbia Waste Rock Pile Research Committee. Thanks are extended to Mr. Tom Dereniwski of OSLO, Dr. Andy Stokes of Canmet, and Mr. Tim Eaton, chairman of the rock pile committee, for their support of the projects carried out for this thesis research. several coal mines also deserve special mention for providing access and field support for the waste dump research: Greenhills Mine, Fording River Coal, Quintette Operating Corporation, and Line Creek Mine.

The highly competent and hard working geotechnical technicians provided a large amount of laboratory and field assistance during my graduate student tenure at the university. Special thanks are due to Gerry Cyre, Christine Hereygers, and Steve Gamble.

Several of my graduate school colleagues also assisted me in various aspects of my research endeavors. In particular, I would like to thank Richard Stahl and Peter Skopek for their very capable assistance both in the field and in the laboratory, and to Dr. Wei Hu Gu for his numerical verification of the collapse process in mine waste dumps.

The support and encouragement of my familly is the main reason I was able to carry out this ambitious endeavor at this stage in my life. To all of you; Sandra, Vanessa, Michael, and Morgan, thank-you. I will not forget.

TABLE OF CONTENTS

1- INTRODUCTION 1
2- GEOTECHNICS OF MINE WASTE AUDITS* 11
    2.1 INTRODUCTION 11
    2.2 REGULATORY TRENDS 12
    2.3 MINE WASTE GEOTECHNICS 13
        2.3.1 DRY WASTE STREAMS 14
        2.3.2 WET WASTE STREAMS 18
    2.4 MINE WASTE AUDITS 24
    2.5 CONCLUSIONS 25
    2.6 REFERENCES 26
3- TAILINGS MANAGEMENT IN COLD REGIONS - THIN LAYERED FREEZING AND THAWING STRATEGIES 41
    3.1 INTRODUCTION 41
    3.2 GROUND TEMPERATURE CONSIDERATIONS 42
    3.3 MOISTURE TRANSFER PROCESSES IN FREEZING SOILS 44
    3.4 DESIGN CONCEPTS 45
        3.4.1 FREEZE CONTROLLED STRATEGY 46
        3.4.2 THAW CONTROLLED STRATEGY 47
    3.5 SELECTED STUDIES 49
    3.5 CONCLUSIONS 52
    3.6 REFERENCES 53
4- FREEZE-THAW DEWATERING OF OIL SANDS FINE TAILS 66
    4.1 INTRODUCTION 66
    4.2 BACKGROUND STUDIES 66
    4.3 OSLO LEASE 41 FREEZE-THAW FIELD STUDY 67
    4.4 FREEZE-THAW DEWATERING DESIGN CONCEPTS 71
        4.4.1 THERMAL CONSIDERATIONS 71
        4.4.2 DRAINAGE AND CONSOLIDATION 72
    4.5 DESIGN SCENARIOS 74
    4.6 CONCLUSIONS 76
    4.7 REFERENCES 77
5- STATIC COLLAPSE OF MINE WASTE EMBANKMENTS 95
    5.1 INTRODUCTION 95
    5.2 SHEAR STRENGTH OF LOOSE GRANULAR MATERIAL 96

5.3 FLOWSLIDES IN MINE WASTE EMBANKMENTS 98
5.4 STEADY STATE AND COLLAPSE BEHAVIOUR 100
5.5 TRIGGER MECHANICS 102
5.6 PROGRESSIVE FAILURE 104
5.7 CONCLUSIONS 104
5.8 REFERENCES 105
6- FLOWSLIDES IN ROCKY MOUNTAIN COAL MINE WASTE DUMPS-FIELD AND LABORATORY STUDIES 118
6.1 INTRODUCTION 118
6.2 FIELD STUDY OF THREE FLOWSLIDE EVENTS 119
6.2.1 FIELD METHODS 120
6.2.2 FLOWSLIDE CASE HISTORIES 122
6.2.3 FACTORS AFFECTING STABILITY 127
6.3 GEOTECHNICAL PROPERTIES OF WASTE DUMP SANDY GRAVELS 128
6.3.1 VOID RATIO RELATIONSHIPS 129
6.3.2 TRIAXIAL TESTS 130
6.4 COLLAPSE MODEL 133
6.5 CONCLUSIONS 134
6.6 REFERENCES 135
7- FLOWSLIDES IN ROCKY MOUNTAIN COAL MINE WASTE DUMPS-ANALYSIS AND MITIGATION 164
7.1 INTRODUCTION 164
7.1 FINITE ELEMENT ANALYSES 164
7.1.1 MODELING METHODS AND PARAMETERS 165
7.1.2 MODELLING RESULTS 167
7.2 LIMIT EQUILIBRIUM ANALYSES 170
7.3 MITIGATIVE STRATEGIES 172
7.3.1 PRE-CONSTRUCTION STRATEGIES 172
7.3.2 CONSTRUCTION STRATEGIES 174
7.3.3 ABANDONMENT STRATEGIES 176
7.4 CONCLUSIONS 177
7.5 REFERENCES 178
8- CONCLUSIONS 197
8.1 MINE WASTE EMBANKMENT STABILITY 197
8.2 RECLAMATION 199

8.3 WASTE HANDLING METHODS 200
8.4 POLLUTION CONTROL 200
8.5 CONCLUDING REMARKS 201
APPENDIX A-FINE TAILS CONSOLIDATION TESTS 202
APPENDIX B-FREEZING AND THAWING MODELS 214
APPENDIX C-WASTE ROCK TRIAXIAL TESTS 218

LIST OF TABLES

TABLE 2.1- FEDERAL MINE EFFLUENT REGULATIONS 31
TABLE 2.2- RECOMMENDED ROCK DRAIN PROPERTIES 32
TABLE 2.3 ATTENUATION POTENTIAL OF SOME DISSOLVED CHEMICALS 33
TABLE 3.1 PORE WATER CHEMISTRY OF OIL SANDS FINE TAILS 55
TABLE 4.1 FORT MCMURRAY CLIMATE DATA 79
TABLE 5.1 INDEX PROPERTIES OF FINE QUARTZ SANDS 108
TABLE 5.2 INDEX PROPERTIES OF SANDY GRAVELS 109
TABLE 5.3 SUMMARY OF COLLAPSE AND FLOW PROPERTIES 110
TABLE 6.1 WASTE DUMP FLOWSLIDE CHARACTERISTICS 138
TABLE 6.2 RUNOUT MATERIAL CHARACTERISTICS 139
TABLE 6.3 FIELD CHARACTERISTICS OF TRIAXIAL SAMPLES 139
TABLE 6.4 TRIAXIAL SAMPLE PROPERTIES 140
TABLE 7.1 INITIAL STRESS ANALYSIS PARAMETERS 180
TABLE 7.2 LIQUEFACTION ANALYSIS PARAMETERS 181
TABLE 7.3 SAFETY FACTORS (BISHOP'S METHOD) 182
TABLE 7.4 MITIGATION STRATEGIES 182

LIST OF FIGURES

Figure 1.1 Some Mining Regions of Western Canada 7
Figure 1.2 Typical Oilsands Mine Waste Streams 8
Figure 1.3 Typical Coking Coal Mine Waste Streams 9
Figure 1.4 Typical Porphyry Copper Mine Waste Streams 10
Figure 2.1 Generalized Minesite Layout 34
Figure 2.2 Shear Strength of Australian Coal Mine Spoil 35
Figure 2.3 Rocky Mountain Coal Mine Runout Statistics 36
Figure 2.4 Stages in the Formation of AMD 37
Figure 2.5 Normalized Collapse Surface for Angular Quartz Sands 38
Figure 2.6 Effects of Fines Content on Steady State Behaviour 39
Figure 2.7 Typical Soil Cover to Control AMD Production 40
Figure 3.1 Permafrost Region of Canada 56
Figure 3.2 Ground Temperature Profiles 57
Figure 3.3 Calculated Tailings Sand Frozen Thicknesses 58
Figure 3.4 Calculated Tailings Sand Thawed Thicknesses 59
Figure 3.5 Total Containment by Frozen Cell Construction 60
Figure 3.6 Consolidation Due to Thaw Strain 61
Figure 3.7 Thaw Controlled Dewatering Schematic 62
Figure 3.8 Lupin Mine Active Layer Stratigraphies 63
Figure 3.9 Giant Mine Tailings Impounment Temperature Data 64
Figure 3.10 Oil Sand Fine Tails Thaw Strain 65
Figure 4.1 OSLO Fine Tails Geotechnical Properties 80
Figure 4.2 OSLO Lease 41 Fines Pond No. 1 81
Figure 4.3 OSLO Initial Versus Final Solids 82
Figure 4.4 OSLO Initial Solids Versus Thaw Strain 83
Figure 4.5 Lease 41 Compressibility Data 84

Figure 4.6 Lease 41 Permeability Data 85

Figure 4.7 Lease 41 Normalized Compressibility and Permeability Plots 86

Figure 4.8 Thin Layered Freeze Thaw Disposal Scheme 87

Figure 4.9 freezing Depths at Fort McMurray 88

Figure 4.10 Thawing Depths at Fort McMurray 89

Figure 4.11 Freeze Thaw Dewatering Consolidation Behaviour 90

Figure 4.12 Finite Strain Consolidation Model 91

Figure 4.13 Cumulative Thickness for 3m per Year Frozen Thickness 92

Figure 4.14 Cumulative Thickness for 4.5m per Year Frozen Thickness 93

Figure 4.15 3m per Year Single Versus Double Drainage 94

Figure 5.1 Constant Volume Collapse of a Loose Sand 111

Figure 5.2 Normalized Collapse Stress Paths 112

Figure 5.3 Western Canadian Coal Mine Flowslide Statistics 113

Figure 5.4 Steady State and Collpase Behaviour of Fine Sand 114

Figure 5.5 Steady State and Collpase Behaviour of Angular Sand 115

Figure 5.6 Steady State Behaviour of Sandy Gravels 116

Figure 5.7 Collapse Due to a Rising Water Table 117

Figure 6.1 Rocky Mountain Coal Mine Flowslide Study Sites 141

Figure 6.2 Coal Mine Waste Dump Stability Statistics 142

Figure 6.3 Quintette Marmot 1660 Flowslide 143

Figure 6.4 Marmot 1660 Runout 144

Figure 6.5 Liquefaction Cone in Marmot 1660 Runout 145

Figure 6.6 Fording South Spoil Flowslide 146

Figure 6.7 Fording South Spoil Prior to Failure 147

Figure 6.8 Fording South Spoil Runout Debris Dozer Cuts 148

Figure 6.9 Green Hills Cougar 7 Flowslide 149

Figure 6.10 Cougar 7 Runout 150

Figure 6.11 Fines Layers in Cougar 7 Dump 151
Figure 6.12 Daily Precipitation Prior to Failure 152
Figure 6.13 Runout Grain Size Distributions 153
Figure 6.14 Liquefaction Flowslide Grain Size Distributions 154
Figure 6.15 Field Void Ratio Versus Moisture Content 155
Figure 6.16 Field Saturated Permeability 156
Figure 6.17 Field vs Triaxial Grain Size Distributions 157
Figure 6.18 Typical Triaxial Test 158
Figure 6.19 Steady State Friction Behaviour 159
Figure 6.20 Steady State Void Ratio Behaviour 160
Figure 6.21 Fording Stress Paths 161
Figure 6.22 Brittleness Index Versus Void Ratio 162
Figure 6.23 Conceptual Collapse Model 163
Figure 7.1 Liquefaction Model Stress Paths 183
Figure 7.2 Failure Surface Criteria 184
Figure 7.3 Quintette Marmot 1660 Initial Yield Ratio and Displacements 185
Figure 7.4 Quintette Marmot 1660 Liquefied Yield Ratio and Displacements 186
Figure 7.5 Fording South Spoil Initial Yield Ratio and Displacements 187
Figure 7.6 Fording South Spoil Liquefied Yield Ratio and Displacements 188
Figure 7.7 Greenhills Cougar 7 Initial Yield Ratio and Displacements 189
Figure 7.8 Greenhills Cougar 7 Liquefied Yield Ratio and Displacements 190
Figure 7.9 Stress State of the Potentially Liquefiable Layers prior to Collapse 191
Figure 7.10 Stress State of Peak Values from Triaxial tests 192
Figure 7.11 Undrained Strength Evaluation Criteria 193
Figure 7.12 Influence of Foundation Shearing Resistance on Trigger Potential 194
Figure 7.13 Liquefaction Resistant Dump Construction Methods 195
Figure 7.14 Influence of Re-sloping on Collapse Potential 196

LIST OF SYMBOLS

Stress/Strain/Strength

$\acute{O}'_1$=maximum principal effective stress	
$\acute{O}'_3$=minimum principal effective stress	
$\acute{O}'_V$=vertical effective stress	
K=coefficient of earth pressure	K_0=coefficient of earth pressure at rest
$t=(\acute{O}'_1-\acute{O}'_3)/2$	
$s'=(\acute{O}'_1+\acute{O}'_3)/2$	
$q=(\acute{O}'_1-\acute{O}'_3)$	q_0=initial
	q_{max}=maximum
	q_{cv}=constant volume
	q_{ss}=steady state
	$q_{collapse}$=collapse
$p'=(\acute{O}'_1+2\acute{O}'_3)/3$	p_{ss}=steady state
I_b=brittleness index	
u=pore pressure	u_e=excess pore pressure
Ø'=effective friction angle	Ø'$_{cv}$=constant volume
	Ø'$_{ss}$=steady state
S_u=undrained strength	
B_T=tangent bulk modulus	
E_T=tangent Young's modulus	
K_B=modulus number	
K_E=hyperbolic elastic number	
n=hyperbolic elastic exponent	
m=modulus exponent	
R_F=failure ratio	
R_y=yield ratio	
a,b=hyperbolic elastic strain weakening parameters	
e=void ratio	e_0=initial
	e_{norm}=normalized
	e_{thaw}=thawed
A,B,C,D=material constants for e relationships	
C_v=coefficient of consolidation	

Physical Properties

D_r=relative density
G=specific gravity
G_s=soil solids specific gravity
G_B=bulk specific gravity

w=moisture content
D_n=% by weight finer than n
C_U=D_{60}/D_{10}=uniformity coefficient
k=permeability

Thermal properties

T=temperature
T_a=air
T_G=ground
T_W=water

D_F=total freezing depth
D_T=total thawing depth
P_F=freezing period
P_T=thawing period
h_c=convection coefficient
L'=latent heat of water
L=volumetric latent heat
I=average solar insolation
K=thermal conductivity
K_{sat}=saturated
K_{soil}=soil
K_{water}=water
K_F=freezing
K_T=thawing

Chapter 1

INTRODUCTION

Large quantities of mining and process wastes are byproducts of most mineral extraction and processing operations. Historically, the disposal of these materials has been carried out with little concern for engineered containment strategies that minimize the effects of these materials on the surrounding environment. Worldwide these practices have resulted in billions of tonnes of poorly contained mine waste products. The legacy of past mine waste management practices haunts the more environmentally responsible industry of today.

Canada and other countries that depend to a large extent on their natural resources for their economic growth are faced with a major challenge for managing mine waste products in an environmentally acceptable yet economic manner. Most mine wastes are not initially hazardous substances, yet there is a trend to impose hazardous waste regulations onto the mining industry's waste management practices. The industry should respond by demonstrating that it is accommodating the most feasible technology presently available to mitigate the environmental impact of their waste management practices. Failure to do so could result in the imposition of unnecessarily hindering regulations that prevents economic extraction of much of our mineral wealth.

Mining is an exercise in materials management. The efficient extraction, transport, disposal, and storage of both ore and waste products is perhaps the single most important economical aspect of a mining operation. As a result, ore grade and stripping ratios (for surface mines only) dominate most other mine planning considerations. An evaluation of a mining operations waste and product streams reveals many of the most important mine planning and infrastructure requirements of a mining operation and presents an overview of mine waste management issues. Thus it is appropriate to introduce the thesis by examining some typical waste and product streams for different mineral producers. The emphasis in the discussion is on the solid waste products (including high moisture content slurries) as these are the materials that influence geotechnical aspects of mine waste management. Mine waste effluents, which are comprised mostly of water are beyond the scope of this thesis.

Some typical waste streams for three different Western Canadian resource extraction operations are examined as follows:

1. Northern Alberta oilsands mines

2. Rocky Mountain coal mines

3. Interior British Columbia copper mines

The mines in these categories are all surface mines. These operations were chosen mainly because many of these mines were visited during the course of the research presented here. Detailed studies were carried out at oilsands operations and at Rocky Mountain coal mines for this thesis and thus an evaluation of these waste streams provides a useful background to this work. The "hard rock" copper mines provide a contrast to the other two "soft rock" operations; two of these operations were visited in order to evaluate their mine waste management practices. Figure 1.1 shows the reserve areas and minesites in these three different groups which span a wide range of geological, geographic, and climatic conditions.

• NORTHERN ALBERTA OIL SANDS MINE WASTE STREAMS

The two oil sands operations in the Fort M^{c}Murray Alberta area, Syncrude and Suncor, produce about 15% of Canada's crude oil consumption. These very large surface mining operations produce about 34,000 m^3/day (214,000 barrels/day) of synthetic crude oil. Figure 1.2 shows a typical waste stream balance for these operations relative to $1m^3$(6.3 barrels) of synthetic crude oil product (Dussealt and Scott, 1983). Each $1m^3$ (6.3 barrels) of synthetic crude oil produced results in about $5m^3$ of "dry" overburden waste and $21m^3$ of tailings. The larger oil sands operation, Syncrude produces about 25,000 m^3 of oil per day. This production rate results in annual quantities of about 45 million m^3 overburden and 150 million m^3 tailings. These large quantities are striking and are demonstrative of the very large scale of these operations.

Surficial soils and weak overburden rocks are mined by truck/shovel methods and disposed of in dry waste overburden dumps. The overburden materials are of several different types and as a result exhibit highly variable shear strength properties. In most cases the waste dumps are engineered structures constructed in semi-compacted lifts or with specially designed compacted shells. Waste dumps are constructed up to about 55m in height. Only where potential failures can be contained inside pit limits is uncompacted end-dumping carried out.

The oil sands ore is extracted by employing strip mining methods with draglines, bucketwheel excavators, and more recently by truck/shovel methods. Oil sands ore and large quantities of water are fed to a hot water extraction plant. The plant produces bitumen (which is further processed to produce synthetic crude oil), a small amount of dry rejects, and very large quantities of tailings. The tailings are considered toxic, mainly due to organic compounds released from the ore during processing, and thus the tailings management system is operated as a total containment system. Tailings basins are constructed of compacted tailings sand, compacted earth fill, or with a combination of both construction materials and range from 30m to 90m in height (Morgenstern et al, 1988). Tailings impoundment design, construction, and operation are highly engineered. Significant quantities of high water content fine tailings accumulate in the tailings basins. These materials consolidate at negligibly low rates and thus pose long term containment and abandonment problems.

- ROCKY MOUNTAIN COAL MINE WASTE STREAMS

Metallurgical quality coal is mined at several operations in the Western Canadian Rocky Mountains. Ten surface mines produce about 30-35 million tonnes of coking coal per year for sale mainly to Pacific Rim steel producers. Figure 1.3 shows a typical waste stream balance for these operations relative to 1 tonne of salable metallurgical coal. Each tonne of coal produced results in about 6m^3 of "dry" overburden waste and 3m^3 of processed wastes (dry coarse reject and fine tailings). At a large operation, such as the Fording River Mine capable of producing in excess of 5 million tonnes of coal per year, this would result in 30 million m^3 of overburden and 15 million m^3 of processed wastes.

The Rocky Mountain coal mine open pits are located mostly in steep, rugged terrain and access is a major mine planning consideration. Overburden rocks are drilled, blasted, and mined mostly by truck/shovel methods. The waste rock is end-dumped without any significant compaction in high (commonly 100 to 300m high) angle-of-repose(37-38°) piles on steep(15-25°) foundation slopes. Large runout flowslide type failures are not uncommon, mainly in the British Columbian mines (Dawson et al, 1992).

Run-of-mine coal is excavated mainly by front-end loaders and processed in washeries. The processed waste consists of dry coarse reject and fine tailings. The fine tails are contained in compacted fill embankments constructed of earth fill and coarse reject materials. Fine tails solids settle readily and as a result they do not pose a large containment problem. Coarse reject materials not used for compacted fill are stored in "dry" waste piles. Most effluent is either recycled to the washery or released back into natural water courses.

- INTERIOR BRITISH COLUMBIA COPPER MINES

Several mines produce copper from porphyry copper type deposits in central British Columbia. Byproduct gold and molybdenum are also produced at some operations. While many are currently closed down, higher copper prices are causing renewed interest in these operations and three copper mines are planning to resume operations this year (Northern Miner, 1994). The mines operate in the dry interior British Columbia climate in areas of moderate relief. Figure 1.4 shows a typical waste stream balance for these operations. The large variation in material quantities is due to the large difference in stripping ratios and grades between the different deposits. Each tonne of copper concentrate produced results in about 3-5m^3 of "dry" overburden waste and 200-400m^3 of tailings. The Highland Valley mine, located near Kamloops, is one of the largest copper mines in the world and produces about 160,000 tonnes of copper (about 400,000 tonnes of concentrate) and 2300 tonnes of molybdenum per year (Hanson, 1992). These tonnages result in the production of about 25 million m^3 of overburden and 113 million m^3 of tailings. Tailings and overburden volumes at Highland Valley rival those of a large oil sands operation.

Overburden rocks are drilled, blasted, and mined by truck/shovel methods. The waste rock is dumped in semi-compacted lifts and in free dumped piles, commonly up to 50m in height (Highland Valley Copper, 1992). At the Brenda mine, an alkaline leachate is produced as water percolates through the waste piles. The leachate is high in dissolved molybdenum as a result (Brown, 1992). Flowslide type waste dump failures observed in the Rocky Mountain coal mines do not occur.

Ore is mined by truck/shovel/conveyor and processed along with large quantities of water. Most of the tailings impoundments are located in valleys with hydraulic tailings sand containment constructed in a downstream or centerline fashion. Most of the tailings water is recycled. At Highland Valley, the tailings impoundment is contained between two dams, the largest which is designed for an ultimate height of 160m (Scott and Lo, 1992). A key issue for tailings containment is earthquake resistant design as interior and coastal British Columbia are seismically active areas.

This brief overview of some typical Western Canadian mine waste streams illustrates two significant aspects which are central to mine waste management:

1. Mine waste management is dominated by volume considerations. The economic management of large quantities of both solid and liquid fractions poses both short and long term containment engineering challenges.

2. Significant bulking occurs, both due to addition of water during processing and in uncompacted or partially compacted waste dumps. The chemical and physical stability of relatively loose materials is often a key mine waste management consideration.

This thesis addresses several geotechnical aspects of these issues. The main objectives are as follows:

1. To demonstrate the role that geotechnical engineering plays in aiding the development of best practicable technologies for mine waste management practice.

2. To carry out detailed studies on thin layered freeze-thaw dewatering of oil sands fine tails

3. To carry out detailed studies on instability mechanisms responsible for catastrophic flowslides in British Columbian coal mine waste dumps.

Chapter 2 examines the concept of the mine waste audit and the role that geotechnical engineering plays in the mine waste audit process. A review of geotechnical issues in Chapter 2 results in a synopsis of issues where technical advances are pending. The remainder of the thesis focuses on some of these issues.

Chapters 3 and 4 examine geotechnical aspects of tailings management in cold regions. Chapter 3 provides an overview of thin layered freeze and thaw controlled strategies for tailings management in cold regions. In Chapter 4 a detailed study of a thaw controlled thin layered freeze-thaw dewatering process for oil sands fine tailings is presented.

Chapters 5, 6, and 7 examine static collapse (liquefaction) mechanics of granular materials in mine waste embankments. Chapter 5 discusses emerging concepts of static collapse and presents a generic framework for analysis and mitigative design. In Chapter 6 the results of detailed studies of Rocky Mountain coal mine waste dump flowslides are presented. Chapter 7 follows by presenting some numerical and limit equilibrium analyses of these events and by examining some mitigative strategies for preventing collapse in mine waste dumps.

The last chapter integrates the results of the thesis findings and summarizes the main conclusions.

REFERENCES

Dussault, M.B. and Scott, J.D., 1983. Tailings Pond Behaviour and Characterization of Oil Sands Tailings Sludge, Particulate Science and Technology, vol. 1, pp 293-309.

Brown, R., 1992. Personal communication during a minesite visit, May, 1992.

Dawson, R.F., Morgenstern, N.R., and Gu, W.H., 1992. Liquefaction Flowslides in Western Canandian Coal Mine Waste Dumps, Phase 1. Report to Supply and Services Canada, 100 p.

Hanson, P., 1992. A Temporary Use of the Land at Highland Valley Copper, CIM Bullitin, vol. 85, No. 62, pp 71-72.

Highland Valley Copper, 1992. Mine Dumps and Fill Roads Monitoring and Audits, Minesite Internal Report.

Morgenstern, N.R.; Fair, A.E. and McRoberts, E.C., 1988. Geotechnical Engineering Beyond Soil Mechanics-a Case Study, Canadian Geotechnical Journal, Vol. 25, pp 637-661.

The Northern Miner, 1994. Copper Mines Staging Comeback in British Columbia, August 1, 1994.

Scott, M.D. and Lo, R.C., 1992. Optimal Tailings management at Highland Valley Copper, CIM Bullitin, vol. 85, No. 62, pp 85 88.

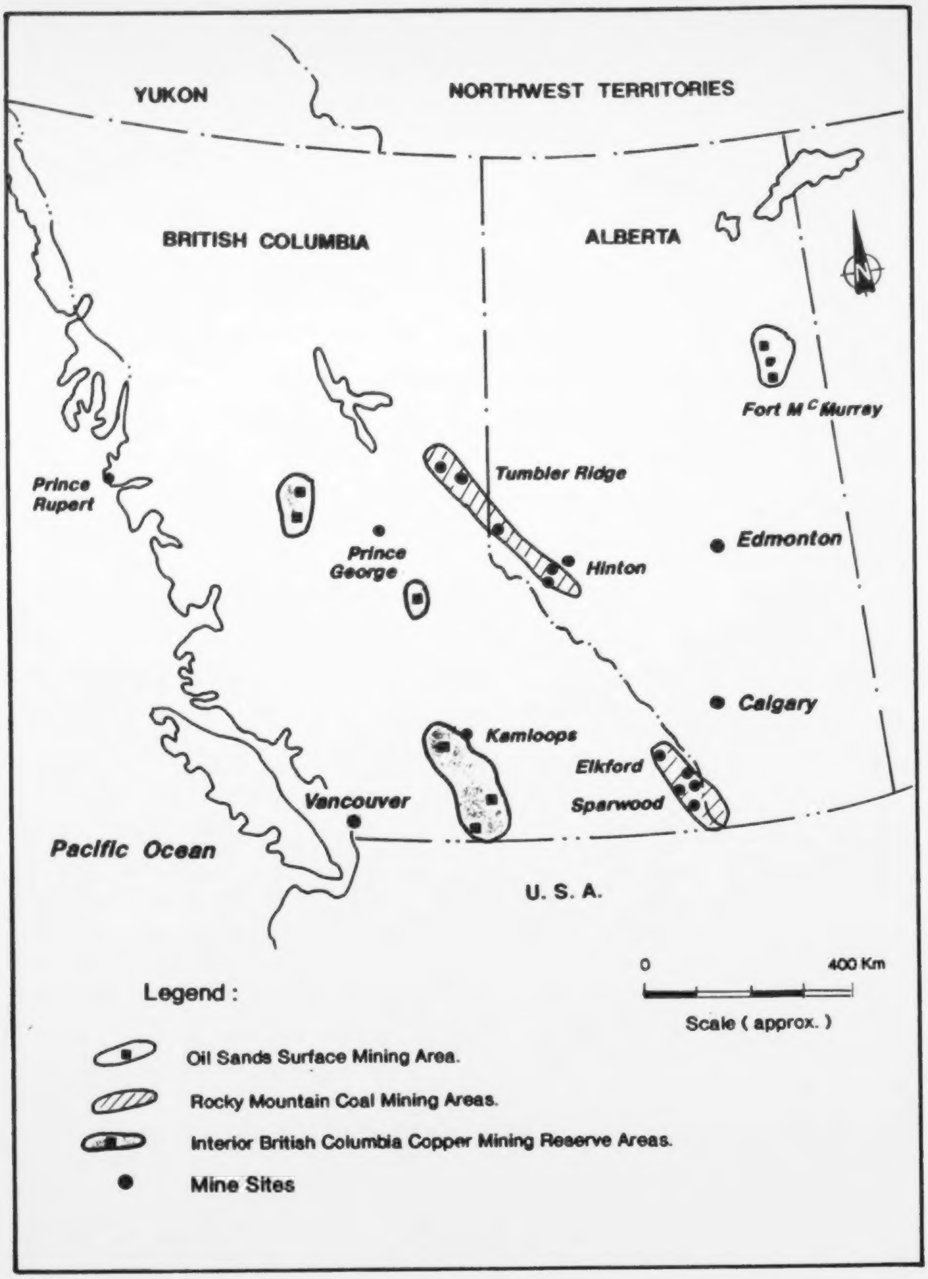

Figure 1.1 Some Mining Regions of Western Canada

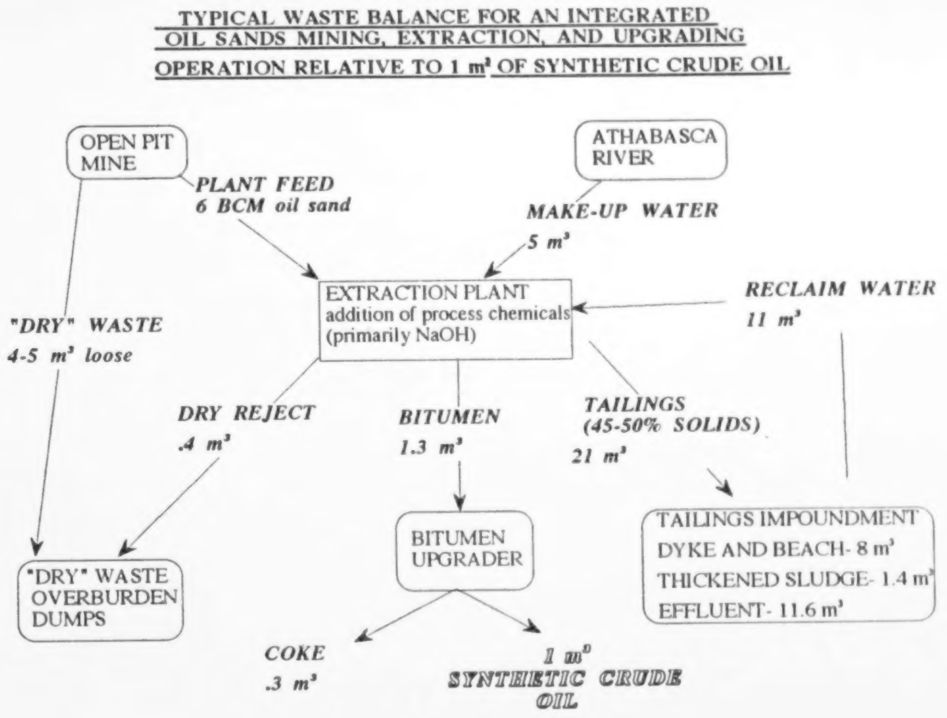
TYPICAL WASTE BALANCE FOR AN INTEGRATED OIL SANDS MINING, EXTRACTION, AND UPGRADING OPERATION RELATIVE TO 1 m³ OF SYNTHETIC CRUDE OIL
OPEN PIT MINE
ATHABASCA RIVER
PLANT FEED 6 BCM oil sand
MAKE-UP WATER 5 m³
EXTRACTION PLANT addition of process chemicals (primarily NaOH)
RECLAIM WATER 11 m³
"DRY" WASTE 4-5 m³ loose
DRY REJECT .4 m³
BITUMEN 1.3 m³
TAILINGS (45-50% SOLIDS) 21 m³
TAILINGS IMPOUNDMENT
DYKE AND BEACH- 8 m³
THICKENED SLUDGE- 1.4 m³
EFFLUENT- 11.6 m³
BITUMEN UPGRADER
"DRY" WASTE OVERBURDEN DUMPS
COKE .3 m³
1 m³ SYNTHETIC CRUDE OIL

Figure 1.2 Typical Oilsands Mine Waste Streams

TYPICAL WASTE BALANCE FOR A WESTERN CANADIAN ROCKY MOUNTAIN COKING COAL MINE RELATIVE TO 1 TONNE OF CLEAN COAL PRODUCT

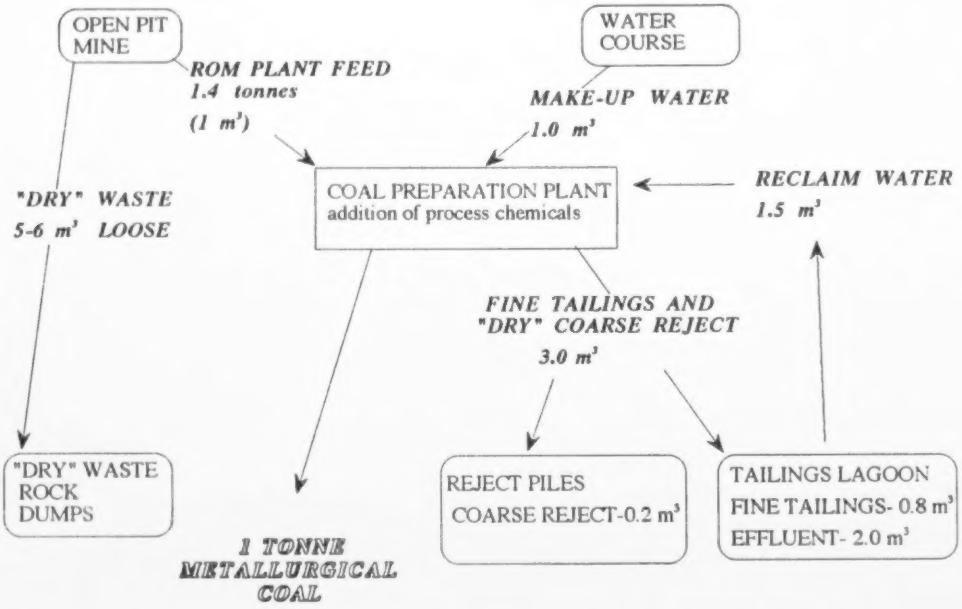

Figure 1.3 Typical Coking Coal Mine Waste Streams

TYPICAL WASTE BALANCE FOR AN INTERIOR BRITISH COLUMBIA COPPER MINE RELATIVE TO 1 TONNE OF COPPER CONCENTRATE

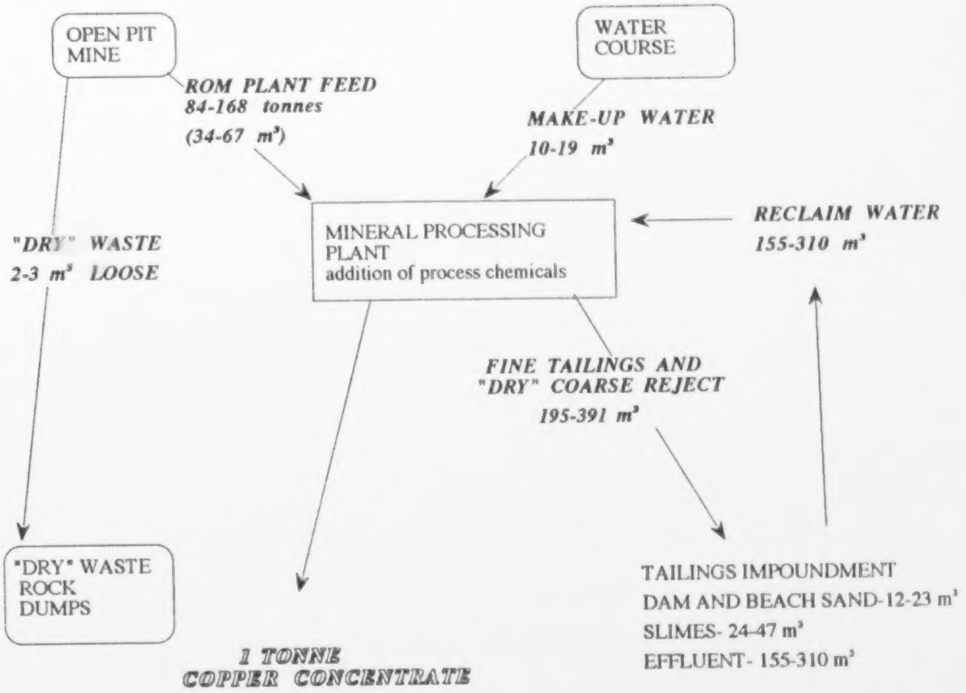

Figure 1.4 Typical Porphyry Copper Mine Waste Streams

Chapter 2

GEOTECHNICS OF MINE WASTE AUDITS*

2.1 INTRODUCTION

Storage and disposal of mine waste is no longer driven only by operational requirements and unit cost economics. Tighter regulatory controls, potential long term environmental liabilities, and social perceptions also play important roles in determining ultimate strategies for disposal. Technical considerations can be overlooked and sound waste management practice becomes more difficult to assess.

The emergence of global environmental concerns has opened new opportunities and has placed new responsibilities on the technical community. Clearly mine waste management, as well as other waste related issues, is an inter-disciplinary activity. It is therefore timely to examine the role of geotechnical engineering for assessing mine waste management practices.

Geotechnical engineering deals with the strength, deformation, and conductivity behaviour of soils, rocks, and geosynthetics. In conventional practice the geotechnical engineer deals mostly with the design of slopes, tunnels, and foundations. Environmental geotechnics is "primarily identified with the geotechnical aspects of waste management" (Morgenstern, 1991). Environmental matters differ significantly from more conventional geotechnical practice in that:

- environmental issues are influenced by an ever increasing variety of regulations.
- environmental issues involve a necessary appreciation for other disciplines not normally encountered in conventional geotechnical engineering practice such as chemistry, biology, and contaminant hydrogeology.
- resolution of environmental issues involves significant legal and public exposure.

---

* A version of this chapter has been published: Dawson,R.F.; Morgenstern,N.R.; and Sego,D.C., 1992. Geotechnics of Mine Waste Audits, Proc 2^{nd} Int'l Conf on Environmental Issues and Management of Waste in Energy and Mineral Production, Calgary, September, 1992, pp1003-1013.

- serviceability time frames far exceed those of conventional practice; issues of longevity pose problems for geotechnical engineers.

A large variety of mine waste products and handling methods further complicates evaluations. Despite these various impediments to establishment of generic standards of practice, a review of various mine waste streams shows that several common problems and concerns emerge.

In this chapter geotechnical issues relevant to the evaluation of mine waste management are discussed. The rational for conducting geotechnical audits that could be used to evaluate mine waste management practice is then presented. A brief comment on the current regulatory environment sets the stage for discussions that follow.

2.2 REGULATORY TRENDS

Control of surface water pollution in Canadian metal mines is regulated federally under the Metal Mining Liquid Effluent Regulations and Guidelines (Environment Canada, 1977). An Environmental Code of Practice for Mines that makes recommendations on technical and operational aspects of water pollution control was also published with the regulations and guidelines. Table 2.1 shows the authorized levels of substances specified in the regulations as compared to U.S. federal regulations. Provincial limits can exceed these levels and also include limits for toxic chemicals such as cyanide. The numerical limits are intended to "control pollution at the source through the application of technology that is in commercial use and is both technically and economically viable" (Environment Canada, 1988). Similar federal regulations governing the management of solid mine wastes and ground water emissions do not currently exist. Compliance oriented regulations (regulations based on prescriptive criteria) are often not well suited to solid waste management issues. Experience in conventional geotechnical practice has shown that performance regulations (regulations based on good standards of practice) are better suited to the changing technologies and inherent uncertainties (mechanical processes and properties) common to engineering evaluations involving geomaterials.

American legislation for the disposal of hazardous wastes suggests some emerging trends. In the United States Federal law assigns the burden of responsibility to the waste generator. Federal policy (1984 US. Hazardous and Solid Waste Amendments to the US. Resource Conservation and Recovery Act, 1976) states:

> *" The Congress hereby declares it to be a national policy of the United States that, wherever feasible, the generation of hazardous waste is to be reduced or eliminated as expeditiously as possible. Waste that is nevertheless generated should be treated, stored, or disposed of, so as to minimize the present and future threat to human health and the environment"*

Regulations and policies designed to accommodate these generic guidelines tend to be restrictive. As a result technological advances can lack innovation and costs of compliance can be excessive. For example, as a matter of policy the US. Environmental Protection Agency (EPA) uses a very simple ground water model (the model conservatively disregards attenuation effects) to assess whether a particular industrial waste is to be listed as hazardous. The waste generator must demonstrate that leachable chemicals from the solid waste would not exceed EPA drinking water standards 500 feet downgradient of the disposal location (U.S. National Research Council, 1990). If the calculated contaminant concentration is above the threshold level then the waste is classified as hazardous and containment obligations are substantially increased. There is little opportunity to demonstrate by other means that environmental risks are sufficiently mitigated.

In order to avoid such a rigid regulatory environment the mining industry must continuously demonstrate that waste is being managed utilizing the best practicable technology currently available to "minimize the present and future threat to human health and the environment." Waste generators are therefore not only obliged to satisfy current regulations but also to continuously evaluate their practices in order to ensure that present and future environmental concerns are met by the application of the best technically and economically viable technology. A concise review of some geotechnical factors necessary to evaluate current mine waste management practices follows.

2.3 MINE WASTE GEOTECHNICS

Technical aspects of waste streams are conveniently divided into four different areas as follows:

1. Waste Handling Methods

2. Waste Embankment Stability

3. Pollution Control

4. Reclamation

These topics are not mutually exclusive; however they form useful categories within which to evaluate waste management practices from a geotechnical perspective.

Handling methods impact on the placed material properties but are largely influenced by issues of economics, mineral processing requirements, scheduling requirements, and equipment availability. An appreciation for the economics and technical aspects of mine waste transport and mineral processing is necessary in order to assess geotechnical aspects of current technologies and to evaluate the merits of new technologies.

Many issues of waste embankment stability are common to other areas of geotechnical engineering. Familiarity with conventional geotechnical principles and practices is an essential starting point for stability evaluations. These issues are extensively discussed elsewhere and need not be repeated here.

Pollution control, in a geotechnical sense, is often dominated by matters of contaminant migration through porous media. This is very much an interdisciplinary field that requires knowledge of basic principles of contaminant hydrogeology and aqueous water chemistry in order to assess control strategies.

For the purpose of this paper, reclamation is defined as post-mining activity that prepares the land surface for ultimate abandonment. Placement of final covers, resloping, revegetation, and erosion control measures all fall within this category.

Figure 2.1 is a pictorial that shows a generalized mine site layout. A distinction between dry waste streams (contained in the waste rock dumps) and wet waste streams (contained in the tailings pond area) is convenient for the discussion of geotechnical issues that follows. Discussions of wet waste streams are confined mostly to slurries and settled solids. Management of surface effluents and runoff are not normally geotechnical matters. Emphasis is placed mainly on current and evolving issues relevant to Western Canadian practice.

2.3.1 DRY WASTE STREAMS

Dry waste consists of unsaturated chunks of rock or overburden transported via truck, dragline or conveyor to waste dumps (also known as spoil heaps, tips, and overburden piles). Waste dumps are normally non-impounding and generally receive less attention during design and operation than tailings embankments.

- Handling and Placement Methods

Waste rock is normally placed by end dumping (truck and shovel mining) or by stacking (drag-line mining). As a direct result of placement methods most waste dumps consist of unsaturated (at time of placement), loose material sloping at their angle-of-repose. The placement methods result in several special design and operational considerations:

- End dumped dry waste material can exhibit considerable natural segregation during disposal along the dump face with the larger more durable rocks rolling to the toe area. While coarser material allows for better drainage in the toe area, the segregated fines may result in undesirable perched zones of low permeability and strength.

- Placement densities of finer unsaturated argillaceous and carbonaceous materials are very sensitive to placement water content. Following detailed studies of the colliery waste flow slides in South Wales Bishop (1973) states "the initial density of loosely placed rock spoil containing fines is very sensitive to placement moisture content, as is also the subsequent decrease in volume on wetting or saturation."

- The rate of placement (rate of loading) can significantly impact dump stability in poorly draining contractant waste and foundation materials. Full saturation is not necessary for excess pore pressure development. A priori predictions of failure are very difficult without ongoing pore pressure measurements within the embankment.

Moisture sensitive materials are particularly sensitive to these handling considerations. The presence of pore pressures within the waste material itself is often not considered.

Waste dumps placed in stream valleys require consideration for maintaining stream flows beneath the dump. Use of the rock fill itself as a flow-through drain (rock drain) is often the conveyance option of choice. Design issues involve consideration of turbulent flow, durability of drain rock, capacity for storm events, weathering effects on long term seepage control, and potential leachate production from the waste rock (Das et al, 1990).

Table 2.2 shows recommended waste rock properties for rock drains. Further work is required to develop a durability classification system for rock drain materials that will provide adequate long term drainage requirements.

- Stability

The many different combinations of waste dump material and foundation conditions result in several different failure modes. Angle-of-repose waste dumps are particularly susceptible to wedge type failure geometries, especially when placed on steep foundations (Campbell, 1986).

As in conventional practice, stability analysis is extremely sensitive to selection of shear strength parameters and knowledge of pore pressures. Design friction angles equal to the angle of repose are often used in stability analysis. Although this may be an appropriate assumption for coarse, strong rock fill it appears to be a questionable practice for poorly graded moisture sensitive waste material. Figure 2.2 shows shear strength results on coal mine spoil from Australia (Seedsman et al, 1980). The coal mine waste shows a dramatic drop in strength due to weathering. These authors suggest that the weathering process is commensurate with poor drainage charactericties (lower coefficient of consolidation) resulting in undrained loading conditions during dumping.

Piteau Associates (1992) have completed a survey of 83 individual dumps at 31 active sites in British Columbia. About 12% of the dumps have exhibited failure events (minor cracking and bulging not included). Figure 2.3, compiled from the database, shows that substantial runouts developed in some of the higher dumps. Most of the failures have taken place at coal mines. Conventional failure mechanics are not able to explain the higher runout events. Eckersley (1991) demonstrates that flow failures in model coal stockpiles initiated under static fully drained conditions were mobilized at secant friction angles less than the steady state Mohr-Coulomb friction angle! Recent advances in liquefaction mechanics of tailings and other loose sands merit consideration.

Stability evaluation of coal measures and other waste rock materials sensitive to moisture infiltration require consideration of weathering processes, undrained loading, and potential liquefaction. A lack of reliable information on these materials is an impediment to better design guidance in this regard.

- Pollution Control

Production and migration of pollutants in mine waste dumps is controlled by infiltration and leaching processes. A central issue has been the production of acidic seepage waters from sulphide bearing wastes. Many consider acid mine drainage (AMD) as the largest environmental problem within the Canadian mining industry today. Steffen, Robertson, and Kirsten (1989) have completed a technical guide on the application of currently available AMD technology. Filion et al (1990) provide a summary of the extensive research programs currently being carried out under federal and provincial guidance. Acid mine drainage is not restricted to waste rock dumps; tailings, open pits, and underground workings are also potential sources. In Western Canada, acid mine drainage production from base metal mine waste dumps is of particular concern (Barton-Bridges and Robertson, 1989) and thus the issue is discussed here with respect to dry waste streams; the discussion is equally applicable to wet waste streams. The majority of Western Canadian coal mine wastes are non-acid producing .

Acid mine drainage (AMD) is defined as " contaminated drainage that occurs as a result of natural oxidation of sulphide minerals contained in rock which is exposed to air and water " (Barton-Bridges and Robertson, 1989). Acid production occurs in a series of continuously accelerating reactions. Figure 2.4 shows the generally accepted form of these reactions for pyrite. The basic reactions are modified and reaction rates are affected by a variety of effects including, availability of oxygen and water, the presence of oxidizing bacteria (biological catalyst), and neutralizing minerals (notably carbonates). These and other geochemical and hydogeological factors render prediction and long term control difficult issues.

Laboratory tests and mathematical models have been developed to predict rates and duration of AMD generation. Results are sensitive to sample representivity, test duration, size effects, boundary conditions, and climatic conditions; familiar factors to geotechnical engineers. Lawrence et al (1989) provide an assessment of various AMD test prediction methods.

The most effective options which have long term control potential are water covers, soil covers, and collection and chemical treatment of the acidic (Barton-Bridges and Robertson, 1989). Disposal of acid generating waste under water is technically the most desirable abatement measure (Nolan, Davis and Associates, 1987). However water cover options are restrictive as outlined by Steffen, Robertson, and Kirsten (1989):

-unconfined open water disposal is discouraged by current legislation and potential for other environmental problems.

- flooding involves construction of water impounding structures unless the waste can be disposed in mined out pit or undergound workings. Disposal in mined out areas often involves significant re-handle costs.

Collection and treatment has proven effective and is currently practiced at four mines in British Columbia. Monitoring of treatment facilities for unspecified periods following abandonment and increasing accumulation of treatment sludges favour placement of soil covers for long term AMD control. Long term effectiveness of soil covers has not been established and long term testing is currently being carrried out at a number of sites. Thus design of walk-away AMD control options is hampered by a lack of information on the long term integrity of soil and geosynthetic covers. Continuous and comparative studies at abandoned sites and operating test sites would go a long way to addressing these deficiencies.

- Reclamation

Reclamation of chemically benign mine waste dumps generally involves re-sloping, placement of top soil, and establishment of suitable vegetative covers. Resloping to the biological angle-of-repose (2:1 slope) appears to be common and sensible practice to control erosion of vegetated slopes and reduce hazards of long term instability. A discussion of soil covers designed to minimize infiltration and prevent migration of leachates is included in the section on wet mine waste streams (tailings) that follows.

2.3.2 WET WASTE STREAMS

Wet mine waste streams normally consist of solid/water slurries (tailings) resulting from mineral processing operations and transported to the disposal area by slurry pipeline. Other forms of wet waste streams are dredging wastes and effluent treatment sludges. Most of the discussions here are confined to tailings. Tailings embankments are frequently water impoundment structures and thus normally receive greater attention during design and operation "dry waste" dumps.

- Handling and Placement Methods

Tailings are usually placed by discharging slurry onto an area and allowing the solids to settle out while the fluids drain away. Preferential settlement of coarse from the fines fraction distinguishes between segregating and non-segregating mixes. Behaviour of slurries as segregating or non-segregating mixes depends on (Kupper,1991):

-carrier fluid rheology

-chemical additives (flocculants/dipersants)

-type and amount of solids

-flow conditions

A fundamental understanding of these controlling factors is currently lacking. Similar behaviour of slurries in pipelines is termed heterogeneous versus homogeneous flow and empirical relationships have been developed to determine the affinity for a particular slurry to develop a concentration gradient under various flow conditions (Wasp, 1977). Similar criteria have not been developed for tailings and other hydraulic fills.

Robinsky (1978) has coined the term "thickened discharge" for tailings handling systems that take advantage of non-segregating material behaviour. Most tailings are initially segregating mixtures and thus require additional thickening to render them non-segregating. Three mines in Canada (all in Eastern Canada) are currently using the thickened discharge method. Deposition curves presented by Salvas (1989) suggest that very high slurry concentrations (>65%) are required to develop non-segregating behaviour for most base metal mine whole tailings. Scott and Cymerman (1984) have examined the "static" segregation behaviour of oil sand tailings; solids contents of 70 % are required to render this material non-segregating. Hydraulic transport is difficult at these high solids contents.

Segregating slurries are normally deposited on a beach (above standing water). Lighthall et al (1989) review the common deposition methods of hydraulic fill construction. In order of increasing placement density and control of embankment slopes, these methods are:

1. Spigotting and Single Point Discharge

2. Cycloning

3. Cell Construction

Knight and Haile (1983) promote a variation on the conventional spigotted deposition, termed "sub-aerial discharge", that involves placement in thin layers, allowing each layer to drain and partially air dry prior to placing the next layer; thus reducing water storage requirements. The system is common in arid regions such as South Africa and Arizona and requires additional underdrain considerations in Canada. Two western Canadian mines have adopted the concept.

Tailings dam configurations are governed by the manner in which the deposition process proceeds. While downstream construction is inherently the most stable configuration it also requires the greatest amount of sand. Upsteam construction requires careful consideration to mitigate against generation of undrained pore pressures in the underlying fines. Adequate pond level control is the key design consideration in this regard.

Predictions of beach geometry are necessary to evaluate different design configurations. Studies by Blight (1987) and others have shown that the concave beach profile of segregating slurries can be adequately described by a dimensionless equation. Kupper (1991) has shown that the average beach angle increases with increasing discharge cross sectional area, average grain size, and slurry solids concentration but with decreasing flow rate. Higher beach slopes were also shown to be coincident with lower density and increased fines capture. This work provides a useful link between handling technology and the resulting geotechnical properties.

The segregated fines that settle in the pond are generally of high moisture content and low permeability. Tailings impoundments must be adequately sized to contain these materials. This often involves estimating the rate of sedimentation and consolidation. Schiffman et al (1988) demonstrate an analytical model that links the two processes. Static segregation, creep, thixotropy, and natural surface processes complicate the consolidation modelling. Large volumes of fine tailings are produced when sedimentary deposits such as oil sands, bauxite, and phosphate ore are processed. Lord, et al (1991) note that the incorporation of large permanent storage ponds into an acceptable mine plan, subject to regulatory approval and public scrutiny, is a difficult task. Tailings handling systems that minimize the production of wet lands are desirable.

- Stability

Stability evaluations of tailings embankments involves considerations of handling methods discussed above, seepage and drainage control, siting, and many other factors. Where borrow material is used for structural control, conventional embankment design and construction is appropriate. Conventional tailings embankment design guidance for site investigations, seepage control, and stability analysis is offered in the Waste Embankments chapter of the Pit Slope Manual (Energy Mines and Resources Canada, 1977). Current and evolving considerations for liquefaction evaluation of granular materials are worth noting here.

There are two approaches for evaluating liquefaction resistance of tailings dams and other hydraulic fill structures:

1. Empirical approaches using in-situ test results
2. Steady state approaches using test results from laboratory samples

Seed and his co-workers have developed empirical correlations relating the corrected Standard Penetration Test (SPT) blowcount $(N_1)_{60}$ and the average cyclic stress ratio determined from back analysis of several liquefied versus non-liquefied sites during earthquakes. The corrected blowcount is determined by applying correction factors for fines content, the in-situ static shear stress, the initial effective overburden stress, and the earthquake magnitude (Seed and Harder, 1990). The empirically driven Seed approach is generally considered to be very conservative. Fear and M^cRoberts (1994) have re-evaluated Seed's data and recommend new design criteria based on a review of Seed's SPT data that is less conservative and differentiates flow from no-flow conditions. Effects of confining stresses, fines content, angularity, and mineralogy on liquefaction potential are not reliably evaluated using in-situ testing techniques and are the subject of ongoing research.

Laboratory test methods are founded on concepts of steady state. The steady state represents the inherent frictional resistance of a particular grain assemblage devoid of initial fabric effects and thus can be determined using remoulded samples. An assessment of in-situ density and stress conditions is necessary however, in order to determine the in-situ "state" relative to steady state. Geophysical density logging and undisturbed sampling are tools finding increasing use in this regard.

Designs based on steady state strengths and static stresses do not allow for an assessment of static and dynamic mechanisms that could potentially trigger liquefaction failure. Sladen et al (1985) have proposed the existence of a collapse surface that represents the peak strength for loose contractant granular materials. Figure 2.5 shows normalized collapse surfaces for angular quartz sands following Sladen's work. Note that the collapse surface defines a failure envelope at lower stress ratios than the steady state friction angle. Gu et al (1992) have demonstrated the mechanism of collapse and progressive failure through back analysis of the San Fernando dam flow slide which was triggerred by an earthquake.

A complete evaluation of liquefaction potential involves an assessment of the static stresses, void ratio, steady state behaviour, collapse mechanics, and triggering mechanisms. Although these are areas of active research, practical applications that allow for rational assessment of all these factors are not currently available. The effects of fines content on liquefaction potential deserves special attention. Figure 2.6 shows the effects of increasing fines content on the steady state behaviour of angular quartz sands. Finer materials can be readily deposited in a contractant state as evidenced in the figure. Segregation control is necessary in order to preserve the structural integrity of tailings embankments where sufficient fines are in evidence. Designers and operators of tailings dams and waste dumps must be kept abreast of recent developments in this area in order to ensure that construction is consistent with the best applicable technology.

- Pollution Control

There are two primary sources of pollution from wet waste streams:

1. Process chemicals and suspended solids contained in the effluent

2. Leachates from milled ore and process precipitates

Ritcey (1989) reviews the toxicity of mining and milling reagents to the environment. An evaluation of whether seepage control is necessary is a complex issue involving several disciplines. In the event that pollution control is required options are varied and include barrier systems, return systems, and liner systems. Vick (1983) reviews several conventional options. Design, installation, and monitoring of compacted clay and geosynthetic liner systems follows fairly well established conventions as developed for hazardous waste landfills. Most jurisdictions have guidelines in place to aid the designer. For many base metal and sedimentary ores, processing effluents are not considered hazardous and the segregated fines blanket that settle in the tailings pond assists the seepage control. Special considerations for seepage control are normally required for operations that employ cyanidation (gold mines in particular) and for uranium mines (uranium tailings contain much of the initial radioactivity of the original ore before processing). Ritcey (1989) provides an extensive review of gold and uranium processing operations and discusses pertinent chemical considerations. There seems to be a lack of information in the literature on mine site contaminant migration and pollution control performance. Table 2.3 illustrates the attenuating potential for different chemical constituents common to mining effluents. Field data would establish guidelines that could be used to take advantage of attenuating mechanisms for pollution control.

In addition to issues of acid mine drainage already discussed, pollution control of leachates from effluent treatment sludges merits consideration. Effluent treatment sludges are produced from the treatment of mine wastewaters to meet discharge criteria. Leaching studies carried out by by MacDonald et al (1989) show that metals are readily leached from the high moisture content sludges. In most cases effluent treatment sludges are transported for disposal in tailings ponds. There is no current information examining the consolidation characteristics of the material; self-weight or other consolidation processes would result in lower permeabilities with a strong potential for reduced leachability. Current disposal practices deserve attention in this regard.

- Reclamation

Issues of long term embankment stability, fine tailings strength and volume enhancement, and placement of soil covers are discussed here with respect to tailings reclamation.

Embankment stability following closure is potentially affected by erosion and material degradation. Oversteepening of loose granular slopes and strength loss due to weathering processes are potential triggers for static liquefaction processess. Robertson and Clifton (1987) discuss erosion and erosion control studies conducted for uranium tailings. The effects of slaking and other weathering propereties on the contractant behaviour of granular materials merit further study.

While segregating slurries provide for better constuction materials for tailings embankment shells the segregated fines form weak, wet areas that are difficult to reclaim as dry landscapes. Stahl and Sego (1992) document the effects of natural processes on the surface enhancement of coal mine tailings. Where large volumes of very high moisture content materials are produced more aggressive enhancement measures may be necessary, sometimes involving rehandling material. Options include mechanical dewatering, "aggressive" drainage, blending with dry material, and thin layered systems which allow for drying or freeze-thaw dewatering.

Soil and geomembrane covers to control infiltration have received considerable attention in the last 10 years. Steffen, Robertson, and Kirsten (1989) review design considerations for covers to control AMD. Multi-layered cover designs are perceived to be most effective. Figure 2.7 shows a design schematic for a soil cover used to control AMD production at an abandoned copper mine in British Columbia (Healey and Robertson, 1989). The two soil cover layers are each 0.5 m thick. Confidence in the long term effectiveness of covers is hampered by a lack of field performance data.

2.4 MINE WASTE AUDITS

A financial audit is a "searching examination of accounts to ensure that financial histories accurately represent the performance of an organization" (Munro, 1985). Rovet (1988) defines an enviromental audit as:

> *" a systematic, thorough review by trained persons of the operations and practices of a business to determine whether the business is meeting environmental requirements, to verify compliance with regulatory standards, to evaluate the effectiveness of environmental controls already in place, and to generally assess environmental risk"*

Enviromental audits for the mining industry are common in the United States and increasingly undertaken in Canada (Nancarrow and Amirault, 1989). The geotechnical component of environmental audits has not previously been defined. In keeping with the above definition and with emerging regulatory trends a geotechnical waste audit is defined here as "*a systematic, independent, and thorough review by trained persons of geotechnical issues related to mine waste management practices that are responsible for ensuring that the best practicable technology is in place to minimize the present and future threat to human health and the environment.*" Some of the geotechnical factors necessary for this evaluation have been discussed in this paper. In addition to geotechnical issues a complete mine waste audit would require an assessment of effluent treatment and handling technologies; these issues are beyond the scope of this paper.

A review of current and evolving issues relevant to geotechnical aspects of mine waste audits reveals that these evaluations need to be conducted in a periodic, comparative, and consistent fashion. Continuously evolving political, technological, and socio-economic considerations dictate that today's practices might not be appropriate tomorrow. Waste audits would achieve the following objectives:

1. Provide regulatory guidance.

2. Evaluate the current state of practice.

3. Provide an arm's length assessment such that due diligence is demonstrated.

These objectives can be achieved at each operation by identifying various waste streams and handling technologies, and assessing the relevant stability, pollution control, and reclamation practices currently in place. Economically achievable standards of practice that are guided by industry and not imposed by regulations would evolve in a progressive manner.

2.5 CONCLUSIONS

A brief discussion of emerging regulatory issues suggests that mining operations should continually monitor their solid waste management practices in order to maintain standards of practice that prevent the imposition of restrictive regulations while still meeting environmental obligations. From a geotechnical standpoint, regular and consistent mine waste audits conducted by qualified independent professionals would satisfy this objective. A discussion of some of the issues relevant to geotechnically sensitive mine waste audits illustrates some technical factors involved. These technical issues are evolving very rapidly and many currently available design guides are out of date. Compliance with current practice may not be adequate in the future.

Drawing from the geotechnical overview presented above, a number of issues emerge where further geotechnically oriented research could significantly improve the current state of practice. Most of these issues are concerned with the management of large volumes of relatively loose materials. In the remainder of this thesis, the results of research and the development of waste management strategies are presented that deal with some specific aspects of loose mine waste materials in"wet" waste tailings streams (Chapters 3 and 4) and "dry" waste rock streams (Chapters 4, 5 and 6).

2.6 REFERENCES

Barton-Bridges, J.P.; Robertson, A.MacG. (1989) "Geotechnical considerations in the control of acid mine drainage" Geotechnical Aspects of Tailings Disposal and Acid Mine Drainage, Vancouver Geotechnical Society, Vancouver, 1989, 16 p.

Bishop, A.W. (1973) "The stability of tips and spoil heaps" Quarterly Journal of Engineering Geology, Vol. 6, 1973, pp. 335-376.

Blight, G.E. (1987) "The concept of the master profile for tailings dam beaches" Prediction and Performance in Geotechnical Engineering, Calgary, 1987, pp. 361-365.

Campbell, D.B. (1986) "Stability and performance of waste dumps on steeply sloping terrain" Proc. of International Symposium on Geotechnical Stability in Surface Mining, Calgary, pp. 317-325.

CANMET (1977) "Pit slope manual- waste embankments" Mining Research Laboratories, CANMET, Energy, Mines and Resources Canada, Report 77-01.

Das, B.M.; Claridge,F.; Garga, V.K. (1990) "The use of rock drains in surface mine waste dumps" CIM Bulletin, Vol. 83, No. 942, 1990, pp. 78-83.

Eckersley, D. (1990) "Instrumented laboratory flowslides" Geotechnique, Vol. 40, No. 3, 1990, pp. 489-502.

Environment Canada (1977) "Metal mining liquid effluent regulations and guideline Report EPS 1-WP-77-1, Ottawa.

Environment Canada (1988) "Status report on water pollution control in the Canadian metal mining industry (1986)" Report EPS 1/MM/3, Ottawa, 27 p.

Fear, C.E. and M^{c}Roberts, E.C.(1994) "A Re-consideration of the Initiation of Liquefaction in Sandy Soils" Submitted to ASCE Journal of Geotechnical Engineering, December, 1993.

Ferguson, K.D. and Erickson, P.M. (1988) "Pre-mine prediction of acid mine drainage" in Environmental Management of Solid Waste, Springer-Verlag,Holland, pp. 25-43.

Filion, M.P.; Sirois, L.L.; Ferguson, K. (1990) "Acid mine drainage in Canada" CIM Bulletin, Vol. 83, No. 944, 1990, pp. 34-40.

Gu, W.H.; Morgenstern, N.R.; Robertson, P.K. (1992) "Progressive failure of the lower San Fernando dam" Canadian Geotechnical Journal, (in press).

Healey, P.M.; Robertson, A.MacG. (1989) "A case history of an acid generation abatement program for an abandoned copper mine" Geotechnical Aspects of Tailings Disposal and Acid Mine Drainage, Vancouver Geotechnical Society, Vancouver, 1989,11 p.

Hutchinson, I.P.G. (1990) "Mine waste disposal initiatives in California" Geotechnical News, March, 1990, pp. 28-32.

Knight, R.B.; Haile, J.P. (1983) "Sub-aerial tailings deposition" Proc. 7th ISSMFE Pan-American Conference, Vol. 2, Vancouver, 1983, pp. 627-639.

Kupper, A.M.A.G, (1991) "Design of hydraulic fill" Unpublished PhD Thesis, Department of Civil Engineering, University of Alberta, Edmonton, Alberta, 525 p.

Lawrence, R.W.; Poling, G.W.; Ritcey, G.M.; Marchant, P.B. (1989) "Assessment of predictive methods for the determination of AMD potential in mine tailings and waste rock" Proceedings of the International Symposium on Tailings and Effluent Management, Halifax, 1989, pp. 317-331.

Lighthall, P.C.; Watts, B.D.; Rice, R. (1989) "Deposition methods for construction of hydraulic fill tailings dams" Geotechnical Aspects of Tailings Disposal and Acid Mine Drainage, Vancouver Geotechnical Society, Vancouver, 1989, 15 p.

Lord, E.R.; Mimura, D.W.; Scott, J.D. (1991) "Disposal of oil sands fine tails (sludge) in overburden waste dumps" Proc. 1st Canadian Conference on Environmental Geotechnics, Canadian Geotechnical Society, Montreal, 1991, pp.129-138.

MacDonald et al (1989) "Generation of, and disposal options for Canadian mineral industry effluent treatment sludges" Proc. of the International Symposium on Tailings and Effluent Management, Halifax, 1989, pp. 139-157.

Morgenstern, N.R.(1991) "The emergence of environmental geotechnics" Proc. of 9th ISSMFE Asian Regional Conference, Bangkok, Thailand, Vol. 2, (in press).

Nancarrow, R.; Amirault, J. (1989) "Environmental audits for the mining industry" Proc. of the International Symposium on Tailings and Effluent Management, Halifax, 1989, pp. 119-128.

Nolan, Davis and Associates (1987) "Study of acid waste rock management at Canadian base metal mines" Prepared for Energy, Mines and Resources Canada, CANMET, DSS No. 23317-6-1738/01-SQ.

Piteau Associates (1991) "Mined rock and overburden piles, investigation and design manual" B.C. Mine Waste Rock Pile Research Committee.

Ritcey, G.M. (1989) "Tailings management, problems and solutions in the mining industry" Elsevier, 970 p.

Robertson, A.M.; Clifton, A.W. (1987) "Design considerations for the long term containment of uranium tailings" Proc. 40th Canadian Geotechnical Conference, Regina, Saskatchewan, pp. 345-354.

Robertson, P.K.; Woeller, D.J.; Finn, W.D.L. (1992) "Seismic CPT for evaluating liquefaction potential under cyclic loading" Canadian Geotechnical Journal, (in press).

Robinsky, E.I. (1975) "Thickened Discharge- A new approach to tailings disposal" CIM Bulletin, Vol. 68, No. 764, 1975, pp. 47-59.

Rovet, E. (1988) "Self examination. The environmental audit" in The Canadian Business Guide to Environmental Law, International Self Cousel Press, Vancouver, pp. 71-77.

Salvas, R.J. (1989) "Beneficial characteristics of slopes tailings deposits" Proceedings of the International Symposium on Tailings and Effluent Management, Halifax, 1989, pp. 215-226.

Schiffman, R.L.; Vick, S.G.; Gibson, R.E. (1988) "Behaviour and properties of hydraulic fills" Hydraulic Fill Structures, ASCE Geotechnical Special Publication No. 21, pp.166-202.

Scott, J.D. and Cymerman, G.J. (1984) "Prediction of viable tailings disposal methods" Symposium on Sedimentation and Consolidation Models, ASCE, pp. 522-544.

Seed, R.B.; Harder, L.F. (1990) "SPT based analysis of cyclic pore pressure generation and undrained residual strength" H. Bolton Seed Memorial Symposium Proceedings,Vol. 2, Bitech Publishers Ltd. pp. 335-350.

Seedsman, R.W.; Richards, B.G.; Williams, D.J. (1988) "The possibility of undrained failure in Bowen Basin spoil piles" Proc. of 5th Australian/New Zealand Conference on Geomechanics, Sydney, 1988, 6 p.

Sego, D.C.; Dawson, R.F. (1992) "Freeze thaw dewatering of OSLO cold water process fine tails" unpublished research report, University of Alberta, 76 p.

Sladen, J.A.; D'Hollander,R.D.; Krahn, J. (1985) "The liquefaction of sands, a collapse surface approach" Canadian Geotechnical Journal, Vol.22, 1985, pp. 564-578.

Stahl, R.P.; Sego, D.C. (1992) "Influence of natural surface processes on reclamation of the Coal Valley tailings impoundment" Proc. 2nd International conference on Environmental Issues and Management of Waste in Energy and Mineral Production, Calgary, Alberta,1992, 12 p.

Steffen Robertson and Kirsten (B.C.) Inc. (1989) "Draft acid rock drainage technical guide, volume 1" British Columbia Acid Mine Drainage Task Force Report.

U.S. National Research Council (1990) "Ground water models, scientific and regulatory applications" National Academy of Sciences, 303 p.

Vick, S.G. (1983) "Planning, design, and analysis of tailings dams" John Wiley and Sons, 368 p.

Wasp, E.; Kenny J.; Gandhi, R. (1977) "Solid liquid flow slurry pipeline transportation" Series on Bulk Materials Handling, Vol. 1, No. 4, Trans Tech Pub.

TABLE 2.1- FEDERAL MINE EFFLUENT REGULATIONS

Parameter	Environment Canada (Total Metals, mg/L)	United States EPA (Total Metals, mg/L)
Arsenic	0.50	
Copper	0.30	0.05
Lead	0.20	0.20
Nickel	0.50	
Zinc	0.50	0.20 (mine); 0.50 (mill)
Suspended Solids	25.0	20
Ra^{226} (pCi/L)	10.0	3.0
pH	6.0 or higher	6.0-9.0

TABLE 2.2- RECOMMENDED ROCK DRAIN PROPERTIES
(modified after Das et al, 1990)

ROCK TYPES	
Coal mines	- Sandstone and Hard Siltstone
Metal mines	- Igneous and Hard Metamorphics
MECHANICAL PROPERTIES	
Los Angeles Abrasion Test	- < 40%
Uniaxial Compresion Test	- >50 MPa
PHYSICO-CHEMICAL PROPERTIES	
Freeze/thaw	- under study
Slake Durability	- >90%
ROCK GRADATION (mm)	MAXIMUM PERCENT PASSING
1000	90
500	70
100	20
50	0-5

TABLE 2.3 ATTENUATION POTENTIAL OF SOME DISSOLVED CHEMICALS

(modified after Hutchinson, 1990)

	SOIL PHYSICAL PROPERTIES PHYSICAL PROPERTIES					SOIL/PORE WATER CHEMISTRY				
						pH			Eh	
	CLAY	SILT	SAND	GRAVEL	FRAC'D	< 6	6-8	> 8	Oxid.	Red.
copper	**H**	**M**	**L**	**L**	**M**	**L**	**M**	**H**	**L**	**H**
lead	**H**	**M**	**L**	**L**	**M**	**L**	**M**	**H**		
nickel	**H**	**M**	**L**	**L**	**M**	**L**	**M**	**H**		
zinc	**H**	**M**	**L**	**L**	**M**	**L**	**M**	**H**		
arsenic	**H**	**M**	**L**	**L**	**M**	**H**	**L**	**L**	**L**	**L**
cyanide	**H**	**M**	**L**	**L**	**M**	**H**	**M**	**L**	**H**	**L**

NOTE: H= High attenuation potential

M= Medium attenuation potential

L= Low attenuation potential

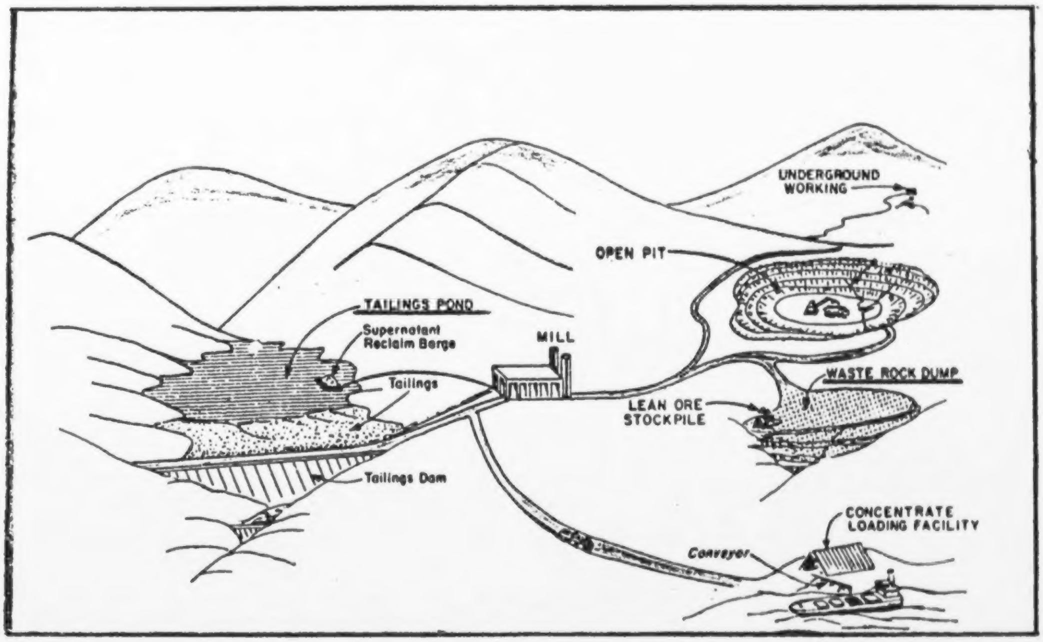

Figure 2.1 Generalized Minesite Layout
(modified after Ferguson and Erickson, 1988)

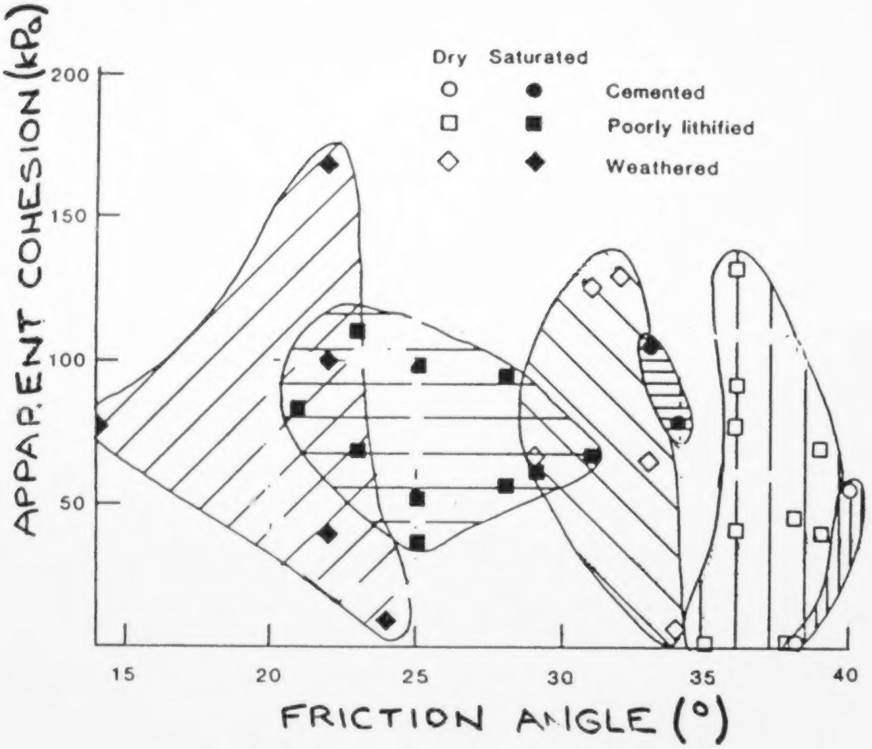

Figure 2.2 Shear Strength of Australian Coal Mine Spoil
(modified after Seedsman et al, 1988)

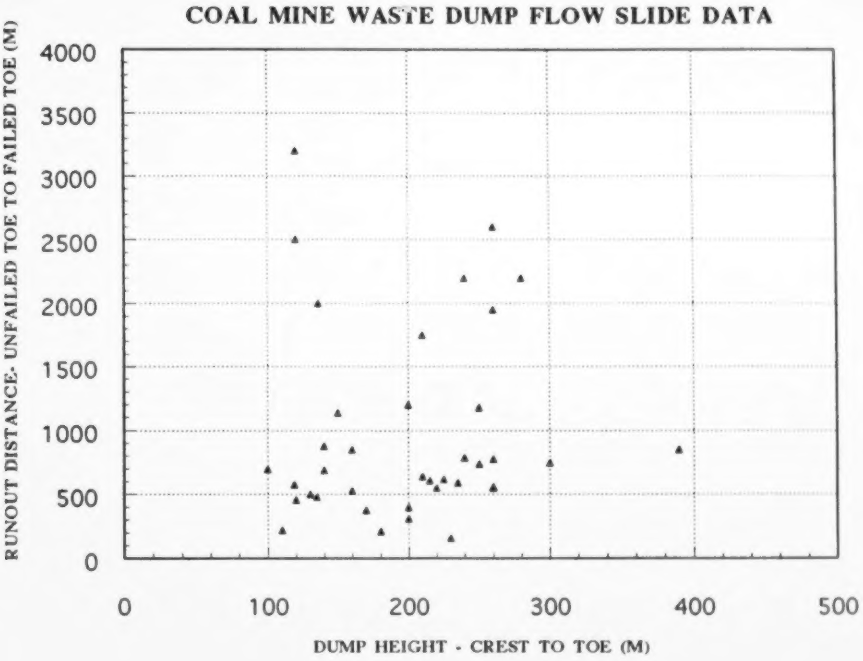

Figure 2.3 Rocky Mountain Coal Mine Runout Statistics

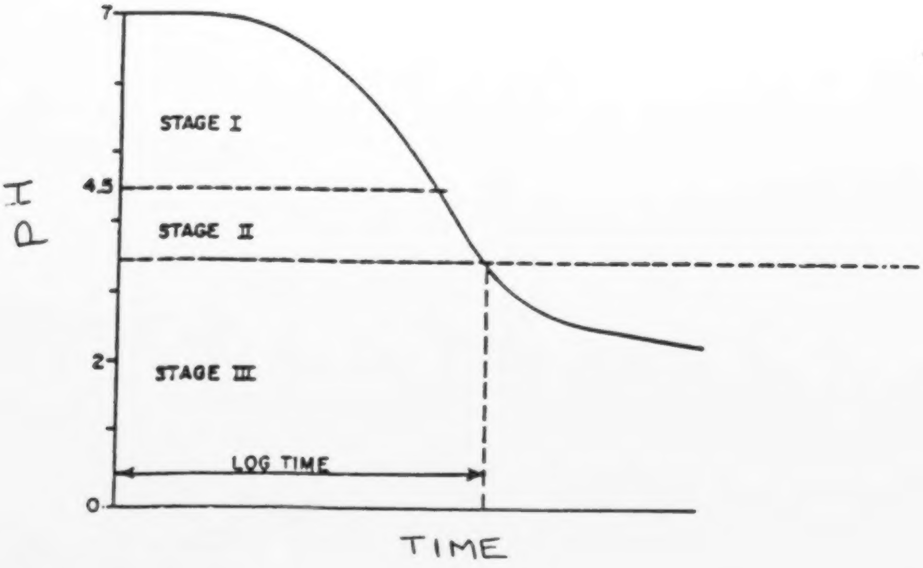

Figure 2.4 Stages in the Formation of AMD
(modified after Nolan and Associates, 1987)

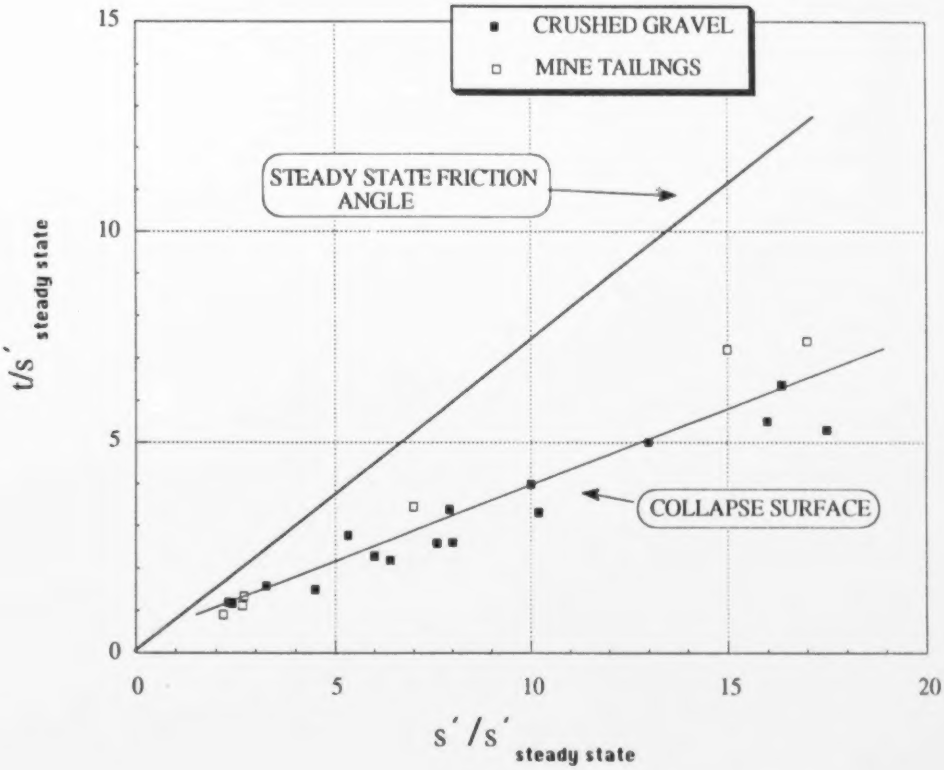

Figure 2.5 Normalized Collapse Surface for Angular Quartz Sands

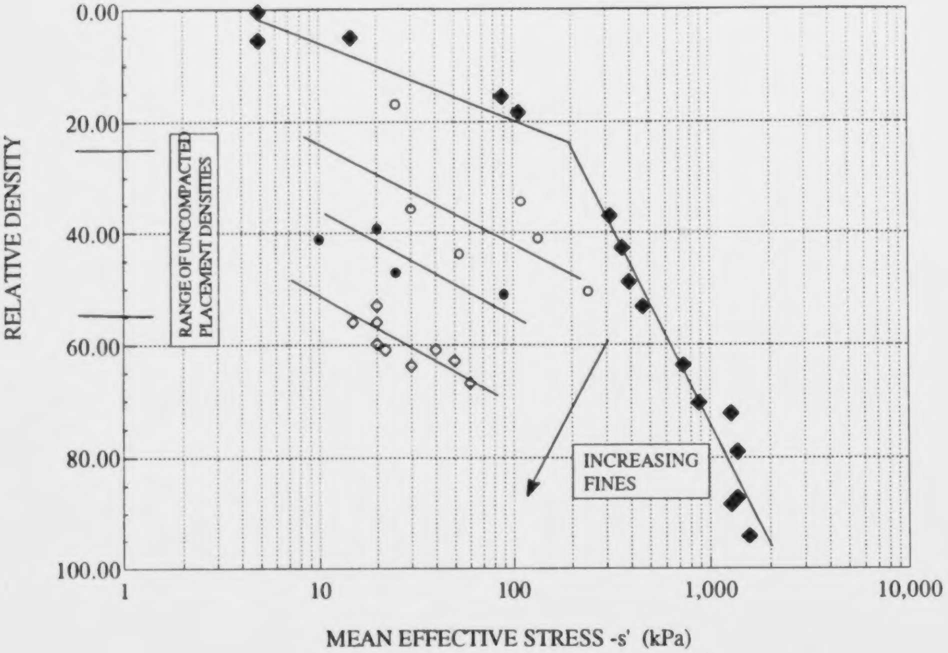

Figure 2.6 Effects of Fines Content on Steady State Behaviour

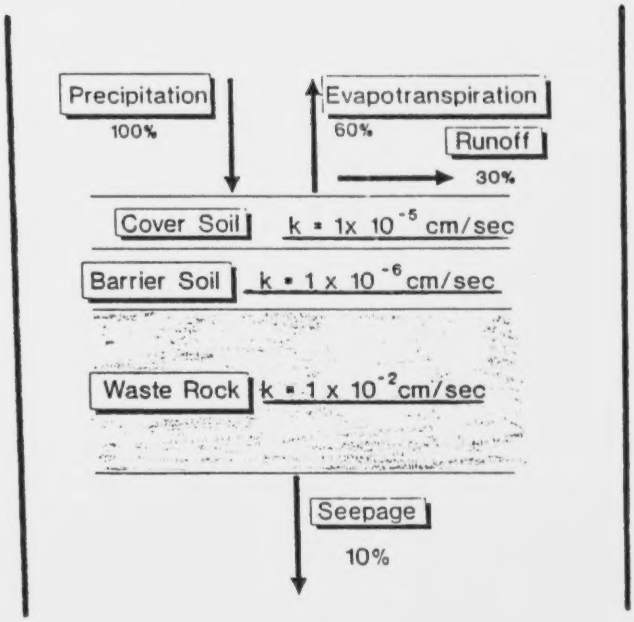

Figure 2.7 Typical Soil Cover to Control AMD Production
(modified after Healey and Robertson, 1989)

Chapter 3

TAILINGS MANAGEMENT IN COLD REGIONS - THIN LAYERED FREEZING AND THAWING STRATEGIES

3.1 INTRODUCTION

Many of Canada's resources are located in cold regions. Permafrost engineering has evolved as a specialized branch of geotechnical engineering along with the development of infrastructure to access and exploit resources in these areas. Central to the study of permafrost engineering is the effect of temperature on the phase change of water to ice (and ice to water) with respect to the strength, deformation, and permeability of geo-materials. Thus the study of freezing and thawing of soil and rock materials differentiates permafrost engineering from more conventional geotechnical practice where thermal considerations are not routinely considered.

The 1990's are witnessing a resurgence of mining exploration and development activity in Canada's North. Examples include intensive exploration and development activities for diamonds in the Northwest Territories and expansion of uranium mining activity in Northern Saskatchewan. Potential expanded infrastructure requirements to develop these resources is also leading to a renewed interest in the exploration for base and precious metals. Thus it is anticipated that there will be several new northern mines in production by the turn of the century. Commensurate with these developments will be a requirement to ensure that tailings management practices are sensitive to current and emerging mine waste containment design and construction issues.

This chapter examines mine waste strategies that take advantage of thin layered freezing and thawing processes. Freezing immobilizes pore water fluids and thus freeze controlled processes can be used to provide engineered physical and chemical containment. Fine grained materials can exhibit significant pore water migration during freezing. Upon thaw, appreciable dewatering and chemical segregation can take place. Thus both freeze and thaw controlled processes can be used to improve mine waste management practices in cold regions.

3.2 GROUND TEMPERATURE CONSIDERATIONS

Canada's cold regions are most easily defined by those areas containing permafrost. Figure 3.1 shows that over 50% of Canada's land mass is underlain by permafrost, an area that contains a large proportion of our natural resources.

Ground surface temperatures are warmer than air surface temperatures. Figure 3.2 shows some typical average and seasonal ground temperature profiles (natural ground conditions) at selected stations in different permafrost regions. These profiles, known as trumpet curves, illustrate some important points:

1. Seasonal variations in ground temperature are about 5° in the discontinuous permafrost region to 10° in the continuous permafrost region. These variations converge to a constant ground temperature at depths of 10 to 15 meters below the ground surface. This depth is known as the depth of zero annual amplitude.

2. Near the surface there is a zone of seasonal thawing which is called the active zone. The active zone is very sensitive to local ground conditions. In general, the active zone is less than 1m in the high Arctic and 1 to 5m in the discontinuous permafrost zone.

3. Zero amplitude ground temperatures are very close to 0°C in discontinuous permafrost and vary from about -4 to -12°C within the continuous permafrost region (Geocon, 1993).

Factors that affect freezing and thawing conditions within the active zone are of particular interest for managing mine wastes in cold regions by ambient freezing and thawing processes. The factors that affect the rate and thickness of ground freezing and thawing within the active zone are surface air temperature (and air/ground thermal boundary conditions), geothermal gradient, and thermal properties. A discussion of these factors follows:

1. Air Temperature - Air temperature has the most dominant effect on freezing ground conditions. This is best exemplified by the relationship between the permafrost regions and average annual air temperatures shown in Figure 3.1. The boundary between continuous and discontinuous permafrost regions corresponds roughly to the -8°C average air temperature isotherm. The discontinuous zone is divided into widespread and scattered regions. An average air temperature of about -4°C separates these two regions.

In addition to air temperature, the temperature boundary conditions at the air/ground interface also govern heat flow. These thermal boundary conditions are mainly influenced by climatic factors such as wind speed, barometric pressure, and relative humidity.

2. Thermal Parameters - Material thermal parameters (unfrozen and frozen thermal conductivity, specific heat, and latent heat) are mostly related to mineralogy, porosity, degree of saturation, and unfrozen water content. Note that thermal parameters do not vary significantly with temperature.

Soil mineralogy affects thermal conductivity. In general, thermal conductivity is higher for coarser grained quartz rich soils (most tailings sands) and lower for finer grained materials containing clays and other softer minerals (fine tailings and sludges).

Freezing and thawing thermal parameters (thermal conductivity and latent heat) vary with the percentage saturation and porosity. Thermal conductivity's (unfrozen and frozen) increase with saturation and porosity. Conversely the latent heat decreases with increasing saturation and porosity. As a result unsaturated soils freeze and thaw much faster than saturated materials.

Water has a lower thermal conductivity than ice by a factor of about four. Therefore materials containing appreciable amounts of unfrozen water (proportion of the weight of water to the weight of dry soil at a temperatures below 1°C) will freeze and thaw faster at temperatures close to 0. Unfrozen water content varies with temperature, mineralogy, and pore water chemistry. The unfrozen water content in high plastic bentonitic soils can exhibit a 40% unfrozen water content (Anderson and Morgenstern, 1973). Pore water chemistry can also have a significant effect on the unfrozen water content. Hivon (1991) showed measured unfrozen water contents of 10 to 30% for natural sands and silty sands that contained salinity's of 30 parts per thousand. Tailings pore water chemistry may have a profound effect on unfrozen water contents.

3. Geothermal Gradient - The geothermal gradient influences the rate of freezing and thawing and the depth of the zero annual amplitude temperature. The geothermal gradient can vary between 1°C/22m to 1°C/160m (Geocon, 1994).

3.3 MOISTURE TRANSFER PROCESSES IN FREEZING SOILS

Significant moisture transfer can take place during freezing of saturated soils. Mine waste management practices must be sensitive to moisture transfer processes which take place as a result of two processes:

1. Expulsion of water due to the 9% volume change that accompanies the water to ice phase change.

2. Attraction of water as a result of capillary suctions set up at the ice-water interface.

These two opposing moisture transfer processes are a function of many factors including drainage conditions, overburden stresses, temperature gradients, soil composition, and pore fluid chemistry. A very substantial effort has been devoted to understanding the relationships between these factors, principally focused towards issues related to frost heave and frost susceptible soils. In general, sandy soils tend to expel water and finer grained soils (silts and clays) tend to attract water. Davila (1992) has developed surface area criteria that shows the influence of plastic fines on the moisture transfer (expulsion versus attraction) of freezing soils. Similar criteria could be usefully applied to tailings materials.

Most sandy soils will expel water during freezing. If the drainage during freezing is unimpeded then 9% of the water volume will flow away from the freezing front. If impeded then this change in volume can lead to heaving and cracking and accumulation of large amounts of ground ice. This process forms pingos in natural ground conditions. Unfrozen tailings underlain and overlain by frozen material will eventually freeze and could form similar accumulations of ground ice that may have a detrimental effect on reclaimed landscapes.

Fine grained plastic soils will attract water during freezing. As a result heaving and cracking can occur both due to the phase related volume change and the additional water drawn towards the advancing freezing front. Frost heave may also cause undesirable effects on reclaimed landscapes.

Moisture transfer processes during freezing are important considerations that need to be addressed during materials placement and disposal in order to preserve the integrity of reclamation efforts in cold regions. In addition, soils with high unfrozen water content values can still exhibit considerable moisture migration following freezing that can potentially negate the benefits of frozen containment. Processed tailings that contain chemical additives may exhibit significantly high unfrozen water contents.

3.4 DESIGN CONCEPTS

Design concepts that take advantage of thin layered freezing and thawing processes are presented here. Freeze controlled strategies rely on permanent freezing to contain pore fluids. Thaw controlled strategies depend on thawing to release free water formed during freezing of soils that are susceptible to a net attraction of water during freezing.

The net amount of mine waste that can be frozen during the winter months and thawed the subsequent summer is the main consideration that controls the waste management strategy employed. Researchers at the US Cold Regions Research and Engineering Laboratory (CRREL) have developed simple models to estimate freezing and thawing thicknesses of sewage sludges placed in specially designed freeze-thaw beds (Martel, 1988). These models have been adopted for use here (Appendix B) in order to provide estimates of saturated sand tailings thicknesses that can be frozen and thawed in different permafrost regimes. The models are also used in the next chapter to estimate frozen and thawed thicknesses of oil sands fine tails.

Waste management systems designed for frozen containment can take advantage of freezing several thin layers rather than one thick layer in order to maximize the total frozen thickness. The hydraulic transport and disposal systems (slurry pipelines) normally used for tailings management make this a viable option as it is relatively easy to place thin layers of material by hydraulic deposition. Figure 3.3 shows total frozen thickness estimates, derived from the relationships contained in Appendix B, for beached tailings sand (70% solids) frozen under different ambient air temperature conditions (expressed in terms of the freezing index in °C days below 0°). Note that the total freezing layer thickness varies in a nonlinear fashion with the placement layer thickness. For example, at a freezing index of 3900° C days (approximate division between continuous and discontinuous permafrost regions), the total freezing thickness varies between 3.6m for a single placement layer to over 10m for a 1m multiple layer placement. In the high Arctic total frozen thicknesses in excess of 15m are possible by placing and freezing thin layers of about 1m.

When tailings are frozen in thin layers, far less material can be thawed than frozen. Figure 3.4 shows the total thawed thickness for tailings sand (70% solids) at different thaw indices and for ground temperatures varying between 2 and -4°C. The figure shows that at the boundary between the continuous and discontinuous permafrost zones (thaw index of about 1400° C days) the active zone can be expected to be about 1 to 2.6m thick for ground temperatures varying between -4 and 2°C respectively. The influence of the ground temperature is dramatic; a small increase in ground temperature causes a large increase in the amount of ground that will thaw.

3.4.1 FREEZE CONTROLLED STRATEGY

It is clear from the calculations shown in Figure 3.3 that significant quantities of material can be frozen by placing and freezing thin layers. Even in the southern extremes of the discontinuous permafrost zone (freezing index of 2200°C) it is possible to freeze 5m of saturated sand tailings by placing and freezing 1m thick layers. A strategy that takes advantage of this process for providing total containment by freezing thin layers is presented below (see Figure 3.5):

1. A compacted fill starter dike is first constructed in order to provide initial containment. The starter dike would eventually freeze.

2. In the first winter season following completion of the starter dike (A in figure 3.5), frozen perimeter dikes are constructed from tailings sand. The perimeter dikes could be constructed using cell construction techniques (Lighthall et al, 1989). Specialized frozen cell construction techniques would need to be developed that maximize frozen thickness and control overboarded decant water and fine tails. The construction would also require an interactive thermal monitoring program to ensure that the dikes are adequately frozen. The perimeter dike would need to be designed to allow for sufficient freeboard that takes the active layer thickness into account.

3. In the first summer season (B in Figure 3.5), tailings could be overboarded into the pond area. The overboarded unfrozen tailings would cause some of the underlying frozen tailings to thaw.

4. In the second and subsequent winters (C in Figure 3.5), frozen cell construction would continue. A layer of unfrozen tailings would be trapped beneath the frozen tailings. This trapped layer of frozen material would freeze by the end of the winter, before thaw was initiated at the surface the subsequent summer (D in Figure 3.5).

The construction sequence of the thin layered freezing strategy presented above is essentially the same as an upstream construction tailings dam. The difference is that in addition to designing for adequate control of sand, fines, and water, the construction must also allow for adequate freezing and thawing control that will assure long term containment. At the end of construction it is likely that there will be thick accumulations of unfrozen fine tails beneath the pond area. The reclamation plan could allow for freezing this material by pumping it up onto itself in the winter months.

3.4.2 THAW CONTROLLED STRATEGY

The dewatering of fine grained slurries by freeze-thaw processes has been recognized for several decades. When water saturated fine grained slurries are subjected to below freezing temperatures, negative pore water pressures are set up between the unfrozen water surrounding the mineral particles and ice filling the voids. Negative pore pressures develop because of surface tension differences between ice and unfrozen liquid pore water. These negative pressures (suctions) cause water to migrate to the growing ice crystals which results in a distinct segregated reticulate ice/fine grained "ped" structure forming in the resulting frozen mass. Segregated ice/soil structures are common in naturally occurring permafrost soils (McKay, 1972).

Two classes of segregated ice/fine grained systems can be distinguished. In an open system, such as occurs in nature when the soil freezes downward, steady state thermal conditions are eventually set up between the advancing freezing front and warmer soil beneath. These conditions result in the formation of horizontal ice lenses just above the 0°C isotherm as water is drawn from the unfrozen soil below. In a closed system, where complete freezing is permitted to take place without access to free water, horizontal ice lenses comprised of externally derived water do not form. However, a reticulated ice structure forms as ice crystals grow in place by removing water from within the matrix of the freezing soil. A thaw controlled dewatering system is best carried out by freezing thin layers (less than .5m thick) that freeze within a closed freezing system. This prevents buildup of ice lenses due to water migration in an open freezing system.

Following work by Nixon and Morgenstern (1973) in permafrost soils, the process of closed system freeze-thaw in fine grained materials is conveniently illustrated by considering a void ratio versus effective stress plot. Using Figure 3.6 to illustrate, consider the following discussion. Assume a fine tailings frost susceptible material first exists at point A having first undergone some sedimentation and consolidation in a settling basin. Following removal from the pond the fine tails swells marginally to point B under conditions of approximately zero effective stress. If the fine tails sample at B is now frozen in thin layers, an increase in volume to point C results due to expansion of the pore water as ice forms in the void spaces between the mineral particles. As the frozen material thaws, water is released from the reticulate ice formed during freezing and the mineral peds settle. The resulting volume change from B to D is known as thaw strain. The thaw strain represents the change in volume due to freeze-thaw that occurs under negligible change in average effective stress. Further post thaw loading causes the material to consolidate along a path, D-E. Previous research work has shown that many soils after undergoing thaw strain will return to the virgin compression line with continued loading (Nixon and Morgenstern, 1973). The stress at which the post thaw consolidation line intersects the virgin compression line is analogous to the pre-consolidation stress in over-consolidated soils.

The process of closed system thaw strain can be used to advantage for dewatering high moisture content fine tails. Figure 3.7 shows the design concept developed during the course of research for this thesis. Fine tails are pumped from a settling basin to pairs of freeze-thaw cells. The unfrozen material is deposited in thin layers so that it freezes quickly and under closed system freezing conditions. As the previously deposited layer in one cell freezes, a new layer is placed in the adjacent cell thus permitting uninterrupted hydraulic transport and deposition. The winter pumping and placing process continues until the total design thickness of frozen material is achieved. During the spring and summer months thawing occurs. Surface water released during thaw is removed to maximize the thaw depth. Sand blanket under drains and surface water decant systems must be designed to resist freeze-up and handle water released as the material thaws. After each yearly cycle of freezing and thawing the process is continued and the previously thawed layers beneath the most recently placed frozen layers consolidates further due to surcharge loading of the newly placed frozen fine tails. Drainage layers placed at regular intervals within the previously placed and thawed layers can be incorporated to accelerate the post thaw consolidation (dewatering) process.

3.5 SELECTED STUDIES

This chapter reviews some tailings management studies carried out for mines in cold regions. Data from mines in the continuous permafrost, widespread discontinuous permafrost, and scattered discontinuous permafrost zones is reviewed. The information illustrates the potential for the strategies discussed above.

- Lupin Mine Tailings Freeze Controlled Containment

The Lupin gold mine is located in the northern part of Canada's Northwest Territories in the continuous permafrost region. The average annual air temperature is -12°C and the ground temperature at the zero amplitude depth is about -8°C. Mean air freezing and thawing indices are about 4700 and 500°C days respectively

The tailings area was constructed using frozen core compacted fill perimeter dams in order to provide total containment. Temperatures within the dams themselves and within the contained tailings materials were monitored extensively and a large amount of data was obtained. Geocon (1994) provides a review of the findings of these investigations. Figure 3.8, derived from the Geocon report, illustrates the depth of the active layer within several different stratigraphies. Discussion of Figure 3.8 follows:

- Figure 3.8a shows that the active layer in bedrock varies between about 2.5 to 4m depending on the degree of surface vegetation. The 2.5m active zone depth was observed in bedrock beneath a 300mm thick organic layer whereas the 4m thick active layer was observed below a bare rock surface.

- Figure 3.8b shows the active layer to be about 1m in depth in natural silty sand soils covered by a 300mm organic cover.

- Figure 3.8c shows the active layer in silty sand (no cover) under the dam crest. The depth of the active layer varied between 2.5 to 3.2m; the variation being due to differences in levels of saturation.

- Figure 3.8d shows the active layer in mine tailings covered with a 600mm sandy gravel cover. This figure shows an active zone depth of about 2.5m.

Thermal monitoring investigations at the Lupin Mine suggests that freeze controlled containment in continuous permafrost regions should consider active zone depths of 2.5 to 3m for partially saturated sandy tailings materials and up to 4m for bare rock surfaces. Calculations in Figure 3.4 show that saturated tailings should result in an active layer thickness of between about .5 and 1.5m for underlying ground temperatures of 0°C and a thawing index of 500°C days. A comparison of actual active zone thicknesses and calculated values support the contention that higher levels of saturation will result in a thinner active layer thickness. This will be an important design consideration for freezing controlled containment.

- Giant Mine Tailings Impoundment Temperature Data

The Giant gold mine is located in Canada's widespread discontinuous permafrost region. The average annual air temperature at the Giant Mine is about -5°C and the temperature at the zero amplitude depth is about -1°C. The mean air freezing and thawing indices are about 3600 and 1600°C days respectively.

Geocon (1994) reports on temperature monitoring data obtained from the Giant Mine tailings impoundment. Thermistor strings were installed upstream and downstream of a dike that separates an active from an inactive tailings area. The tailings in the active upstream area were covered with a 1.8m water cap. The phreatic surface in the inactive downstream area is not indicated but is assumed to lie well below the ground surface.

Figure 3.9 shows temperature measurements during May (maximum freezing) and October (maximum thaw) that illustrate the distribution of frozen tailings material when ground temperature conditions are at the coldest and warmest respectively. In the partially saturated inactive area the tailings below the 6.8m depth remained frozen throughout the year. Above 6.8m the tailings froze and thawed from the ground surface seasonally. The very deep freezing and thawing demonstrates the accelerating influence of partial saturation on rate of freezing and thawing.

Figure 3.9 shows that in the saturated upstream active area the water cap froze completely to about a 4m depth during the winter. The total frozen depth is similar to the 3.5m depth predicted in Figure 3.3 for single layer freezing of tailings sand at a freezing index of about 3600°C days. During the summer months the whole 4m frozen thickness thawed. Calculated thawing thicknesses from Figure 3.4 show that at a thawing index of about 1600°C days it is possible to thaw between about 2.0 and 2.6m of frozen sand tailings at ground temperatures of 0° and 2°C respectively. Figure 3.9 shows that the summer ground temperatures below the frozen material were about 4.4°C (40°F). At this ground temperature calculations suggest an active layer thickness of about 3m. Thus the calculated and actual thawed thickness values differ by about 1m (difference between calculated value of about 3m for thaw with 4.4°C underlying ground temperature and the measured value of 4m.). This difference is attributed to the warming influence of the water cap.

Thermal monitoring data from the Giant mine suggests that freeze controlled containment in Canada's discontinuous permafrost region would require special considerations for permafrost enhancement due to warm underlying ground temperature conditions and relatively low mean air thaw indices thaw indices. Costs of different enhancement options that incorporate insulation, thermosyphons, and rock convection covers have been worked out by Geocon (1994). Costs for a 10 hectare tailings area vary from $700,000 to $900,000. These costs, when considered for larger tailings facilities, may be prohibitive especially if the design requires consideration for climate warming effects.

- Thaw Controlled Dewatering of Oil Sands Fine Tails

The Alberta oil sands mines (Suncor and Syncrude) are located near Fort M^{c}Murray, Alberta at the southern boundary of the scattered discontinuous permafrost zone. The average annual air temperature at Fort M^{c}Murray is about -1°C and the zero amplitude ground temperature is about 2°C. The mean air freezing and thawing indices are about 2200 and 1800°C days respectively.

The University of Alberta has been conducting geotechnical engineering studies on freeze-thaw dewatering of oil sands fine tails for 4 years. Studies have been carried out on fine tails from the two commercial operations (Syncrude and Suncor) which utilize a hot water process for bitumen extraction and fine tails from the OSLO cold water extraction (OCWE) process. The commercial process utilizes sodium hydroxide to promote bitumen release within the extraction process.

The studies have advanced from bench scale lab tests (Sego and Dawson, 1992a, 1992b) through to field tests (Sego and Dawson, 1993) and field pilot scale demonstration tests (Sego et al., 1993). The earlier bench scale laboratory tests lab tests were mostly carried out using 15cm thick layers of fine tails frozen in cells with top and bottom cold plates at temperatures of -15 and -8C respectively. Following freezing, samples were thawed and the decant water due to thaw strain was drained. Solids contents (ratio of the weight of dry solids to the total slurry weight) of the thaw dewatered tails were measured. Figure 3.10 shows results of initial solids contents of three different oil sands fine tails derived from the results of the bench scale tests. The results show considerable variation in settled solids contents. At a 30% initial solids content the Syncrude fine tails exhibits only a 5 percentage point increase in settled solids following thaw whereas the OSLO fine tails exhibits an increase in settled solids of 18 percentage points at the same initial solids content. This latter increase equates to a thaw strain (change in volume/initial volume) of about 50%.

X-ray diffraction analyses of the three different fine tails from Figure 3.10 showed that all the materials exhibited a similar mineralogy composed of about 60% hydrous mica and 40% kaolinite (Dudas, 1993). Chemical tests of the pore water derived from the different samples indicated that the different thaw strain results may have been due to different concentrations of the major dissolved cations (sodium, magnesium, and calcium). Table 3.1 shows that the OSLO material clearly had a much lower sodium concentration, primarily due to a different extraction process which did not involve addition of sodium hydroxide. Soil scientists frequently employ the Gappon equation to describe the dispersion potential of saline soils.

$$ESR = .015\left(\frac{[Na]}{\sqrt{[Ca + Mg]}}\right)$$

Where: ESR = Exchangeable Sodium Ratio
[ ] = concentration of dissolved cation

Exchangeable sodium ratios (ESR) greater than .10 indicate a high potential for dispersion. Table 3.1 shows that all the fine tails have ESR values greater than .10 but that the ESR for the OSLO material is considerably lower than the other two materials. Pore water chemistry appears to be influencing the relative thaw strain behavior of these materials. This observation has lead to research involving addition of chemicals to promote enhanced thaw strain behavior in the commercially produced materials (Sego, 1992).

3.5 CONCLUSIONS

Tailings management in cold regions requires appropriate considerations for freezing and thawing ground conditions. Freezing and thawing processes can be used to advantage for providing total containment and in dewatering of fine tails respectively. The brief review of these processes presented here illustrates the following points:

1. In the continuous permafrost region, thin layered freeze controlled containment appears to be a viable strategy where the design accommodates consideration for a 2 to 3m thick active layer. It should be possible to develop hydraulic fill placement frozen cell construction methods that provide an adequate level of containment. Calculations demonstrate that it should be possible to freeze over 10m of tailings sand when the saturated sands are deposited in thin layers about 1m thick.

2. In the discontinuous permafrost region, a deep active layer may develop due to warm underlying ground temperatures and where the tailings are largely unsaturated. This may limit the feasibility of freeze controlled containment in the discontinuous permafrost region without consideration for permafrost enhancement. Previous work indicates that permafrost enhancement costs may be prohibitively high.

2. Thaw controlled dewatering of fine tails may be a viable method for dewatering high moisture content clay rich (highly plastic) mine waste materials. This strategy is most applicable in the discontinuous permafrost region where thawing depths (active layer thickness) are greater.

3. Mine waste pore water chemistry is an important consideration for both freezing and thawing controlled strategies. High salinity's can cause high unfrozen water contents that decrease the containment integrity of frozen tailings and reduce the thaw strain potential.

Encouraging results from laboratory studies on the freeze-thaw dewatering behavior of oil sands fine tails has lead to further investigations. Results of a study on field frozen fine tails at the OSLO Lease 41 site and design calculations that predict thaw controlled dewatering benefits are presented in the next chapter.

3.6 REFERENCES

Anderson, D.M. and Morgenstern, N.R., 1973. Physics, Chemistry and Mechanics of Frozen Ground: a review, Proc. 2nd Int'l Conf on Permafrost, Yakutsk, USSR, pp257-288.

Davila, R., 1992. The Influence of Fines Content and Specific Surface Area on Freezing of Sandy Soils. MSc Thesis, University of Alberta, Edmonton, Alberta.

Dudas, M.J., 1993. Preliminary Characterization of Suncor, Syncrude, and OSLO Sludges, Internal University of Alberta report, January, 1993.

Geocon, 1994. Preventing of AMD by Disposing of Reactive Tailings in Permafrost, MEND Program report, December, 1993, 98p.

Hivon, E.G., 1991. Behaviour of Saline Frozen Soils, PhD Thesis, University of Alberta, Edmonton, Alberta.

Lighthall, P.C.; Watts, B.D.; Rice, R., 1989. Deposition methods for construction of hydraulic fill tailings dams, Geotechnical Aspects of Tailings Disposal and Acid Mine Drainage, Vancouver Geotechnical Society, Vancouver, 1989, 15 p.

M^{c}Kay, R.J., 1972. The World of Underground Ice, annals of the association of American Geographers, Volume 62, No. 1, pp 1-22.

Nixon, J.F. and Morgenstern, N.R., 1973. The Residual Stress in Thawing Soils. Canadian Geotechnical Journal, 10: 571-580.

Sego, D.C. and Dawson, R.F, 1992a. Freeze-thaw dewatering of OSLO cold water process fine tails. Submitted to ESSO Resources Ltd., April 1992. 76p.

Sego, D.C. and Dawson, R.F, 1992b. Influence of freeze-thaw on behavior of oil sand fine tails. Submitted to Alberta Oil Sand Technology and Research Authority, June 1992, 77p.

Sego, D.C., 1992. Influence of pore fluid chemistry on freeze-thaw behavior of SUNCOR oil sand fine tails (Phase 1). Submitted to Reclamation Research Technical Advisory Committee, Alberta Environment, 35p.

Sego, D. C. and Dawson, R.F., 1993. Freeze-thaw enhancement studies on Oslo Lease 41 Field Frozen Samples. Submitted to ESSO Resources Ltd., April 1993, 36 p.

Sego, D., Burns, R., Dawson, R., Dereniwski, T. Johnston, R. and Lowe, L., 1993. Dewatering of fine tails utilizing the freeze-thaw process. Proceedings of Fine Tails Symposium, Oil Sands Our Petroleum Future Conference, Edmonton, Alberta April 4-7, 1993, F17-1 to F17-25.

TABLE 3.1 PORE WATER CHEMISTRY OF OIL SANDS FINE TAILS

	pH	Ca (mg/l)	Mg (mg/l)	Na (mg/l)	EXCHANGEABLE SODIUM RATIO
SYNCRUDE	8.4	4.8	5.1	480	.54
SUNCOR	8.4	4.2	4.4	400	.49
OSLO	8.2	3.6	3.0	84	.12

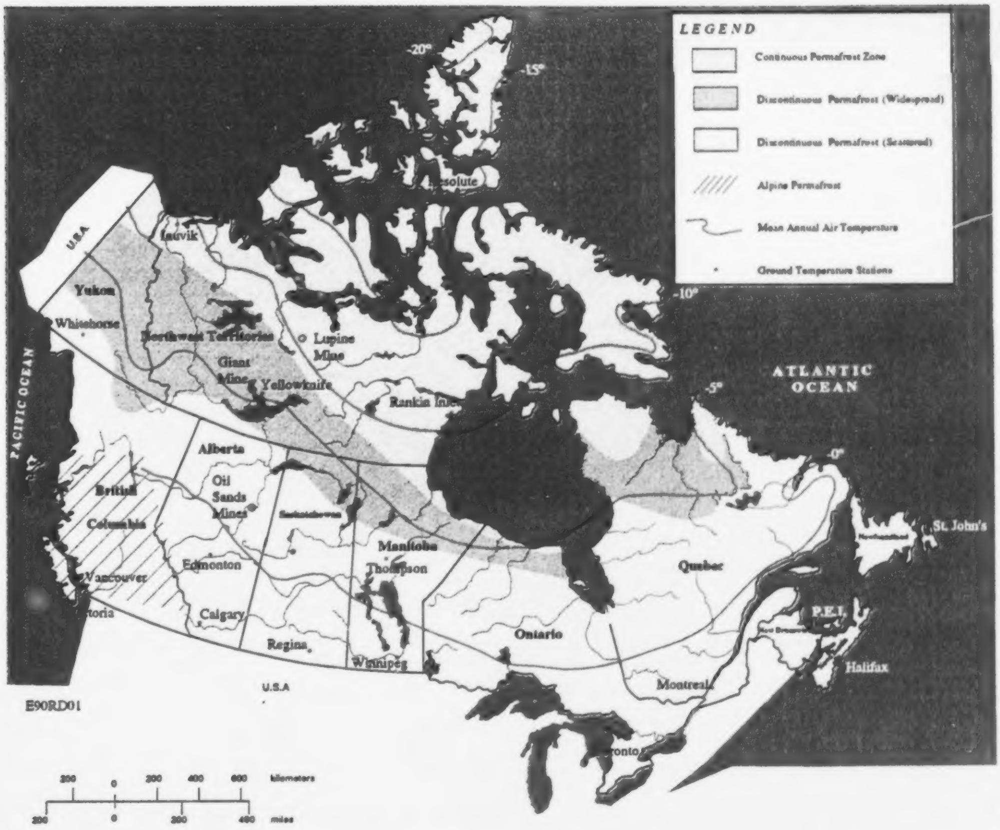

Figure 3.1 Permafrost Region of Canada
(modified after Climatic Atlas of Canada)

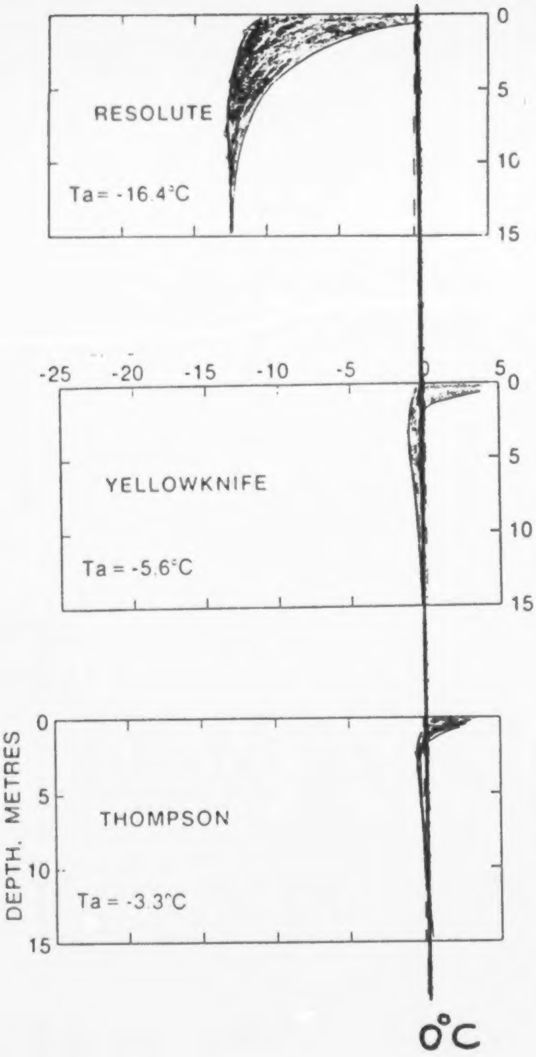

Figure 3.2 Ground Temperature Profiles

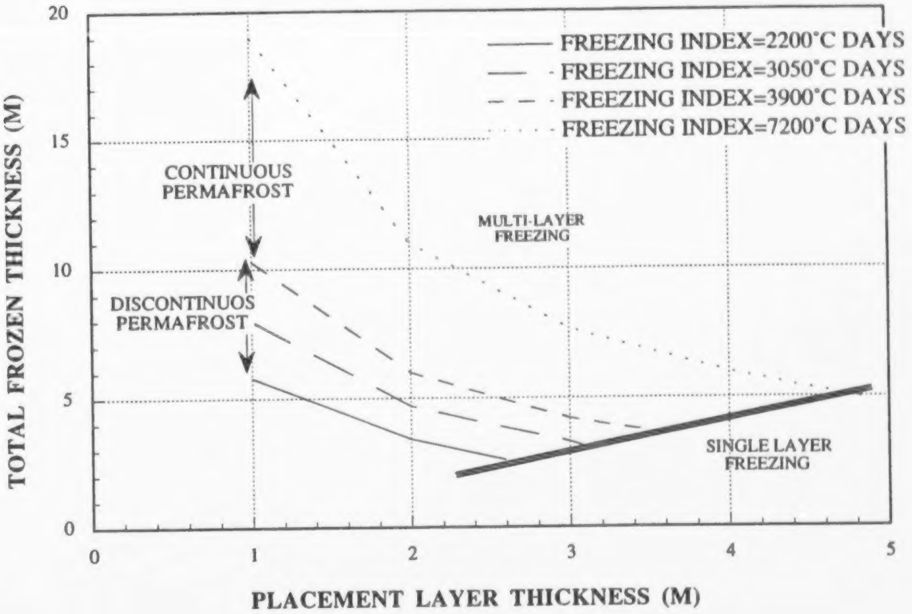

TAILINGS SAND FREEZING LAYER THICKNESSES

Figure 3.3 Calculated Tailings Sand Frozen Thicknesses

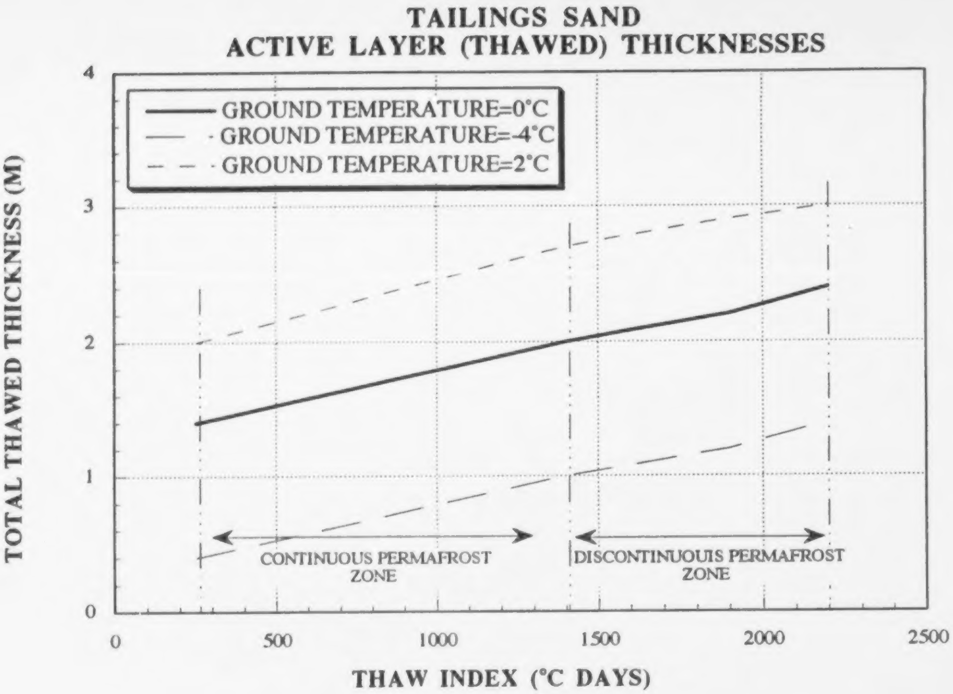

Figure 3.4 Calculated Tailings Sand Thawed Thicknesses

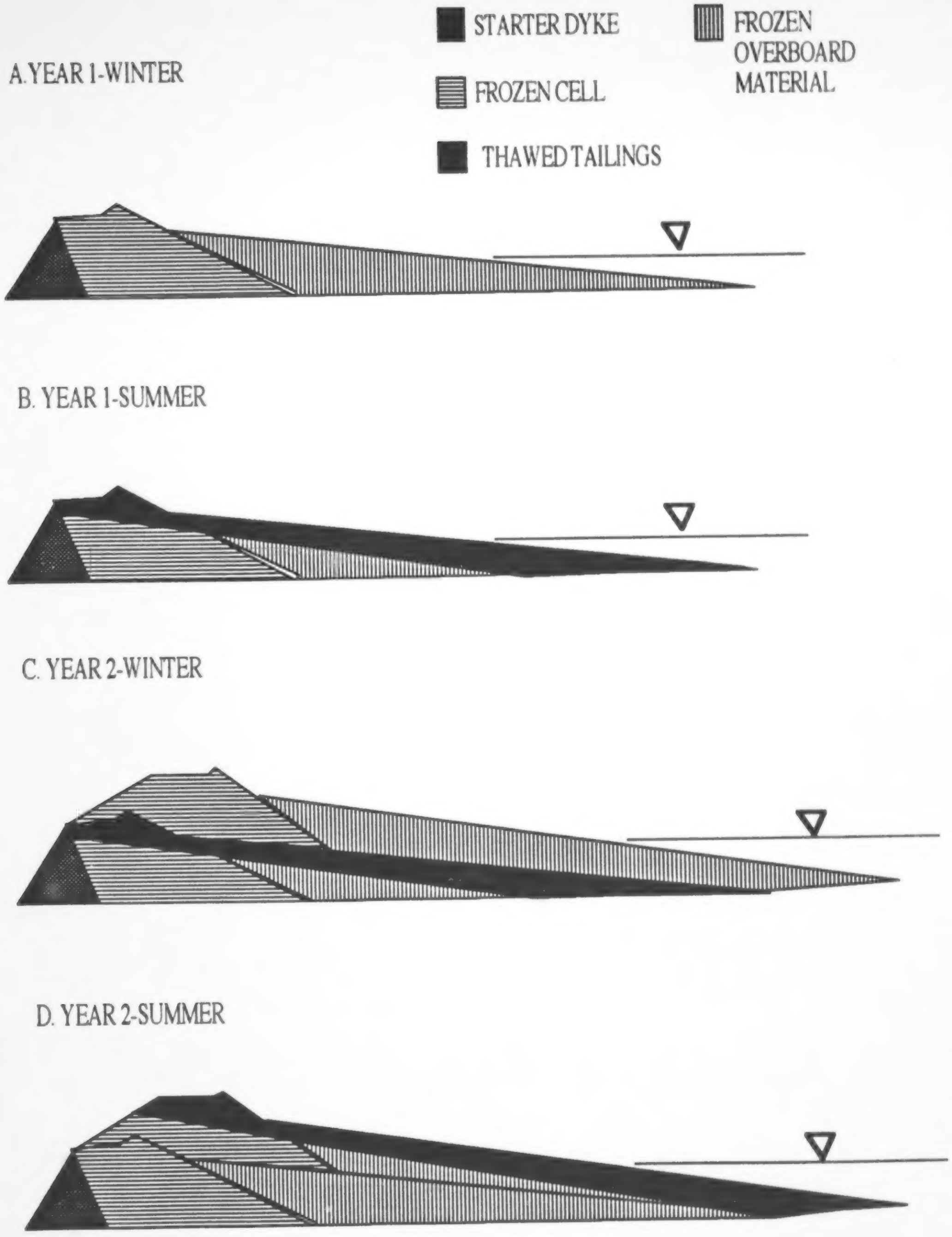

Figure 3.5 Total Containment by Frozen Cell Construction

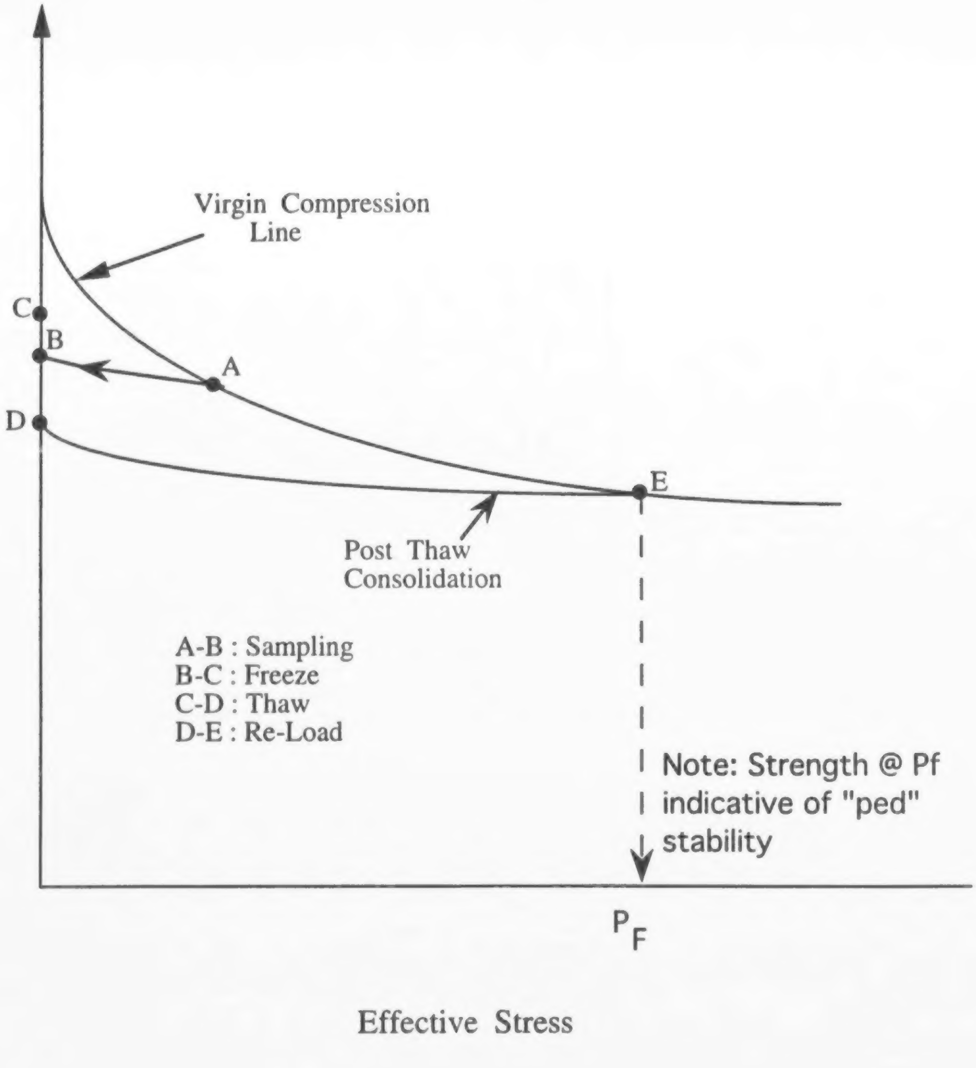

Figure 3.6 Consolidation Due to Thaw Strain

A. WINTER PLACEMENT

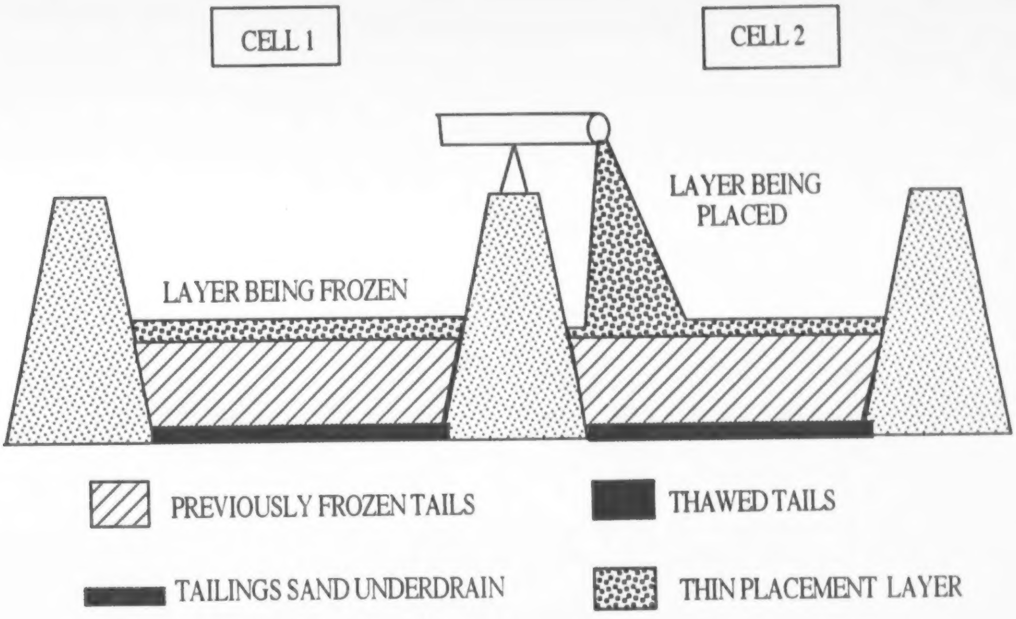

B. SUMMER THAW

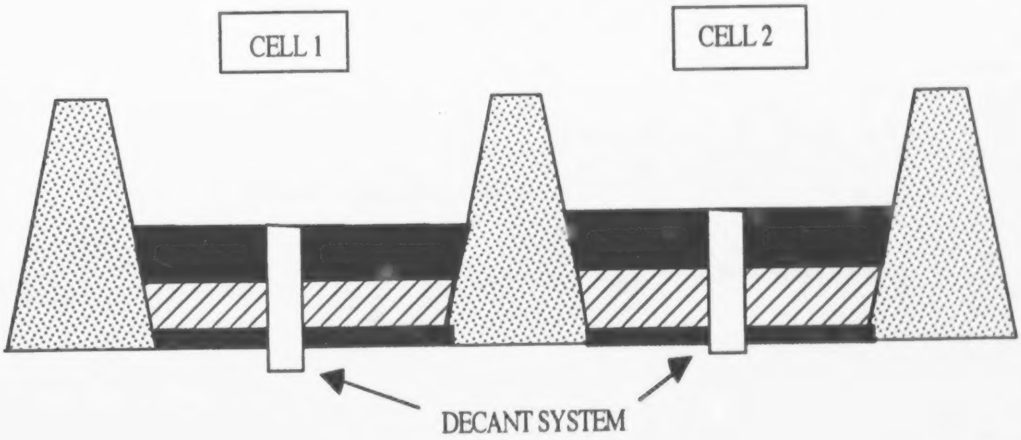

Figure 3.7 Thaw Controlled Dewatering Schematic

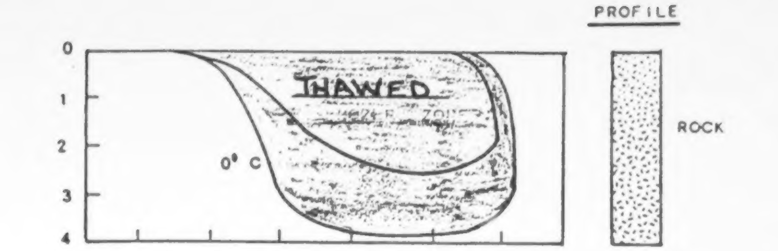

(a) SOUND AND FRACTURED ROCK

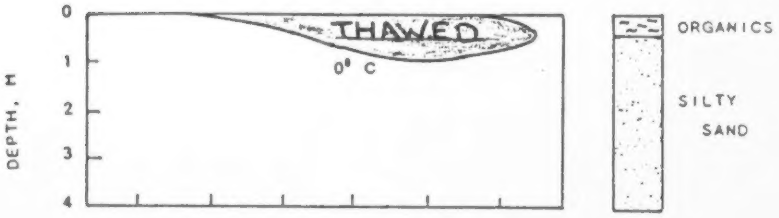

(b) SOIL WITH ORGANIC COVER

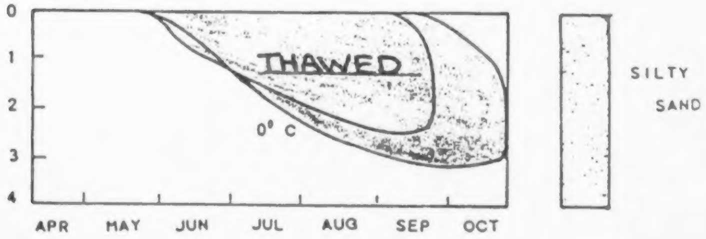

(c) SILTY SAND UNDER DAM CREST

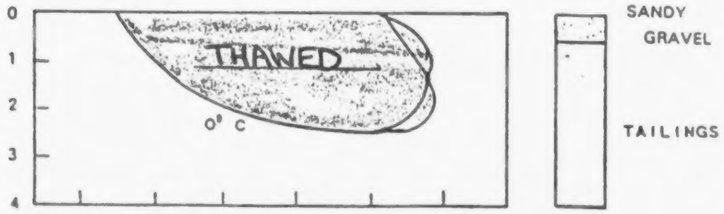

(d) TAILINGS COVERED WITH SAND

Figure 3.8 Lupin Mine Active Layer Stratigraphies
(modified after Geocon, 1994)

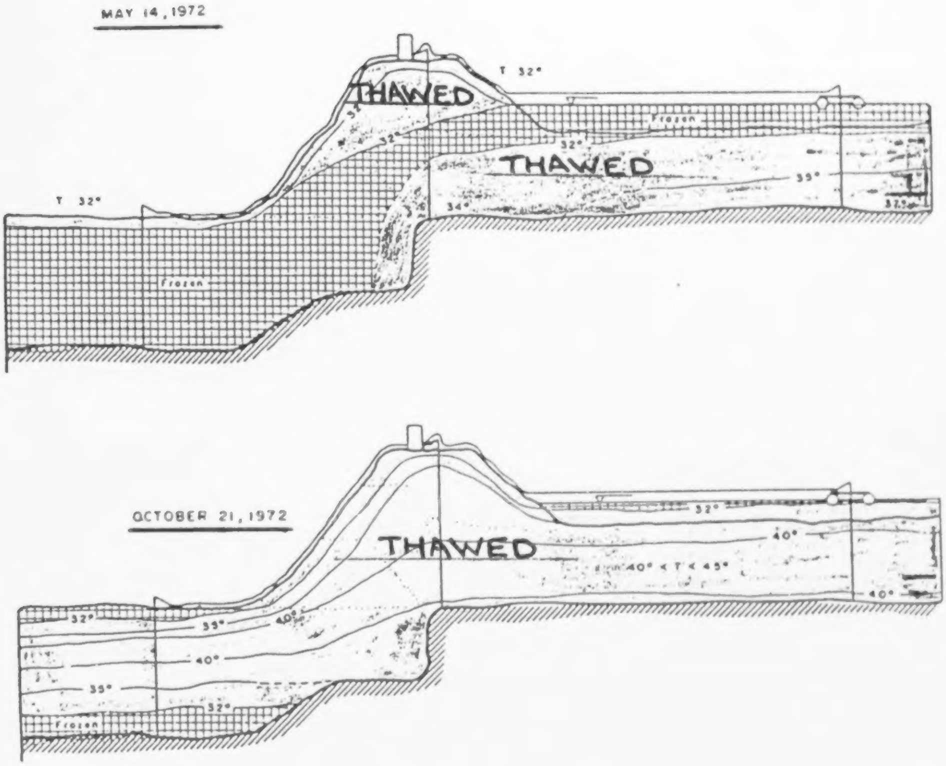

Figure 3.9 Giant Mine Tailings Impounment Temperature Data
(modified after Geocon, 1994)

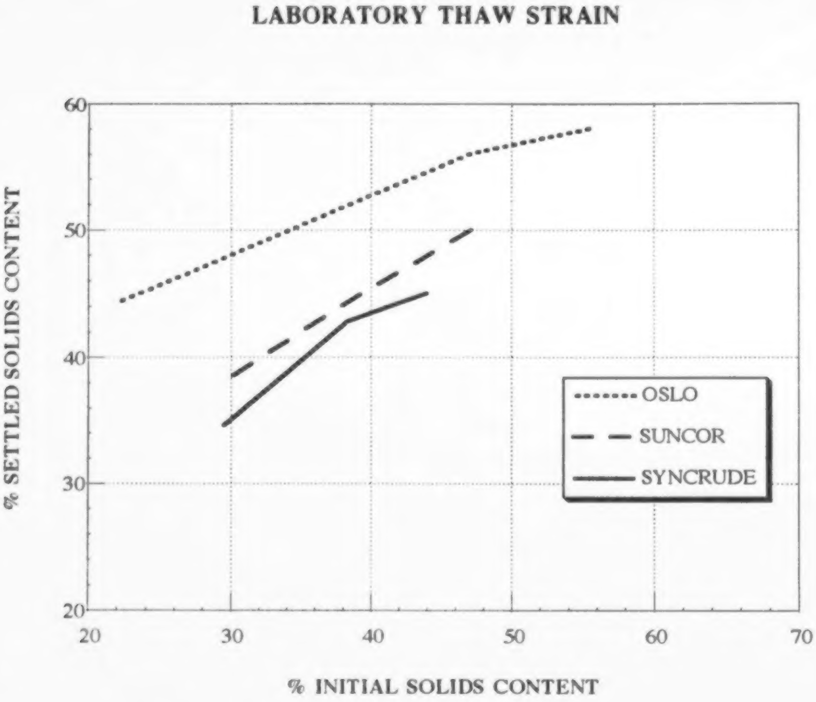

Figure 3.10 Oil Sand Fine Tails Thaw Strain

Chapter 4

FREEZE-THAW DEWATERING OF OIL SANDS FINE TAILS

4.1 INTRODUCTION

The Alberta oil (tar) sands are a vast petroleum resource containing 214 billion m^3 of bitumen. About 6% of the total resource is recoverable with current surface mineable technology. Presently, two commercial operations (Syncrude and Suncor) mine oil sands ore and extract then upgrade the bitumen to produce over 30,000 m^3/day of synthetic crude oil. This represents over 15% of Canada's total crude oil production.

The very large scale of commercial oil sands operations results in the accumulation of large volumes of mine waste. Under current production conditions, a plant producing 15,900 m^3/day (100,000 bbl/day) of synthetic crude requires the processing of 100,000 bank m^3/day ore which results in a tailings stream consisting of 100,000 m^3 of loose sand and 20,000 m^3 of 30% solids content fine tails (Morgenstern *et al*, 1988). Thus a nominally sized oil sands mine produces about 7.2 million m^3/year of mature fine tails (30% solids).

Storage and disposal of the vast amounts of high moisture content fine tailings remains one of the major problems associated with the current oil sands mining and processing technology. Consequently, considerable research efforts directed towards more environmentally acceptable waste management practices are underway. The University of Alberta has been interrogating the feasibility of dewatering oil sands fine tails through natural freeze-thaw processes for 4 years. This chapter examines some fine tails dewatering properties and design concepts that have evolved as a result of this research.

4.2 BACKGROUND STUDIES

In 1971, the United States Bureau of Mines completed a laboratory study of freeze-thaw dewatering on Florida phosphate rock slime (Stancyzyk *et al.*, 1971). Samples of 13.7% solids phosphate fine tails were frozen in a freezer at different freezing rates. The layer thickness used and actual temperature boundary conditions were not presented in the report. After an 8 hour freezing period the settled solids contents increased from 14% to 32% following thaw, representing a settled solids increase of 134%. It was unclear whether sedimentation occurred during freezing which might mask the effects of freeze-thaw alone. For shorter freezing periods, substantially lower settled solids was in evidence. When samples were frozen quickly (less than 1 hour) there was no change in settled solids content when thawed.

The US Cold Region Research and Engineering Laboratory (CRREL) has been conducting a pilot scale study on freeze-thaw dewatering of sewage sludges (Martel, 1988). The CRREL researchers designed and constructed a concrete lined sludge freezing bed for freezing, thawing, and decanting dewatered sludge. During the winter sludge was applied in 5 to 15 cm thick layers to a total thickness of about 1 meter. As the sludge thawed during the spring and summer the melt water was drained away as the previously frozen sludge settled. Thaw strain values of 70% were realized for sewage sludge containing initial solids contents of about 5%.

Researchers at the Alberta Environmental Center in Vegreville, Alberta (Johnson *et al*, 1989) have examined freeze-thaw dewatering of commercial oil sand fine tails. Extensive laboratory and field testing consistently demonstrated substantial increases in solids content. The field tests showed that the water released as a decant during thaw could be drained from a V-notch ditch established along one side of the retention cell. Two meters of frozen fine tails thawed under ambient Fort McMurray conditions. Reed Canary grass was successfully cultivated on fertilized thawed fine tails to assist in further dewatering of the fine tails by evapotranspiration.

4.3 OSLO LEASE 41 FREEZE-THAW FIELD STUDY

The OSLO New Ventures group, which studies new oil sands technologies, set up a pilot plant for processing oil sands using the OSLO cold water bitumen extraction (OCWE) process. Various schemes for dry landscape disposal of oil sands fine tails were piloted following the processing operation including layered disposal (Been et al., 1991) and freeze thaw dewatering reported here.

Figure 4.1 shows some typical grain size distributions and material properties for the OSLO OCWE process fine tails. Fine tails solids are comprised of 45 to 50% clay sized fraction (-2 micron). The clay fraction consists of about 60% hydrous mica and 40% kaolinite. Bitumen contents range from 1 to 4%. The material typically has a plastic index of about 30.

Bench scale laboratory testing, discussed in Chapter 3, has established that the OSLO fine tails exhibit better thaw strain dewatering potential than fine tails from the two commercial operations. Although the difference has been attributed to pore water chemistry a fundamental understanding of the different chemical processes taking place during freezing is lacking.

The OSLO Lease 41 test site is located approximately 8 km south of the SUNCOR plant site near Fort McMurray, Alberta. During the winter of 1992 frozen cores were obtained from the No. 1 fines pond area. The fines pond is approximately 1375 m^2 (55m x 25m) and was used for the disposal of oil sands tailings during pilot plant processing operations conducted at the site. The pond is lined with a synthetic liner to control seepage. Most of the pond was covered with up to 10 cm. of fine sand placed during sand spray tests carried out in 1991.

The coring was carried out with a 103mm CRREL core barrel attached to a power auger. The site was drilled on two separate occasions and two separate sets of core were obtained; 12 holes were cored on February 14 (numbered from 1 to 12) and 5 additional holes were cored on March 14, 1992 (identified from A to G). Four cores from the earlier February drilling (numbered series) and all of the March core (lettered series) were returned to the University of Alberta for laboratory thawing and post thaw consolidation tests and the test results are reported here. Figure 4.2 shows a plan of the Lease 41 Fines Pond No. 1 with the 1992 bore holes noted. All of the holes for this study were drilled to the liner at the base of the pond.

The test specimens machined from the frozen core obtained from the field were tested in plexi-glass oedometer test cells which were specially designed and constructed to accommodate the frozen tailings and to accurately measure material characteristics (thaw strain, compressibility, and permeability) under low stress conditions. Details of the test procedures and individual test results are contained in Appendix A.

Figure 4.2 shows the pond plan with the spatial distribution of initial measured solids content in the pond. The higher solids content samples occur in the north, upstream end of the pond. Multiple freezing cycles in this portion of the pond are probably responsible for these higher solid contents. Previous laboratory testing showed that fine tailings originally at 30% solids approaches solids contents of 60% after two cycles of freeze-thaw (Sego and Dawson, 1992a) .

Figure 4.3 shows the relationship between initial and final solids content for the field samples as compared with 15 cm laboratory frozen and thawed samples (double sided freezing of 15 cm long samples). This plot demonstrates that the field frozen samples exhibit a parallel and slightly improved thaw behaviour to the laboratory samples. This improvement is attributed to the following factors:

1. For the field frozen samples tested in the laboratory apparatus it was necessary to apply a nominal seating load of 0.5 kPa during thaw to maintain a reasonably level sample surface prior to the post thaw consolidation tests. This load had not been applied to the laboratory frozen and thawed samples on which the thawed solids content were measured.

2. Freezing in the pond was from one direction only and occurred over a layer about 40 cm thick, as compared to the double sided freezing of the 15 cm thick laboratory frozen samples. Previous work for AOSTRA has demonstrated that smaller freezing temperature gradients result in greater solids enhancement upon thaw (Sego and Dawson, 1992b).

Figure 4.4 shows a straight line relationship between initial solids content and thaw strain measured for the field frozen and laboratory thawed samples. One cycle of freeze thaw results in thaw strains in excess of 50% which is consistent with previous findings with OSLO fine tails (Sego and Dawson, 1992a). The trend of the thaw strain line suggests that the volume reduction due to thaw strain approaches zero at a fine tails solids content of about 70% (void ratio of about 1.0).

Figures 4.5 and 4.6 show the compressibility (void ratio versus effective stress) and permeability (void ratio versus permeability). behaviour respectively for the tests on frozen fine tails. These two figures demonstrate the following findings:

1. Thawed fine tailings behave like an overconsolidated soil and approach the never frozen fine tails compressibility line (virgin consolidation line) at stresses in excess of 10 kPa.

2. The thawed fine tails exhibit enhanced permeability values up to two orders of magnitude greater than the never frozen fine tails at similar void ratio upon thaw.

The large scatter in the laboratory results are due to differences in the initial void ratio after thaw and at the beginning of the post thaw consolidation test. In addition, the permeability measured for sample C-1 was influenced by the presence of a sand pocket which created a preferred drainage path within the sample. This explains the distinct jump in the void ratio versus permeability behaviour recorded for this sample. The compressibility and permeability relationships of high moisture content soils and slurries are often expressed as power law relationships of the form (Somogyi, 1980):

$$e = A\sigma_V^B$$

$$e = Ck^D$$

Where: e = void ratio
σ_V = vertical effective stress
k = permeability
A, B, C, D are material constants

Figure 4.7 shows plots of the compressibility and permeability data versus normalized void ratio. The void ratio data has been normalized as follows:

$$e_{norm} = {}^{e}\!/_{e_{thaw}}$$

Where: e = void ratio at a particular stress after thaw
e_{thaw} = void ratio immediately after thaw under 0.5 kPa stress
e_{norm} = normalized void ratio

Data from the two samples with very low initial void ratio (A-2 and B-1) are not included in these figures as these materials were apparently subjected to more than one cycle of freeze-thaw. The log-log plots exhibit a reasonably well defined straight line relationship between void ratio and stress or permeability that can be incorporated into analytical models which illustrate the benefits of using a freeze-thaw disposal system.

4.4 FREEZE-THAW DEWATERING DESIGN CONCEPTS

The ongoing research has been guided by a thin layered freezing design concept as illustrated schematically in Figure 4.8. Mature fine tails (25 to 35% solids) are pumped from a settling basin to pairs of freeze-thaw cells. The unfrozen material is deposited in thin layers so that it freezes quickly and under closed system freezing conditions. As the previously deposited layer in one cell freezes, a new layer is placed in the adjacent cell thus permitting uninterrupted hydraulic transport and deposition. The winter pumping and placing process continues until the total design thickness of frozen material is achieved. During the spring and summer months thawing occurs. Surface water released during thaw is removed to maximize the thaw depth. Sand blanket under drains and surface water decant systems must be designed to handle water released as the material thaws. After each yearly cycle of freezing and thawing the process is continued and the previously thawed layers beneath the most recently placed frozen layers consolidates further due to surcharge loading of the newly placed frozen fine tails. Drainage layers placed at regular intervals within the previously placed and thawed layers can be incorporated to accelerate the post thaw consolidation (dewatering) process. Bitumen contents as high as 4% do not seem to clog up the sand drainage layers ((Sego and Dawson, 1992a).

The technical and practical feasibility of freeze-thaw management systems is influenced by several geotechnical factors. Thermal boundary conditions and drainage/consolidation considerations are of particular interest. A quantitative evaluation of each of these factors and their influence on natural freeze-thaw dewatering disposal schemes for oil sands fine tails are presented here.

4.4.1 THERMAL CONSIDERATIONS

The amount of material that can be frozen and/or thawed is a function of the site climatic conditions, material thermal properties, and the thermal boundary conditions. Table 4.2 shows a summary of Fort McMurray climatic data from the Climatic Atlas of Canada. The data shows that the freezing season is about 150 days (November to March) with an average freezing temperature of -14°C (freezing index of 2160°C days). Similarly, the thawing season is also about 150 days with an average thawing temperature of 12° (thawing index of 1770°C days). The mean global solar radiation, is 208 watts/m^2 during the thaw period. These average values are incorporated into the simple freezing and thawing design calculations presented below. The effects of variations from these mean values was not addressed.

Researchers at the CRREL (Martel, 1988) have developed simple design thermal models to predict the freezing and thawing depths of sewage sludges placed in specially designed freeze-thaw beds. These models are presented in Appendix B are used here to estimate freeze-thaw dewatering design thicknesses for fine tails placed at Fort M^{c}Murray.

The average climatic factors (Table 4.2) and thermal parameters derived from empirical relationships based on moisture content (see Appendix B) can be used to estimate freezing and thawing depths for layered freeze-thaw dewatering systems in the Fort M^{c}Murray area. Calculated freezing depths, shown in Figure 4.9, are factored by one-half to allow for the filling of one cell while the other is freezing. Figure 4.9 shows that it is possible to obtain a total frozen thickness of 2 to 4.5 m by placing and freezing thin layers 0.1 to 0.5 m thick respectively under average winter conditions.

Thaw depths are calculated by summing the amount of material that thaws during the summer (upper and lower thaw fronts) and the thaw that occurs at depth (lower thaw front) only in the subsequent winter. Figure 4.10 shows the total ambient thaw and warm water cap thaw thicknesses over a range of appropriate temperature conditions. A nominal thaw depth of 0.5 m is assumed for the thawing at depth during the winter. Figure 4.9 indicates average thaw thicknesses of 3.0 and 4.5 m for ambient and warm water thaw depths respectively.

A comparison of Figures 4.9 and 4.10 reveals that it is normally possible to freeze more material than will thaw per year, even when the frozen depths are divided by one-half to allow for handling considerations and a warm water cap is used to accelerate the thaw process. Thus a freeze-thaw dewatering system in the Fort M^{c}Murray area is governed by thawing considerations

4.4.2 DRAINAGE AND CONSOLIDATION

The unique consolidation characteristics (high permeability and high compressibility) of the thawed fine tails allow for dewatering rates several orders of magnitude faster than corresponding rates for mature unfrozen fine tails at the same void ratio. These unique characteristics are best portrayed by examining the void ratio versus coefficient of consolidation relationship for the thawed and never frozen fine tails. The coefficient of consolidation can be calculated from the power law constants as:

$$C_v = \frac{ce^d(1+e_0)}{-\gamma_w ab(e/a)^{\frac{b-1}{a}}}$$

Where: C_v = coefficient of consolidation

e = void ratio

e_0 = initial void ratio

γ_w = unit weight of water

a, b = compressibility power law functions

c, d = permeability power law functions

The void ratio(e) versus coefficient of consolidation (C_V) relationship for mature fine tails and thawed fine tails is shown in Figure 4.11 to illustrate drainage and consolidation behaviour for a 3m thick frozen and thawed layer of fine tails. The power curve compressibility and permeability constants for thawed fine tails are derived from the normalized compressibility and permeability plots shown in Figure 4.7 for e_0=2.3; this corresponds to an initial solids content of 30% which undergoes thaw strain to 52% solids content (Figure 4.2). The power curve compressibility and permeability constants for never frozen fine tails are derived assuming that the consolidation characteristics for unfrozen and thawed fine tails meet at a void ratio of 1.1, corresponding to an effective stress of 100 kPa.

As the mature frozen fine tails layer thaws (A-B in Figure 4.11) the void ratio decreases from 5.8 to 2.3 (30 to 52% solids content) virtually instantaneously as the dense peds settle. Assuming downwards drainage, following thaw appreciable self weight consolidation takes place to a void ratio of about 1.7. Additional surcharge loading from an overlying frozen layer placed the following winter results in an additional decrease in void ratio to about 1.25, assuming that all excess pore pressures can dissipate. As surcharge loading continues in subsequent years, the effective stress path approaches the compressibility line for never frozen fine tails.

An under drain placed below the freeze-thaw cells is considered an essential element of the management strategy for several reasons:

1. To maintain the steady state seepage pressures at zero as a result of downwards flow.

2. To ensure that drainage is not fully impeded from frozen layers overlying previously thawed, underconsolidated fine tails.

3. To facilitate drainage water management by minimizing surface ponded water.

For layers 3 to 5 meters thick most of the volume reductions benefits are apparent in the first two freeze-thaw cycles as volume change is most pronounced at low effective stresses. In addition excess pore pressures dissipate rapidly at void ratios greater than about 1.5 corresponding to coefficient of consolidation of 1 m^2/yr. Below a void ratio of 1.5 the volume change is markedly reduced and increases in strength rather than volume reduction are more significant.

In order to calculate the highly nonlinear volume change with time relationship for a thin layered thaw dewatering process a finite strain program was developed (Pollock, 1993). The program is based on the solution for finite strain consolidation developed by Somogyi (1980) and discussed in detail by Pollock (1988). Figure 4.12 shows the boundary conditions and governing equation used by the program to track the thaw consolidation process. The program allows for placing a drainage blanket each year (double drainage) or for placing each layer without an intervening blanket (single drainage). The dewatering benefits for different handling scenarios are illustrated in the next section.

4.5 DESIGN SCENARIOS

Several handling strategies have been developed, following the rational presented above, to maximize volume reduction and increase the shear strength of thawed fine tails. Thermal boundary conditions dictate two main approaches:

1. Freeze Controlled- Thin layers are placed throughout the winter to maximize the total frozen fine tails thickness. Calculations presented above show that this approach will result in a larger mass of frozen material than can be thawed the following summer. Figure 4.9 shows that it may be possible to freeze between 4 and 5 metres of fine tails each year, assuming that thin (.1 to .15 meters) placement layers are deposited. This approach would result in the accumulation of 1 to 2 meters of frozen material each winter. The advantages are that more material can be placed each year. Disadvantages include uncertainties with respect to thawing at depth, impedance of drainage from deep

frozen layers, and longer term maintenance of the drainage system. Alternatively, a freeze controlled strategy could be carried out by placing material every other year thus allowing two years for thawing to take place.

2. Thaw Controlled- The total thickness of fine tails frozen each winter is controlled by the amount that can be thawed the following summer (two way heat flow) and at depth the following winter (one way heat flow). Thus frozen material does not accumulate at depth and most of the dewatering occurs during the summer thaw period. At present, a thaw controlled approach to freeze-thaw dewatering appears more environmentally acceptable.

The thaw strain layered consolidation program discussed above was used to calculate the dewatering benefits of thaw controlled dewatering schemes. Figure 4.13 shows the calculated frozen versus thawed cumulative thicknesses (single drainage condition) for a 3m per year (ambient thaw) frozen placement thickness scheme. After five years of deposition at 3 m/yr. (15 m cumulative frozen thickness) the cumulative thawed thickness would be about 5.5 m (volumetric strain of 63%). Similarly, Figure 4.14 shows the calculated frozen versus thawed cumulative thicknesses (single drainage condition) for a 4.5m per year (thaw with warm water cap) frozen placement thickness scheme. After five years of deposition at 4.5 m/yr. (22.5 m cumulative frozen thickness) the cumulative thawed thickness would be about 8.3 m (volumetric strain of 63%). The potential volume reduction benefits of freeze-thaw dewatering are dramatic as these two figures clearly illustrate.

The consolidation calculations for Figures 4.13 and 4.14 were carried out assuming single drainage conditions (no intermediate sand drains). Figure 4.15 compares the single versus double drainage condition (sand drainage layers placed each year) for a 3 m/yr. frozen placement scenario. Note that the difference in the total thawed thickness is only about 0.3 over the five year period as most volume change occurs in the first two years of placement.

A nominally sized oil sands mine produces about 7.2 million m^3/year of mature fine tails (30% solids). A thaw controlled freeze-thaw disposal scheme designed for ambient thaw conditions (3.0 m thick frozen placement per year) would require an area about 300 hectares in size (includes an additional 25% for dikes and materials handling infrastructure) to accommodate a freeze-thaw disposal system that manages one years fine tails production. Similarly, a thaw controlled disposal scheme designed for warm water cap thaw (4.5 m thick frozen placement per year) would require an area about 200 hectares in size. These are very large areas and it is unlikely that it would be practical to devote this much space to a freeze-thaw management facility. However, it is envisaged that in practice other management technologies would be coupled with freeze-thaw dewatering to reduce the ultimate stored volumes of fine tails. Thus freeze-thaw management facilities of 50 to 100 hectares in size are more realistic.

4.6 CONCLUSIONS

Design considerations presented in this chapter illustrate the potential dewatering benefits of layered oil sands fine tails freeze-thaw dewatering systems. Design calculations show some important points:

1. Material placement considerations are governed by thawing. Average yearly thaw thicknesses of 3.0 and 4.5 m are calculated for ambient and enhanced warm water cap thaw conditions respectively.

2. Volume change is most significant in the first two years following placement.

3. After five years of deposition (3 and 4.5 m frozen thickness per year) total volumetric strains approaching 65% are realized.

4. Intermediate sand drains placed every year result in only a small difference in the dewatering benefits as compared with an under drain only situation.

Detailed study of a prototype field freezing experiment is required to validate and refine the concepts presented here. Such an experiment is being carried out at the SUNCOR oil sands mine site (Sego et al., 1993b). Other high moisture content mine waste slurries, including acid mine drainage treatment sludges, may also be amenable to similar natural freeze-thaw dewatering schemes.

4.7 REFERENCES

Been, K., Hachey, J., Dereniwski, T. and Paul, R., 1991. Layered Disposal and Consolidation of OCWE Process Fine Tailings, 44th Canadian Geotechnical Conference Proceedings, Calgary, Alberta, pp. 52-1, 52-10.

Johnson, R.L., Bork, P. and Layte, P., 1989. The Effect of Freezing and Thawing on the Dewatering of Oil Sands Sludges. International Symposium on Reclamation, A global Perspective, Calgary, Alberta, pp. 687-694.

Martel, C.J., 1988. Development and Design of Sludge Freezing Beds, USA Cold Regions Research and Engineering Laboratory, CRREL Report 88-20.

Morgenstern, N.R., Fair, A.E., and M^{c}Roberts, E.C., 1988. Geotechnical engineering beyond soil mechanics-a case study. Canadian Geotechnical Journal, 25: 637-661.

Pollock, G.W., 1988. Large Strain Consolidation of Oil Sand Tailings Sludge, unpublished University of Alberta MSc Thesis, 276p

Pollock, G.W., 1993. University of Alberta Finite Strain Freeze Thaw Consolidation Program.

Sego, D.C. and Dawson, R.F, 1992a. Freeze-thaw dewatering of OSLO cold water process fine tails. Submitted to ESSO Resources Ltd., April 1992. 76p.

Sego, D.C. and Dawson, R.F, 1992b. Influence of freeze-thaw on behavior of oil sand fine tails. Submitted to Alberta Oil Sand Technology and Research Authority, June 1992, 77p.

Sego, D. C. and Dawson, R.F., 1993a. Freeze-thaw enhancement studies on Oslo Lease 41 Field Frozen Samples. Submitted to ESSO Resources Ltd., April 1993, 36 p.

Sego, D., Burns, R., Dawson, R., Dereniwski, T. Johnston, R. and Lowe, L., 1993b. Dewatering of fine tails utilizing the freeze-thaw process. Proceedings of Fine Tails Symposium, Oil Sands Our Petroleum Future Conference, Edmonton, Alberta April 4-7, 1993, F17-1 to F17-25.

Somogyi, F., 1980. Large strain Consolidation of Fine Grained Slurries. Presented at the Canadian Society for Civil Engineering Conference, Winnipeg, Manitoba, May 19-29, 1980.

Stancyzyk, M.H., et al., 1971. Dewatering Florida Phosphate Pebble Rock Slime by Freezing Techniques. USBM Report of Investigations, Number 7520.

TABLE 4.1 FORT M^{C}MURRAY CLIMATE DATA

Month	Mean Temperature (°C)	Mean Global Solar Radiation (W/m^2)	Mean Precipitation (mm)
January	-22	32	<10
February	-15	70	<10
March	-10	137	<10
April	1	198	<10
May	8	233	30
June	12	244	50
July	15	238	80
August	15	195	75
September	9	128	50
October	3	70	10
November	-8	35	<10
December	-17	23	<10

For Freeze Thaw Design:

- Freezing Index = 2160°C days (Nov. - March)
- Thawing Index = 1770°C days (May - Sept.)
- Average Thaw Insolation = 208 W/m^2 (May - Sept.)

* Source: Climatic Atlas of Canada, Environment Canada, 1987

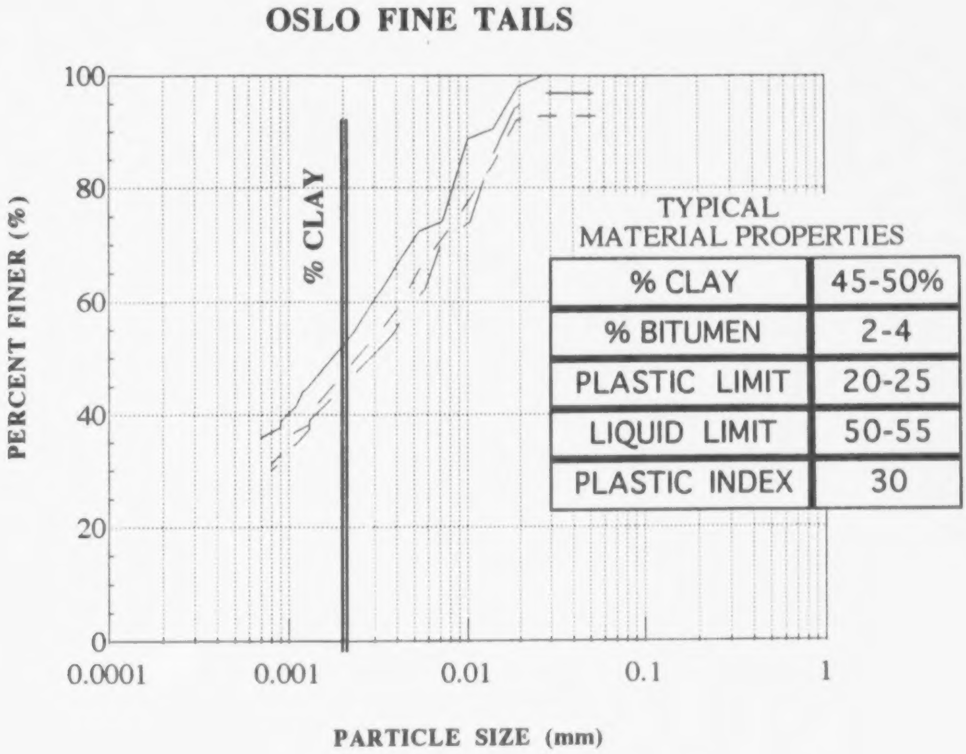

% CLAY	45-50%
% BITUMEN	2-4
PLASTIC LIMIT	20-25
LIQUID LIMIT	50-55
PLASTIC INDEX	30

Figure 4.1 OSLO Fine Tails Geotechnical Properties

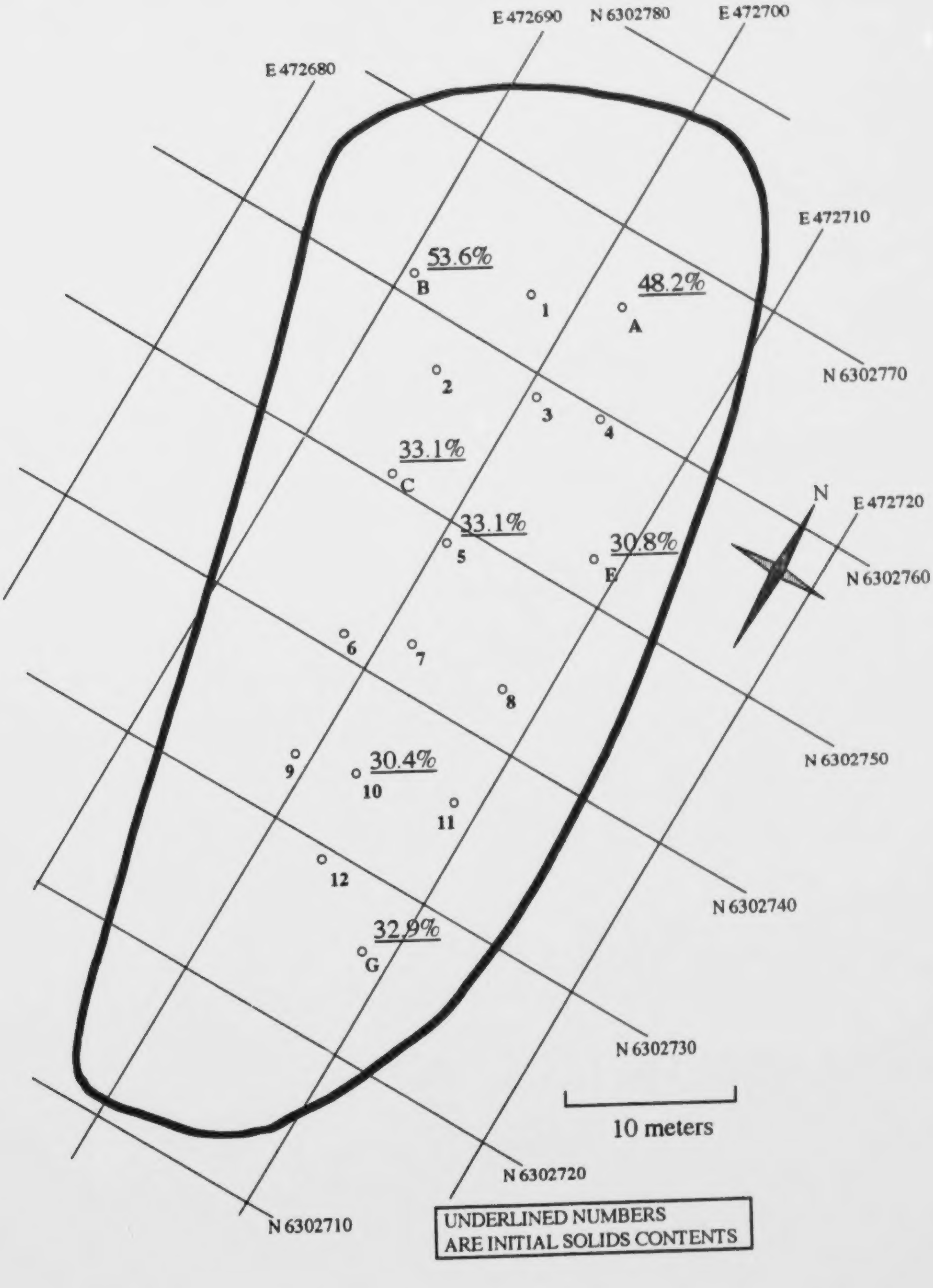

Figure 4.2 OSLO Lease 41 Fines Pond No. 1

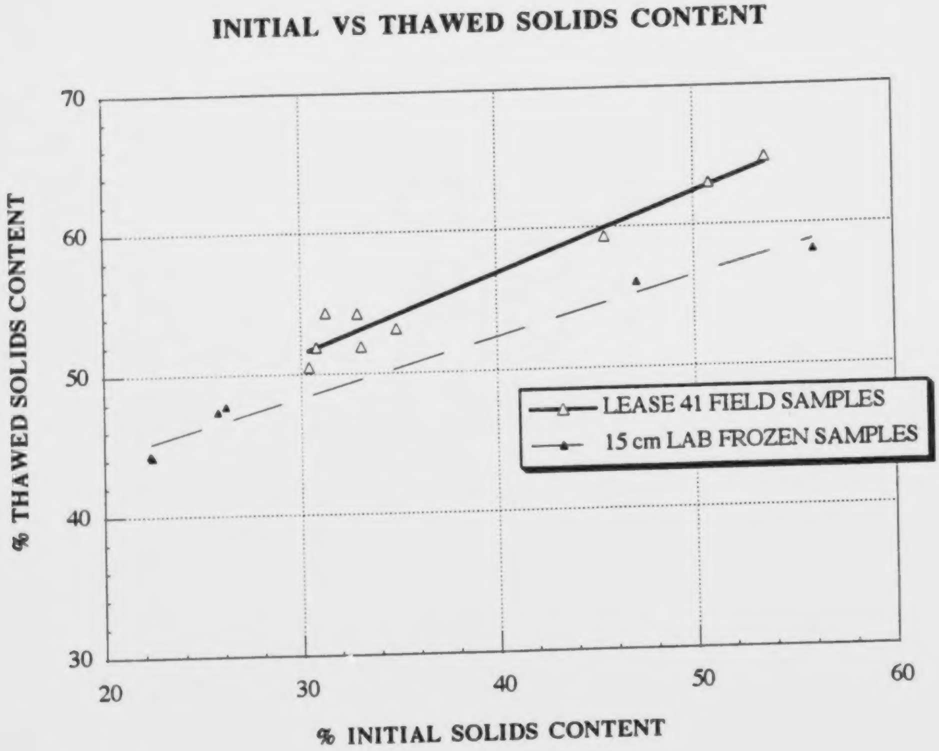

Figure 4.3 OSLO Initial Versus Final Solids

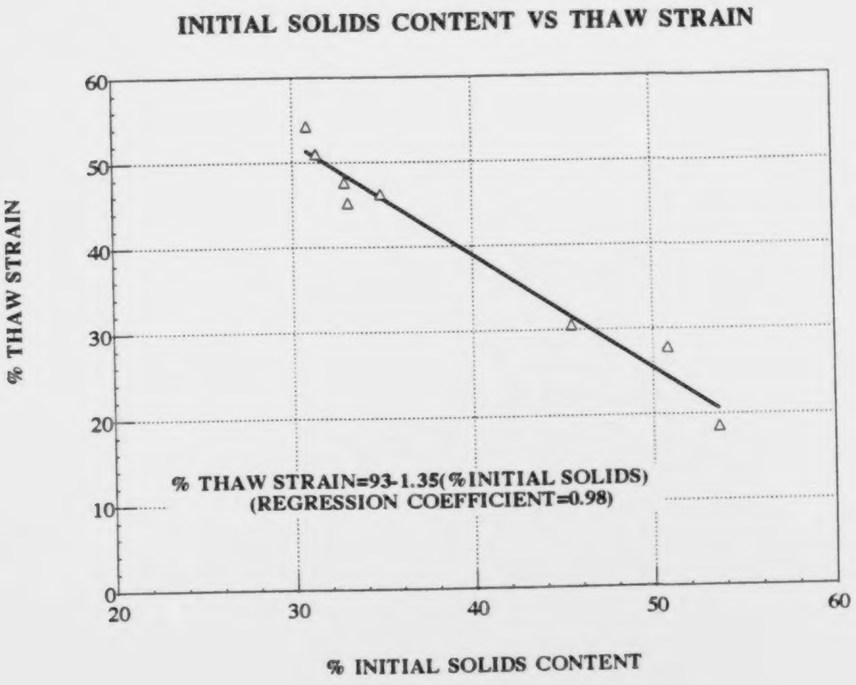

Figure 4.4 OSLO Initial Solids Versus Thaw Strain

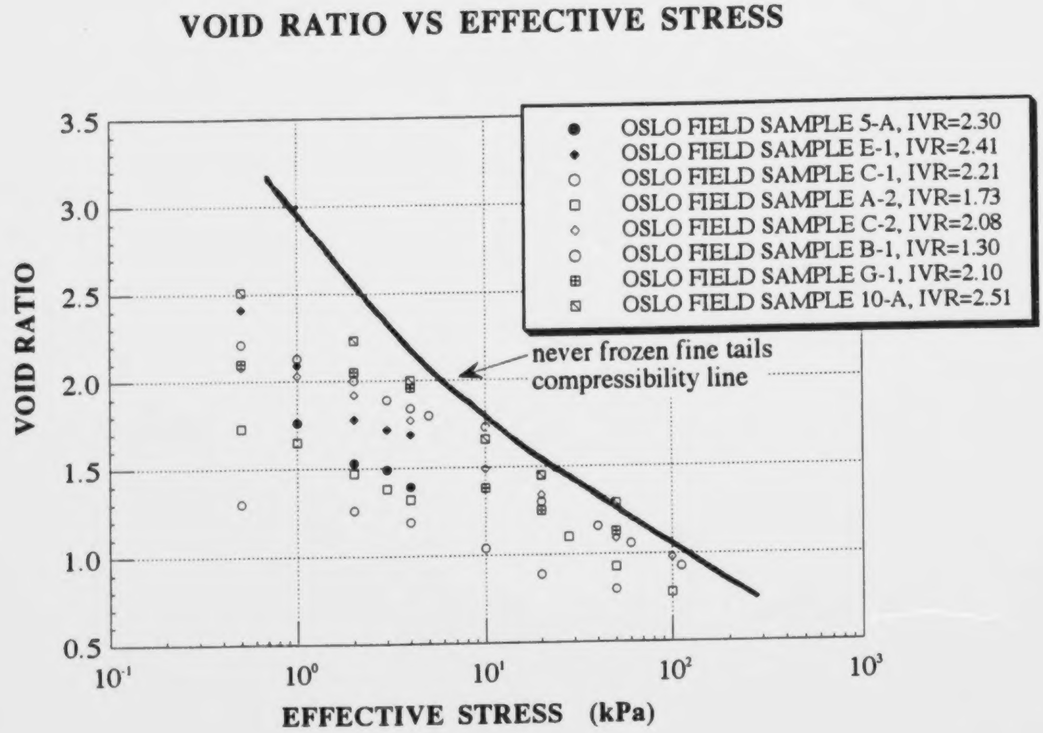

Figure 4.5 Lease 41 Compressibility Data

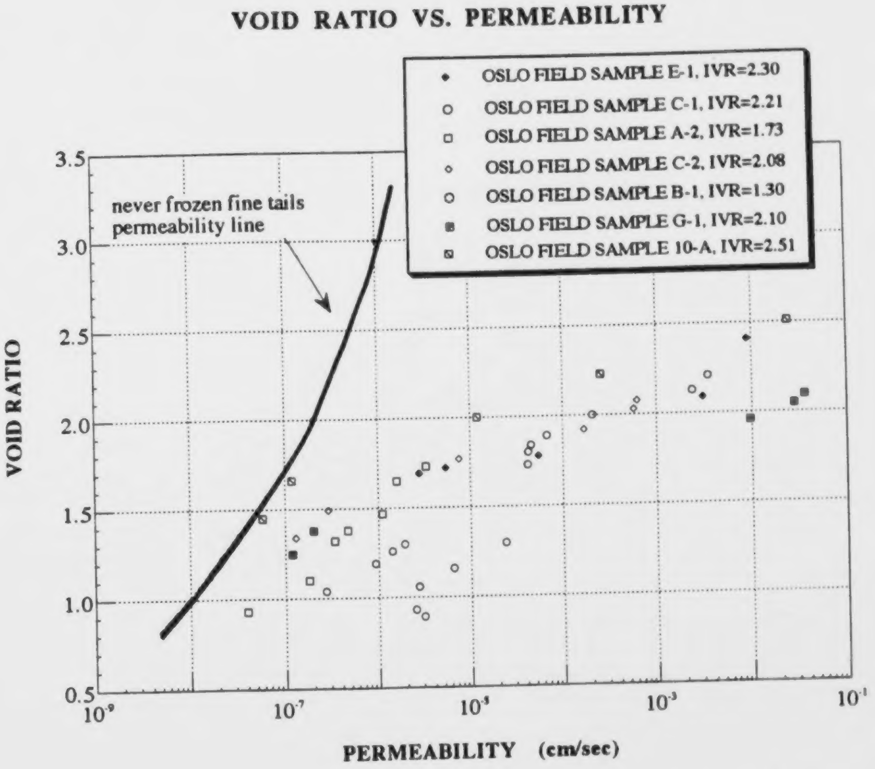

Figure 4.6 Lease 41 Permeability Data

A. NORMALIZED VOID RATIO VS EFFECTIVE STRESS

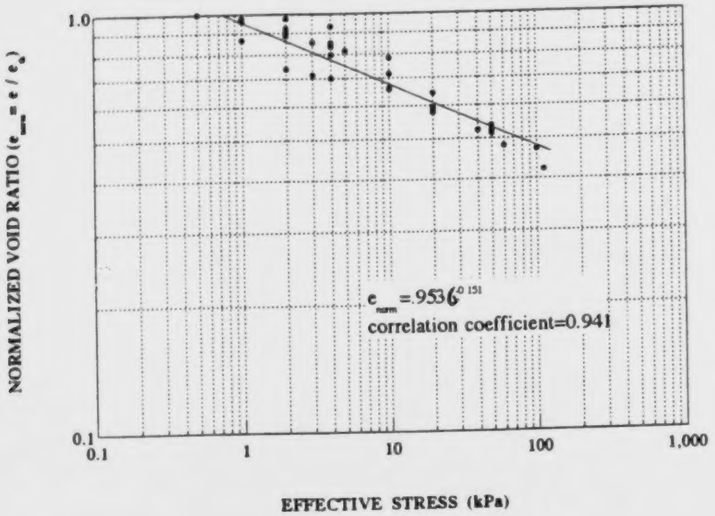

B. NORMALIZED VOID RATIO VS PERMEABILITY

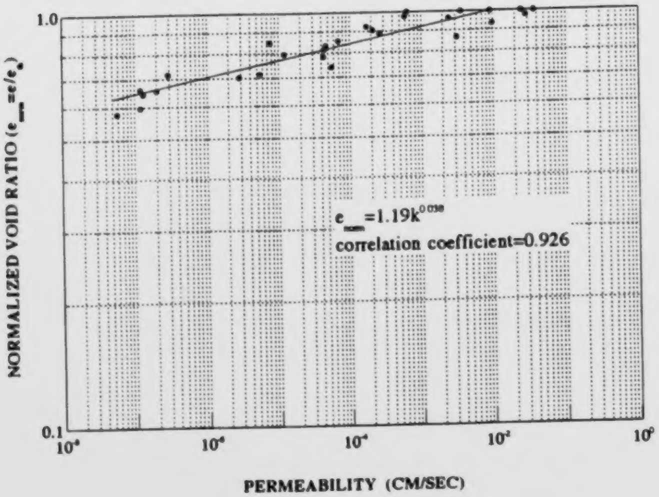

Figure 4.7 Lease 41 Normalized Compressibility and Permeability Plots

A. WINTER PLACEMENT

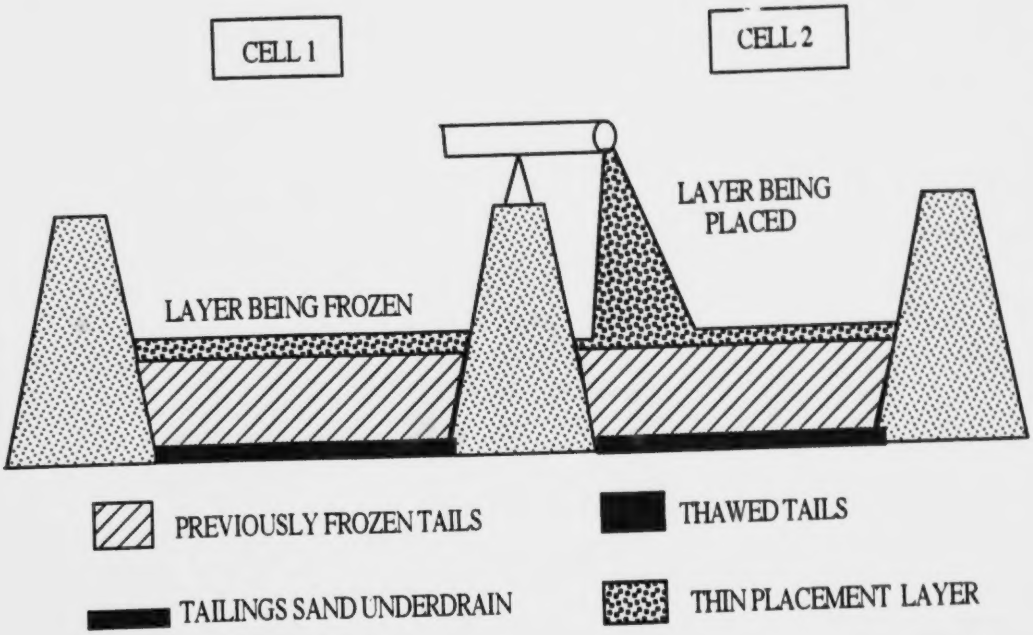

B. SUMMER THAW

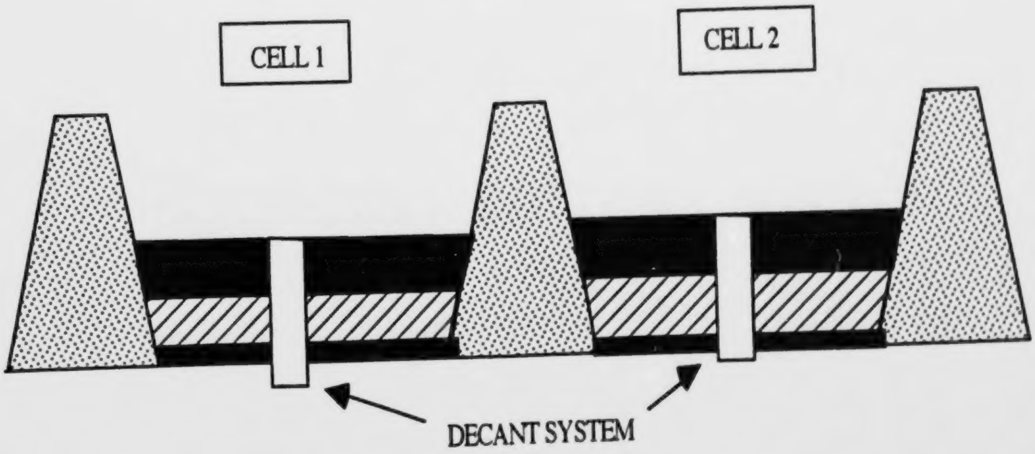

Figure 4.8 Thin Layered Freeze Thaw Disposal Scheme

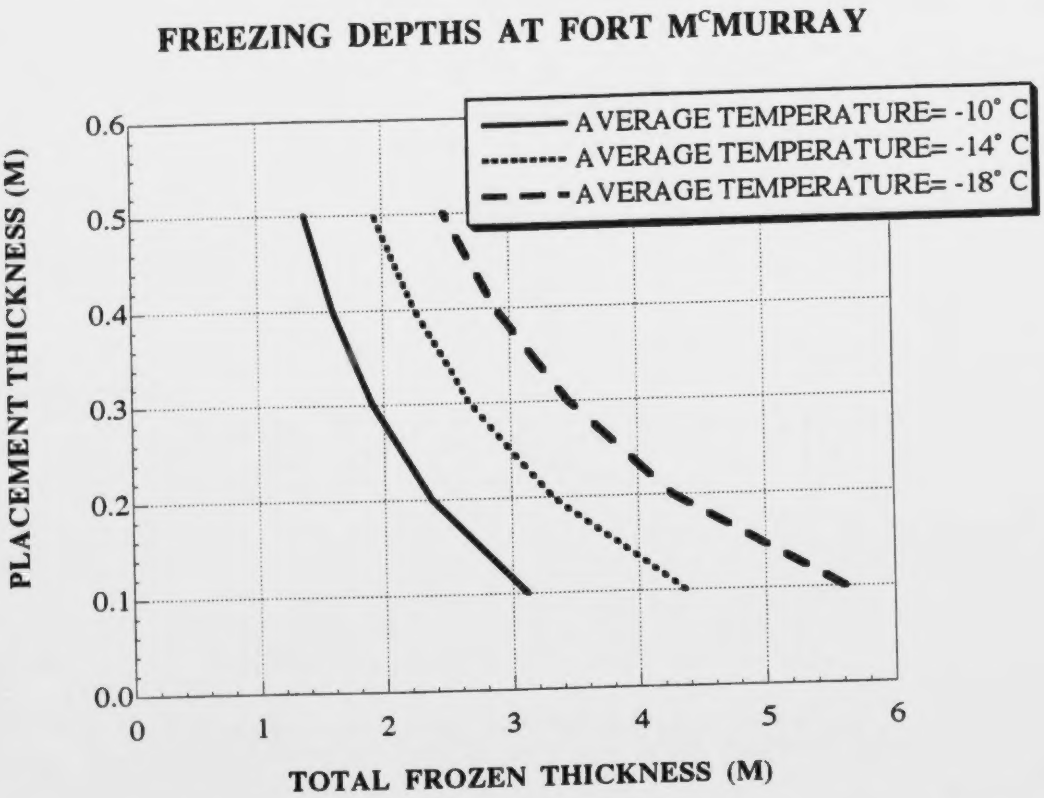

Figure 4.9 freezing Depths at Fort M^{c}Murray

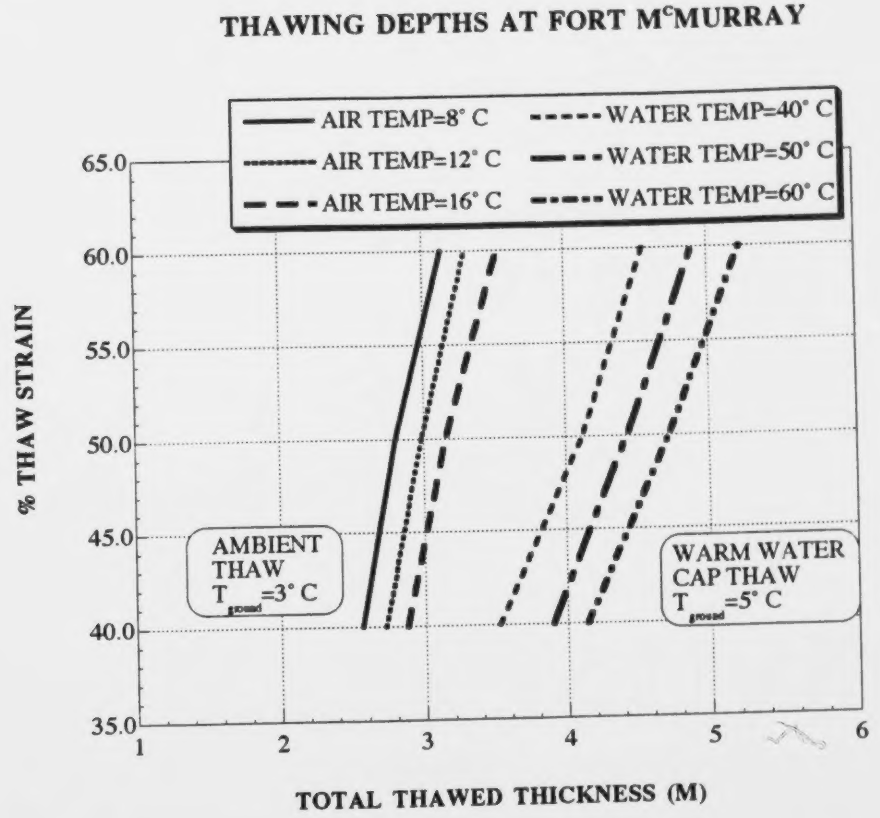

Figure 4.10 Thawing Depths at Fort M^{c}Murray

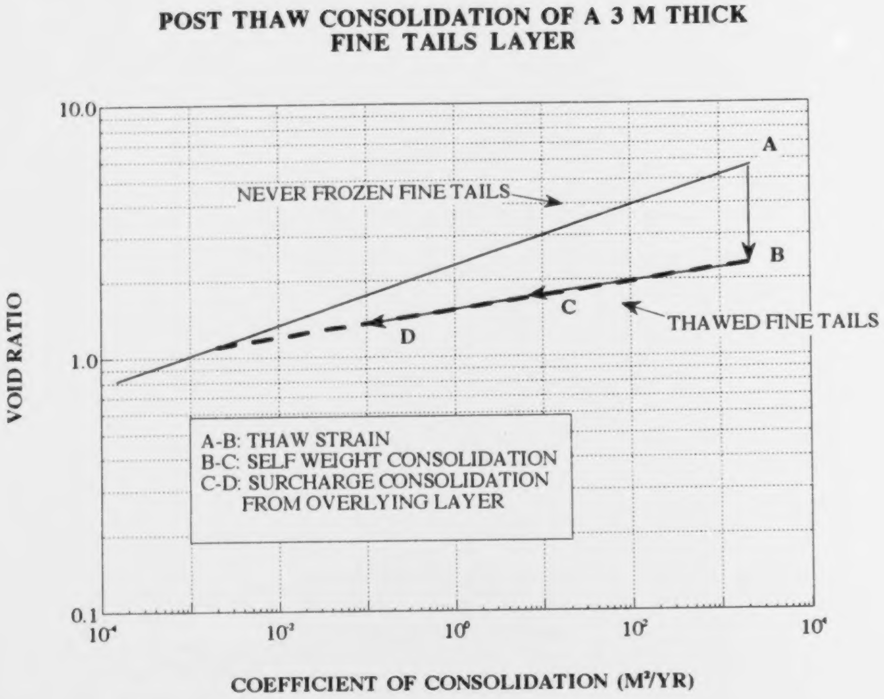

Figure 4.11 Freeze Thaw Dewatering Consolidation Behaviour

A. BOUNDARY CONDITIONS FOR THIN LAYERED THAW CONSOLIDATION

1. FREE DRAINING UPPER BOUNDARY
(SURFACE INTERFACE OR SAND BLANKET)

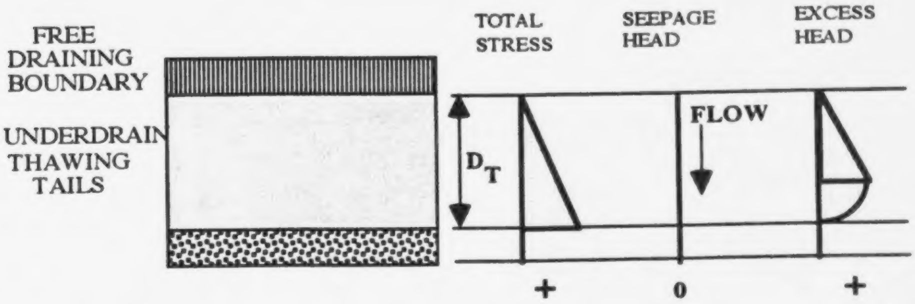

2. UNDRAINED UPPER BOUNDARY

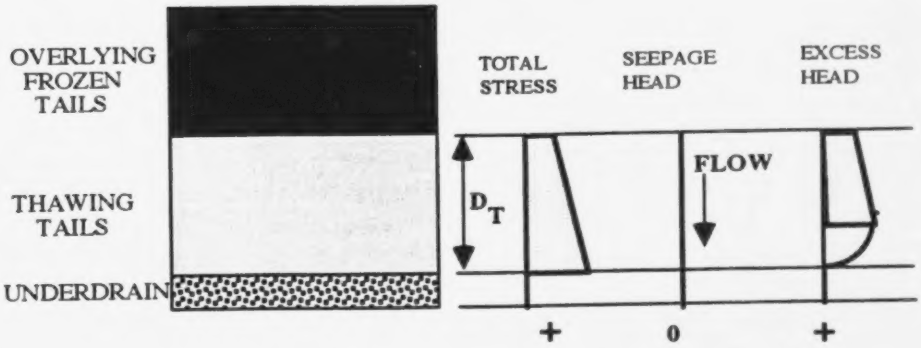

B. GOVERNING EQUATION FOR FINITE STRAIN CONSOLIDATION
(after Somogyi, 1980)

$$\frac{\partial}{\partial z}\left[-\frac{k}{\gamma_w(1+e)}\frac{\partial u}{\partial z}\right]+\frac{de}{d\sigma'}\left[(D_R-1)\gamma_w\frac{d(\Delta z)}{dt}-\frac{\partial u_e}{\partial t}\right]=0$$

Where: z = material coordinate

k = permeability

e = void ratio

u_e = excess pore pressure

σ' = vertical effective stress

γ_w = unit weight of water

t = time

D_R = relative density

Figure 4.12 Finite Strain Consolidation Model

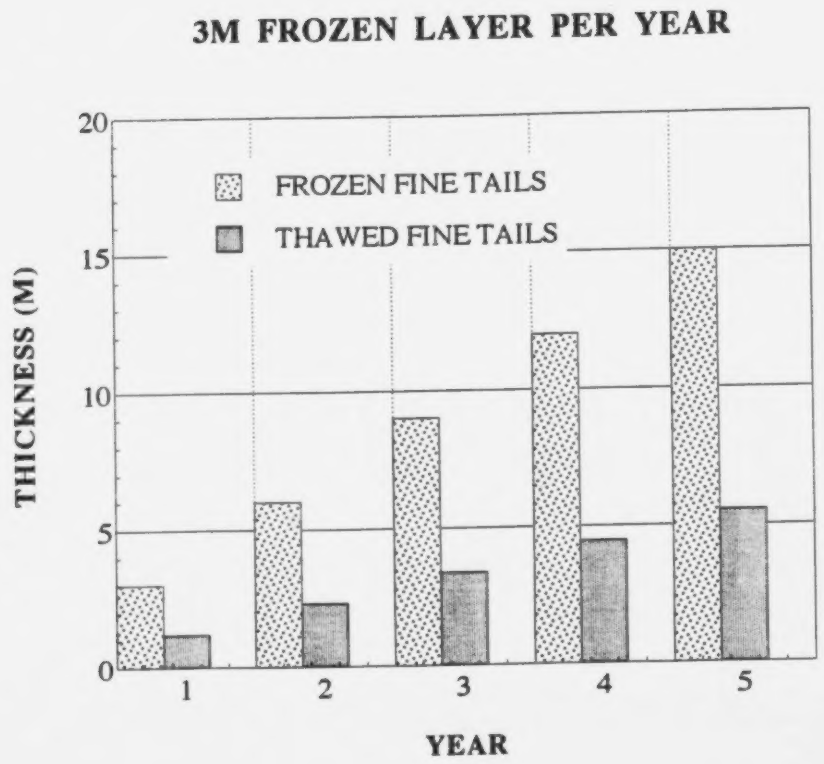

Figure 4.13 Cumulative Thickness for 3m per Year Frozen Thickness

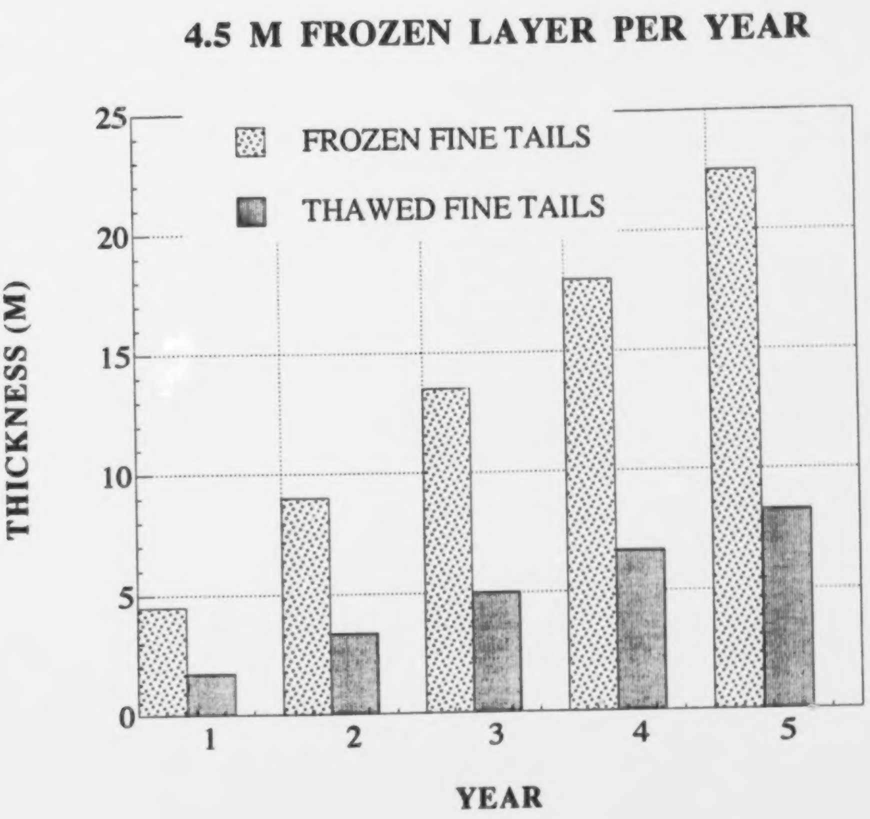

Figure 4.14 Cumulative Thickness for 4.5m per Year Frozen Thickness

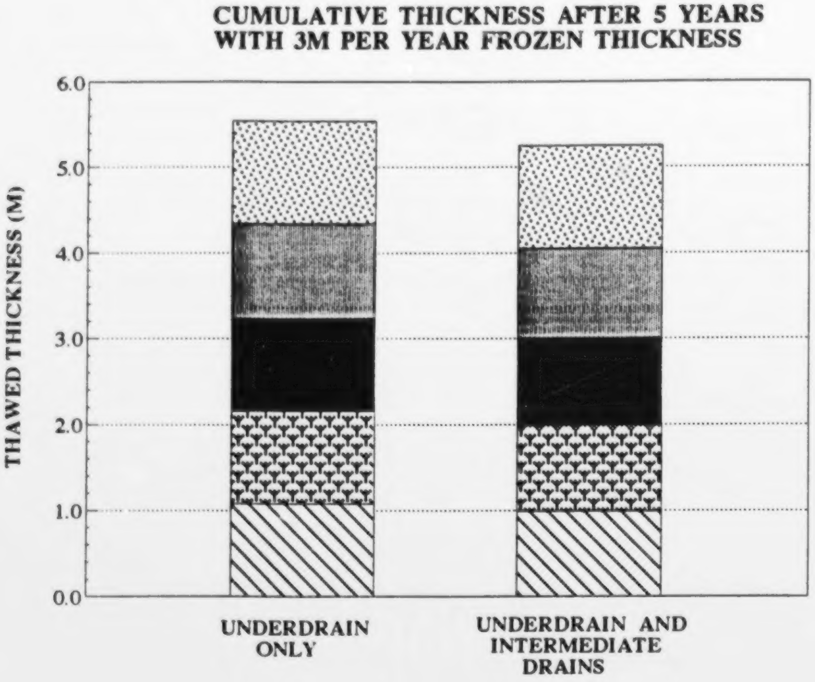

Figure 4.15 3m per Year Single Versus Double Drainage

Chapter 5

STATIC COLLAPSE OF MINE WASTE EMBANKMENTS

5.1 INTRODUCTION

An underlying premise of soil mechanics is that shear strength is a function of effective normal stress and is largely determined by frictional forces arising during slip between particles. Frictional strength is relied upon for the structural integrity of all engineered soil and rock structures.

Fundamental studies by Rowe (1962) and others on granular materials that tend to increase in volume (dilate) when sheared have shown that frictional resistance is comprised of four components: grain to grain sliding (intrinsic friction), grain re-arrangements, resistance to volume change (dilation), and crushing. Higher initial densities and confining stresses result in increased strength. Crushing moderates this effect causing a curved strength envelope. The peak shear strength is coincident with the maximum principal stress ratio at failure. An assessment of density (or void ratio) and confining stresses guides the selection of design friction angles in dilatant granular materials. Conservative designs assume zero dilation and frictional resistance equal to the constant volume friction angle ($\text{Ø}'_{cv}$).

The shear strength of granular materials that tend to decrease in volume (contract) when sheared is normally assumed to be equal to the constant volume friction angle ($\text{Ø}'_{cv}$) which is often taken to be similar to the angle-of-repose. Emerging laboratory and field evidence shows that this may not be a conservative assumption as the operational strength of collapsible materials is stress path dependent and thus may sometimes be less than $\text{Ø}'_{cv}$.

Many mine waste embankments are designed with uncompacted fills. A lack of understanding of the static collapse mechanics initiating flow is an impediment to good design practice and operational serviceability of these structures.

5.2 SHEAR STRENGTH OF LOOSE GRANULAR MATERIAL

For any assemblage of granular particles there is a critical void ratio and confining stress for which shearing produces zero change in volume. Castro (1982) defined this state as the steady state and proposed the following definition:

> *"The steady state of deformation for any mass of particles is that state in which the mass is continuously deforming at constant volume, constant normal effective stress, constant shear stress, and constant velocity. The steady state of deformation is achieved only after all particle orientation has reached a statistically steady state condition and after all particle breakage, if any, is complete, so that the shear stress needed to continue deformation and the velocity of deformation remain constant.."*

The inter-particle frictional behaviour of granular materials at the steady state is not totally understood although the work of Horner (1969) and others provides insight. The steady state is achieved when the original meta-stable structure is broken down due to shear and a new flow structure is formed. Flow of granular material takes place at steady state conditions (Hungr, 1980).

Many granular materials loose of steady state will lose strength (strain weaken) when sheared under conditions of negligible volume change. The strength loss is due to collapse as the loose structure is re-arranged. This material behaviour is known as a brittle response and is often described by the undrained brittleness index (I_b) which is defined as follows:

$I_b = \Delta q / q_{max}$

Where: Δq = difference between peak and steady state deviator stress

q_{max} = peak or maximum deviator stress

The brittle behaviour is a function of the initial confining stress and the stress path to failure. Some tests by Sasitharan (1993) with Ottawa sand illustrate this point clearly. Figure 5.1 shows results of two constant volume tests, one undrained and the other fully drained, consolidated to the same isotropic stress and void ratio. Both tests were then sheared at a constant rate of deformation of 0.15 mm/min. The drained constant volume test stress path was achieved by adjusting the back pressure during loading such that the sample volume remained relatively unchanged. As the figure shows, both effective stress paths and stress/strain curves are essentially identical showing that the stress paths and not the external drainage conditions govern collapse behaviour. The effective friction mobilized at failure is less than the steady state value. The peak strength is reached at a strain of less than 1% and the steady state strength is about one third the peak value. This dramatic drop in strength that occurs at very small strains is responsible, under constant volume conditions, for the generation of high pore pressures that sustain mobile flowslides. The pore pressures that are generated need not be a result of seismic or other "undrained" loading triggers.

A similar reduction in effective strength has been observed by Eckersley (1991) during studies of flow failure in model coal stockpiles:

> *" flowslides can initiate under essentially static, drained conditions, and liquefaction occurs subsequent to failure initiation with excess pore pressures being generated in relatively thin shear zones."*

The sudden loss in strength of loose materials is attributed to collapse of a meta-stable structure. Sladen et al (1985) have shown that for a constant void ratio the peak strengths of samples tested at different confining stresses lie on a straight line, referred to as the collapse surface. Stress paths normalized to the steady state strength define a line, joining the maximum shear peaks. Figure 5.2 shows this phenomenon for constant volume (in this case undrained) stress paths of Erksak sand (Been et al,1991).

Dry sand also exhibits collapse behavior at effective friction angles less than those associated with the steady state condition (Skopek et al, 1994). In collapsing dry sands the sudden volume change may not be sufficiently impeded (air is compressible and water is relatively incompressible) and thus a drop in shear strength commensurate with excess pore pressure development does not take place. As a result the collapse of a wet material results in a more mobile flow than the collapse of the same material in a dry state.

Flow failures of wet granular materials, often termed liquefaction flowslides, are explainable in terms of collapse and steady state flow mechanics. The term liquefaction implies a complete loss of static shear strength (zero frictional resistance), although this is seldom the case. At normal stress levels often encountered in engineering practice significant static shear strength is mobilized at the steady state. The high mobility of wet granular flows is due to the dramatic drop in effective stresses caused by excess pore pressures generated during collapse.

5.3 FLOWSLIDES IN MINE WASTE EMBANKMENTS

Highly mobile, accelerating, and rapidly initiating flow failures are potentially serious safety and environmental hazards. Hutchinson (1988) has defined a liquefaction flowslide as :

> " *characterized by the sudden collapse and extensive, very to extremely rapid run-out of a mass of granular material or debris, following some disturbance. An essential feature is that the material involved has a meta-stable, loose or high porosity structure. As a result of the disturbance this collapses transferring the overburden load wholly or partly onto the pore fluid, in which excess pressures are generated. The consequent loss of strength gives the failing material, briefly a semi-fluid character and allows a flow slide to develop.* "

Bishop (1973) first pointed out the important relationship between potential mobility of a failing slope and brittleness of the soil materials prior to failure. Bishop published compelling examples demonstrating that more highly mobile flow-like slope movements tended to be associated with significant brittle behaviour of the embankment materials, particularly the undrained brittle behaviour which results in the generation of excess pore pressures.

Work by Castro (1982) and others on the undrained brittle behaviour of loose sands has resulted in a rational framework for understanding flowslides initiated by seismic and other rapid loading dynamic triggering phenomenon. Flowslides initiated by static processes are not as well understood and thus are often not adequately considered during design.

TAILINGS EMBANKMENTS

Vick (1991) has reviewed the runout risks associated with 32 tailings dam flow failures. Over 50% of the flowslides occurred without any related seismic activity. The cause of failure for the non-seismic events was variously attributed to piping, seepage, overtopping, slope instability, and erosional breach by pipeline rupture. In many cases the non-seismic instability mechanisms are not clear.

Many flowslides occur with little warning and a lack of preparedness results in little opportunity for piecing together reliable historical information for back analyses. Oftentimes, tailings related flowslides are accompanied by the discharge of underconsolidated slimes (mud) that are released when the structural tailings sand shell fails. Evidence required for understanding the instability mechanics is often obscured by the mud flow.

The failure of a large tailings pile in Zimbabwe, Africa (Shakesby and Whitlow, 1991) is a particularly compelling example of static collapse and flow of tailings sands. On January 31, 1978 a tailings embankment at the Arcturus Gold Mine in north-eastern Zimbabwe collapsed with a "loud bang" and 30,000 tonnes of material flowed 300 metres downslope killing one child and injuring another. Heavy rains occurred prior to failure. The facility was designed so that significant dewatering occurred due to evaporation and most of the surface water drained down through the penstock, even during heavy rainfalls similar to the events that preceded the failure. The investigation conducted by Shakesby and Whitlow (1991) revealed that "the high void ratios of the basal tailings through which the failure scars passed, are similar to or exceed the critical void ratios calculated for comparable fine tailings." Loss of cohesion due to wetting caused collapse and flow of the loose granular material.

WASTE ROCK PILES

Until the Aberfan disaster (Bishop,1973) in 1966 it was not generally recognized that flowslides could occur in coarser materials deposited initially in a "dry" state. At Aberfan a flowslide occurred when over 100,000 cubic metres of colliery waste (sandy gravel texture) failed and flowed 600 metres into the town of Aberfan in Wales. The flowslide resulted in the loss of 144 lives, mostly children attending a Junior School, which was demolished by the flow. There was no seismicity associated with the catastrophe.

Rocky Mountain coal mine waste dumps in Western Canada have suffered numerous high runout failure events. Golder Associates (1991) have compiled historical data on 42 British Columbian coal mine waste dump flow slides. Figure 5.3 shows the dump height versus runout distances for these events. More than half of the events exhibited runouts exceeding 500 meters and there are 8 flow slides documented for which runouts exceeded 1 kilometer. The areas in which these coal mines are located are relatively aseismic and none of the events has been attributed to seismic activity. An earlier study of coal mine waste dumps in British Columbia by Golder Associates (1987) states :

> *"It is quite probable that the presence of significant zones of finer-grained, less durable material has contributed to either failure events or periods of high crest*

deformation which have not been reported as being linked to the presence of fine material...

We consider that a significant number of factors which have been attributed primarily to such factors as excessive precipitation and also steep foundations slopes may, in fact, also have been affected by the presence of weaker, fine grained material."

Detailed study of three coal mine waste dump flowslides by Dawson et al (1994) presents convincing evidence that the waste material in the dumps are susceptible to collapse and flow processes.

Stability evaluations for granular fill embankments containing loose materials requires special considerations for evaluating the potential rapid loss in strength that results in collapse and subsequent flow. This involves an assessment of:

1. Steady state and collapse surface behaviour

2. Trigger mechanics

3. Progressive failure

These issues are examined in the text that follows mainly with respect to data from triaxial testing.

5.4 STEADY STATE AND COLLAPSE BEHAVIOUR

Most tailings embankments consist of fine sands deposited hydraulically. Most mine waste dumps consist of sandy gravels and coarser materials deposited in a "dry" state. This chapter reviews the steady state and collapse behaviour of sands and gravels as determined from triaxial tests.

Table 1 shows the index properties for some fine quartz sands, listed in order of increasing uniformity coefficient (C_u). Figure 5.4 shows the steady state and collapse surface behaviour for the first two sands in Table 5.1, a sub-rounded marine sand dredged from the Beaufort Sea (Been et al,1992) and an angular mine tailings sand (Castro,1982). The two data sets are representative of collapse and flow behaviour over a wide stress range and illustrate several important points as follows:

1. STEADY STATE UNIQUENESS: For each data set, the steady state points lie on a unique line in void ratio (e) - mean stress (p') - deviator stress (q) space. The e - p' relationship is commonly plotted as e - log p' in order to linearize the relationship. Been et al (1991) point out that the steady state for each test specimen must be chosen carefully and after deformations proceed without any further changes in stress conditions. In some cases very high strains in excess of 15 to 20 % are required to reach steady state.

2. BREAK POINT: Each steady state data set exhibits a break point stress separating two roughly bilinear segments. The break point is due to crushing (Been et al, 1991). Vesic and Clough (1968) referred to this point as the breakdown stress and pointed out that it is a function of mineral composition, gradation, and particle shape. The break point,where clearly distinguishable, appears to be an intrinsic material property. Beyond the break point true steady state behaviour is often difficult to discern due to continuous crushing. At a stress level of about 1 MPa both data sets converge onto a common envelope.

3. COLLAPSE PROPERTIES: The collapse surface of the angular tailings is steeper than the more rounded marine sand. Hird and Hassona (1990) show a similar trend of increasing steepening collapse surface with increasing angularity. Beyond the break point the stress strain curves show a marked decrease in brittleness. The effects of crushing on collapse and steady state behaviour merits further investigation.

Figure 5.5 shows the steady state and collapse properties for the four angular materials in Table 5.1. The steady state behaviour of the mine tailings sand forms an envelope for the other three crushed gravel materials. The crushed quartz gravel data (De Matos, 1988) shows that the effects of grading on steady state behaviour are dramatic. At a given confining stress, the steady state void ratio decreases with increasing uniformity coefficient (grading). Thus very broadly graded sandy materials are more susceptible to liquefaction due to the high relative densities at steady state. Small amounts of clay and silt sized particles that increase compressibility may reduce this trend however. Hassona (1990) demonstrates that the presence of small amounts (greater than 10%) of fine mica particles reduces the liquefaction potential of fine sands. Taylor (1984) determined that coal mine tailings from the U.K. with liquidity indices greater than 10 were unlikely to liquefy. Presumably the higher plasticity materials were more compressible and thus less brittle. Compressibility appears to have a major influence on undrained brittle behaviour. As compressibility increases brittleness appears to decrease.

Table 5.2 shows the index properties of some gravely materials derived from several literature sources and a recently completed University of Alberta study (Dawson et al , 1994). Steady state behaviour of the sandy gravels is shown in Figure 5.6. Despite the range in material types, mean grain sizes and grading, a remarkably consistent trend of steady state behaviour is observed. The steady state is achieved at void ratios lower than the most widely graded crushed gravel in Figure 5.6. Uniformity coefficients for the gravel materials range from 20 to 60. The collapse surface of the more friable sandy gravel materials decreases with increasing confining stress indicating that crushing during consolidation is eliminating the brittleness (Dawson et al, 1994).

Table 5.3 shows a summary of the steady and collapse behaviors for the different materials discussed above. The summary data is representative of the tests where significant crushing was not taking place (i.e. before the break point). Apart from the very shallow steady state slope of the sub rounded marine sand, the other sands exhibit similar steady state gradients when expressed on a log scale (note that the slope beyond the break point was not considered). The steady state friction angle ($\emptyset_{ss}$) is notably larger for the sandy gravel materials. By far the greatest variable is the position of the steady state line with respect to void ratio, denoted in Table 5.3 by the e_{10} intercept (void ratio at p'= 10kPa). The shallow slope of the steady state line and high void ratio sensitivity to material gradation are inherent difficulties for liquefaction evaluations. The placement density with respect to the steady state (at zero mean effective stress) will determine whether consolidation is initiated in a loose or dense state.

5.5 TRIGGER MECHANICS

Although the framework of steady state and collapse surface define necessary boundary conditions for collapse and flow they are not sufficient conditions. Collapse must be triggered and pore pressures sufficiently impeded to produce a mobile flow. It appears that two related conditions must be satisfied in order for collapse and subsequent strain weakening behaviour to occur: :

1. The triggering stress path must approach the collapse surface in such a fashion as to force a rapid, rather than gradual, structural re-adjustment.

2. Pore pressures must be sufficiently impeded during structural collapse so that excess pore pressures develop and a significant loss of strength occurs.

Figure 5.7 shows the results of two triaxial tests conducted by Sasitharan et al. (1993) to demonstrate "drained" collapse caused by a rising water table. The undrained stress path shown in Figure 5.7 shows the collapse and steady state surfaces for a void ratio of 0.804. Another sample was consolidated isotropically to the same void ratio (initial consolidation state) and a constant q test was carried out to simulate pore pressure increase due to a rising water table. The sample followed the constant q stress path until the average effective stress was about 140 kPa and then the sample immediately collapsed. Collapse occurred so rapidly that it was not possible to collect test data. At the point of collapse "the sample reached such a large momentum during collapse that when the loading head hit the restricting nuts the entire laboratory felt the vibration" (Sasitharan et al., 1993). Prior to collapse the stress state was very close to the stress path defined by the undrained test.

The stress path resulting from wetting, when expressed in terms of effective stress, is the same as that for a rising water table. Wetting results in a loss of apparent cohesion due to matric suction in unsaturated soils. This is the mechanism responsible for "collapsible foundations". The same process can occur in an embankment. If the material is sufficiently saturated during collapse then excess pore pressures will develop that can lead to a liquefaction flowslide. Sassa (1988) demonstrates that degrees of saturation of about 85% are sufficient to initiate excess pore pressures.

Other static triggers may also be possible although further research is necessary to explore individual stress paths. It seems rational to assume that loading paths resulting in decreases or small increases in average effective stresses accompanied by small volume changes are particularly collapse sensitive. Collapse might also occur due to high shear strains, weathering, creep, and other processes. Foundation strains are known to have triggered liquefaction of hydraulic fill structures (Morgenstern and Küpper, 1988).

The conventional safety factor approach does not provide a conservative assessment of collapse potential. With reference to Figure 5.7, the factor of safety with respect to the constant volume friction angle ($q_{cv}/q_{initial}$) is always greater than a factor of safety with respect to the collapse surface ($q_{collapse}/q_{initial}$). Conventional engineering analysis does not directly recognize static collapse processes and the "lower bound" safety factor is normally calculated with respect to the constant volume friction angle. For waste dump design, the constant volume friction angle is approximately equal to the angle-of-repose.

Once collapse is initiated excess pore pressure will only be generated if drainage is sufficiently impeded due to geometry (length of flow path) or hydraulic characteristics (permeability). Critical drainage lengths and permeability values have not been measured for different collapse processes. Experience suggests that most sands and sandy gravel embankment materials exhibit sufficiently low permeability's to sustain excess pore pressures if collapse is initiated.

5.6 PROGRESSIVE FAILURE

Triggering of localized yield zones in strain softening materials will cause stress re-distributions that can lead to progressive failure. The release of driving shear stress from the peak to the steady state must induce re-distribution of stresses in an embankment. If not contained these re-distributions can lead to overall collapse and flow. Progressive failure is responsible for overall collapse as the initial trigger does not usually render the whole embankment unstable.

Gu (1992) demonstrates initial triggering (caused by an earthquake), collapse, progressive failure, and flow of the Lower San Fernando dam. The initial yielding zones caused by the earthquake were very small compared to the total volume of the flow that occurred about 30 seconds after the main shaking stopped.

Dawson et al (1994) demonstrate static collapse, progressive failure, and flow of coal mine waste dumps. Significant unspent collapse energy at failure may be contributing to the high mobility of the runouts. Strain weakening of finer collapsible materials within the dumps causes considerable yielding of coarser non-collapsible material.

5.7 CONCLUSIONS

Uncompacted fills contained in mine waste embankments are prone to static collapse processes. A brief review of flowslides in mine waste embankments shows that the initiating mechanisms are not always due to seismic loading and other rapid loading phenomena. Flowslides can also be initiated by static "drained" loading mechanisms. A conceptual framework for understanding and evaluating liquefaction flowslide potential, discussed in this paper, illustrates the following points:

1. The steady state strength and collapse surface, determined from conventional undrained triaxial tests define the static collapse potential of a soil element.

2. Collapse can be initiated by a rising water table and other triggers that require further research in order to better define.

2. Conventional limit equilibrium factor of safety calculations are not conservative with respect to collapse potential.

3. Progressive failure can rapidly contribute to overall flow failure once local collapse has been initiated.

The design and construction of mine waste embankments should be sensitive to static collapse processes despite uncertainties with respect to a fundamental understanding of these processes.

5.8 REFERENCES

Balasubramanium, A.S., Lee, L.H., and Wyeyakulasiruya, V., 1987. Stress-Strain Behaviour of Rockfill. Proceedings 8th Asian Reg. Conference on Soil Mechanics and Foundation Engineering, Kyoto, Japan, Vol. 1, pp. 21-25.

Been, K., Jefferies, M.G., and Hackey, J., 1991. The Critical State of Sands. Geotechnique, Vol 41, No. 3, pp. 365-381.

Bishop, A.W., 1973. The Stability of Tips and Spoil Heaps, Quaternary Journal of Engineering Geology, Vol. 6, pp. 335-376.

Bolognesi, A.J.L. and Mecucci, C.A., 1987. Steady State and Deformation in Gravels. Proceedings 8th Pan Am Conference on Soil Mechanics and Foundation Engineering, Vol. 2, pp. 521-532.

Brown, A.J., 1988. Use of Soft Rockfill at Evreton Dam. Geotechnique, Vol 38, No. 3, pp. 333-354.

Castro, G., Poulos, S.J., France, J.W., Enos, J.L., 1982. Liquefaction Induced by Cyclic Loading. Report to National Science Foundation, Washington, D.C.

Dawson, R.F., Morgenstern, N.R., and Gu, W.H., 1994. Liquefaction Flowslides in Western Canandian Coal Mine Waste Dumps, Phase 2: Case Histories. Report to Supply and Services Canada, File No. XSG42-00138(608), 112 p.

DeMatos, M.M., 1988. Mobility of Rock and Soil Avalanches. Ph.D. Thesis, University of Alberta.

Eckersley, J.D., 1985. Flowslides in Stockpiled Coal. Engineering Geology, Vol. 22, pp. 13-22.

Eckersley, J.D., 1990. Instrumented Laboratory Flowslides. Geotechnique, Vol. 40, No. 3, pp. 489-502.

Golder Associates Ltd., 1991. Runout Characteristics of Debris from Dump Failures in Mountainous Terrain. Report to Supply and Services Canada, Contract No. 23440-0-9198/01-X8G.

Gu, W.H., 1992. Liquefaction and Post Earthquake Deformation Analysis. Ph.D. Thesis, University of Alberta.

Hassona, F.A.K., 1990. The Effect of Fines on the Liquefaction Behaviour of Cohesionless Soils. Proceedings of 6th International Congress of Association of Engineering Geologists, Rotterdam, Vol. 3, pp. 1595-1602.

Hird, C.C. and Hassona, F.A.K., 1990. Some Factors Affecting the Liquefaction and Flow of Saturated Sands in Laboratory Tests. Engineering Geology, Vol. 28, pp. 149-170.

Horne, M.R., 1965. The Behaviour of an Assembly of Rotund, Rigid, Cohesionless Particles. Proceedings of the Royal Society, Vol. 286, pp. 62-97.

Hungr, O., 1981. Dynamics of Rock Avalanches and Other Types of Slope Movements. Ph.D. thesis, University of Alberta.

Hutchinson, J.N., 1988. General Report. Morphological and Geotechnical Parameters of Landslides in Relation to Geology and Hydrogeology. 5th International Symposium on Landslides, Lausanne, Switzerland, Vol. 3, pp. 3-35.

Rowe, P.W., 1962. The Stress Dilatance Relation for Static Equilibrium of an Assembly of Particles in Contact. Proceedings Royal Society, Vol. 269, pp. 500-527.

Sasitharan, S., Robertson, P.K., Sego, D.C., and Morgenstern, N.R., 1993. A State Boundary Surface for Sand and its Practical Implications. Canadian Geotechnical Journal (in press).

Sassa, K., 1985. The Mechanism of Debris Flows. Proceedings of 11th International Conference on Soil Mechanics and Foundation Engineering, Vol. 3, pp. 1173-1176.

Skopek, P., Morgenstern, N.R., Robertson, P.K., and Sego, D.C., 1994. Collapse of Dry Sand. Submitted to the Canadian Geotechnical Journal.

Sladen, J.A., D'Hollander, R.D., and Krahn, J., 1985. The Liquefaction of Sands, a Collapse Surface Approach. Canadian Geotechnical Journal, Vol 22, pp. 564-578.

Taylor, R.K., 1984. Composition and Engineering Properties of British Colliery Discards. London: Mining Department, National Coal Board, London, 244p.

Vesic, A.S. and Clough, G.W., 1968. Behaviour of Granular Materials Under High Stresses. ASCE Journal of Soil Mechanics and Foundations, Vol. 94, No. 5, pp. 661-688.

TABLE 5.1 INDEX PROPERTIES OF FINE QUARTZ SANDS

DESCRIPTION	SOURCE	D_{50} (mm)	C_U	- 200M (%)	e_{max}	e_{min}
SUB ROUNDED MARINE SAND	Been et al, 1991	0.330	1.80	0.7	0.753	0.527
ANGULAR TAILINGS SAND	Castro et al, 1982	0.256	2.71	6.5	1.08	0.62
CRUSHED GRAVEL #1	De Matos, 1988	0.15	3.0	16.8	1.013	0.416
CRUSHED GRAVEL #3	De Matos, 1988	0.15	13.4	33.7	0.908	0.500
CRUSHED GRAVEL #6	De Matos,1988	0.15	24.6	38.8	0.867	0.708

TABLE 5.2 INDEX PROPERTIES OF SANDY GRAVELS

DESCRIPTION	SOURCE	D_{50} (mm)	C_U
QUARRY LIMESTONE	Brown, 1988	5.0	60
IGNEOUS GRAVEL	Bolognesi and Micucci, 1987	4.3	40
COAL	Eckersley, 1991	2.0	40
SANDSTONE ROCKFILL	Balasubrumanium et al, 1991	2.0	30

TABLE 5.3 SUMMARY OF COLLAPSE AND FLOW PROPERTIES

DESCRIPTION	e- intercept @ 10 kPa	e- log p' slope	$\O_{ss}$	$\O_{col}$
SUB ROUNDED MARINE SAND	0.78	0.03	32	17
ANGULAR TAILINGS SAND	1.05	0.06	34	27
CRUSHED GRAVELS #1 #3 #6	0.89 0.70 0.56	0.05	30	22-24
SANDY GRAVELS	0.37-0.47	0.08	35-42	5- 20

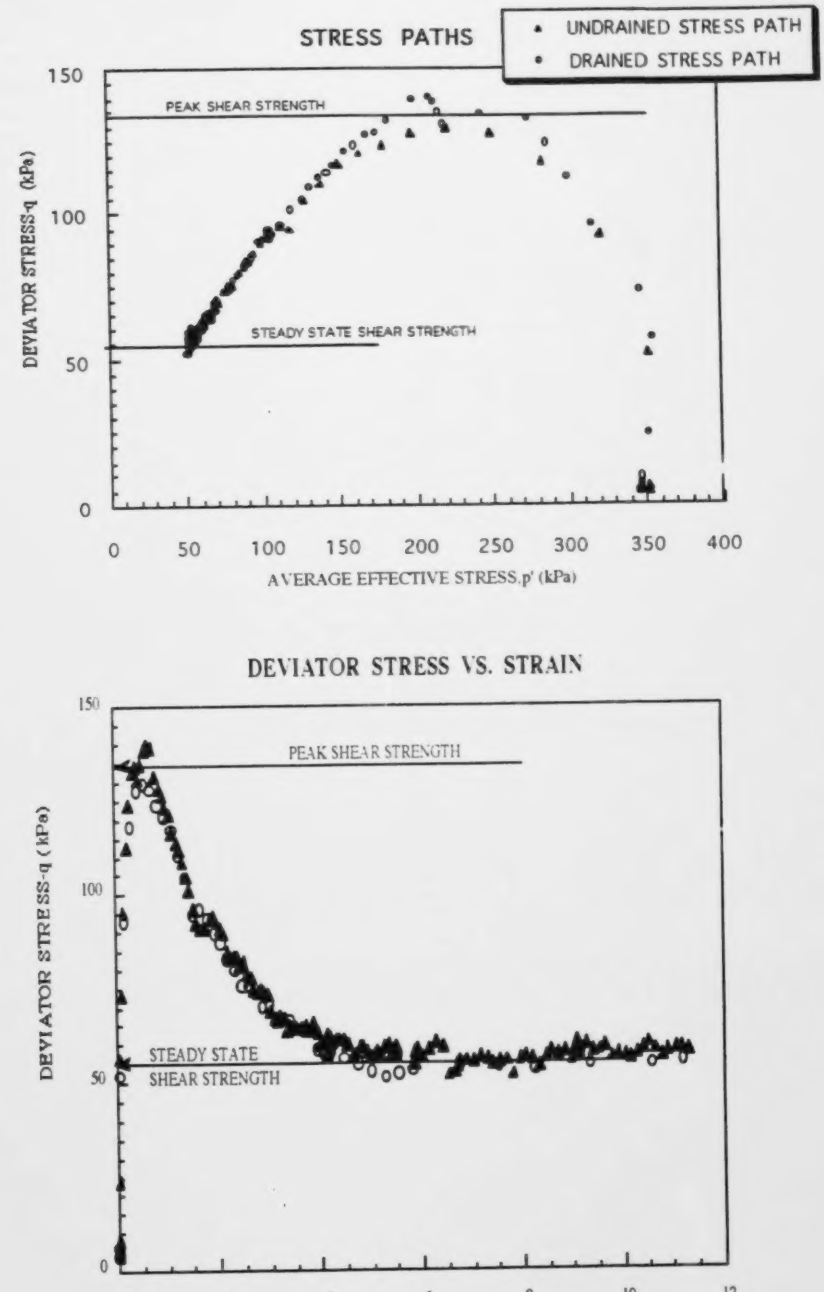

Figure 5.1 Constant Volume Collapse of a Loose Sand

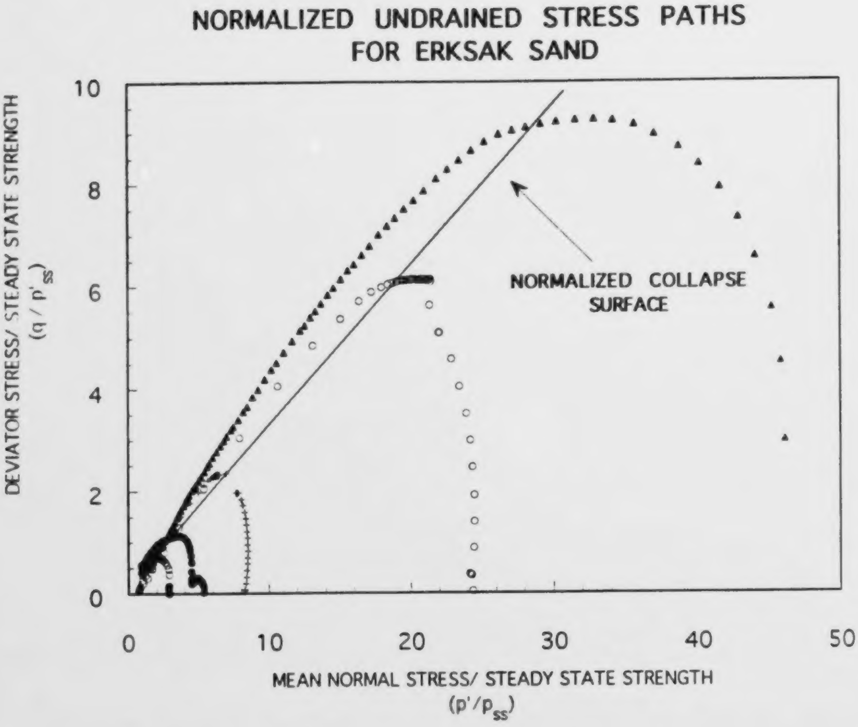

Figure 5.2 Normalized Collapse Stress Paths

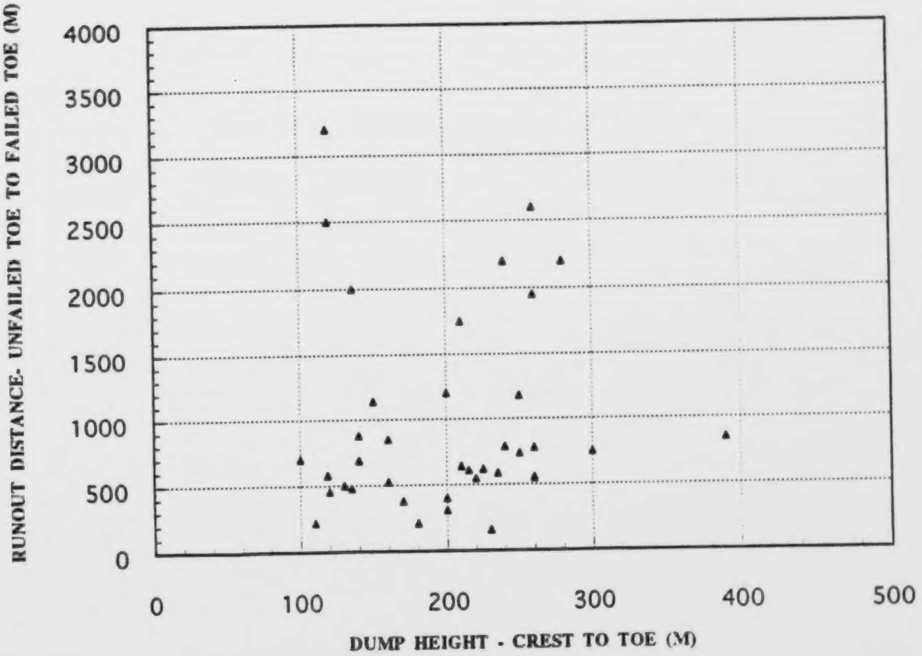

Figure 5.3 Western Canadian Coal Mine Flowslide Statistics

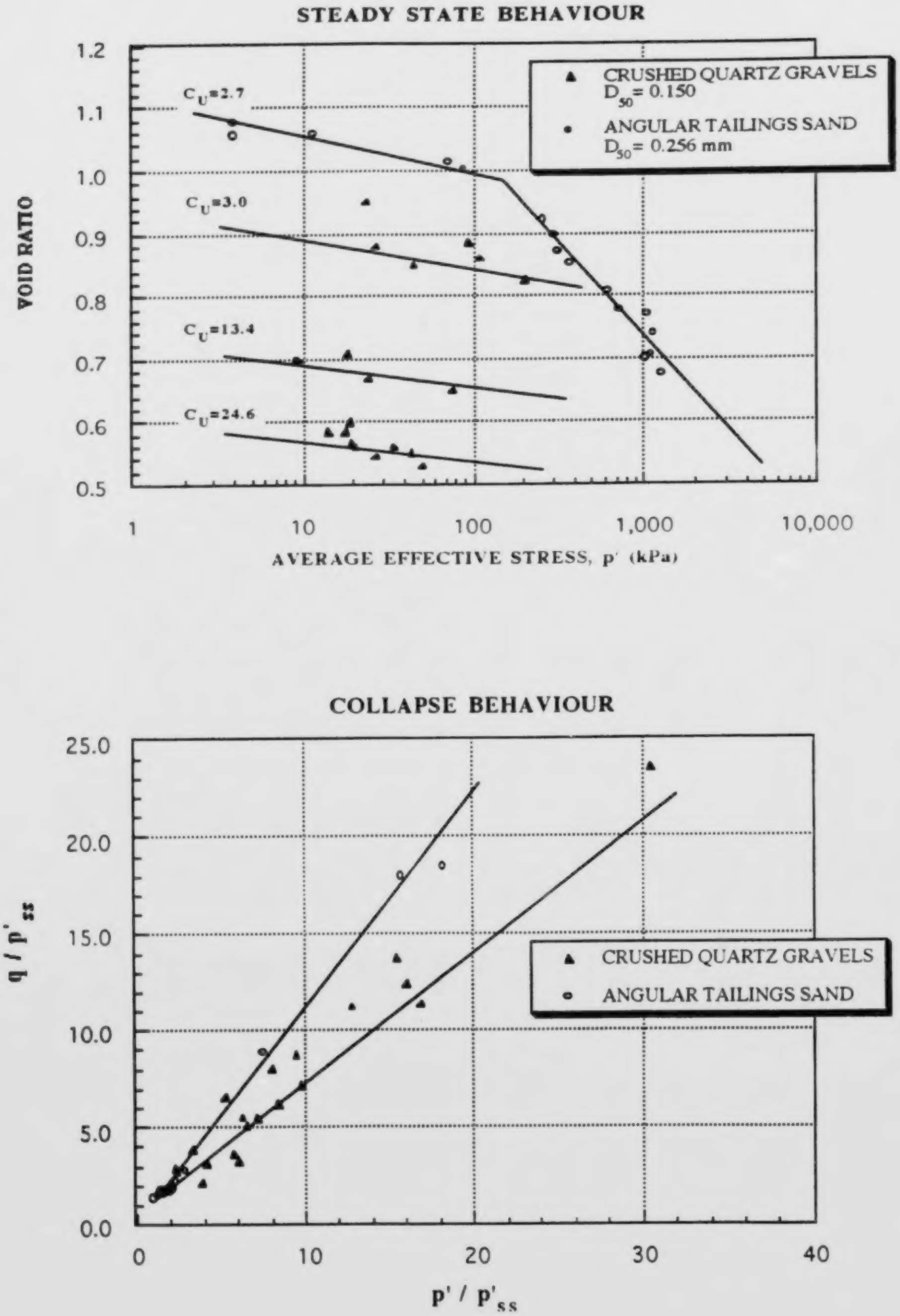

Figure 5.4 Steady State and Collapse Behaviour of Fine Sand

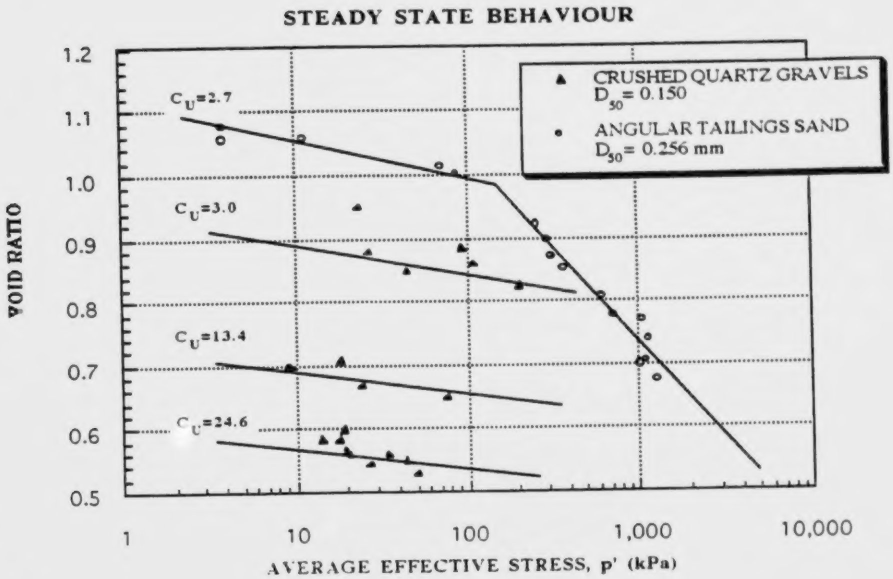

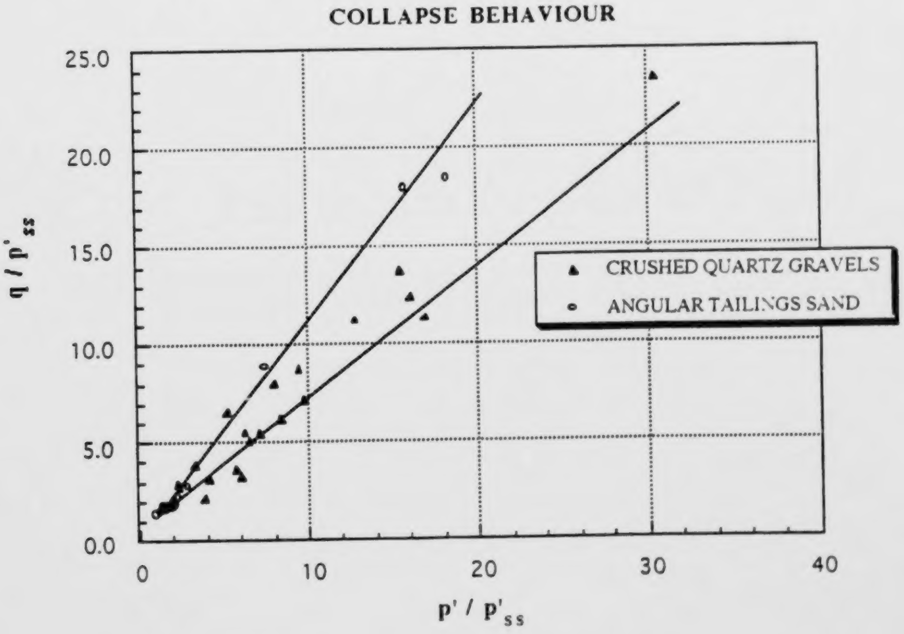

Figure 5.5 Steady State and Collapse Behaviour of Angu

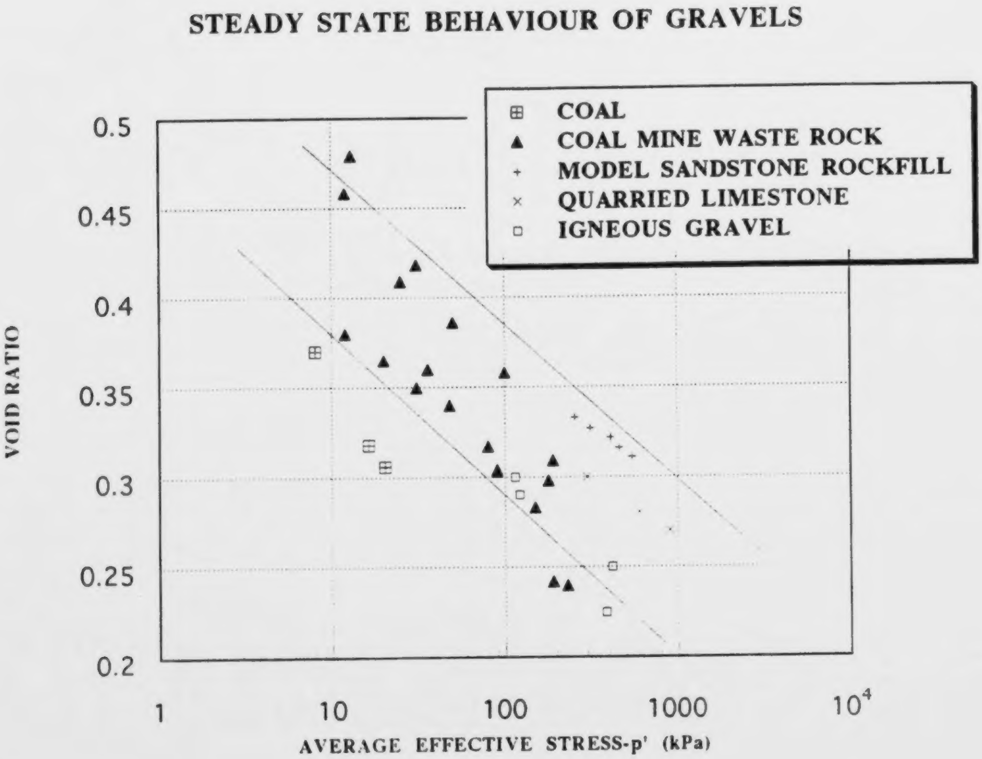

Figure 5.6 Steady State Behaviour of Sandy Gravels

CONSTANT q TEST
(after Sassitharan et al, 1993)

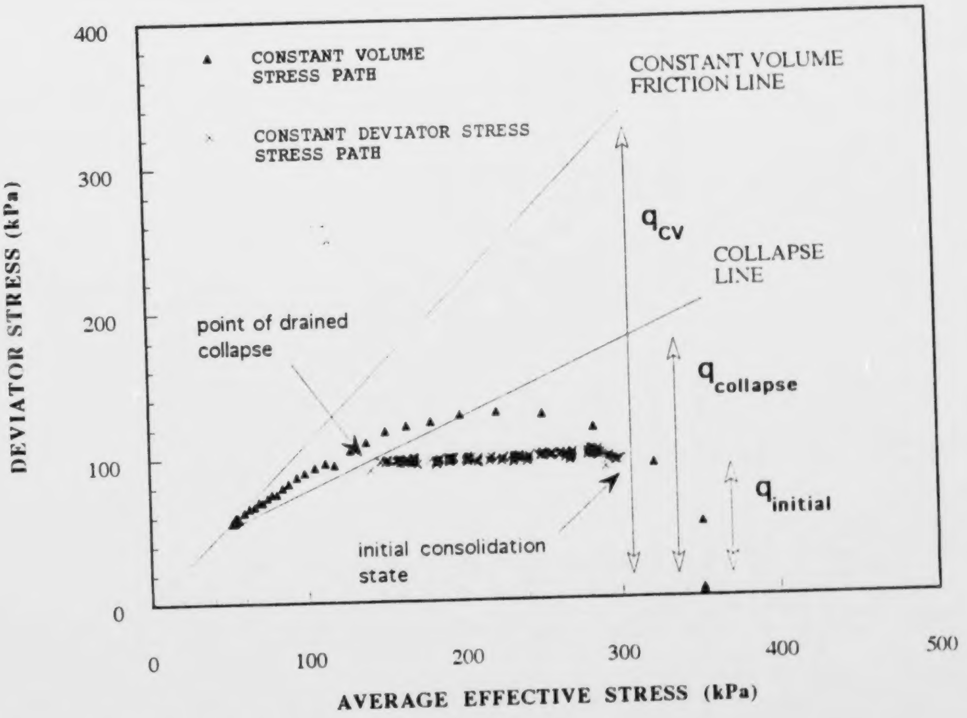

Figure 5.7 Collapse Due to a Rising Water Table

Chapter 6

FLOWSLIDES IN ROCKY MOUNTAIN COAL MINE WASTE DUMPS-FIELD AND LABORATORY STUDIES

6.1 INTRODUCTION

There are currently 10 Western Canadian Rocky Mountain coal mines producing about 30 million tonnes of coal annually, mainly for the export metallurgical market (Figure 6.1). It is estimated that these mines haul over 100 million BCM (bank cubic m) of waste rock per year. The waste material is excavated and transported mostly by truck/shovel methods to waste dumps near to the open pit areas. Mining is carried out in steep mountainous terrain and haulage costs are very sensitive to the proximity of the free dumped waste piles to the pit areas. Since the late 1960s when higher production mining was initiated there have been incidences of long runout waste dump flowslides, mostly in the British Columbia mountain coal mines. As more coal mines came into production during the 1980s the number of incidences increased substantially and efforts to improve waste dump management practices were initiated.

Most mountain coal mine waste dumps in British Columbia are end-dumped fills placed on foundation slopes steeper than 20°. The foundation materials overlying the bedrock typically consist of granular colluvium derived from weathering and slope wash and/or alpine dense stony glacial tills. Laboratory tests on these materials show effective friction angles ranging between 29 and 41° (Golder Associates, 1987).

Mobile waste dump flowslides run out large distances over relatively flat ground (commonly less than 20°). Thus the runout path normally consists of a steeper portion beneath the original unfailed dump toe and a shallow runout zone over which the failed material is deposited.

Despite the fact that many of the mountain mine waste dumps in British Columbia fail on very steep foundations, the runouts extend for greater distances than would be expected for "dry" material with an angle of repose of 37-38°.

A recent industry survey (Piteau Associates, 1991) conducted at 31 active sites in British Columbia documented 18 instabilities (minor sloughs and slumps not included) out of 81 individual dumps. Figure 6.2 shows data from 49 individual waste dumps included in the survey. The upper figure shows that most of the failures occurred on dumps with overall slope angles greater than 35°, close to the angle of repose. The figure also shows that there was an increase in the percentage of failures as dump height increases. At heights greater than 200 m all but one dump exhibited large-scale instability.

The lower graph in Figure 6.2 shows that there were 14 documented events with runouts exceeding 100 m. A review of the data and some field reconnaissance carried out for this thesis suggests that weak foundation conditions were clearly identifiable as the main cause of failure for only 4 of these events. The others all occurred at coal mines. These events represented 12% of the 83 dumps surveyed or 31% of the coal mine waste dumps surveyed. These statistics suggest that up to 30% of "active" coal mine waste dumps are potential high runout flowslide hazards.

The documentation for the 10 events with runouts exceeding 100 meters shows that these dumps were either founded on relatively strong till or colluvium foundations or that wet fines were noted in the runout debris. As a result, weak foundations were not clearly responsible for the instabilities.

6.2 FIELD STUDY OF THREE FLOWSLIDE EVENTS

Field work was carried out at three British Columbia mountain coal mine sites (Quintette Coal, Fording River, and Fording Greenhills) during the summer of 1992. The objective of the field work was to examine waste dump materials, study the runout zones of three flowslides (one at each site), and sample potentially liquefiable materials for laboratory characterization and triaxial testing. Figure 6.1 shows the locations of the three mines where detailed flowslide studies were carried out. The three flowslides chosen for detailed study were selected based on initial dump height, runout distance, location (one at each site), and accessibility.

Field investigations consisted of site reconnaissance, trenching, sampling, and in-situ density and infiltration testing. Drilling was not carried out.

6.2.1 FIELD METHODS

Field work was carried out in order to examine the runout zones of the three flowslide events and to characterize typical finer grained runout materials. In addition, samples of similar finer grained materials in the unfailed portions of waste dumps were obtained for triaxial testing to evaluate their collapse potential. The field work included in-situ tests and sampling on the surface of active dumps as well as on the runout zones of the three flowslide events.

Waste rock material field properties were determined by conducting in-situ tests. Samples were taken of loose heaped waste rock piles placed on the dump surface and of in-place waste material that was being re-handled. The heaped materials represented freshly placed waste prior to it being subjected to any significant self loading due to burial. The re-handled material was dug out of an existing dump and thus had been subjected to prior loading.

Material was collected from the runout zone by trenching and surface sampling. A backhoe was used to excavate a trench up to 5m deep. Trenching, testing, and sampling areas were all selected based on the presence of finer grained sandy gravel sized materials. These materials were present in the runout zones of each flowslide event studied.

At each site in-situ density and infiltration tests were conducted and runout zones were mapped. A brief explanation of the field activities follows:

Density Tests - In-situ density tests were carried out in the runout zones and on the surfaces of stable dumps. The purpose of these tests was to establish void ratio measurements at placement, prior to, and following failure. The procedure for carrying out the tests was as follows:

1. A relatively undisturbed area containing sandy gravel materials was chosen and a 1m diameter by 15cm high ring was placed on the site. Plastic was placed inside the ring and the ring was filled with water to establish a zero reference plane. Water was weighed with bathroom scales. The water and plastic was then removed, being careful not to spill water on the in-situ material.

2. A sample of waste rock was excavated (about 50 kg), placed in sealed 20l plastic pails, and weighed. Plastic was then placed inside the excavation and water was again added up to the top of the ring.

3. The difference in the weight of water in 1 and 2 above was used to establish the volume occupied by the sampled waste rock ($1m^3$=9.81kN of water). The total unit weight at each site was readily determined from the weight of sample and excavated volume measurements.

4. The waste rock from each site was returned to the laboratory for grain size analyses, in-situ moisture content, and bulk specific gravity measurements. It was then possible to calculate the in-situ void ratio for each site as follows:

$$e = \frac{G_B \gamma_w \ (1+w)}{\gamma_T} - 1$$

Where: e = void ratio
GB = bulk specific gravity
γ_W = unit weight of water
w = moisture content
γ_T = total unit weight

Infiltration Tests - Constant head infiltration tests were conducted at the in-situ density sites. The infiltration tests were carried out in order to estimate the field saturated hydraulic conductivity (permeability). Tests were conducted by sealing a 30 cm diameter plastic cylinder in the ground with bentonite pellets and measuring volume of water required to maintain a constant head. The infiltration rate was converted to permeability using an empirical relationship (Swiss Technical University, 1975).

$$k = \frac{Q}{7\pi D h_m}$$

Where: k = permeability
Q = steady state infiltration rate
D = cylinder diameter
h_m = *height* of constant head in test cylinder

The purpose of the infiltration tests was to establish the range of permeability's for different void ratios in order to provide an indication of whether sufficient pore pressure impedance might occur during collapse.

Runout Mapping - In addition to the sampling and testing program the field work included mapping of the runout zones. Each runout path was traversed in order to examine and record characteristic features within and around the edges of the flowslide. Although foundation materials were not sampled for testing, field descriptions of the surficial soils around each slide area were made. Data from the field mapping was combined with information obtained from minesite records in order to characterize the engineering geology of each flowslide event.

6.2.2 FLOWSLIDE CASE HISTORIES

The three flowslides chosen for detailed study were selected based on initial dump height, runout distance, location (one at each site), and accessibility. Table 6.1 lists the physical features of the three waste dumps and their associated runout zones. The three case histories span a broad range of dump heights (100 to 400 m) and runout distances (700 to 2200 m) and thus should be representative of many of the flowslides that have occurred at British Columbian mountain coal mines.

• QUINTETTE MARMOT 1660 FLOWSLIDE

Several mine waste dump flowslides have occurred at Quintette Coal near Tumbler Ridge, British Columbia. On September 9, 1985, at about 0600 hours, the Marmot 1660 dump failed and about 2.5 million cubic meters (1.9 million bank cubic metres) of material flowed down the Boulder Creek valley for a distance of 2200 m. There were no personnel or equipment involved in the slide.

Figure 6.3 shows a plan of the area affected by the flowslide and a cross section through the waste dump and runout zone. Aerial photographs taken just after the slide are shown in Figure 6.4. A post failure synopsis report prepared by Piteau Associates Engineering Ltd. (1985) documents the following events preceding the runout:

1. Construction of the Marmot 1660 Dump began in July 1984 and at the time of the failure approximately 12 million BCM (bank cubic metres) of waste rock had been placed.

2. Dumping rates during July and August, 1985 averaged about 80 BCM per linear meter of dump crest area per day with peak placement rates as high as 200 BCM per linear meter per day. Dump displacement rates, measured by wireline extensometers, were generally in the 2 to 4 cm/hour range throughout dump construction with peak rates

of 10 cm/hour occurring periodically. These rates are considered normal for Quintette. Continuous monitoring records prior to failure were not available.

3. Dumping in the failure area had not been taking place immediately prior to failure; it had ceased on August 31, 1985. Elsewhere on the dump, waste placement had continued until September 5, but was halted from September 5 to 7. Dumping was resumed and continued until a few hours before the failure when activities were shut down due to the presence of large cracks. Major cracking and bulging were not evident until just before failure.

The Piteau Associates (1985) report attributes the failure to be due "to the presence of fines in the waste rock, accompanied by a buildup of pore pressures in the part of the dump occupying the Boulder Creek Valley." The wide, partially super-elevated runout path indicates that the flowslide reached a high velocity.

Foundation conditions underlying the runout zone, determined from the failure reports, test pits (only TP4, TP6, and D reached the original ground level), two drill holes, and field mapping are shown on Figure 6.3. Thin colluvium underlies the original dump and extends to about the 1350 m elevation. Note that the Boulder Creek valley extends up underneath the original dump. The creek was flowing in August of 1992 when the runout field study was undertaken.

Below 1350 m the foundation consists of till ranging from 2 to 10 m thickness. Both the till and colluvial materials are dense (Piteau Associates, 1985). Below the 1225 m elevation the Boulder Creek Valley steepens and the foundation conditions are assumed to have been mostly organic soils as evidenced by piled up organic material in the runout toe zone.

Down to the 1250 m elevation the surface of the runout zone consisted of a central zone of carbonaceous sandy gravels following the Boulder Creek valley flanked by coarser gravels and boulders on either side. This material is distinguished on the photograph in Figure 6.4 as a darker wet looking zone. Test pits in the finer material at Sites A and C encountered about 5 m of this material and did not reach original ground. Below the 1250 m elevation the finer materials were absent at the surface and the runout zone consisted of the coarser gravels and boulders. The central zone of finer sandy gravel is exposed as a window of finer material and is believed to have been the original underlying liquefied material that initiated the event and contributed to the very high mobility. As the slide proceeded down-slope the overlying coarser material "slid off" creating a large splash zone along the west side of the Boulder Creek valley (above the 1250 m elevation) and below the sedimentation pond A on the east side of the valley. As the valley narrowed below the 1225 m elevation the liquefied materials propelling the slide may have been exhausted and the runout continued due to inertia and higher pore pressures generated in the underlying organic foundation soils.

A unique feature of the runout zone was the presence of isolated sandy gravel cones situated in the coarser gravel and boulder sized materials. These cones appear to be related to pore pressure relief (piping) within pockets of liquefied material trapped below the slide. Similar features were also observed in an adjoining flowslide where they were much more frequent and seemed to contain till-like materials. Figure 6.5 shows a photograph of one of these unusual features. Similar debris cones formed in rock avalanche deposits are referred to as molards (Cassie et al., 1988)

• FORDING SOUTH SPOIL FLOWSLIDE

The Fording River Mine is located near Elkford, British Columbia, across the Fording River from the Greenhills Mine. On October 26, 1989 at about 0600 hours a major failure occurred on the 400 m high South Spoil Stage 1 waste dump. Approximately 3.9 million cubic metres (3.0 million BCM) of waste rock failed and flowed 800 m down slope over the mined out Blackwood Pit and into the Kilmarnock Creek valley. The leading edge of the runout carried up the opposite slope of the valley to a height of 30 m above the valley floor.

Figure 6.6 shows a plan of the area affected by the flowslide and a cross section through the waste dump and runout zone. Aerial photographs of the waste dump prior to and after failure are shown in Figure 6.7. Information gathered from consultant's reports (Golder Associates, 1989, 1990) and minesite records document the following site conditions prior to and immediately following the failure event:

1. Construction of the South Spoil Stage 1 Dump started in November 1987. The dump contained over 10 million BCM of material prior to failure.

2. The dump was active until October 24, 1989 at which time the dump was closed because of high rates of movement. Wireline extensometer movements of about 10 cm/hour were observed on that day. On October 25 movements accelerated rapidly and reached values in the 100 to 130 cm/hour range before catastrophic failure occurred on the following day.

3. The Kilmarnock creek was dammed by the failure debris for about 6 days following the event.

4. The flowslide must have attained considerable velocity as evidenced by air blast damage to nearby foliage and dust around the perimeter of the slide area.

The dump was developed in a draw, referred to as the Blackwood Gully, between two prominent sandstone ridges. The pre-failure topographic plans show that the Blackwood Gully contained an intermittent stream.

Foundation conditions underlying the dump and runout zone were determined from a review of the failure reports, air photos, and field mapping carried out for this study. Beneath the original unfailed dump the foundation consisted of "a relatively thin veneer of relatively coarse granular colluvial soils overlying bedrock" (Golder Associates, 1989). At the time of failure the dump toe was advancing out over the mined out Blackwood Pit. Foundation conditions in the runout zone consisted of the shaly Blackwood access embankment material, a till bench above the valley floor, and sand/gravel alluvium in the Kilmarnok flood plain (see Figure 6.6).

Most of the runout material was deposited in the valley since only a thin blanket of boulders was apparent up on the till bench and around the Blackwood pit area. In the valley bottom the runout zones consisted predominantly of sandy gravels and boulder materials. The finer materials appears to have been associated with the base of the slide. Figure 6.8 shows photographs at Site A taken at the leading edge of the slide zone and at Site D taken at the lateral edge of the slide. Note the finer materials and sharp contact with the underlying foundation.

• GREENHILLS COUGAR 7 FLOWSLIDE

On May 11, 1992, at about 0700 hours, the Cougar 7 Dump at the Greenhills Mine located near Elkford, British Columbia failed. Approximately 200,000 cubic metres (160,000 BCM) of failure debris slid off the 100 m high waste dump, traveled across an access roadway, and flowed downslope for a total runout distance of 700 m. A service truck and driver traveling along the access road near the dump toe were swept off the road by the failure material.

Figure 6.9 shows a plan of the area affected by the flowslide and a cross section through the waste dump and runout zone. Aerial photographs taken just after the slide are shown in Figure 6.10. Information collected from reports of post failure geotechnical investigations conducted by Golder Associates (1992) and the British Columbia Ministry of Energy, Mines and Petroleum Resources (1993) document the following site conditions prior to and immediately following the failure event:

1. The dump was constructed in the winter of 1991 between February and May. Heavy rains occurred during the spring of 1991. There were approximately 450,000 BCM of material in the dump derived mainly from surficial soils (till and colluvium) and near surface rock excavated from an adjacent mining area.

2. The dump was inactive and remained stable for 13 months prior to the failure. An access roadway was constructed entirely from fill below the dump toe in March and April, 1992. The roadway did not interfere with the Cougar 7 dump toe.

3. On the morning of May 11, 1992 just prior to the failure, cracks were noticed on the dump face defined by a snowfall (approximately 4 cm) the previous night. Seepage zones were also noticed. At the time of failure there were no monitors on the dump to indicate displacement rates.

4. There were no eyewitness accounts of the dump failure but a judgment of the short time that the service truck must have been exposed to the hazard suggests that the failure occurred very rapidly, and that the debris attained considerable velocity. Excavation of failure debris indicated that the access road remained virtually intact.

5. Buried snow and ice lenses were observed in dozer cuts along the edge of the unfailed portion of the dump.

Foundation materials beneath the original dump and throughout most of the runout zone consisted mostly of sand, and gravel colluvium. A dozer cut at Site D in Figure 6.9 showed that the colluvium was 0.3 to 0.5 m thick beneath the dump. Exploration road cuts near the runout zone exposed 1 to 1.5 m of colluvial material. A coal seam sub-crops beneath the dump. The dump was developed in the headwater area of Cataract Creek. Water was observed flowing through the runout debris below the original dump toe during the site study conducted in August, 1992.

The runout zone of the Cougar 7 dump consisted predominantly of sandy gravel materials. The coarser gravel and boulder material referred to in the previous case history were noticeably absent. A dozer cut at Site D in Figure 6.9 revealed a wet sandy gravel layer at the foundation contact. Similar fines layers were observed near the dump crest and in the failure debris. Photographs of the fines layer are shown in Figure 6.11. It is clear that the dump was riding on a saturated fines layer.

6.2.3 FACTORS AFFECTING STABILITY

Factors affecting the stability of mine waste dumps have been discussed at length in previous studies and a dump stability rating scheme has been proposed (Piteau Associates, 1991). With respect to the field studies presented here, a number of factors known to contribute to instability are compared and contrasted below:

1. Foundation Conditions: It is particularly noteworthy that all the runouts were developed in incised gullies or creek beds. Surface water was evident in these drainage paths during the site studies for both the Marmot 1660 and Cougar 7 flowslides. Surficial soils within these drainages were reported to consist of thin (less than 0.5 m) relatively free draining colluvial materials. Failures occurred despite the three dimensional confinement offered by the foundation geometry's. Foundation slopes in the toe areas of the Marmot 1660 dump and South Spoil ranged from 20 to 25° while the Greenhills foundation was steeper at 25 to 30°. South Spoil was advancing out over the mined out Blackwood pit highwall prior to failure.

2. Dump Configuration: Dump heights ranged from 100 to 400 m and all the dump slopes were at an angle-of-repose of 37-38°.

3. Construction Conditions: All three dumps were constructed as loose, end dumped fills. Active dumping in the failure area had ceased two days prior to failure on South Spoil, 10 days prior to failure at Marmot 1660, and one year before the Cougar 7 flowslide.

4. Construction Materials: Carbonaceous sandy gravel materials were observed in the runout zones of all three events. These materials appeared to be closely associated with the base of the runout zone.

5. Climate: Figure 6.12 shows plots of daily rainfall prior to each of the failure events. Significant rainfall of 30 cm to 35 cm within two weeks prior to failure was apparent for both the Marmot 1660 and South Spoil events. Similar rainfall intensities did not precede the Cougar 7 failure. However, this dump was constructed under very wet conditions the previous spring and snow and ice were observed in the unfailed portion of

the dump just after the failure occurred. Several days of warm weather contributing to snow melt preceded the failure at Cougar 7.

It is difficult to discern the relative importance of the above factors without a mechanism to link them together. Careful consideration reveals that the factors necessary for a liquefaction flowslide may have been present in each case and that the framework of static collapse potential, collapse trigger, and overall progressive failure (discussed in the previous chapter) could explain the instabilities that preceded the flowslides:

Collapse Potential - Finer grained, loosely deposited "layers" of sandy gravel materials were seen in each slide. These materials when deposited loosely (end dumped) and loaded under high angle-of-repose shear stress conditions, may have produced a potential collapse state for these materials within the dumps prior to failure.

Collapse Trigger - Chapter 5 clearly demonstrated the manner in which a rising water table or wetting could initiate collapse. All three case histories provide evidence that sufficient water was available to provide the collapse trigger.

Progressive Failure - Overall progressive failure can only occur if there is insufficient containment to control the collapsible material. Steeper foundation slopes in the toe zone areas may have contributed to the loss of support that eventually must have occurred for the flowslides to develop.

Weak foundation materials and loading rate did not seem to be significant contributing factors in these events. The most important common denominator was the presence of fine grained materials, apparently associated with the base of the slides.

6.3 GEOTECHNICAL PROPERTIES OF WASTE DUMP SANDY GRAVELS

The sandy gravel materials sampled from the runout zones of the three flowslides discussed in the previous section were taken to the laboratory for characterization work. Grain size curves for the sandy gravel materials are shown in Figure 6.13. The materials all exhibit similar grain size distributions with average grain sizes (D_{50}) of 4 to 10 mm and sand contents (-2 mm) in the 20 to 35% range. Table 6.2 shows the characteristics of the different materials. Carbonaceous shales dominate the lithological makeup of all three materials. The Greenhills material has the highest carbonaceous content as demonstrated by the lowest ash content (weight percent of non-carbonaceous material) and highest amount of carbonaceous shale. The Fording runout material exhibits the least amount of carbonaceous shale.

The average grain size distributions from each of the three runout zones are compared in Figure 6.14 with the range of grain size distributions from the Aberfan and other flowslide events taken from various literature sources. Sand contents of these materials vary from 10 to 55% and mean grain sizes from about 1 to 10 mm. The most distinguishing characteristic of all these events appears to be grading. All the grain size distributions exhibit subparallel grain size distribution curves. These broadly graded materials, when placed in a loose condition, may be particularly susceptible to forming loose meta-stable structures capable of collapse.

6.3.1 VOID RATIO RELATIONSHIPS

Void ratio is an important material property that can be correlated with many engineering properties. It is especially important for studies involving potentially collapsible materials. The field void ratio relationships presented here were determined for three different sources of sandy gravel material :

1. Heaped Samples - As placed, end dumped material. Density testing was conducted on piles placed by haul trucks during the site study period. The heaped void ratio is an estimate of the end dumped initial void ratio prior to self-weight consolidation as the material becomes buried within the dump. End dumping may produce a slightly different initial void ratio due to the flow of material down the dump face, however the heaped void ratio should be reasonably representative of this condition.

2. In-place Samples - In-situ material subjected to prior self-weight loading. Density testing was conducted at three sites where re-handling of waste dump material was being conducted. Thus it was possible to obtain density tests of material that had been subjected to prior loading It was not possible to measure the amount of swell due to unloading.

3. Runout Samples - Material from the runout zones of the study flowslides. The density testing in the runout zones was confined to areas where sandy gravel textured materials were exposed. Sites were chosen that appeared to be relatively undisturbed; however, the site investigations were carried out up to 7 years after the failure event. The effects of

prior disturbance, snow loading, and weathering were impossible to evaluate and thus corrections for these processes have not been considered.

Figure 6.15 shows the moisture content (partial saturation) versus void ratio relationship for runout and heaped materials. The failed runout materials exhibit void ratios of about 0.3 whereas the freshly placed heaped materials show placement void ratios greater than 0.4. These two trends show that, for heaped moisture contents greater than about 5%, significant volume change occurs between the initial unfailed and final failed states. At a moisture content of about 4% the difference in void ratio is much less. It appears that the initial moisture content may be contributing to the formation of a loose structure. Note that at moisture contents less than about 4% the runout and heaped void ratios converge.

Bishop (1973) observed that materials in the Aberfan flowslide showed a minimum placement density (maximum void ratio) at moisture contents of between 6 and 8%. On either side of this moisture content range the placement density increased (void ratio decreased). Clearly, the formation of a loose initial structure in the Aberfan colliery spoil materials was also sensitive to initial moisture content conditions.

Infiltration tests were conducted at each density test site in order to obtain approximate correlations between field saturated permeability and void ratio. The infiltration test methods are described in the previous chapter. Figure 6.16 shows the permeability versus voids ratio relationship for the various tests. The data are contained within a band that demonstrates a linear relationship between void ratio and the logarithm of permeability. Within the void ratio range of 0.3 to 0.5, average permeability's of 0.001 to 0.1 cm/s are in evidence. These permeability's are within the range of values capable of impeding drainage during collapse. Eckersley (1985) quotes a field saturated permeability of 0.01 cm/s for collapsible stockpiled coal.

6.3.2 TRIAXIAL TESTS

Testing was conducted with "fresh" sandy gravel materials obtained from the crest zones of active waste dumps at the Greenhills, Quintette, and Fording River mine sites. Sampled materials from the runout zones were not used for testing as crushing during self weight loading, failure, and subsequent flow as well as weathering may have significantly changed the mechanical behaviour of these materials. A comparison of the characteristics of the test materials shown in Table 6.3 with the characteristics of the actual runout zone materials shown in Table 6.2 demonstrates that the test materials adequately represent typical runout zone materials.

The characteristics of the three materials are believed to vary significantly enough to represent a broad range of typical sandy gravel coal mine waste dump materials. The Quintette field sample was the finest material and was notably weathered. The Greenhills material exhibits relatively low ash (high carbonaceous) content as evidenced by the significant quantity of coal. The Fording material was derived from the re-handle zone of the South Spoil waste dump and is the least carbonaceous (highest ash content) and most broadly graded material. This waste product appears be more similar to the material found in the runout zones than the other test materials.

The coarse and angular waste rock proved to be a difficult test material. Thus most of the testing was carried out as conventional undrained tests on lab prepared samples (ICU tests) in 10.2 cm (4 inch) diameter cells. Details of the test procedures and complete records of all the successful tests are contained in Appendix B. Data from the triaxial testing program were reduced to average effective stress (p') and deviator stress (q) according to the following conventional relationships:

$p' = (\sigma'_1+2\sigma'_3)/3$
$q=(\sigma'_1-\sigma'_3)$
Where: σ''_1 = major principal stress
σ'_3 = minor principal stress

The coarse top size (150 mm) of the sampled materials prevented the use of the full gradation for testing purposes. Thus it was necessary to prepare test triaxial samples by removing oversize particles (-20 mm) from the field sampled material. Fragaszy et al. (1992) have examined the effects of oversize particles on the strength and deformation behaviour of sandy gravels. These authors have demonstrated that oversize particles (less than approximately 40% by weight) floating in a matrix of finer material do not have an appreciable impact on the strength and deformation behaviour. Thus testing of the matrix material should provide a reasonable approximation of the strength and deformation properties of the total material.

Figure 6.17 shows the field versus laboratory prepared grain size distributions for the three test samples. All the test samples contain less than 40% by weight of particles greater than 20 mm. Geotechnical properties of each of the three triaxial test materials are shown in Table 6.4. All the materials have similar average grain sizes (2-3 mm). The main distinguishing properties are the different sand and ash contents.

Several tests at a range of cell pressures ranging from 50 to 500 kPa (limit of the load cell) were undertaken for each of the three different sample materials. Results for a typical strain weakening, undrained isotropically consolidated test sample are shown in Figure 6.18. This sandy gravel waste sample was prepared at a void ratio of 0.51 and consolidated isotropically to a void ratio of 0.40 at an average effective stress level of 200 kPa (point A in Figure 6.18). The drainage ports were then closed and the specimen was sheared in a conventional strain controlled undrained fashion (constant cell pressure and increasing axial load). Figure 6.18 demonstrates that the sample behaved in a contractant fashion (decreasing effective stress) until the peak strength was reached (point B) at an axial strain of about 2%. At point B in Figure 6.18 strain weakening was initiated and a loss of strength occurred to a steady state strength (q_{ss}) of about 80 kPa, shown as point C in Figure 6.18. The steady state condition was not achieved until the axial strains approached 20%. Apart from the large strains required to reach the steady state condition the behaviour of the test specimen was similar to that of a loose sand.

Figure 6.19 shows the average effective stresses and deviator stresses at the steady state for all the test samples. The steady state points all lie on a straight line defined by a slope of 1.5 which is equivalent to an effective friction angle ($\emptyset'$) of 37°. Despite the differences in the sand and coal contents of the three test materials, the steady state friction angles are all essentially the same and close to the field gradation waste dump angle-of-repose value of 37-38°.

Figure 6.20 shows the effective stress versus void ratio relationship at the consolidation and steady states for the three different materials. The steady state trends for each material type exhibit similar slopes and steady state void ratios mostly in the 0.3 to 0.5 range. The consolidation lines are roughly subparallel to the steady state lines. The more carbonaceous Greenhills material exhibits generally lower void ratios at a given consolidation stress.

Collapse behaviour in undrained tests is manifested as a strain weakening response as indicated in Figure 6.18. Not all the tests exhibited this behaviour as there tended to be a loss of brittleness as consolidation stresses increased. Figure 6.21 shows this phenomenon for the Fording material. At average stresses of 50 to 300 kPa brittle behaviour is well defined, the stress paths in this range show a collapse surface with a slope of about 0.5. At 500 kPa consolidation stress the collapse surface is almost horizontal and thus brittle behaviour is negligible. The other two materials exhibit similar behaviour as consolidation stresses increase and the difference between the consolidation and steady state void ratios (often referred to as the state parameter) decreases. This important aspect of the behaviour of these materials is examined further below.

The undrained brittleness index (I_b) is a parameter that describes the amount of strain weakening following collapse. It is defined as follows:

$I_b = \Delta q / q_{max}$

Where: Δq = difference between peak and steady state deviator stress

q_{max} = peak or maximum deviator stress

Thus a brittleness index of 0.5 denotes a 50% loss in strength due to collapse. Figure 6.22 shows a plot of void ratio versus percent brittleness index for all the triaxial test samples. This figure demonstrates the drop in the collapse potential as the void ratio decreases due to consolidation. Crushing during consolidation appears to reduce brittleness by breaking down the collapsible structure. At a void ratio of about 0.3 the brittleness index approaches zero for these loosely deposited materials.

6.4 COLLAPSE MODEL

Study results presented here show some convincing evidence that collapse and flow processes caused the initial instabilities that lead to the mobile flowslides within the three events under study. With reference to Figure 6.23 consider the following stress paths leading to collapse within a coal mine waste dump:

1. During construction of a waste dump, layers of finer sandy gravel materials are periodically deposited parallel to the face. These layers do not necessarily need to extend down to the foundation but must be sufficiently fine grained and of sufficient thickness to be able to sustain a water table and impede the drainage of pore pressures should collapse occur. Figure 6.23-(1) shows a sandy gravel layer (shaded) parallel to the dump slope. For a thin layer the initial stresses are very low and the void ratio is equal to the placement void ratio.

2. As construction continues an element originally at Point A (Figure 6.23-(1)) in the embankment follows a consolidation path from A to B (Figure 6.23-(2)) as overburden loading takes place. Consolidation occurs at a high principal stress ratio due to the steep angle-of-repose slopes. Thus significant shear stresses are mobilized during consolidation. At point B the element is potentially collapsible as it exhibits a static stress state higher than the steady state strength.

3. High moisture contents in the finer layers can develop due to consolidation, snow melt, and rainfall infiltration which approach saturated water contents potentially high enough to generate excess pore pressures during collapse. As the water table rises or wetting occurs the average effective stress decreases towards the collapse surface under constant shear stress and with only small changes in void ratio. At the point of collapse excess pore pressures are generated and strain weakening behaviour initiates the load transfer process that eventually results in overall progressive failure. Other processes such as shearing in the toe region, creep, and weathering may also act as a collapse trigger.

Note that the conventional factor of safety prior to collapse, as defined in Figure 6.23, is greater than the factor of safety with respect to the collapse surface. This is the case even when pore pressures are taken into consideration. Conventional practice does not directly recognize collapse processes.

6.5 CONCLUSIONS

Detailed studies of three flowslide events have been carried out. The results explicitly illustrate the role of liquefaction in these events. The main study findings are as follows:

1. Finer grained sandy gravel layers were present near the base of the runout zones. These layers were believed to have been originally deposited parallel to the dump face and were present as loose, moisture sensitive, potentially liquefiable zones in the unfailed dumps prior to failure.

2. Significant moisture was available to trigger collapse as evidenced by precipitation prior to failure, snow in the runout debris, and/or underlying spring water conditions.

3. Testing of materials similar to those sampled within the runout zones showed brittle behaviour during constant volume testing. Brittleness decreased with increasing consolidation stresses.

4. A conceptual model has been introduced that demonstrates the manner in which liquefaction flowslides may have been initiated in these events.

The next chapter presents numerical and limit equilibrium analyses of these events and examines mitigative strategies that could be employed for reducing the risk of a flowslide.

6.6 REFERENCES

Bishop, A.W., 1973. The Stability of Tips and Spoil Heaps, Quaternary Journal of Engineering Geology, Vol. 6, pp. 335-376.

British Columbia Ministry of Energy, Mines and Petroleum Resources, 1993. Geotechnical Investigation of the Westar Greenhills North Cougar Access Road Dump Failure.

Cassie, J.W., Van Gassen, W. and Cruden, D.M., 1988. Laboratory Analogue of the Formation of Molards, cones of rock avalanche debris, Geology, Vol. 16, pp. 735-738.

Dawson, R.F., Morgenstern, N.R., and Gu, W.H., 1994. Liquefaction Flowslides in Western Canandian Coal Mine Waste Dumps, Phase 2: Case Histories. Report to Supply and Services Canada, File No. XSG42-00138(608), 112 p.

Eckersley, J.D., 1985. Flowslides in Stockpiled Coal. Engineering Geology, Vol. 22, pp. 13-22.

Eckersley, J.D., 1990. Instrumented Laboratory Flowslides. Geotechnique, Vol. 40, No. 3, pp. 489-502.

Evans, M.D., Seed, H.B., and Seed, R.B., 1991. Membrane Compliance and Liquefaction of Sluiced Gravel Specimens. ASCE Journal of Geotechnical Engineering, Vol. 118, No. 6, pp. 856-872.

Fragaszy, R.J., Gu, W., Giddigi, F.H., 1990. Effects of Oversize Particles on the Density of Clean Granular Soils. Geotechnical Testing Journal, Vol 13, No. 2, pp. 106-114.

Golder Associates Ltd., 1987. Regional Study of Coal Mine Waste Dumps in British Columbia. Report to Supply and Services Canada.

Golder Associates Ltd., 1989. Failure on South Face of South Spoil Stage I, October 26, 1989. Internal Rept to Fording Coal Ltd.

Golder Associates Ltd., 1990. South Spoil Failure Debris. Internal Report to Fording Coal Ltd.

Golder Associates Ltd., 1992. Failure of a Waste Rock Dump on the Morning of May 11, 1992 at the Westar Greenhils Operations. Internal Report to Westar Greenhills Operations.

Golder Associates Ltd., 1992. Runout Characteristics of Debris from Dump Failures in Mountainous Terrain. Report to Supply and Services Canada, Contract No. 23440-0-9198/01-X8G.

Klohn Leonoff Ltd., 1991. Operation and Monitoring of Mine Dumps: Interior Guidelines. Report to British Columbia Ministry of Energy, Mines and Petroleum Resources.

Nichols, R.S., 1986. Rock Segregation in Waste Dumps. Proc. of the International Symposium on Flow-Through Rock Drains, Cranbrook, British Columbia, pp. 105-120.

Piteau Associates Engineering Ltd., 1985. Marmot 1660 N Dump Analysis of Slide on September 9, 1985. Internal Report to Quintette Coal Limited.

Piteau Associates Engineering Ltd., 1986. Marmot 1660 N Dump Foundation Conditions on Failure Lobe and Impact on Future Dumping. Internal Report to Quintette Coal Limited.

Piteau Associates Engineering Ltd., 1991. Investigation and Design of Mine Dumps: Interim Guidelines. Report to British Columbia Ministry of Energy, Mines and Petroleum Resources.

Swiss Technical University, 1975. Technical Research Memorandum, Zurich, Switzerland.

TABLE 6.1 WASTE DUMP FLOWSLIDE CHARACTERISTICS

WASTE DUMP NAME	HEIGHT (M)	FAILURE DATE	FAILED VOLUME (10^3M^3)	RUNOUT DISTANCE (M)	FDN TOE SLOPE (°)	RUNOUT SLOPE (°)
QUINTETTE MARMOT 1660	240	SEPT 9,1985	2500	2200	20-25	7
FORDING SOUTH SPOIL	400	OCT 26,1989	3000	800	20-25	10
GREENHILLS COUGAR 7	100	MAY 11,1992	200	700	25-30	13

TABLE 6.2 RUNOUT MATERIAL CHARACTERISTICS

RUNOUT SOURCE	D_{50} (mm)	% SAND (-2 mm)	%ASH CONTENT	LITHOLOGY
QUINTETTE MARMOT 1660	5-10	20-33	75-85	60% carbonaceous shale, 20% siltstone, 20% sandstone, minor coal
GREENHILLS COUGAR 7	7-10	28-33	70	70% carbonaceous shale, 20% siltstone, 10% coal, PART WEATHERED
FORDING SOUTH SPOIL	4-10	20-25	75-85	50% carbonaceous shale, 40% siltstone, 10% sandstone, minor till

TABLE 6.3 FIELD CHARACTERISTICS OF TRIAXIAL SAMPLES

SOURCE	D_{50} (mm)	% SAND (-2 mm)	%ASH CONTENT	LITHOLOGY
QUINTETTE MARMOT P1	4	38	74	WEATHERED 50% carbonaceous shale, 25% siltstone, 20% sandstone, 5% coal
GREENHILLS NORTH DUMP	7	20	62	60% carbonaceous shale, 20% coal, 10% siltstone, 10% sandstone
FORDING SOUTH SPOIL RE HANDLE	8	38	81	40% carbonaceous shale, 40% siltstone, 20% sandstone, trace coal

TABLE 6.4 TRIAXIAL SAMPLE PROPERTIES

SOURCE	D_{50} (mm)	% SAND (-2 mm)	BULK SPECIFIC GRAVITY	% ASH CONTENT	% OVERSIZE PARTICLES (+20 mm)
QUINTETTE MARMOT P1	2	50	1.95	70	25
GREENHILLS NORTH DUMP	3	30	1.85	60	30
FORDING SOUTH SPOIL RE HANDLE	3	24	2.20	78	35

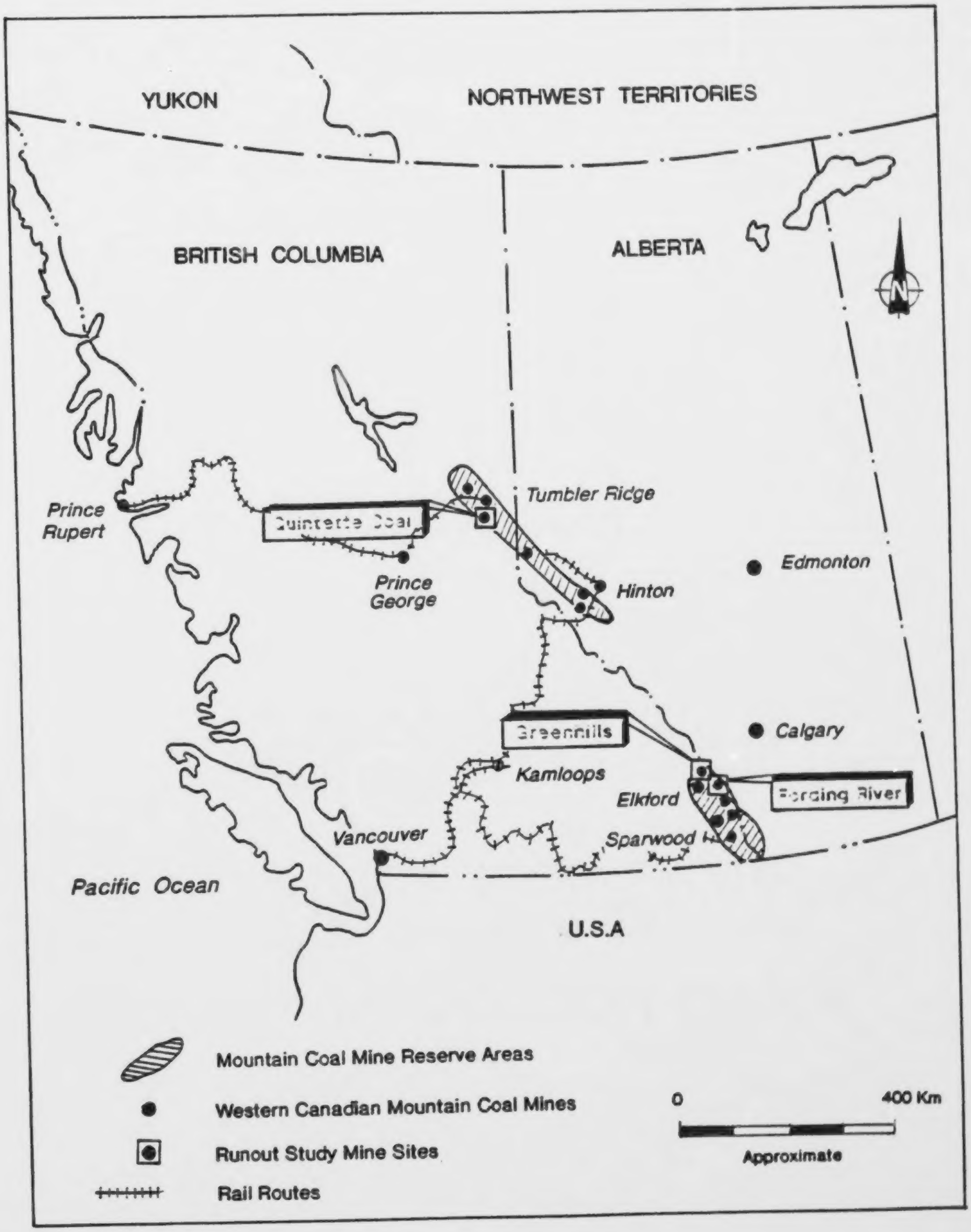

Figure 6.1 Rocky Mountain Coal Mine Flowslide Study Sites

STABLE VS UNSTABLE
DUMP GEOMETRIES

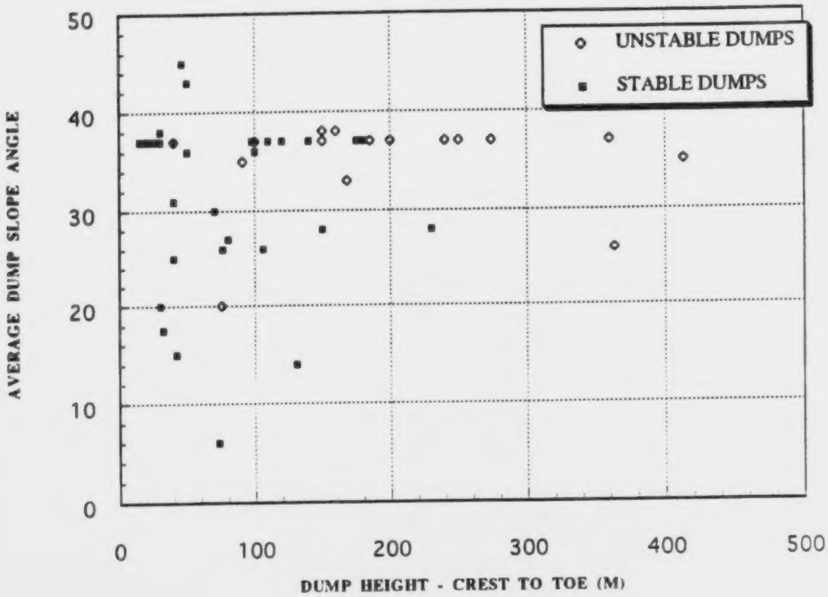

RUNOUT DISTANCES

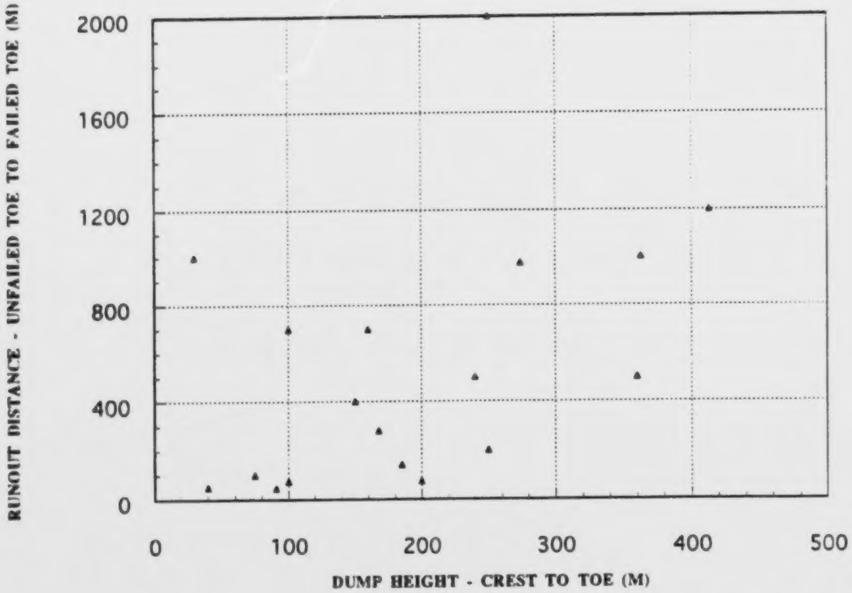

Figure 6.2 Coal Mine Waste Dump Stability Statistics

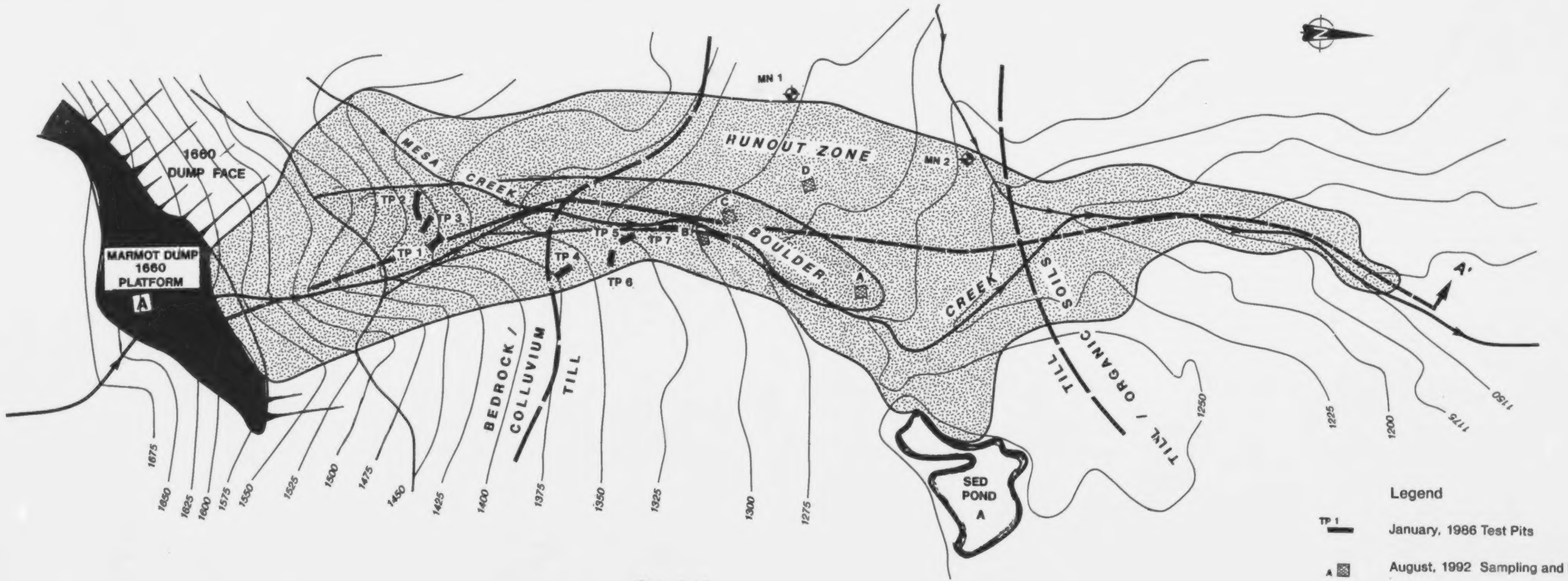

PLAN

Legend

- TP 1 — January, 1986 Test Pits
- A ▨ — August, 1992 Sampling and In - Situ Site Locations. (this study)
- ◈ — October, 1989 Foundation Testholes
- ▨ — Flowslide Runout Zone.
- ▩ — Window of Finer Sandy Gravel Runout Material

0 100 200 300 400 500

Scale (m)

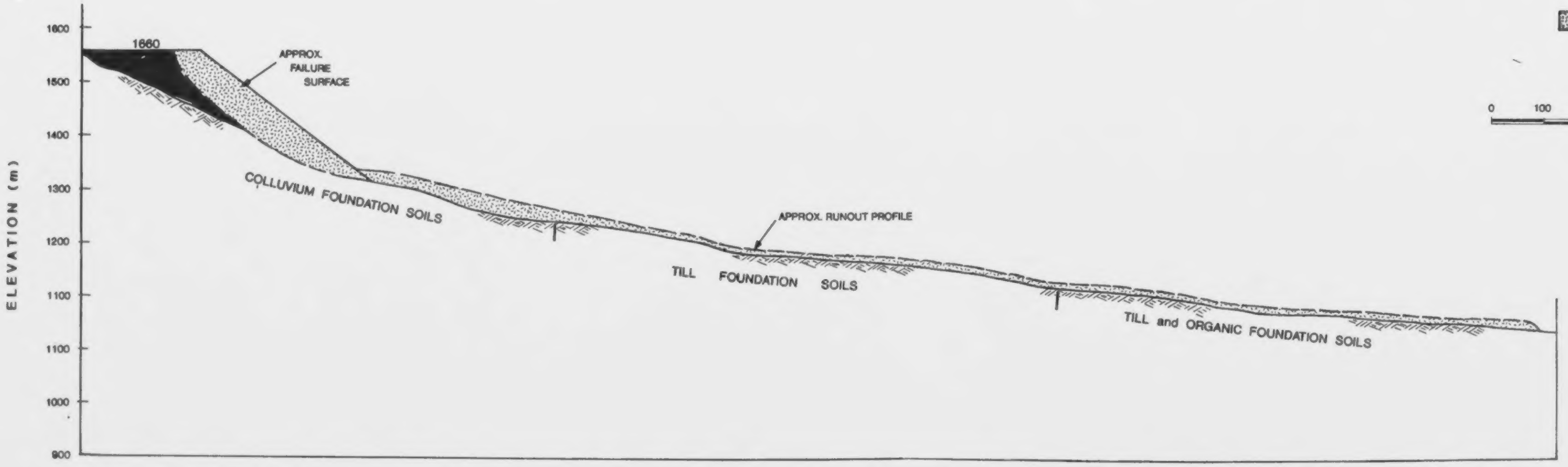

SECTION A - A'

QUINTETTE MARMOT 1660
SEPTEMBER 1985 FLOWSLIDE

SCALE As noted DATE Nov./93 MADE RD/YK CHKD RD APPD RD

JOB No CG25013 Figure 6.3 REV

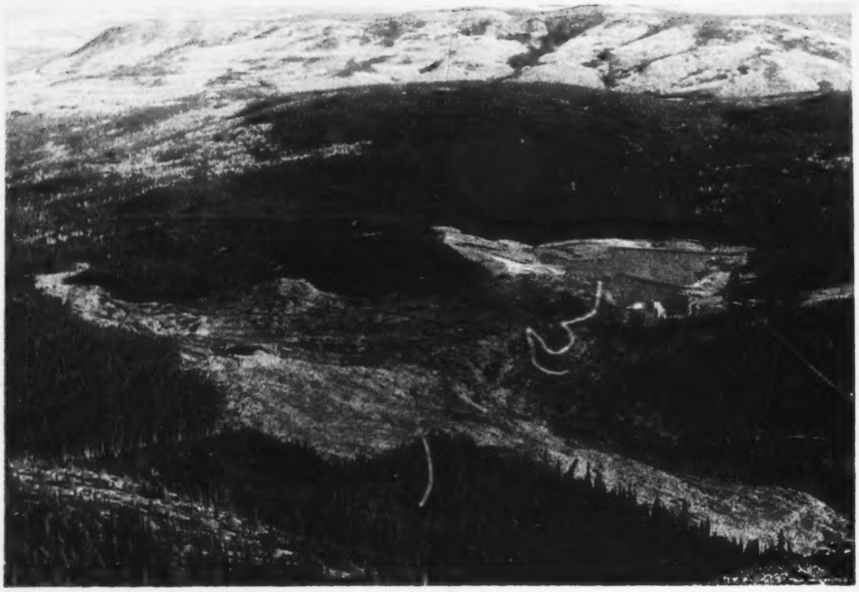

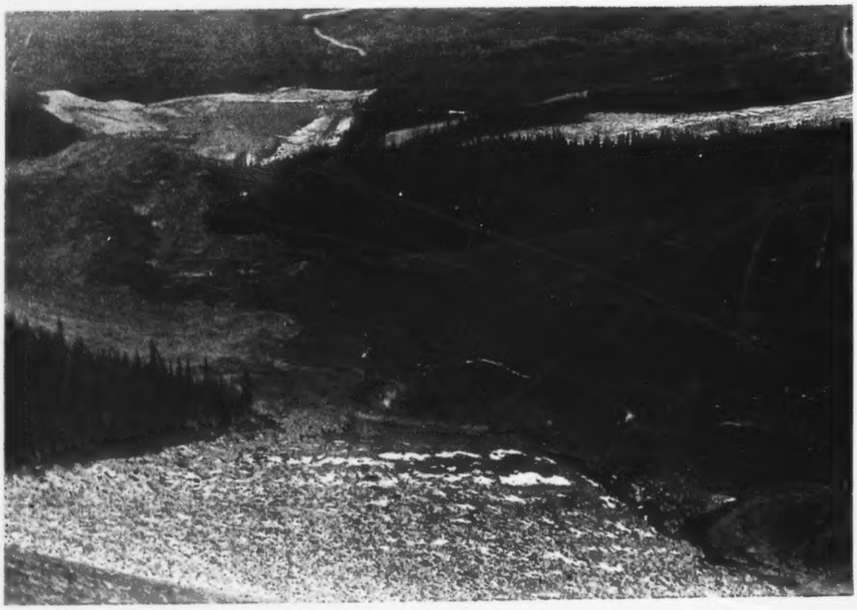

Figure 6.4 Marmot 1660 Runout

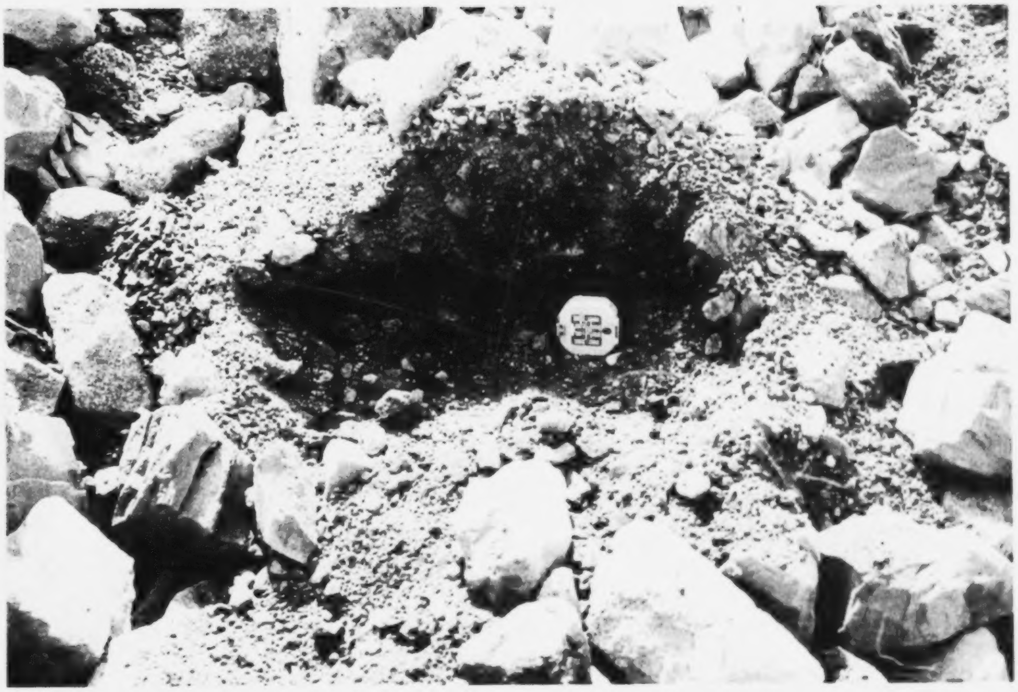

Figure 6.5 Liquefaction Cone in Marmot 1660 Runout

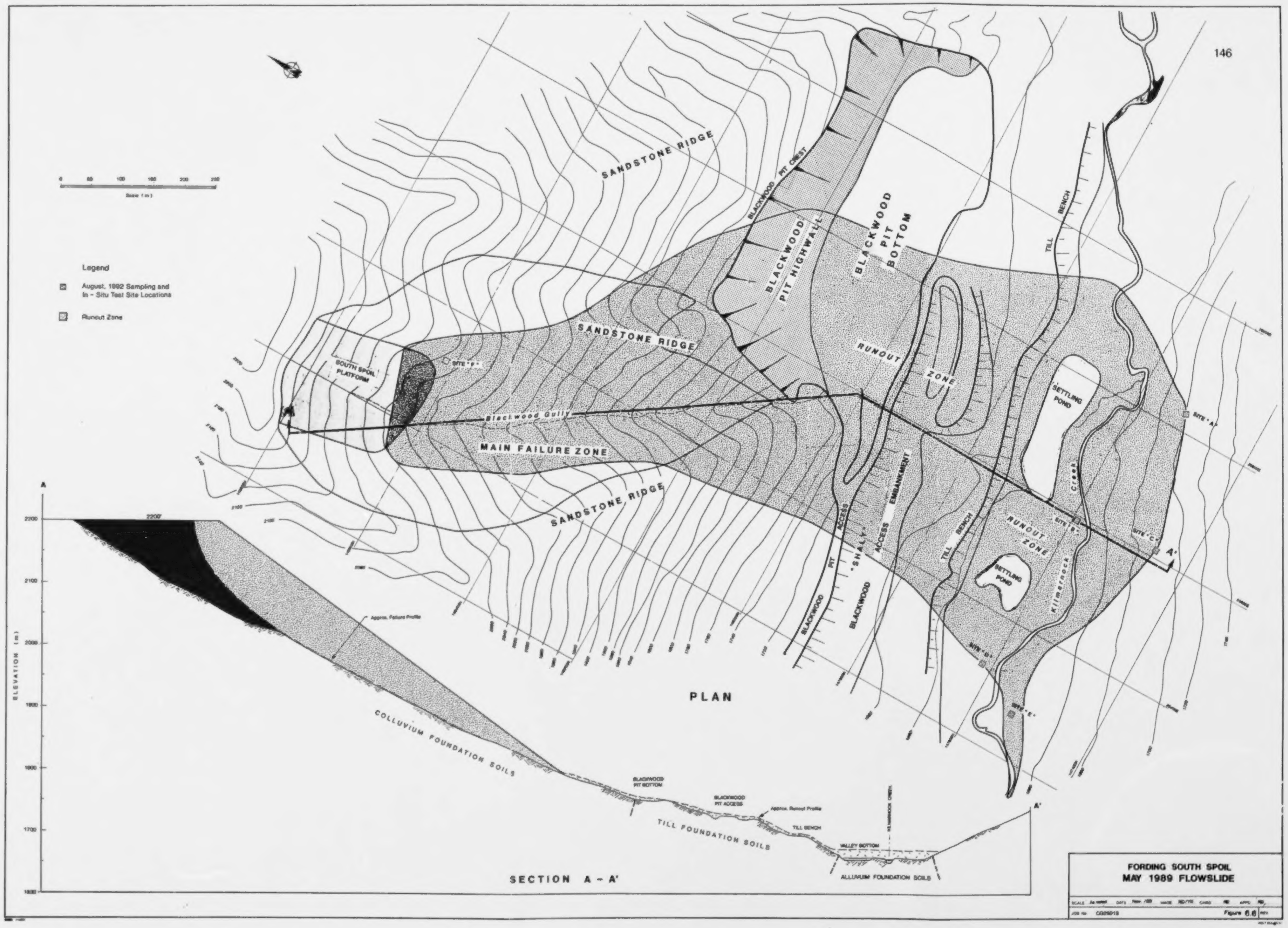

FORDING SOUTH SPOIL
MAY 1989 FLOWSLIDE

Figure 6.6

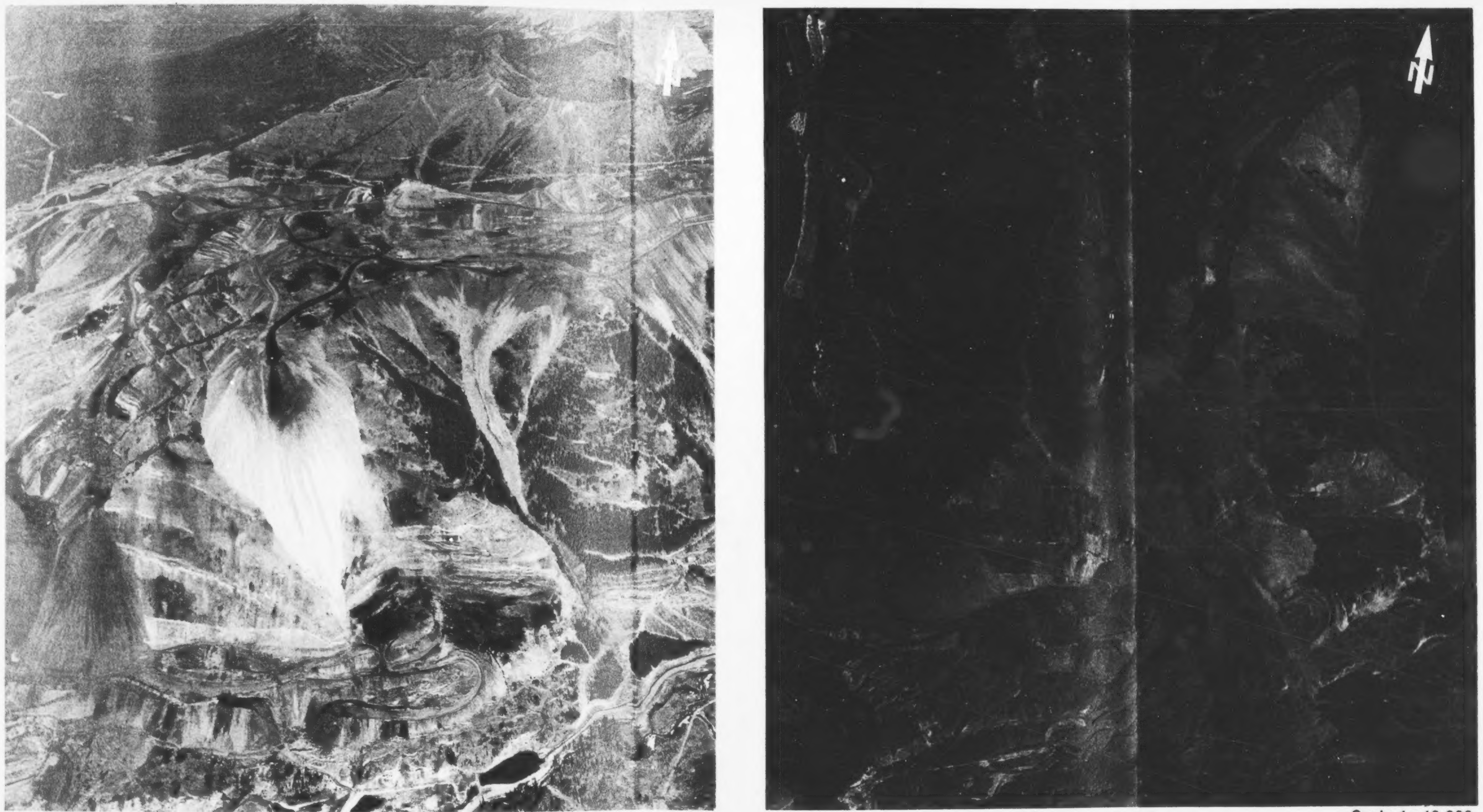

July 1989 Approx. Scale 1 : 11 000

Fording South Spoil 3 Months Before Failure

August 1990 Scale 1 : 10 000

Fording South Spoil 10 Months After Failure

Figure 6.7 Fording South Spoil Before and After Failure.

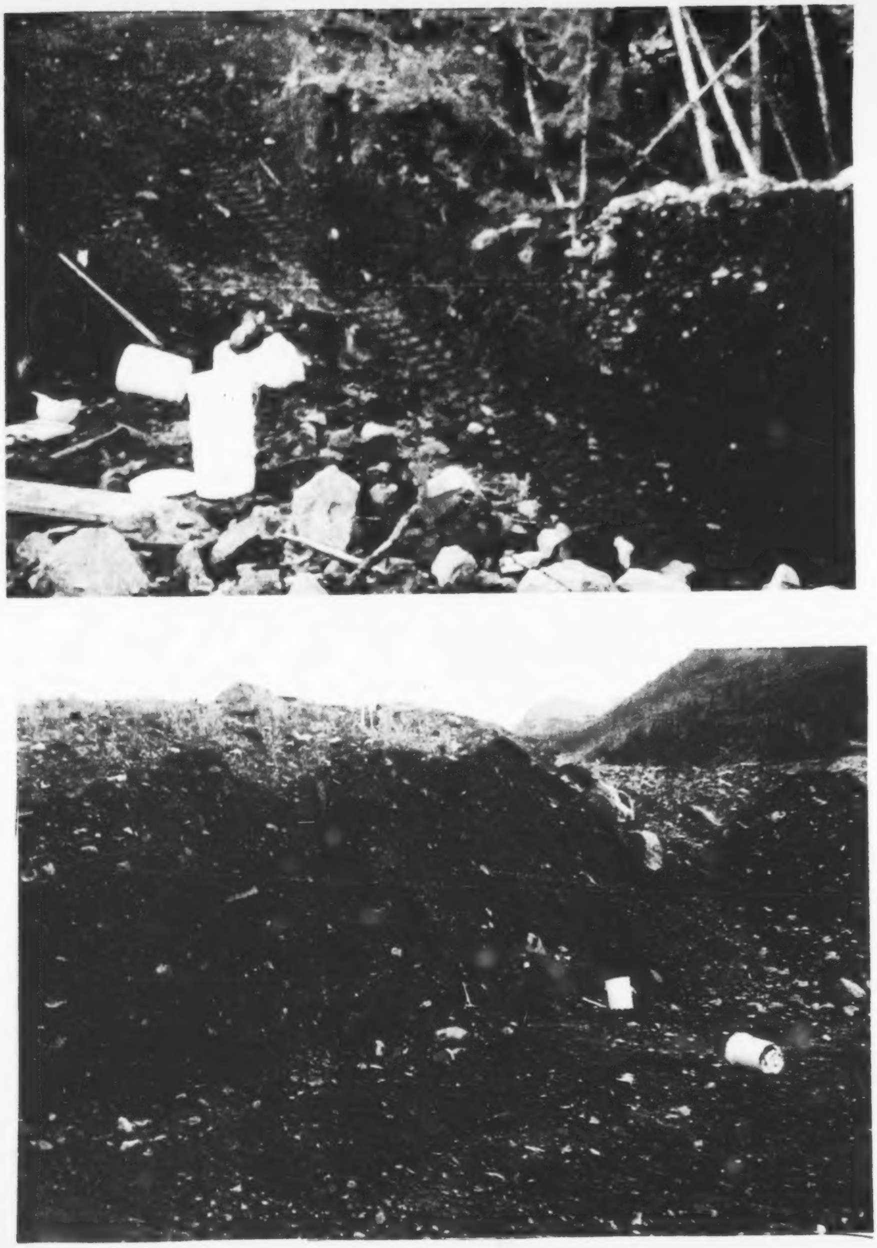

Figure 6.8 Fording South Spoil Runout Debris Dozer Cuts

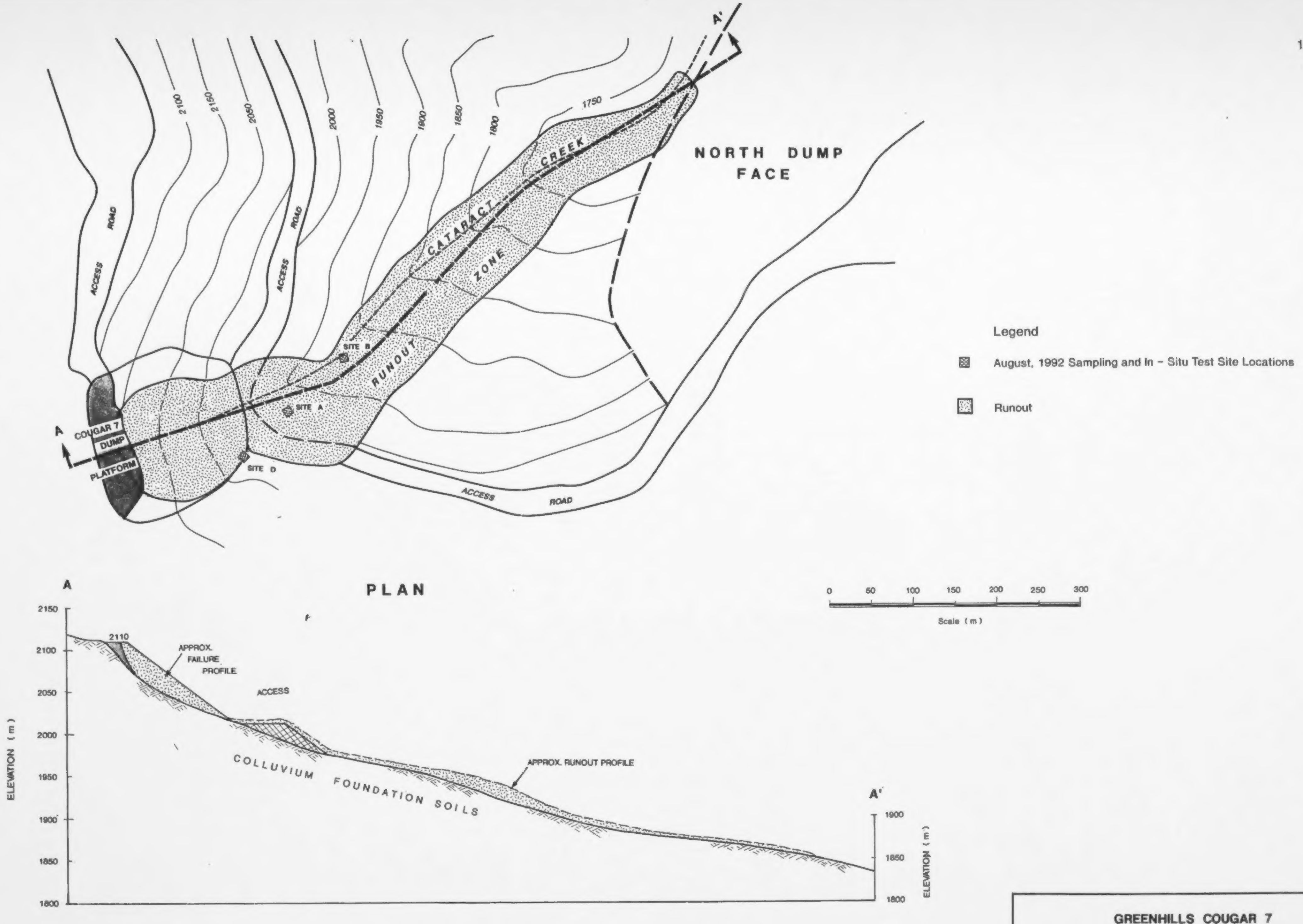

PLAN

SECTION A - A'

GREENHILLS COUGAR 7
MAY 1992 FLOWSLIDE

SCALE As noted DATE Nov. /93 MADE RD/YK CHKD RD APPD RD
JOB No. CG25013 Figure 6.9 REV

Figure 6.10 Cougar 7 Runout

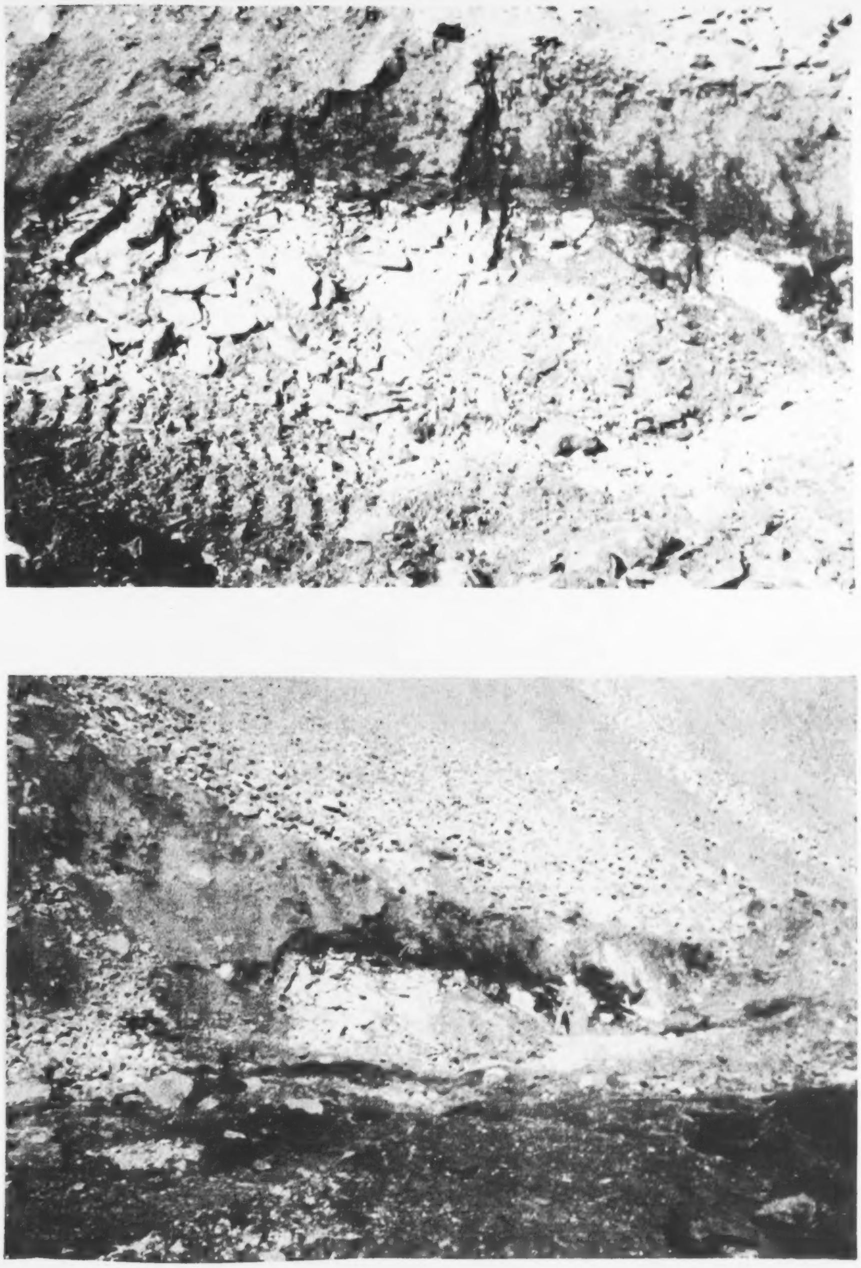

Figure 6.11 Fines Layers in Cougar 7 Dump

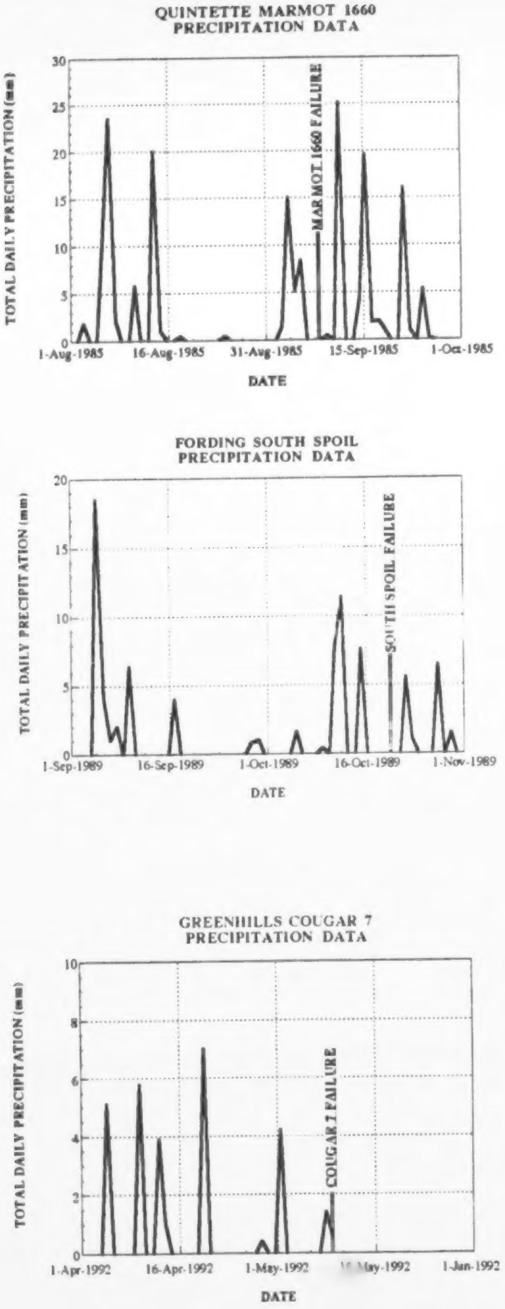

Figure 6.12 Daily Precipitation Prior to Failure

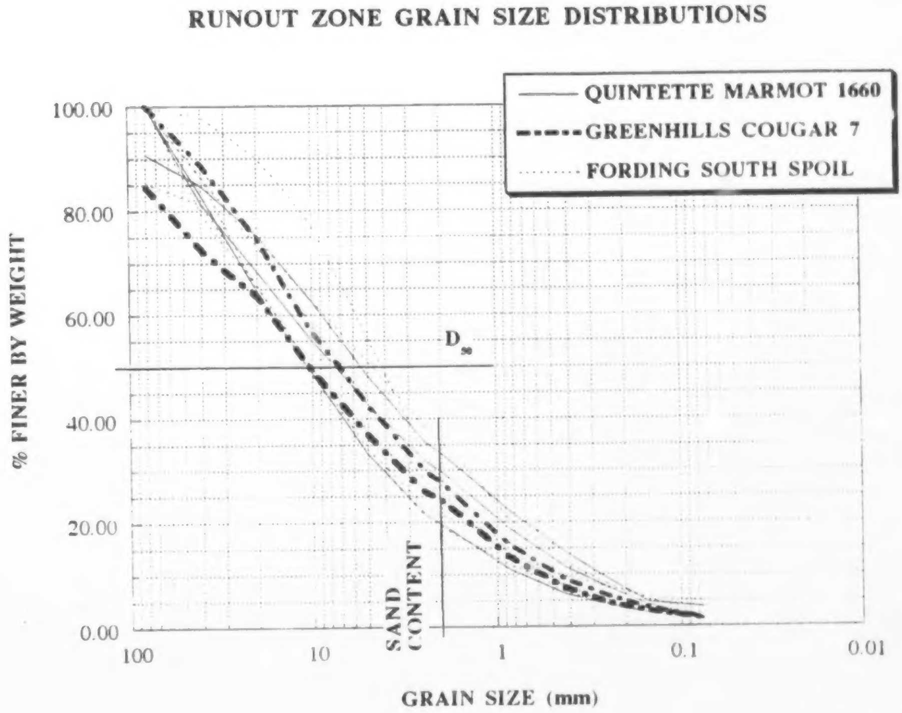

Figure 6.13 Runout Grain Size Distributions

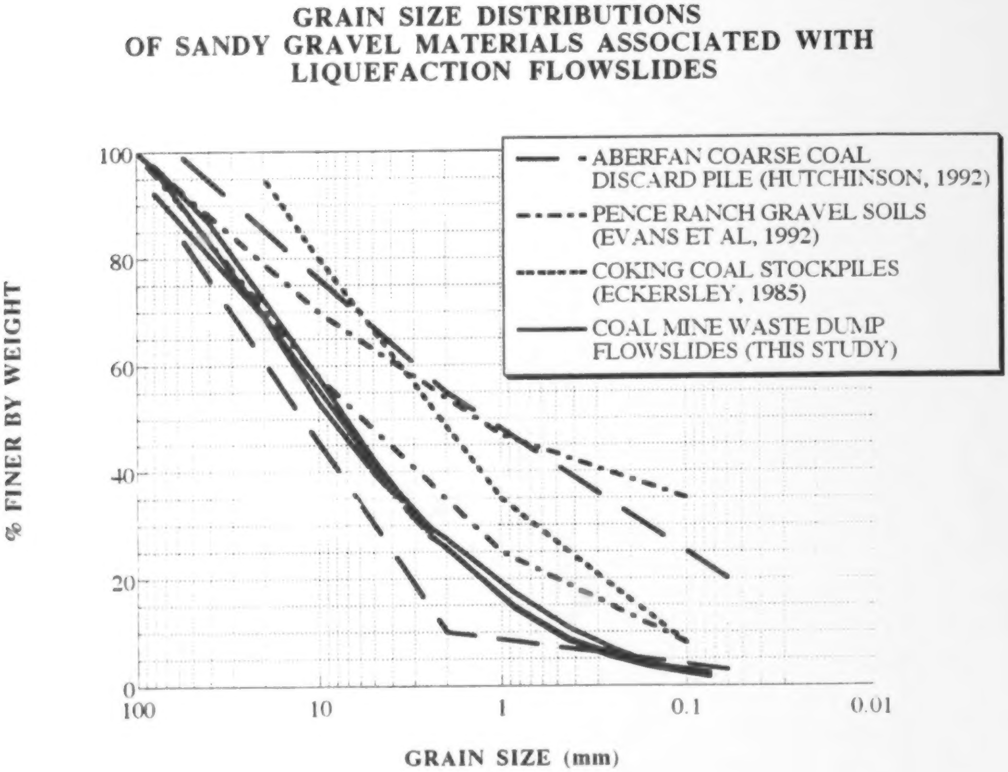

Figure 6.14 Liquefaction Flowslide Grain Size Distributions

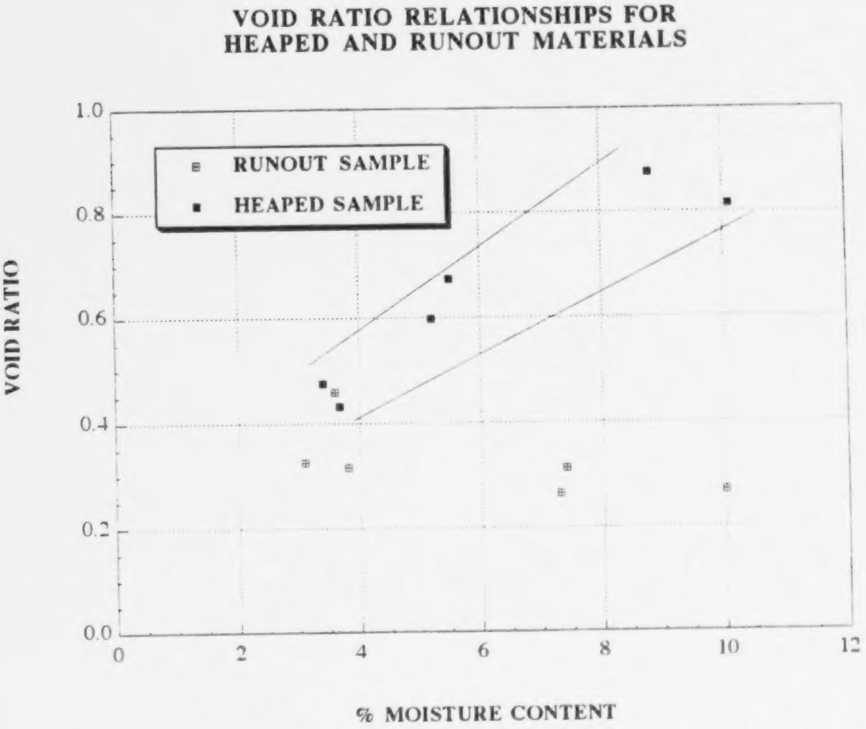

Figure 6.15 Field Void Ratio Versus Moisture Content

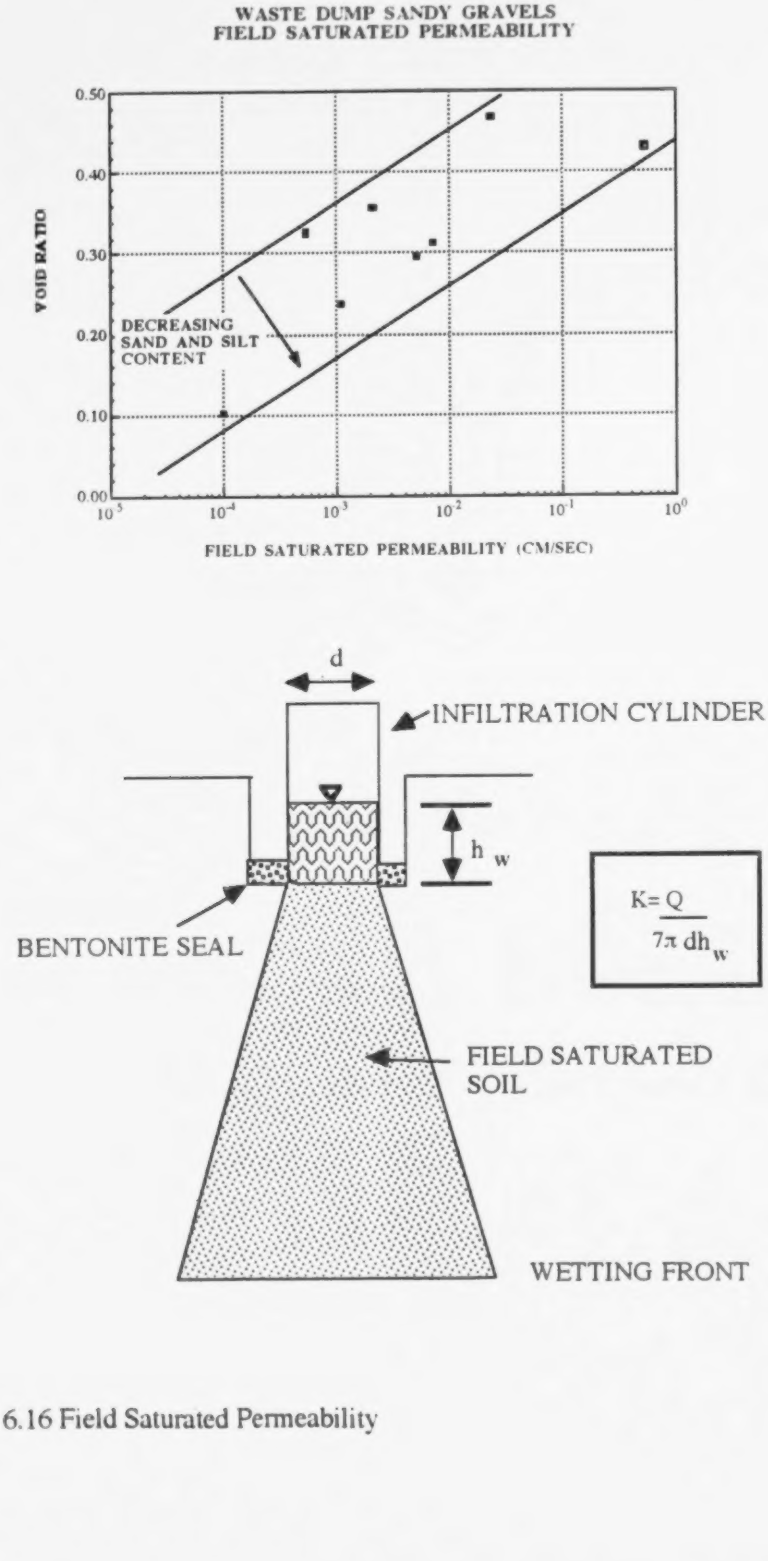

Figure 6.16 Field Saturated Permeability

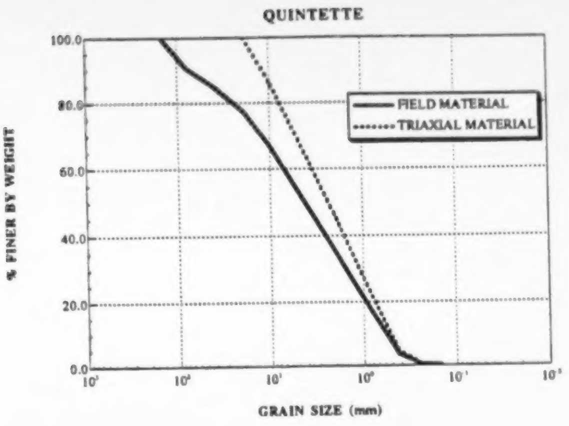

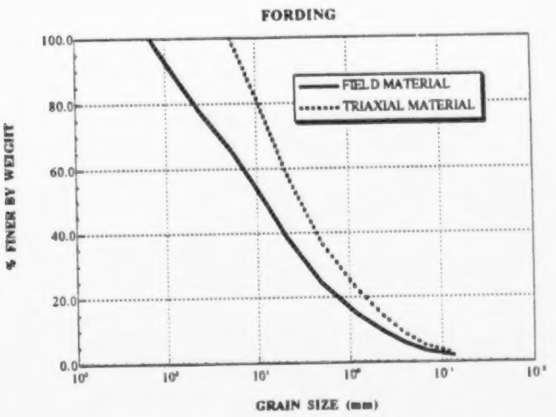

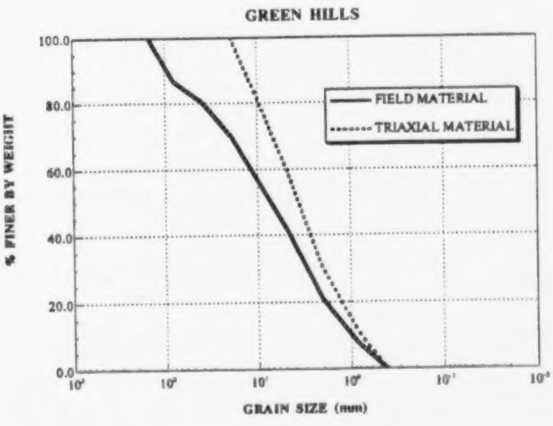

Figure 6.17 Field vs Triaxial Grain Size Distributions

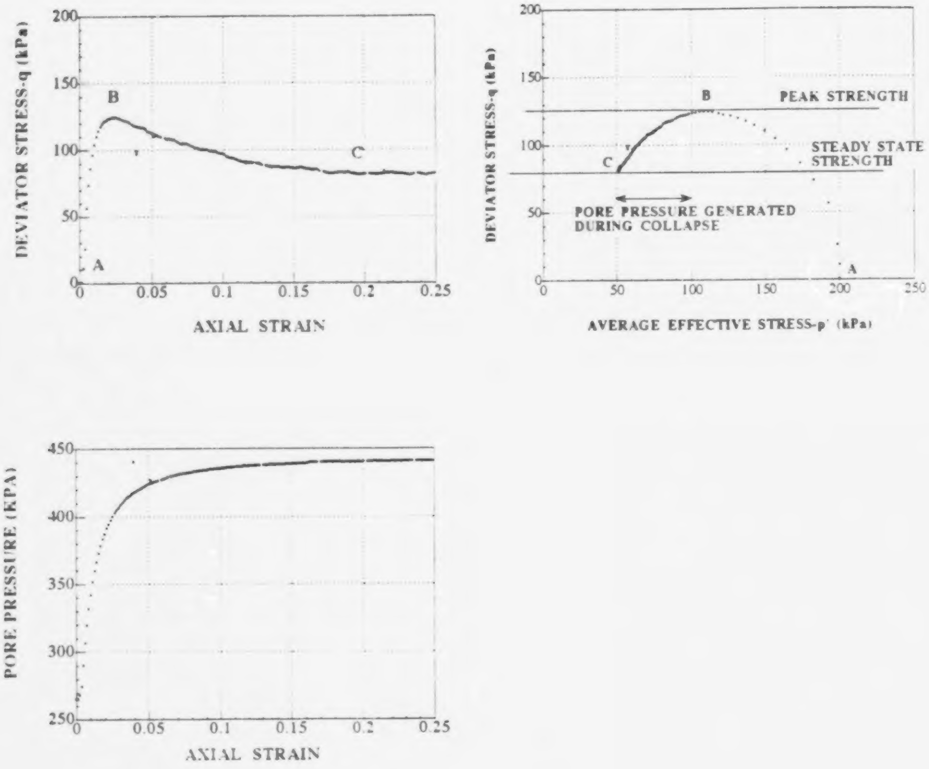

Figure 6.18 Typical Triaxial Test

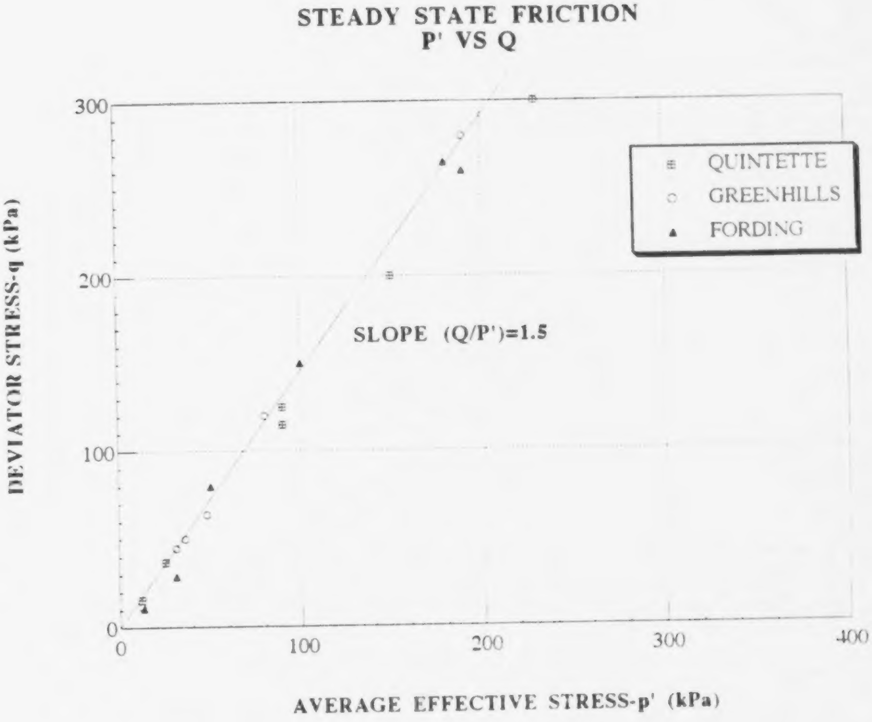

Figure 6.19 Steady State Friction Behaviour

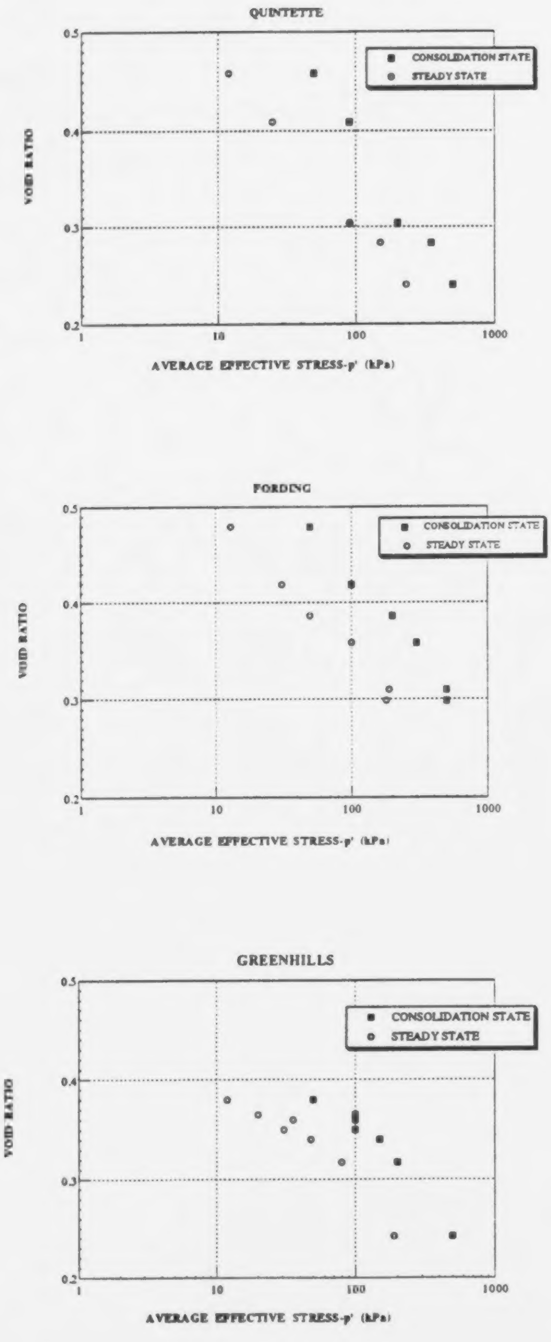

Figure 6.20 Steady State Void Ratio Behaviour

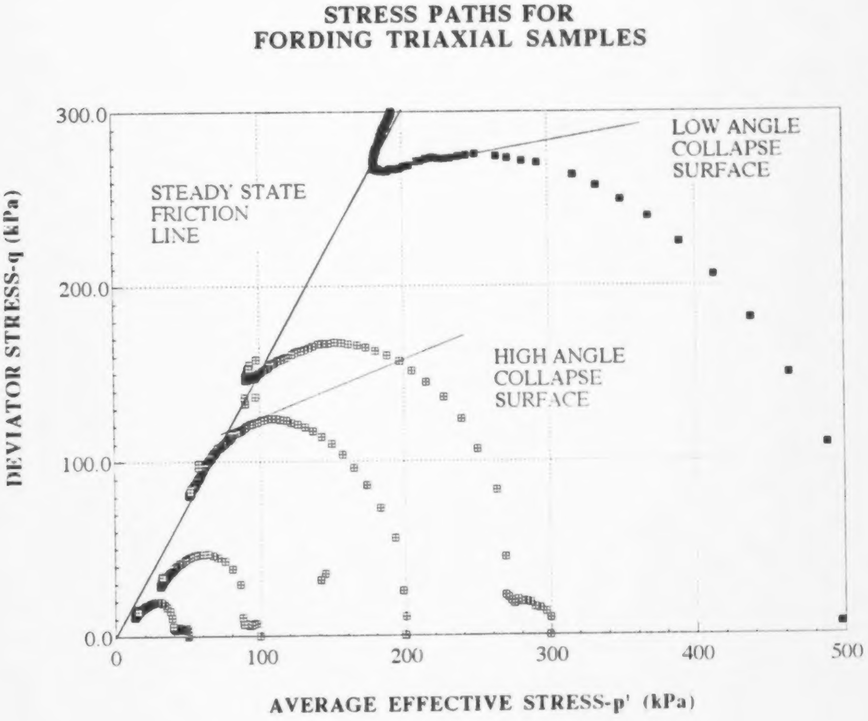

Figure 6.21 Fording Stress Paths

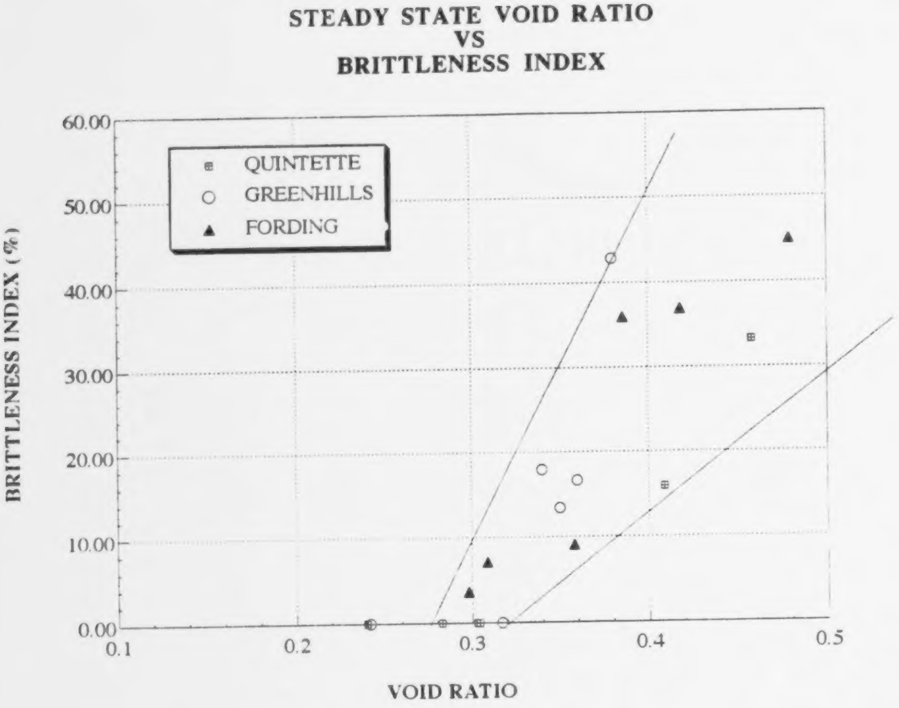

Figure 6.22 Brittleness Index Versus Void Ratio

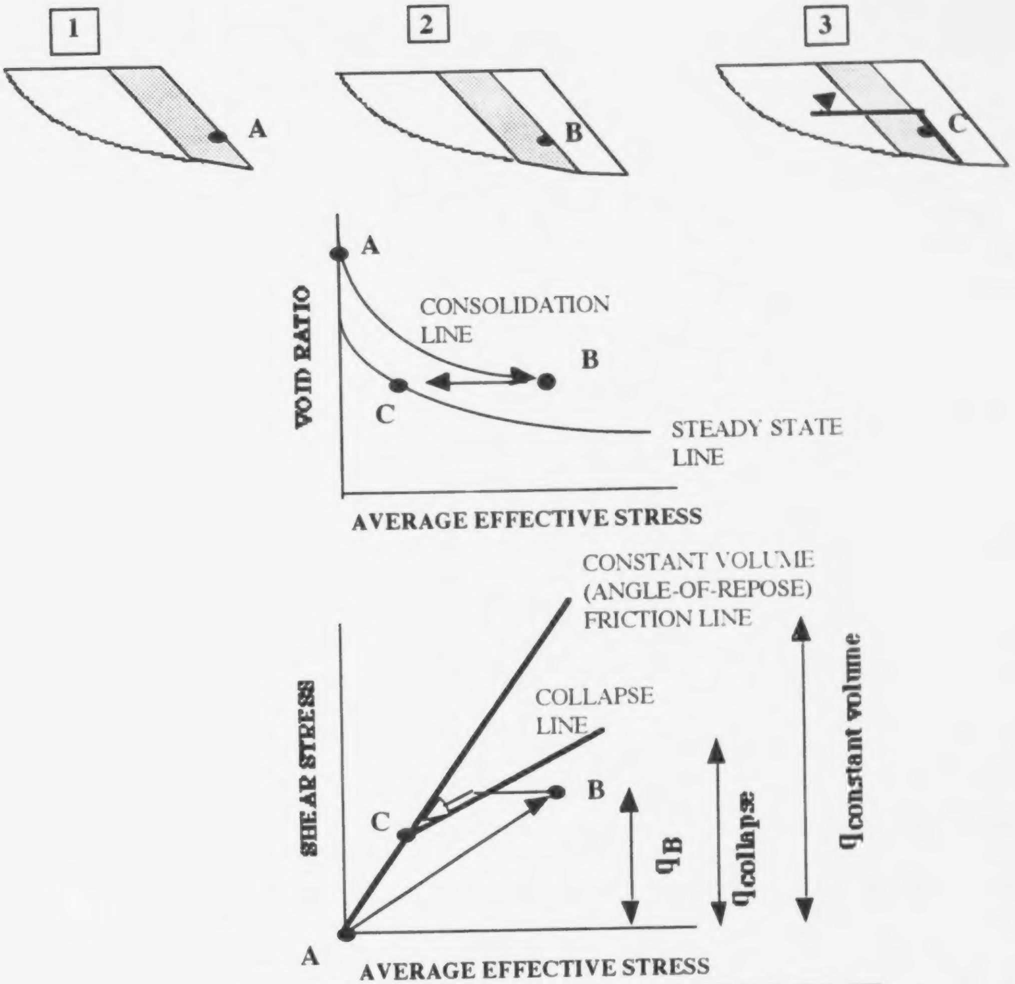

$$\text{CONVENTIONAL FACTOR OF SAFETY AT POINT B} = \frac{q_{\text{constant volume}}}{q_B}$$

$$\text{COLLAPSE FACTOR OF SAFETY AT POINT B} = \frac{q_{\text{collapse}}}{q_B}$$

Figure 6.23 Conceptual Collapse Model

Chapter 7

FLOWSLIDES IN ROCKY MOUNTAIN COAL MINE WASTE DUMPS-ANALYSIS AND MITIGATION

7.1 INTRODUCTION

In chapter 5, a framework for understanding and evaluating collapse processes in mine waste embankments (tailings dams and waste rock dumps) was presented. Chapter 6 examined three Rocky Mountain coal mine waste dump case histories and presented convincing evidence that collapse processes are responsible for the instabilities that resulted in long runout flowslide events.

This chapter presents results of finite element and limit equilibrium analyses carried out on each of the three flowslide events discussed in detail from Chapter 6. These events were fully documented in Chapter 6 and therefore the discussion here is restricted to the stability conditions prior to and following collapse. The analyses verifies the validity of the collapse mechanism.

Some mitigative strategies for reducing the liquefaction hazard are also discussed and highlighted by limit equilibrium analyses.

7.1 FINITE ELEMENT ANALYSES

The finite element analytical method is a very powerful and insightful tool and is used extensively in geotechnical engineering, especially in the design of embankments. Results are most useful when the input parameters are well defined and the particular analysis under consideration has been calibrated to field performance. This is not the case for the analyses presented here. Therefore in this chapter the finite element method is used to verify the mechanical validity of the collapse model presented in Chapter 6 and to gain an appreciation for the sense of the resulting displacements.

7.1.1 MODELING METHODS AND PARAMETERS

The modelling was carried out in two main steps. First the initial stresses prior to failure were calculated for each waste dump. Initial stresses were used as inputs to the collapse model which tracked the initiation of collapse and overall progressive failure that preceded the flowslides. Following the model presented in the previous chapter, each dump was constructed with a layer of potentially liquefiable sandy gravel material located near the base of the failure surface as defined by minesite records. The materials above and below this layer were assumed to be non-liquefiable coarser waste rock.

An explanation and discussion of modelling methods and parameters follows. The same parameters were used to model each flowslide event.

INITIAL STATE

The initial stresses were calculated by sequentially "constructing" each waste dump in layers parallel to the dump face (38° slope). Dumps were constructed with between 7 and 15 layers. The hyperbolic soil model (Duncan and Chang, 1970) was used to model the stress/strain response of the dumps during construction. The hyperbolic model calculates a tangent Young's modulus and bulk modulus as follows:

$$E_T = K_E P_A \left|\frac{\sigma_3}{P_A}\right|^n \left|1 - \frac{R_F(\sigma_1 - \sigma_3)(1 - \mathrm{SIN}\phi)}{2c\mathrm{COS}\phi + 2\sigma_3\mathrm{SIN}\phi}\right|^2$$

$$B_T = K_B P_A \left|\frac{\sigma_3}{P_A}\right|^m$$

WHERE: E_T = tan gent Young 's modulus
K_E = hyperbolic elastic number
n = hyperbolic elastic exponent
P_A = atmospheric pressure
$\sigma_1;\sigma_3$ = major and minor principal stresses
R_F = failure ratio
c = cohesion
ϕ = friction angle

B_T = tan gent bulk modulus
K_B = mod ulus number
m = modulus exponent

Table 7.1 shows the parameters used as input to the initial stress analysis. The hyperbolic elastic numbers (K_B) and hyperbolic elastic exponent value (n) were arrived at by examining large diameter triaxial tests from the literature. Results from testing of the angular Pyramid Dam sedimentary rockfill (Marachi et al., 1972) were used as this material exhibited similar initial void ratio, grain shape, lithology, and grain size distribution to "typical" coal mine waste dump materials. In addition test results for Pyramid Dam material were available for very large diameter test samples (0.9 m diameter triaxial cells). A friction angle of 38° was used as input to the hyperbolic model incremental stiffness calculation and a nominal cohesion of 1 kPa was necessary to prevent tensions from occuring in the mesh.

The tangent bulk modulus (B_T) was assumed constant (m=0) and equal to 0.3 for the coarse non-liquefiable material and 0.4 for the potentially liquefiable material. It was necessary to make several runs with different B_T values in order to conrol displacements to acceptable levels and avoid numerical instabilities .

COLLAPSE STATE

Gu (1992) has developed a finite element model to analyse small strain instabilities leading to collapse and flow. The model, while still in early stages of development, is unique in that it incorporates the essential elements of steady state and collapse, triggering, and stress redistributions necessary for evaluating liquefaction. The liquefaction analysis is conducted in the constant volume plane and thus volumetric strains are assumed negligible (ie., pore pressure dissipation is considered to be very small). The stress/strain behaviour of liquefiable materials in the constant volume plane is divided into three zones defined by the steady state strength and collapse surface as shown in Figure 7.1 and briefly described below:

Zone 1: Triggering and unbalanced loading due to stress redisributions resulting from collapse in Zone 2 occur in this zone. Linear elastic stress/strain behaviour is assumed. The stress path is defined by incrementally changing the A pore pressure parameter (q/p') between an initial (A_o) and final (A_m) value (Gu, 1992).

Zone 2: Collapse and strain softening behaviour occurs here. The strength parameters that determine collapse are defined by the peak strength line (q/p' at peak strength) and the collapse line (q/p' during collapse). During collapse displacements are determined by using the inverse hyperbolic stress/strain model, developed by Chan (1986), which takes the following form:

$$q = q_{max}\left|1 - \frac{\varepsilon_p}{a + b\varepsilon_p}\right|$$

WHERE: q = deviator stress

q_{max} = peak deviator stress

ε_p = plastic strain

a = post peak strain behaviour parameter

$$b = \frac{1}{1 - q_{ss}/q_{max}}$$

q_{ss} = steady state deviator stress

In Zone 2, all strains are assumed to be plastic. Unbalanced loads occurring in Zone 2 are transferred to adjacent elements in Zone 1 and Zone 3.

Zone 3: An elastic plastic stress/strain model is used in this zone. The stress path is defined by the steady state line. Excess pore water pressure decreases during loading and increases during unloading in shear.

Following initial triggering, unbalanced loads are brought to equilibrium by iteration. Non-convergence during the iterative process means that equilibrium will not be reached and flow failure is imminent. Further deformations are contolled by large strain flow processes which are beyond the scope of this study.

Table 7.2 shows the parameters used to model the collapse process. The liquefaction model incorporates a constant volume friction line with a slope of 1.5 ($Ø_{cv}$=38°), a peak strength line with a slope of 1.1, and a collapse line with a slope of 0.33 ($Ø'_{collapse}$=9°).

7.1.2 MODELLING RESULTS

Finite element results are portrayed in terms of the yield ratio (R_y) defined as :

$$R_y = q_o / q_f$$

Where: q_o= shear stress

q_f= shear strength

The yield ratio of an element is the inverse of the factor of safety of that element. A yield ratio of 1.0 means that yielding has occurred. Figure 7.1 shows the yield ratio relationships for the liquefaction model. The yield ratio is always less than one in Zone 1, always equal to one in Zone 2, and only equal to one in Zone 3 when the steady state strength is reached. The yield ratio approach allows for a finite element based stability analysis to be undertaken and easily interpreted. In fact, a safety factor can be calculated based on the weighted average yield ratio through a failure zone.

Failure will not occur unless a kinematically admissible displacement field exists. Such a zone can be found by examining results of finite element displacement vectors. It is defined as follows (Gu, 1992):

> *" a kinematically possible slip surface is a surface on which all the displacement vectors point in the same clockwise or anti clockwise tangent directions of the surface, and with two ends on the free boundary surface of the earth structure"*

A failure surface defined by finite element results is a kinematically possible yield surface passing though a continuous yield zone. Figure 7.2 shows a failure surface according to this criterion.

Finite element results for the three case histories are examined with contoured plots of yield ratio and vector plots of displacement in order to capture the growth of the yielding zone due to collapse of the loose sandy gravel layers.

The analyses presented in this section consists of pairs of yield ratio/displacement plots that represent the stress conditions and displacements in the dump just prior to failure (initial condition) and at the point of overall progressive failure. The latter condition was determined when convergence could not be obtained after several iterations. The position of the liquefiable layer for each dump was determined from the failure profile obtained from the minesite; it is shown as a cross-hatched layer on each plot. The yield ratio plots are shaded to show zones with a yield ratio of 1.0. The liquefied yield ratio plots for each dump show the final failure profile (shown as a dashed line with arrows) as determined from minesite records.

Liquefaction is initiated by sequentially increasing the pore pressures in the liquefiable layer elements starting from the lowermost elements in the slope. In all cases only a very small pore pressure increment (several kPa) was required to initiate overall collapse. During collapse all the elements in the liquefied zone are assumed to be potentially liquefiable.

QUINTETTE MARMOT 1660

Figure 7.3 shows the initial yield ratio and initial displacements respectively for the Marmot 1660 dump. The location of the potentially liquefiable layer was assumed to be located about 40 m behind the dump face as based on a post failure cross section obtained from the minesite. The layer drapes over a break in the underlying foundation topography. The initial yield ratio plot shows that maximum yield (R_y=1) behaviour is apparent mostly near the crest and close to the dump face near the toe area. Corresponding displacements appear to be controlled and oriented mostly parallel to the dump face. Most of the movement prior to failure occurs in a zone parallel to the face and in the middle third of the embankment.

As pore pressures are built up in the liquefiable layer, collapse occurs (Figure 7.4). The liquefied yield ratio plot shows that most of the dump has yielded and the post failure profile appears to bound most of the fully yielded zone. The displacement plot shows that the failure occurs as a slab which overrides the passive "toe block." Very large displacements are apparent above the toe block area indicating a rapid release of strain energy in this area.

FORDING SOUTH SPOIL

Figure 7.5 shows the initial yield ratio and displacements for the Fording South Spoil waste dump. The location of the potentially liquefiable layer was assumed to be located about 50 m behind the dump face as based on a post failure cross section obtained from the minesite. The initial yield ratio plot shows that maximum yield (R_y=1) behaviour is apparent mostly near the crest and close to the dump face near the toe area, in a very similar pattern to the Marmot 1660 dump. Corresponding displacements appear to be controlled and oriented mostly parallel to the dump face.

As pore pressures are built up in the liquefiable layer, collapse occurs (Figure 7.6). The post failure profile lies well within the fully yielded zone. The displacement plot shows that the material above the liquefied layer has a distinct movement pattern parallel to the slope and that the failed zone daylights above the toe block. The analysis appears to define the post failure profile nicely.

GREENHILLS COUGAR 7

The initial yield ratio and displacement plots for the Cougar 7 waste dump flowslide are shown in Figure 7.7. A potentially liquefiable layer located about 15 m behind the slope face was assumed for the analysis. The initial yield ratio plot shows a similar pattern of yielding near the crest and slope face as the previous two cases. Initial displacements are controlled and oriented mostly parallel to the slope face. Displacements are relatively smaller than the previous two cases.

Figure 7.8 shows the yield ratio and displacement plots corresponding to the failure condition. Most of the slope has failed and a clear displacement surface is evident that closely matches the post failure profile. The liquefied displacement plot shows that the failure zone daylights above the toe zone area, similar to the previous two cases.

Figure 7.9 shows a series of stress state plots (p-q space) that show the initial stress states calculated from the finite element analyses for potentially liquefiable layer elements in each of the waste dumps analyzed. For each plot in Figure 7.9 the stress state points are shown relative to the peak and steady state lines used for the analyses undertaken in the previous section. All the plots show that the stress state points lie on or just above the peak line demonstrating that only a very small disturbance is necessary to initiate collapse. For the potentially liquefiable points shown in Figure 7.9 the safety factor with respect to the peak line is less than or equal to 1.0 whereas the safety factor with respect to the constant volume line is greater than 1.0. This is the case without any considerations for water pressures in the slope.

7.2 LIMIT EQUILIBRIUM ANALYSES

Although the finite element analysis results are revealing, routine stability analysis of mine waste dumps is carried out by calculating a safety factor with respect to limit equilibrium. A survey of mine waste dumps conducted in British Columbia (Piteau Associates, 1991) shows that many coal mine waste dumps fail with calculated safety factors of 1.1 to 1.2. In most cases the analysis is carried out without any consideration for pore pressures and by assigning a waste rock friction angle equal to the angle of repose. The work presented in the last two chapters of this thesis clearly demonstrates that these assumptions are not valid; not only because they incorrectly predict stable dumps, but more importantly because they do not identify the potential for a liquefaction flowslide.

Limit equilibrium analyses (Bishop's method of slices) were carried out for each of the three case histories in order to derive safety factors that define stability conditions prior to and following collapse. For each waste dump the failure profile used in the stability analyses followed the potentially liquefiable layer down to the foundation contact and passed out through the toe along the dump foundation contact. A unit weight of 19 kN/m^3 was assumed for all waste rock materials. The non-liquefiable waste rock and foundation materials were assumed to be cohesionless with friction angles of 38° and 32° respectively. The shear strength parameters of the liquefiable materials were varied in order to calculate three different safety factors as follows:

1. CONVENTIONAL ANALYSIS: The conventional safety factor was calculated based on an angle of repose friction angle of 38° for all waste rock materials.

2. TRIGGER ANALYSIS: The safety factor with respect to a collapse trigger was calculated by assigning a triggering strength to the potentially liquefiable material based on the peak strengths derived from the triaxial tests in the previous chapter. Figure 7.10 shows a plot of the peak data points from the isotropically consolidated triaxial tests in Appendix B. The laboratory results show that a trigger strength equivalent to a friction angle of 28° ($q/p'=1.1$) provides a reasonable lower bound estimate of the collapse trigger. The collapse trigger derived from the results of isotropically consolidated tests provides a conservative assessment of collapse behaviour. Anisotropically consolidated samples will demonstrate collapse behaviour at higher stress ratios.

3. COLLAPSE ANALYSIS: The most conservative assessment of stability is attained by considering that all the potentially liquefiable material is triggered and that the shearing resistance of this material is defined by an undrained strength value equivalent to the steady state strength. Figure 7.11 shows a plot of brittleness index (I_B)versus the ratio of undrained strength to the vertical effective stress (S_u/σ'_v) at a p/q ratio of 1.0 (equivalent to K_0 conditions) for the triaxial test data in Appendix B. Values of S_U/σ'_v) of 0.15 and 0.2 were used to calculate undrained strength for the undrained analyses. Note that at a brittleness index equal to zero the S_U/σ'_v value is about 0.22.

Table 7.3 shows the results of the stability analyses. The table shows that conventional safety factors of about 1.2 are calculated for each flowslide event and that the trigger analyses computes safety factors of about 1.0. Clearly all three waste dumps were marginally stable against a liquefaction trigger and a negligibly small trigger was required to initiate collapse. The collapse analyses show safety factors considerably less than 1.0 and illustrate the link between instability and potential mobility. Additional strain weakening behaviour following the onset of global instability (at a safety factor equal to unity) provides the energy required to initiate a rapidly moving liquefaction flowslide.

7.3 MITIGATIVE STRATEGIES

The analyses conducted above and detailed studies presented in chapter 6 provide an enhanced understanding of mechanisms responsible for liquefaction flowslides in mine waste dumps. In this section, some strategies that could be employed to reduce the flowslide risk are examined. The discussion is divided into three different periods related to waste dump construction and ultimate abandonment as follows:

1. Pre-construction - period of site preparation work required prior to waste rock placement.

2. Construction - active dump construction period.

3. Abandonment - reclamation period following active dumping.

The various strategies are outlined in Table 7.4 in a matrix format for the different time periods arranged according to practices related to water management, materials management, and construction methods. A discussion of the various strategies which follows the format outlined in Table 7.4 follows.

7.3.1 PRE-CONSTRUCTION STRATEGIES

Steep mountain slopes place some limits on practical pre-construction strategies. Also, it is not practical to exercise the same care and attention to foundation conditions that would be afforded a fluid impounding structure. However, in some cases it may be worthwhile reducing the liquefaction flowslide hazard by undertaking some modest pre-construction strategies. Clearly, a technical evaluation of these factors should be coupled with economic considerations. Discussion here is confined to technical issues.

Water Management - All practices that reduce the influx of water into an embankment will have a positive effect on stability. Diversion of surface water with upslope interceptor ditches and finger drains constructed on the foundation for preventing the buildup of a water table in the dump during subsequent construction are two mitigative measures that could be employed. These more conventional practices are discussed in detail elsewhere and need not be elaborayed on here.

Construction Methods - During the pre-construction period, the liquefaction flowslide hazard can be reduced by employing construction practices that increase the shearing resistance at the waste dump/foundation contact. This would have the added benefits of reducing the potential for triggering a liquefaction flowslide due to foundation straining and preventing a loss of structural containment in the waste dump toe region that could lead to the flow of liquefied material. Construction activities that could achieve these objectives include removal of weak saturated materials and constructing a shear key in the critical toe regions of a waste dump as it advances out over the foundation. Relative stability benefits of removing weak materials can be examined by employing conventional stability analyses which incorporate appropriate undrained strength criteria for the weak foundation materials. Further discussion here is confined to the potential liquefaction stability benefits of incorporating a shear key in the foundation toe region.

Additional analyses for the three waste dump flow slides discussed in Sections 7.1 and 7.2 were carried out employing the triggering analysis discussed above for the potentially liquefiable material (friction angle of 28° for potentially liquefiable material). Figure 7.12 shows the results of the analyses plotted as foundation friction angle versus safety factor. The figure demonstrates that a modest increase in the foundation shearing resistance could have a beneficial effect on stability. It is shown that an increase in frictional resistance from 32° (typical value for a sandy till foundation material) to 38° (similar to the increase afforded by a waste rock shear key) results in an increase in safety factor from 1.0 to about 1.1. Similar analyses carried out with undrained strength values for potentially liquefiable materials (collapse analysis) demonstrated that a similar relative increase in safety factor was achievable but that the increase in foundation shearing resistance was not sufficient to fully contain a flow slide (i.e.. the safety factor was still less than or equal to unity). These results suggest that a shear key may provide short term triggering resistance but that the flowslide potential is still present. In some cases this may be an acceptable strategy, especially where further construction will result in additional stabilizing measures.

7.3.2 CONSTRUCTION STRATEGIES

There are several strategies that could be employed during construction to reduce the potential for a liquefaction flowslide from occurring. Clearly, many conventional practices employing compaction in lifts would also achieve this objective. It is assumed here that a fully compacted dump is not a practical alternative and thus attention is focused towards other strategies that could be employed during construction. As discussed previously the discussion is confined to technical issues although it is recognized that economic considerations need to be evaluated as part of the process of arriving at an acceptable mitigative strategy.

The work presented in Chapter 6 clearly identified the role of finer sandy gravel consist materials in causing the instabilities that could lead to highly mobile flowslide events. This work identified that end dumped carbonaceous sandy gravel waste rock (sand contents greater than 20%) is particularly collapse prone. Further classification and characterization work is required in order to properly predict and track the occurrence of these materials. This work is currently underway (Dawson et al, 1994b) but is beyond the scope of this thesis. In the discussion of construction strategies that follows it is assumed that these materials can be classified and identified. Thus the discussion refers to the finer, high moisture retention collapse prone materials as liquefiable and the coarser, low moisture retention non-collapsible materials as non-liquefiable.

Water Management - Internal drains, formed from coarser non-liquefiable materials could prevent the formation of a water table in a waste dump. Such drains could be end-dumped longitudinally down the dump face and spaced at appropriate intervals. The effectiveness of these drains would depend on saturated/unsaturated seepage conditions present prior to collapse These drains may not be effective in draining partially saturated liquefiable materials and some further study of layered unsaturated flow conditions is required to properly investigate the effectiveness of this strategy. Nonetheless they would serve to break up the formation of laterally continuous liquefiable layers within the dump.

As the Greenhills Cougar 7 case history points out, accumulations of large amounts of snow in the dump can significantly contribute to the water table conditions during melting. Clearly it is impossible to doze the snow off the dump face, however snow should not be dozed over active dump areas where large accumulations could occur within the dump.

Materials Management - Selective management of potentially liquefiable materials is perhaps the most practical and effective way to reduce the liquefaction flowslide hazard during construction. Materials management strategies include eliminating liquefaction prone materials, blending coarse and fine materials, and selectively placing liquefaction susceptible materials in portions of the dump where the risk of collapse is reduced or contained.

Where appropriate it may be possible to store these materials in specially designed compacted fill embankments or in areas where a flowslide poses an acceptable risk to safety, infrastructure, and the environment.

Blending of coarse and fine materials in order to produce a non-liquefiable blended product merits consideration. Blending could potentially be accomplished by hauling and dumping waste rock truck loads at pre-determined ratios to the same dump location. It is not clear whether adequate blending would be achieved and this strategy would require some controlled field scale demonstration.

Selective placement of liquefiable materials could be a very effective strategy where smaller volumes of finer materials are being handled. This strategy would be most effective if the finer materials could be dumped on the crest when an additional lift is required or prior to dump closure. In this case additional compaction would also take place due to truck traffic.

Construction Method - The manner in which waste dumps are constructed controls the development of weak, potentially liquefiable layers and can enhance the structural containment of these layers. Some construction methods that achieve these objectives include terraced construction, dumping perpendicular to the slope, and construction within a containing berm. Figure 7.13 shows some schematic cross sectional and plan views of these strategies and a brief discussion of each follows.

Terraced construction is the most effective strategy as the continuity of the finer layers will be limited by the height of each terrace and the overall dump slope is flattened due to the terracing effect. Economics often restricts terraced construction methods on steep mountain slopes.

Where terracing is impractical weak layers can be restricted by advancing the dump normal to the topography thus causing weaker layers to form normal to the natural topography. This method would require that an initial starter dump be constructed parallel to the natural topography on each pass. In addition, this method does not require any inventory control of potentially liquefiable materials. The effectiveness of this approach will require some further considerations of the width of each dumping pass relative to the potential formation and geometry of liquefiable layers in the dump.

Construction of a containment berm near the toe area prior to or following the main dump construction period could provide sufficient containment that would reduce the overall flowslide potential should collapse of liquefiable material be initiated. This option could be interrogated by assigning undrained strength criteria to the liquefiable materials and using limit equilibrium analyses to examine the size of berm required to contain a collapsing layer. Analyses conducted for the case histories discussed above demonstrated that very large berms are required to provide sufficient containment.

7.3.3 ABANDONMENT STRATEGIES

Following abandonment, additional efforts to reduce the liquefaction risk merit consideration. Offsetting this requirement is the observation that most dumps fail during or slightly after construction. A study by Golder Associates (1992) which documented several coal mine waste dump flowslides indicated that all the events occurred within 6 months of closure. For the events studied in this thesis two occurred during construction. The third event, Greenhills Cougar 7, took place one year after construction. There are no accounts of flowslides taking place on re-sloped waste dumps. Mechanisms responsible for these beneficial weathering effects could include creep, weathering, and wetting due to infiltration.

Despite the apparent benefits of aging, the potential hazards of highly mobile liquefaction flowslides suggests that it may not be prudent to rely on these processes to insure against a flowslide for an angle of repose dump (that contains liquefaction prone material) following closure.

Water Management - Protective soil covers that minimize infiltration are more often considered as moisture barriers to prevent leachate generation in mine waste piles and to provide for vegetation. A cover could also be applied to prevent moisture ingress for stability purposes. Angle-of-repose slopes are too steep to apply covers and must be re-sloped in order for equipment to access the slope. Top soil covers are often applied following re-sloping as part of the reclamation process.

Construction Method - Re-sloping is often carried out to reduce long term erosion and increase long term stability. It is generally considered good practice to re-slope waste dumps from angle-of-repose (38°)to flatter slopes of about 2:1 (27°). Some analyses incorporating undrained strengths (derived from figure 7.11) for potentially liquefiable materials were carried out for the Quintette Marmot 1660 dump. The collapse analysis results are shown in Figure 7.14. The results show that the effects of re-sloping are dramatic; an increase in factor of safety from about 0.7 to 1.5 results. The results are not very sensitive to the assumed undrained strength/vertical effective stress (relates to brittleness) value. This analysis strongly suggests that the current practice of re-sloping waste dumps to 2:1 slopes following closure is sufficient to ensure against flowslides. This is consistent with experience in this regard.

7.4 CONCLUSIONS

Analyses presented in this chapter substantiates the field observations, laboratory results, and collapse model presented in chapter 6. A discussion of mitigative measures suggests that there are some practical strategies that could be employed to reduce the liquefaction flowslide hazard. The main findings are as follows:

1. Numerical analyses carried out with state-of-the-art finite element methods illustrates the manner in which overall collapse occurs and shows how the toe area of a dump serves to prevent failure and store strain energy until overall collapse occurs.

2. Limit equilibrium analyses demonstrates the inadequacy of conventional practice for evaluating liquefaction flowslide potential and shows that an indication of mobility is realized by incorporating triggering and collapse parameters derived from undrained triaxial tests. Further larger diameter tests conducted with coarser grain sized materials that more closely model actual waste rock sandy gravels would lend more confidence to the parameters used in the analysis.

3. A discussion of potential mitigative strategies suggests that the most rational strategies for reducing liquefaction flowslide risks prior to abandonment are to adopt construction practices more sensitive to the occurrence of potentially liquefiable materials. Further work on the classification and handling of potentially liquefiable waste rock materials is required before these strategies can be adopted in practice.

4. Limit equilibrium analyses demonstrates that following abandonment, the current practice of re-sloping from angle of repose (38°) to a 2:1 slope (27°) appears to virtually eliminate liquefaction potential. This is substantiated by field observations.

7.5 REFERENCES

Dawson, R.F., Morgenstern, N.R., and Gu, W.H., 1994a. Liquefaction Flowslides in Western Canandian Coal Mine Waste Dumps, Phase 2: Case Histories. Report to Supply and Services Canada, File No. XSG42-00138(608), 112 p.

Dawson, R.F., Morgenstern, N.R., and Gu, W.H., 1994b. Liquefaction Flowslides in Western Canandian Coal Mine Waste Dumps, Phase 3: Mitigative Strategies. Report to Supply and Services Canada, in preparation.

Duncan, J.M. and Chang, C., 1970. Nonlinear Analysis of Stress and Strain in Soils. ASCE Journal of the Soil Mechanics and Foundation Engineering Division , Vol 16, No. SM5, pp. 1629-1654.

Golder Associates Ltd., 1987. Regional Study of Coal Mine Waste Dumps in British Columbia. Report to Supply and Services Canada.

Golder Associates Ltd., 1992. Runout Characteristics of Debris from Dump Failures in Mountainous Terrain. Report to Supply and Services Canada, Contract No. 23440-0-9198/01-X8G.

Gu, W.H., 1992. Liquefaction and Post Earthquake Deformation Analysis. Ph.D. Thesis, University of Alberta.

Klohn Leonoff Ltd., 1991. Operation and Monitoring of Mine Dumps: Interior Guidelines. Report to British Columbia Ministry of Energy, Mines and Petroleum Resources.

Marachi, N.D., Chan, C.K., and Seed, B.W., 1972. Evaluation of Properties of Rockfill Materials. ASCE Journal of the Soil Mechanics and Foundation Engineering Division, Vol. 90, 5M1, pp. 95-114.

Morgenstern, N.R. and Sangrey, D.A., 1978. Methods of Stability Analysis in Landslides Analysis and Control. Transportation Research Board, National Academy of Sciences, Special Report No. 176, pp. 155-171.

Morgenstern, N.R., 1991. Limitations of Stability Analysis in Geotechnical Practice. (6th Manuel Rocha Lecture), Geotecnia, Rievista da Sociedade Portugesa do Geotecnia, No. 61, pp. 5-19.

Morgenstern, N.R., 1994. Observations on the Collapse of Granular Materials. The Kersten Lecture 42nd Annual Geotechnical Engineering Conference, Minneapolis, Minnesota.

Piteau Associates Engineering Ltd., 1991. Investigation and Design of Mine Dumps: Interim Guidelines. Report to British Columbia Ministry of Energy, Mines and Petroleum Resources.

TABLE 7.1 INITIAL STRESS ANALYSIS PARAMETERS

PARAMETERS	SANDY GRAVEL	COARSE WASTE	FOUNDATION
Unit Weight (kN/m^3)	19.0	19.0	22.0
Young's Modulus (kN/m^2*10^5)	1.0	2.0	10,000
Poisson's Ratio	0.40	0.30	0.40
Cohesion (kN/m^2)	1.0	1.0	
Friction Angle (□)	38	38	
Hyperbolic Elastic Number (Loading/Unloading)	650/1000	650/1000	
Hyperbolic Elastic Exponent	0.25	0.25	
Failure Ratio	0.65	0.65	
Modulus Number	0.40	0.30	
Modulus Exponent	0	0	

TABLE 7.2 LIQUEFACTION ANALYSIS PARAMETERS

PARAMETERS	SANDY GRAVEL	COARSE WASTE	FOUNDATION
Unit Weight (kN/m^3)	19.0	19.0	22.0
Young's Modulus (kN/m^2*10^5)	1.0	2.0	10,000
Poisson's Ratio	0.48	0.30	0.40
Cohesion (kN/m^2)		1.0	
Friction Angle (□)		38	
Constant Volume Friction Line (q/p')	1.5		
Peak Strength Line (q/p')	1.1		
Collapse Line (q/p')	0.33		
Hyperbolic Stress/Strain **a** Parameter	0.5		
Pore Pressure A Parameters (A_o/A_m)	0/4.0		

TABLE 7.3 SAFETY FACTORS (BISHOP'S METHOD)

	CONVENTIONAL SAFETY FACTOR $\phi_{coarse}=38^\circ$ $\underline{\phi_{fine}=38^\circ}$ $\phi_{fdn}=32^\circ$	TRIGGER ANALYSIS SAFETY FACTOR $\phi_{coarse}=38^\circ$ $\underline{\phi_{fine}=28^\circ}$ $\phi_{fdn}=32^\circ$	COLLAPSE ANALYSIS SAFETY FACTOR $\phi_{coarse}=38^\circ$ $(c_U/\sigma_{Vk0})_{fine}=.15\text{--}.2$ $\phi_{fdn}=32^\circ$
Quintette Marmot 1660	1.22	1.01	0.68-0.77
Fording South Spoil	1.17	0.98	0.66-0.73
Greenhills Cougar 7	1.17	0.99	0.64-0.69

TABLE 7.4 MITIGATION STRATEGIES

	PRE-CONSTRUCTION	**CONSTRUCTION**	**ABANDONMENT**
WATER MANAGEMENT	- divert surface water - finger drains	- internal drains	- reduce infiltration
MATERIALS MANAGEMENT		- eliminate liquefaction susceptible materials - blending - selective placement	
CONSTRUCTION METHOD	- foundation preparation - shear key	- terrace construction - dump perpendicular to slope - containment berm	- re-slope

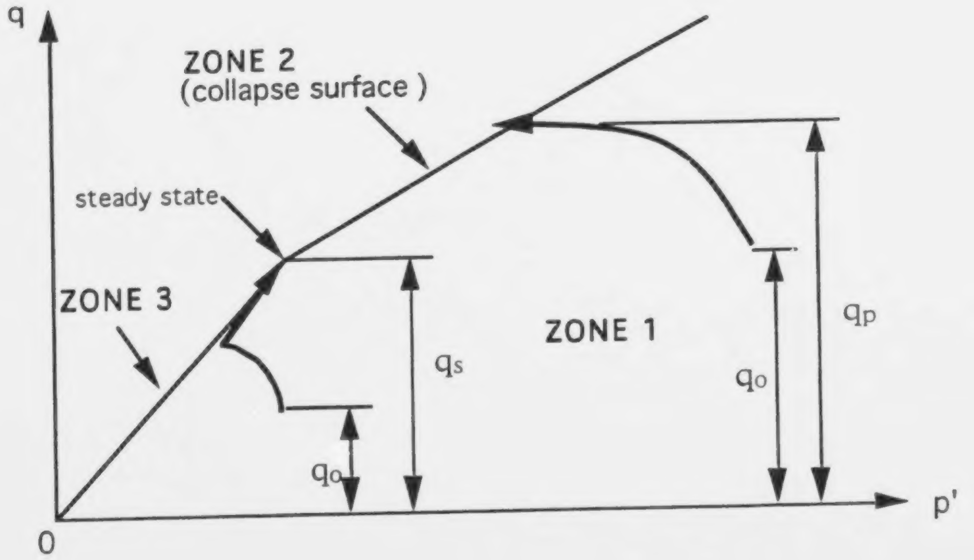

Yield Ratio: $R_y = q_o/q_p$ $(q_p > q_s)$

$R_y = q_o/q_s$ $(q_p < q_s)$

Figure 7.1 Liquefaction Model Stress Paths

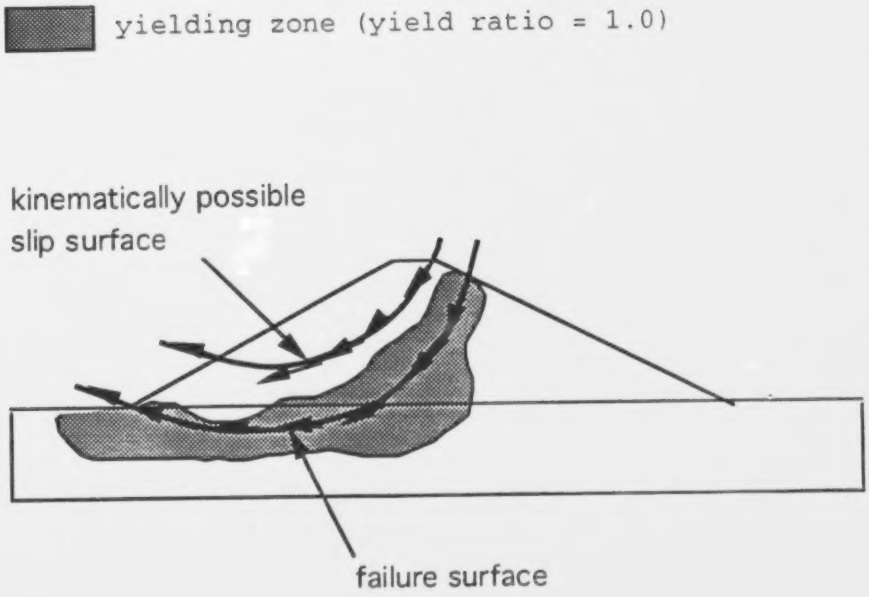
yielding zone (yield ratio = 1.0)
kinematically possible slip surface
failure surface

Figure 7.2 Failure Surface Criteria

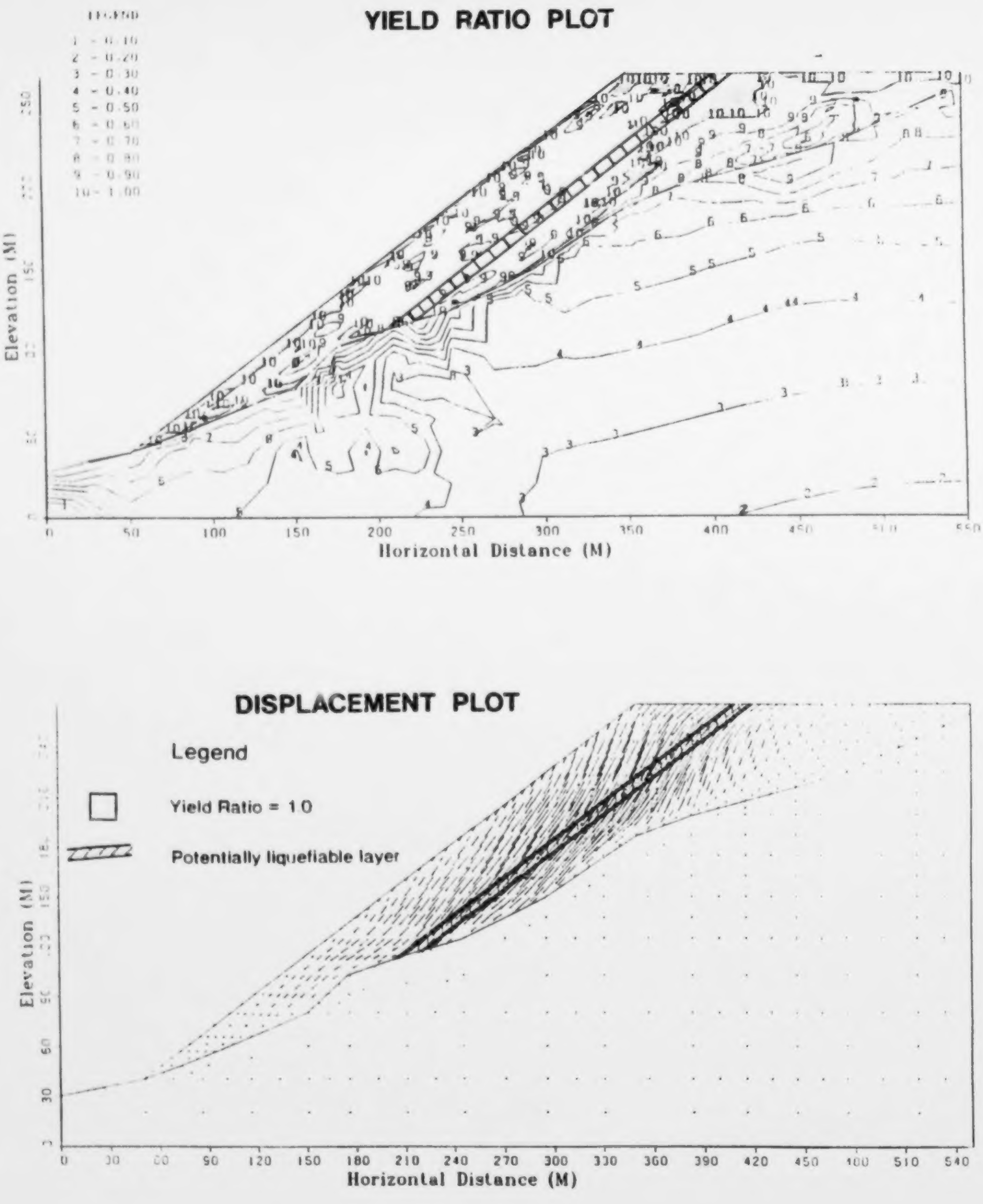

Figure 7.3 Quintette Marmot 1660 Initial Yield Ratio and Displacements

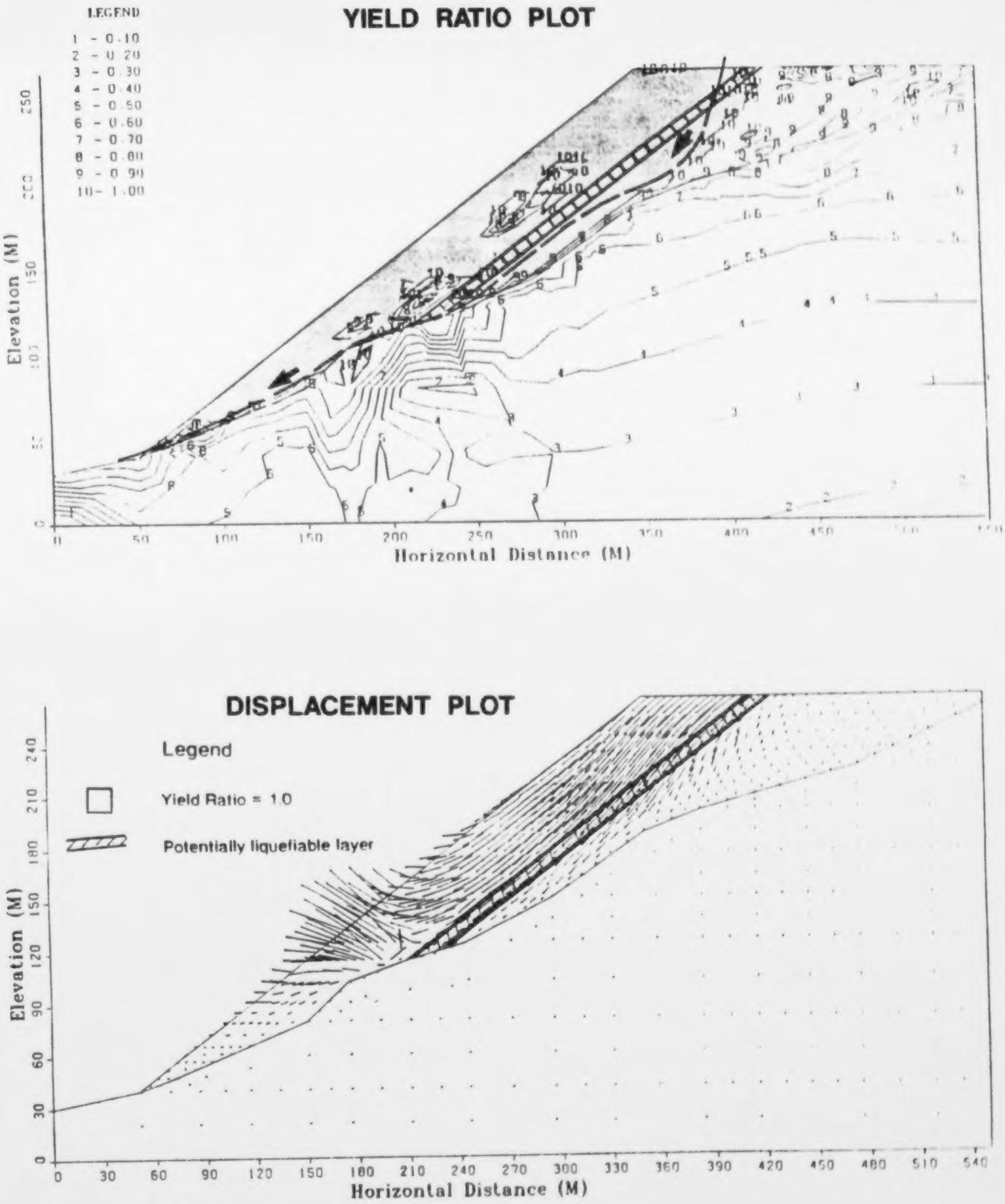

Figure 7.4 Quintette Marmot 1660 Liquefied Yield Ratio and Displacements

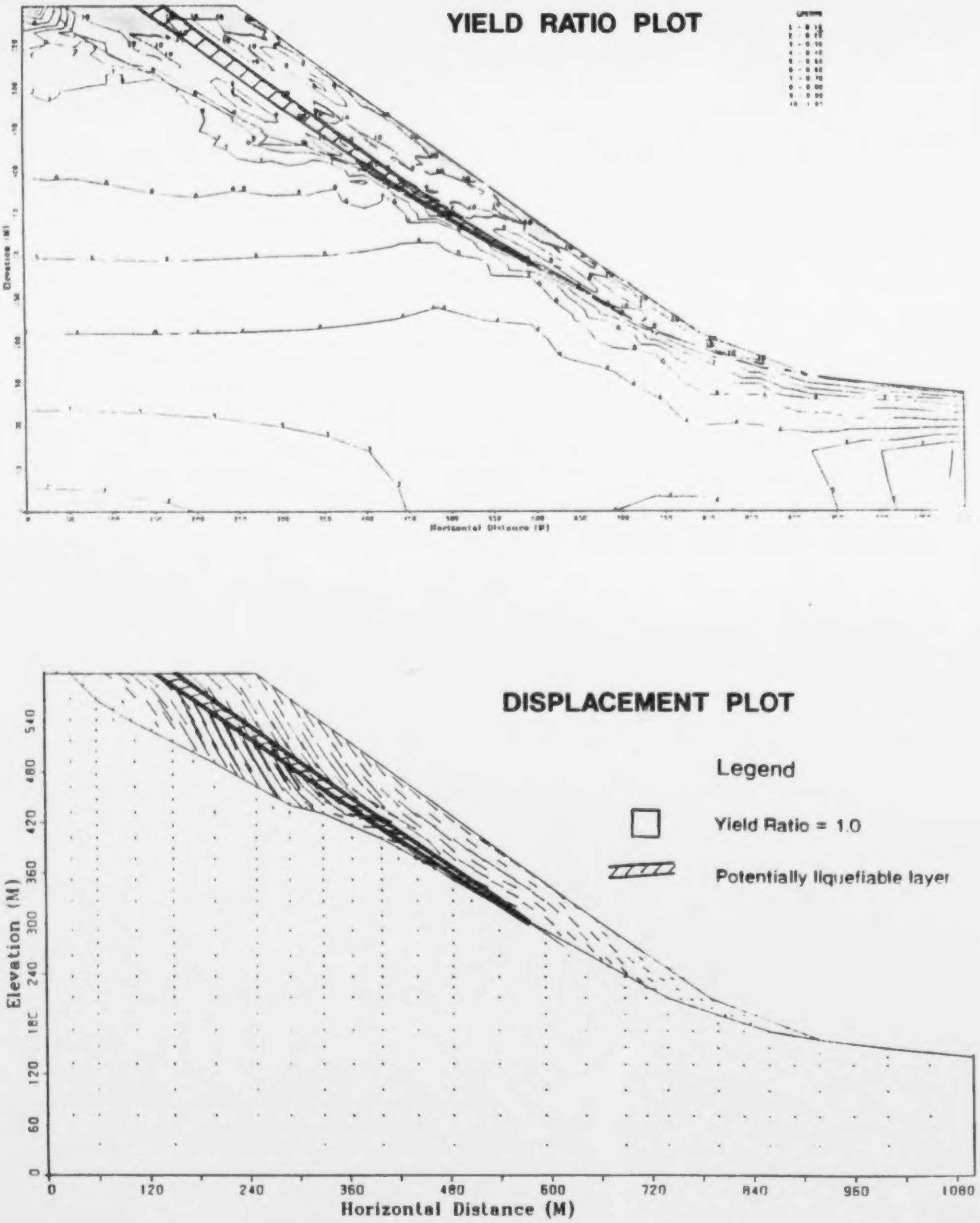

Figure 7.5 Fording South Spoil Initial Yield Ratio and Displacements

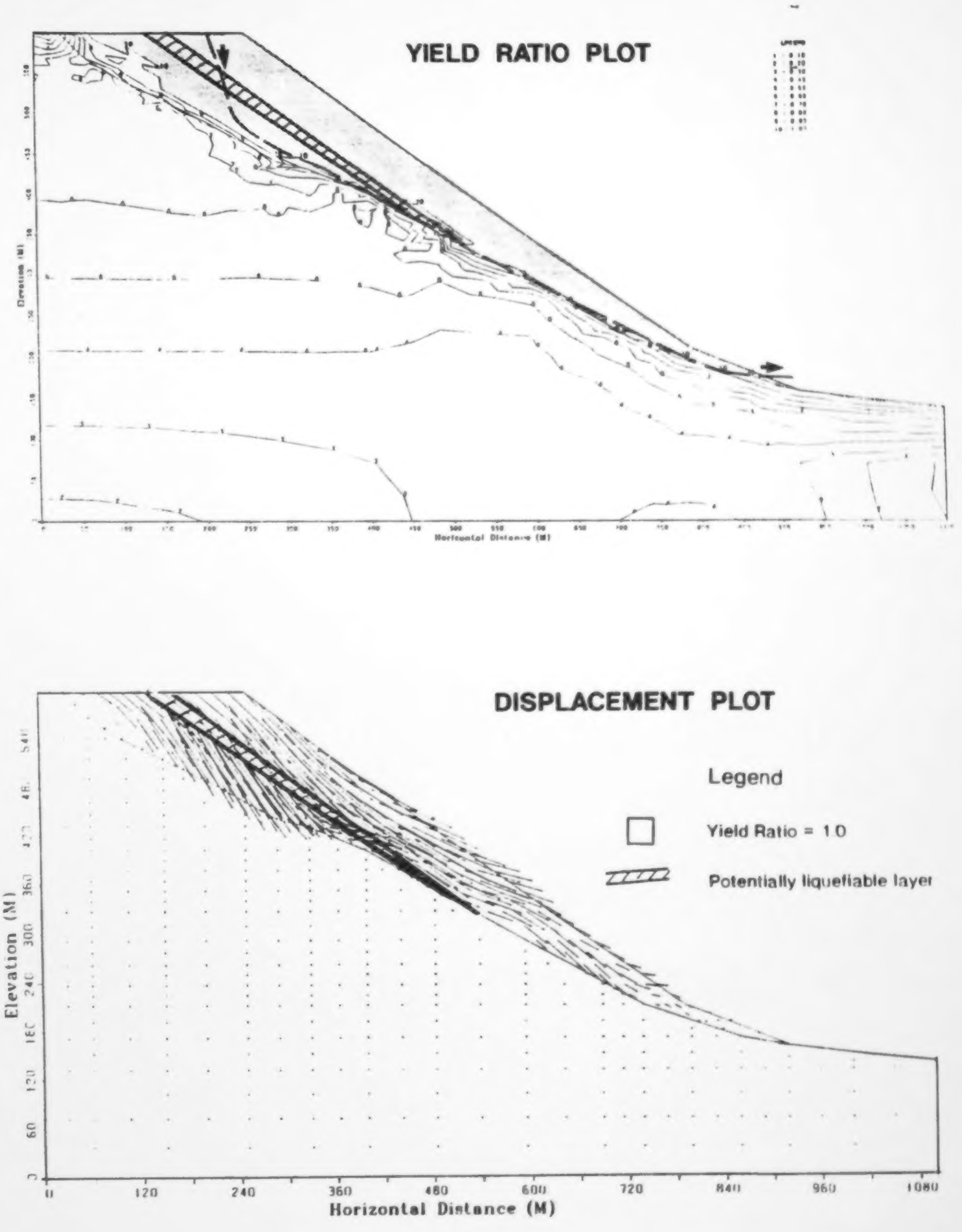

Figure 7.6 Fording South Spoil Liquefied Yield Ratio and Displacements

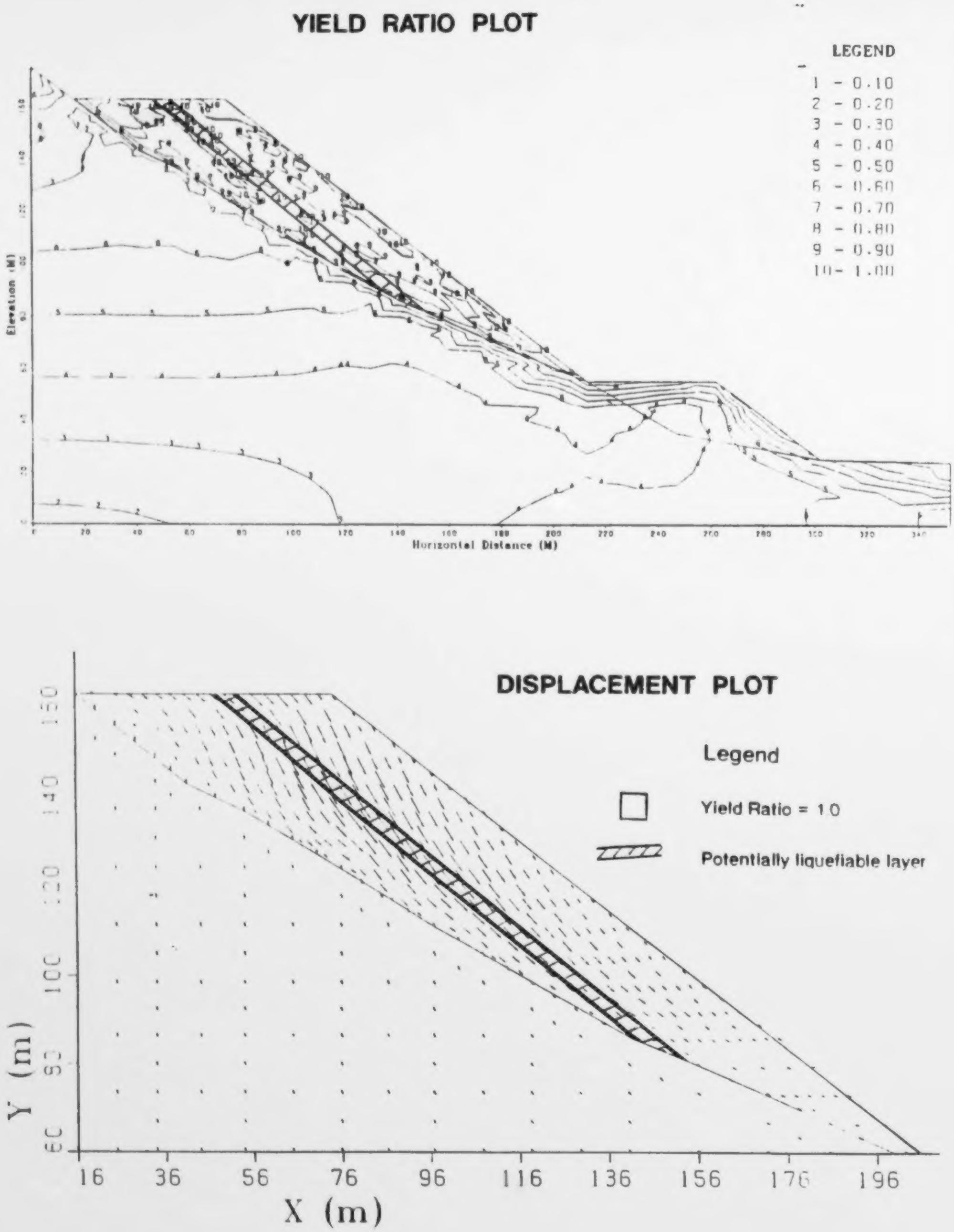

Figure 7.7 Greenhills Cougar 7 Initial Yield Ratio and Displacements

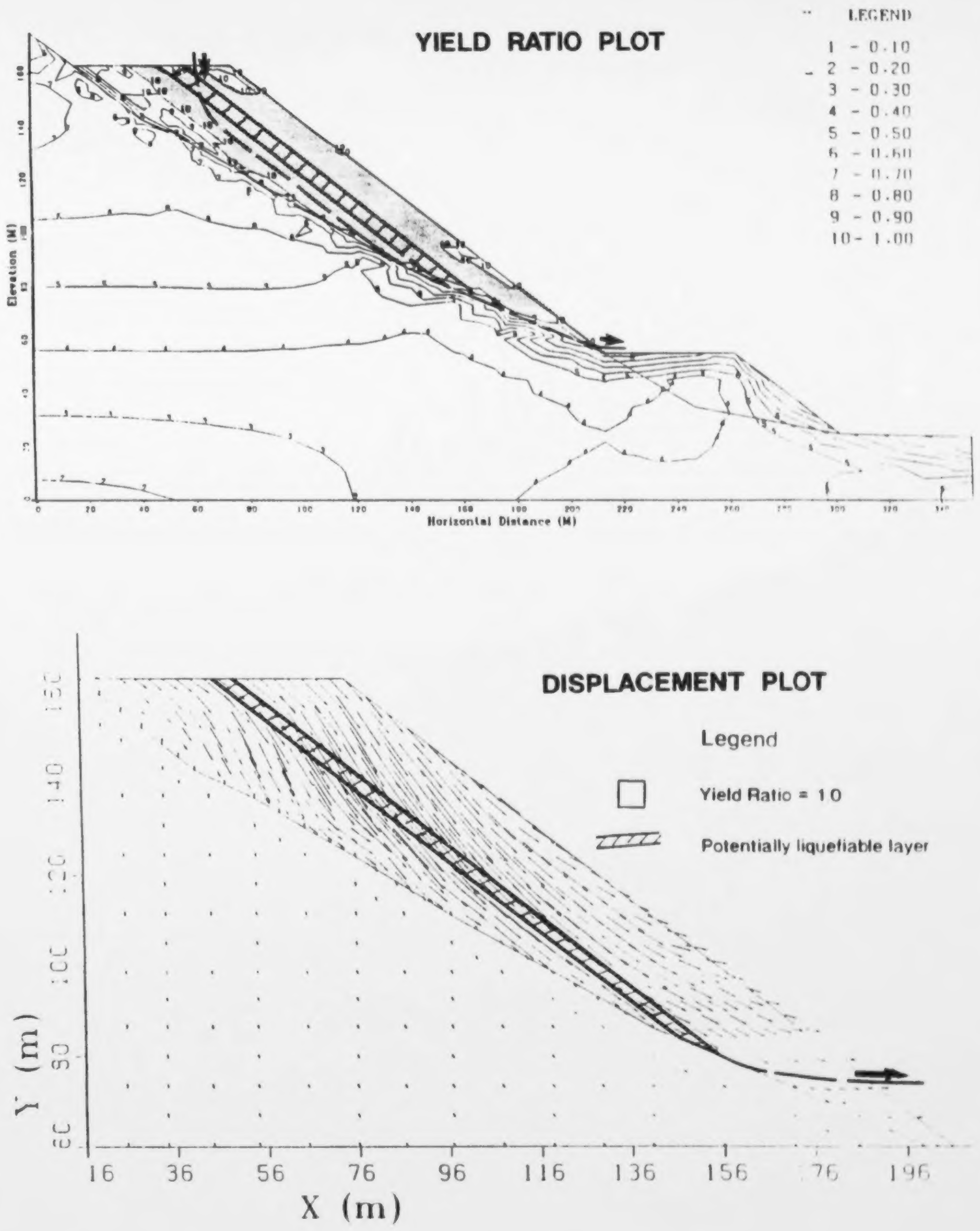

Figure 7.8 Greenhills Cougar 7 Liquefied Yield Ratio and Displacements

GREENHILLS GOUGAR 7

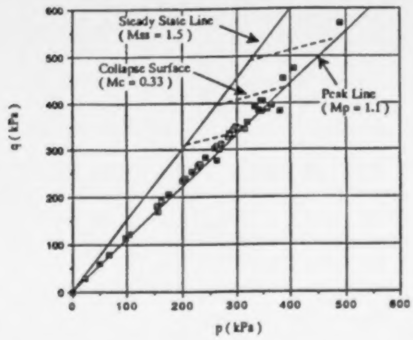

FORDING SOUTH SPOIL

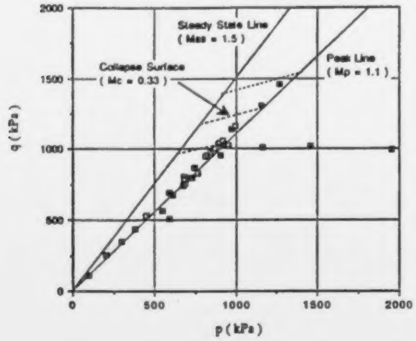

QUINTETTE MARMOT 1660

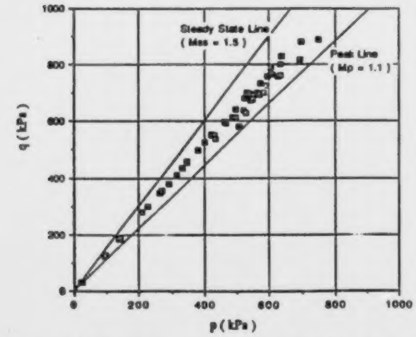

Figure 7.9 Stress State of the Potentially Liquefiable Layers prior to Collapse

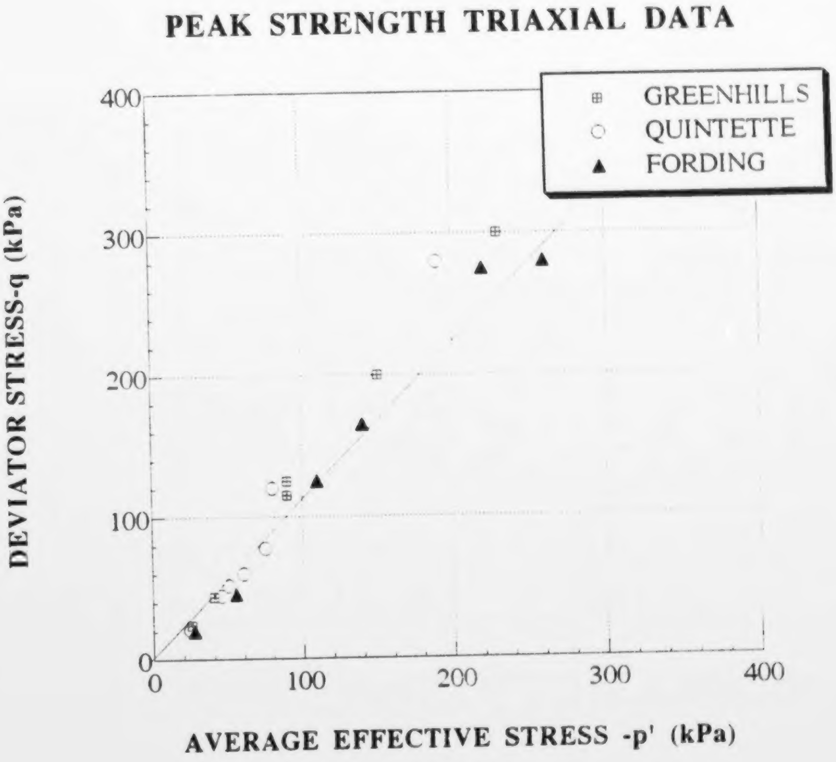

Figure 7.10 Stress State of Peak Values from Triaxial tests

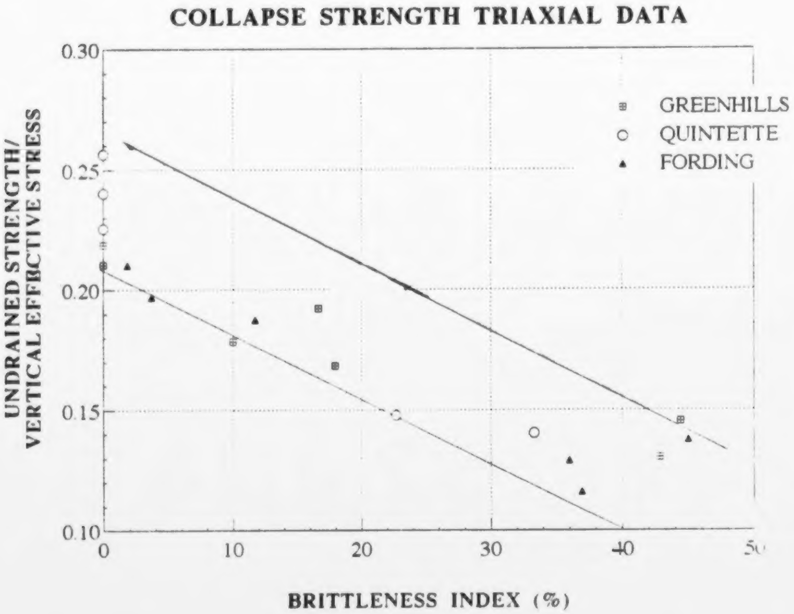

Figure 7.11 Undrained Strength Evaluation Criteria

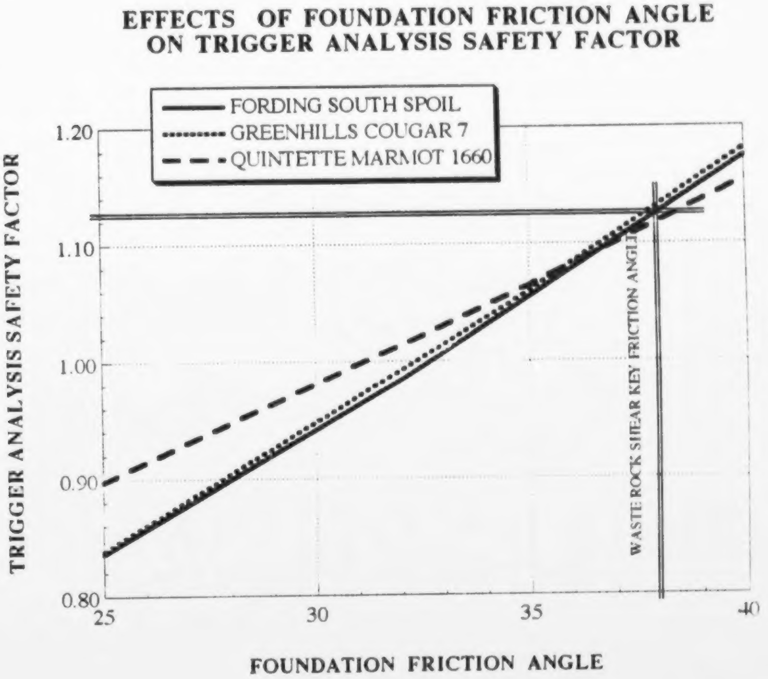

Figure 7.12 Influence of Foundation Shearing Resistance on Trigger Potential

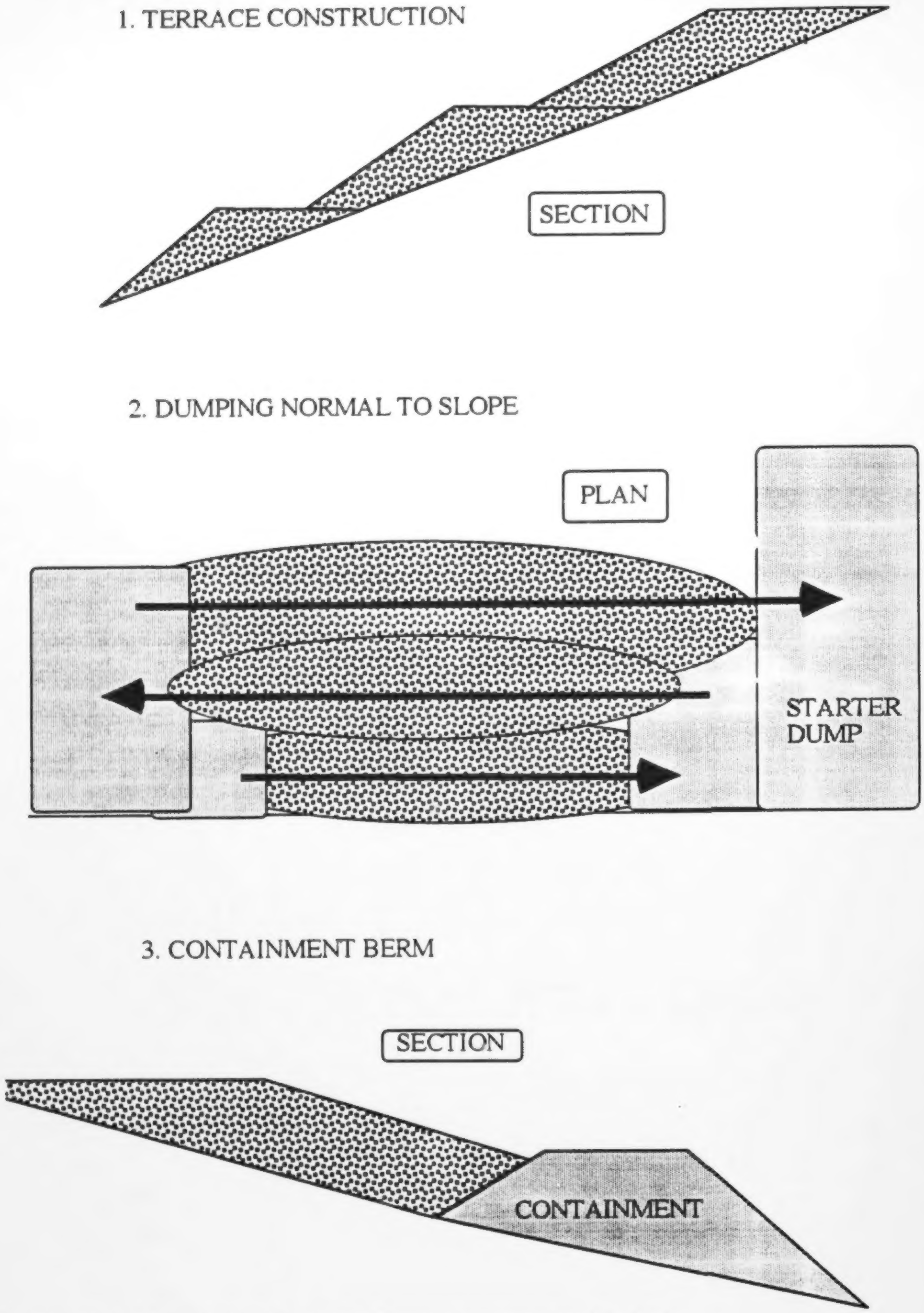

1. TERRACE CONSTRUCTION

2. DUMPING NORMAL TO SLOPE

3. CONTAINMENT BERM

Figure 7.13 Liquefaction Resistant Dump Construction Methods

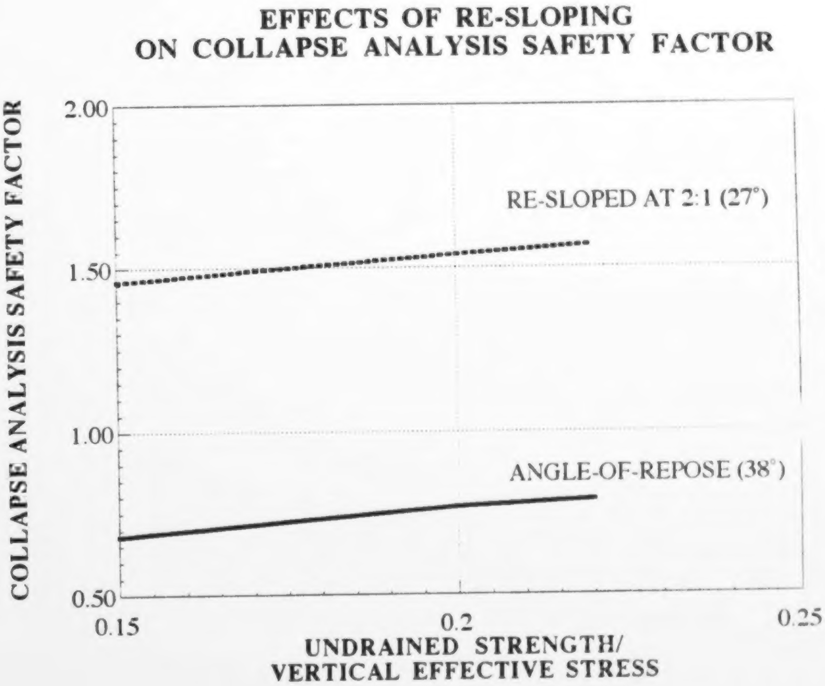

Figure 7.14 Influence of Re-sloping on Collapse Potential

Chapter 8

CONCLUSIONS

This thesis illustrates the role of geotechnical engineering for managing mine wastes. A review of typical mine waste streams in Chapter 1 showed that mine waste management is dominated by volume considerations and by containment strategies sensitive to the behaviour of loose materials. Loose materials take up additional storage space, are highly deformable and sometimes prone to collapse, and are more chemically unstable than dense materials.

Throughout the thesis the role of geotechnics for assessing mine waste products and developing waste management strategies is emphasized. Work conducted for this thesis demonstrates how conventional soil mechanics principles may be used to understand the behaviour of "wet" stream fine tailings (oil sand fine tails) and "dry" stream coarse waste rock. (coal mine waste rock). In each case management strategies resulting from these findings were developed.

Chapter 2 presents an overview of mine waste management practices and reviews geotechnical issues relative to waste handling methods, waste embankment stability, pollution control, and reclamation. In this concluding chapter, each of these issues is revisited with reference to the work presented in the preceding chapters. The main contributions were made in the areas of stability and reclamation. The other two areas received less attention but some shortcomings of current practice were revealed.

8.1 MINE WASTE EMBANKMENT STABILITY

Tailings and mine waste rock are normally loosely placed and thus mine waste embankments formed from these materials are susceptible to liquefaction flowslides. Flowslides triggered by rapid loading events, such as earthquakes, are fairly well understood. Flowslides triggered by "drained" loading conditions are not very well understood. A framework for evaluating liquefaction flowslide potential was developed in this thesis as follows:

1. The evaluation of liquefaction potential can be carried out with reference to the steady state and collapse surfaces. These surfaces are a mappable limiting state surfaces for most granular materials.

2. Potentially liquefiable material must be triggered by an upset condition. Static collapse triggers include a rising water table, wetting, pure shear, and creep. Pore pressures at collapse must be sufficiently impeded to create undrained pore pressures following collapse.

3. Collapse is usually initiated locally. Global failure occurs due to progressive failure as loads are transferred due to brittle collapse.

Flowslides in British Columbian coal mine waste dumps are not rare occurrences. Detailed study of three flowslide events presented convincing evidence supporting the static collapse liquefaction flowslide mechanism. It was demonstrated that sandy gravel materials in the waste dumps form layers parallel to the dump face and can exhibit collapse behaviour at void ratios greater than about 0.3. At void ratios less than about 0.3 (vertical effective stress of about 1MPa) it appears that the brittle behaviour is removed due to crushing during consolidation. Thus there is a limiting depth (about 50m) beyond which collapse cannot occur in these waste rock dumps. A review of runout event case histories seems to corroborate this finding.

Evaluation of collapse potential can be carried out with limit equilibrium methods by assigning an undrained strength to the potentially liquefiable layer. This approach, when applied to three case histories, showed safety factors less than 1. The high mobility partially results from the excess energy that becomes available as strain weakening occurs.

Design strategies that mitigate against liquefaction flowslides in mine waste dumps were developed. During dump construction, better control and selective placement of potentially liquefiable materials will lessen the likelihood of a flowslide event. Classification and characterization criteria needs to be developed in order to manage these materials. Following dump construction the current practice of re-sloping the dump face to 27° appears to eliminate collapse potential.

8.2 RECLAMATION

Minesite reclamation is an integral part of every modern day mining operation. Geotechnical methods can play an important role in the development of reclaimed landscapes, especially where the main objective is to create a "dry" landscape from initially high moisture content materials.

Tailings reclamation in cold regions may be aided by dewatering strategies that take advantage of thaw strain dewatering processes. Work conducted for this thesis has demonstrated that oil sands fine tails, initially at 30% solids content can be dewatered to solids contents of about 60% (50% thaw strain) after one freeze-thaw cycle. The post thaw consolidation properties of the thawed material are enhanced due to the relict structure created by the freezing process. A strategy for taking advantage of the thaw strain process was developed and design calculations were presented that showed the benefits of the process. Mine waste management schemes that take advantage of the thaw strain process should incorporate the following design elements:

1. Fine tailings should be placed in layers thin enough to prevent open system freezing from occurring and to maximize the total frozen thickness (several thin layers freeze faster than an equivalent thick layer). Open system freezing will cause longer freezing times and can result in additional moisture entering into the process. A maximum layer thickness of about .5m is recommended to achieve closed system freezing conditions.

2. An under drain should be placed below the freeze-thaw dewatering cells in order to promote two way drainage and to minimize ponding on the surface. Design calculations that interrogate the advantages of intermittent drainage layers should be carried out.

3. In most cases the depth of thaw will control design. When freezing more material than will thaw in one season permafrost conditions could result. This may not be acceptable reclamation practice in some jurisdictions. If warm process water is available then the heat energy available could be used to promote additional thawing.

4. The collection and handling of the water released during thaw is an important practical consideration that should be studied by pilot scale field tests.

In this thesis thaw strain dewatering of oil sands fine tails was considered as a reclamation procedure for managing tails that had already undergone sedimentation in a tailings basin. As a result of the large quantities of fine tails materials that would require re-handling this process is best considered as a method to augment other oil sands tailings management schemes. Other mining operations that produce lesser quantities of fine tails or thickened products that would not require re-handling could also benefit from thaw strain dewatering. In addition, thaw strain may be particularly well suited to the dewatering of effluent treatment sludges such as acid mine drainage treatment sludge.

8.3 WASTE HANDLING METHODS

Geotechnical aspects of waste handling methods did not receive special attention in this thesis. However the studies of cold weather tailings management and liquefaction flowslides in mine waste dumps revealed two important waste handling considerations:

1. Tailings handling practices in cold regions can take advantage of the cold weather to construct total containment with frozen perimeter dykes. Special cell construction techniques could be developed that maximize freezing by controlling hydraulic fill placement. This may involve maintaining a high water table in the cells in order to promote faster freezing rates.

2. During end-dumping of mine waste rock segregation of free draining coarse rock at the toe and less permeable finer material at the crest does not always occur. Observations of end dumping at coal mines showed that when similarly graded but finer materials are being placed much less segregation takes place. This often results in the formation of fine layers formed parallel to the dump face. These layers can allow a perched water table to build up in a waste dump. Handling practices are not generally sensitive to this observation.

8.4 POLLUTION CONTROL

Pollution control is governed by chemical and hydrological (infiltration, seepage and drainage) considerations. The chemistry of mine waste materials has received much attention in recent years, especially with respect to the acid mine drainage problem. Pollution control aspects of waste pile hydrology has received far less attention, especially with respect to mine waste dumps.

Work presented in this thesis clearly demonstrated the presence of water in mine waste dumps that are normally considered to be "dry". A better understanding of the role that segregation, layering, weathering, and evaporation plays in the flow of water through mine waste piles is required in order to economically design against pollution. This will undoubtedly require attention to unsaturated flow conditions.

8.5 CONCLUDING REMARKS

At the outset of this thesis it was emphasized that the mining industry should adopt the most feasible technology that mitigates the environmental impact of mine waste handling and storage practices. It was suggested that mine waste audits could help to achieve this purpose by helping to set standards of practice sensitive to environmental concerns. In this fashion regulators would not need to impose restrictive, economically punitive regulations.

The work presented in this thesis demonstrates that geotechnically based research can also play a role in developing better mine waste management practices. Studies founded on well established soil mechanics principles can usefully characterize mine waste materials and predict strength, deformation and conductivity (mainly hydraulic, and thermal conductivity) behaviour so that mine waste management strategies can be developed that provide better physical and chemical containment.

Appendix A

OIL SANDS FINE TAILS THAW CONSOLIDATION TESTING

Objective

To determine the consolidation behaviour, change in void ratio with effective stress, and the permeability behaviour, change in permeability with change in void ratio, of oil sand fine tails over a effective stress range of 0.5 to 100 kPa. If the fine tails is initially frozen, the thaw strain can also be determined.

Equipment

- large strain consolidation apparatus including a cell which requires a specimen 100 mm in diameter and between 100 and 130 mm in height
- constant head water reservoir

Procedure

The test procedure involves installing the frozen specimen, allowing it to thaw, commencing consolidation by applying a load, measuring the permeability under a constant head once consolidation is complete, increasing the load to the next effective stress and repeating the cycle.

1. When working with a frozen specimen, it may have to be trimmed to a diameter of 100 mm and a height between 100 and 130 mm.

2. When installing the specimen into the consolidation cell it is essential to de-air the cell and all the tubing. Filter paper should be used to prevent fines from migrating during permeability testing.

3. It is recommended that the cell fluid (and permeant) be selected on the basis of field conditions. For example, pond water instead of tap water or distilled water should be used.

4. Once the specimen is installed and the cell reassembled, the specimen can be allowed to thaw overnight. The specimen LVDT can be used to monitor thaw strain.

5. After thaw the specimen height is measured to calculate thaw strain. A 0.5 kPa nominal load is applied to the specimen as a standard reference stress.

6. When the 0.5 kPa load is applied, both the bottom drainage port and the top port are opened to allow double drainage during consolidation. By monitoring the specimen height changes through the LVDT measurements and by monitoring fluid drainage, consolidation and the void ratio can be evaluated.

7. Once consolidation is complete, the bottom drainage port is closed. The constant head reservoir is adjusted to provide a hydraulic gradient of 1 during permeability testing. The permeability test begins when the bottom port to the reservoir is opened. Fluid volume is measured as it drains from the top port.

8. Based on Darcy's Law, once hydraulic gradient and fluid drainage rate are known, the permeability (hydraulic conductivity) of the fine tails at this stress level and void ratio can be calculated.

9. After the permeability test is finished, the bottom reservoir port is closed, the load is increased to the next effective stress level and consolidation begun by having both top and bottom drainage.

10. The procedure is repeated for effective stresses of 2, 4, 10, 20, and 100 kPa.

11. When the test is completed, the specimen is removed from the apparatus and a oven dried solids content and soxhlet extraction tests are performed to measure the solids content and bitumen content. A vane shear test is also performed to measure the peak and residual undrained shear strength of the specimen.

In the tables that follow, detailed results from the 12 laboratory consolidation and shear strength testing are tabulated. The first nine samples are homogeneous fine tails samples and the last three samples are sand/tails inteface test results.

OSLO Field Sample E-1 Test Data

Effective Stress (kPa)	e theoretical	ΔH (cm)	Δe	e	i	K (cm/s)	e backcalc.
0.5	2.02	0.00	0	2.02	0.69	9.00E-03	2.41
1.0		0.53	0.276	1.75	0.38, 0.85	3.10E-03	2.09
2.0		1.04	0.542	1.48	0.9	5.50E-05	1.78
3.0		1.14	0.595	1.43	2.36	5.40E-06	1.72
4.0		1.21	0.631	1.39	1.9	2.80E-06	**1.68**

BEFORE CONSOLIDATION

Initial solids content = 30.8%
Frozen sample height = 12.69 cm
Frozen sample diameter = 10.05 cm
Initial sample weight = 1122.3 g
Thawed sample height = 5.80 cm (with 0.5 kPa seating load)
Thaw strain = 54.3%
Thawed solids content = 51.9%

AFTER CONSOLIDATION

Final sample height = 4.4 cm (measured)
Final solids content = 60.78%
Bitumen content = 1.24% (dry basis)
Gss = 2.60 (bitumen + mineral solids)
Final void ratio = 1.68

Undrained Shear Strength:
Peak = 3.7 kPa
Residual = 1.2 kPa

OSLO Field Sample C-1 Test Data

Effective Stress (kPa)	e theoretical	ΔH (cm)	Δe	e	i	K (cm/s)	e backcalc.
0.5	2.05	0.00	0	2.05	0.30, 0.70	3.50E-03	2.21
1.0		0.19	0.086	1.96	0.38, 0.75	2.40E-03	2.13
2.0		0.50	0.226	1.82	0.41, 0.79	2.10E-04	2.00
3.0		0.77	0.348	1.70	0.47, 0.89	6.80E-05	1.89
4.0		0.88	0.398	1.65	0.51, 0.94	4.60E-05	1.84
5.0		0.97	0.439	1.61	0.52	4.30E-05	1.80
10.0		1.15	0.520	1.53	0.36	4.20E-05	1.73
20.0		2.16	0.977	1.07	0.55, 1.2	2.40E-05	1.30
40.0		2.50	1.131	0.92	0.75, 1.9	6.50E-06	1.16
60.0		2.73	1.235	0.81	0.75, 2.1	2.70E-06	1.06
112.0		3.05	1.380	0.67	1.0, 2.4	2.50E-06	**0.93**

BEFORE CONSOLIDATION

Initial solids content = 34.9%
Frozen sample height = 12.52 cm
Frozen sample diameter = 10.10 cm
Initial sample weight = 1187.9 g
Thawed sample height = 6.74 cm (with 0.5 kPa seating load)
Thaw strain = 46.2%
Thawed solids content = 53.1%

AFTER CONSOLIDATION

Final sample height = 4.57 cm (measured)
Final solids content = 72.98%
Bitumen content = 4.00% (dry basis) (assumed)
Gss = 2.50 (bitumen + mineral solids)
Final void ratio = 0.93

Undrained Shear Strength:
Peak = 10.7 kPa
Residual = 3.1 kPa

OSLO Field Sample A-2 Test Data

Effective Stress (kPa)	e theoretical	ΔH (cm)	Δe	e	i	K (cm/s)	e backcalc.
0.5	1.78	0.00	0	1.78	1.0, 1.88	3.30E-06	1.73
1.0		0.27	0.088	1.69	1.07	1.60E-06	1.65
2.0		0.86	0.281	1.50	0.94	1.10E-06	1.47
3.0		1.16	0.379	1.40	0.96, 1.03	4.00E-07	1.38
4.0		1.34	0.437	1.34	1.02	3.40E-07	1.32
28.0		2.09	0.682	1.10	1.32	1.80E-07	1.10
50.0		2.63	0.858	0.92	2.09	4.00E-08	0.93
100.0		3.13	1.021	0.76	n/a *	n/a *	**0.78**

* Unable to test permeability due to blocked flow path.

BEFORE CONSOLIDATION

Initial solids content = 45.5%
Frozen sample height = 12.25 cm
Frozen sample diameter = 10.13 cm
Initial sample weight = 1318.7 g
Thawed sample height = 8.51 cm (with 0.5 kPa seating load)
Thaw strain = 30.5%
Thawed solids content = 59.3%

AFTER CONSOLIDATION

Final sample height = 5.9 cm (measured)
Final solids content = 76.30%
Bitumen content = 3.29% (dry basis)
Gss = 2.52 (bitumen + mineral solids)
Final void ratio = 0.78

Undrained Shear Strength:
Peak = 3.7 kPa
Residual = 0.9 kPa

OSLO Field Sample C-2 Test Data

Effective Stress (kPa)	e theoretical	ΔH (cm)	Δe	e	i	K (cm/s)	e backcalc.
0.5	2.23	0.00	0	2.23	0.81, 1.4	6.30E-04	2.08
1.0		0.09	0.052	2.18	0.88, 1.32	5.80E-04	2.03
2.0		0.29	0.169	2.06	0.86, 1.35	1.70E-04	1.92
4.0		0.58	0.338	1.89	1.55	7.60E-06	1.77
10.0		1.09	0.634	1.60	1.79	2.90E-07	1.49
20.0		1.36	0.791	1.44	1.47	1.30E-07	1.34
50.0		1.82	1.059	1.17	n/a *	n/a *	1.09
100.0		2.02	1.176	1.05	n/a *	n/a *	**0.98**

* Unable to test permeability due to blocked flow path.

BEFORE CONSOLIDATION

Initial solids content = 31.3% (assumed)
Frozen sample height = 11.33 cm
Frozen sample diameter = 10.08 cm
Initial sample weight = 1015.9 g
Thawed sample height = 5.55 cm (with 0.5 kPa seating load)
Thaw strain = 51.0%
Thawed solids content = 54.3%

AFTER CONSOLIDATION

Final sample height = 3.65 cm (measured)
Final solids content = 71.56%
Bitumen content = 4.67% (dry basis)
Gss = 2.48 (bitumen + mineral solids)
Final void ratio = 0.98

Undrained Shear Strength:
Peak = 5.0 kPa
Residual = 1.2 kPa

OSLO Field Sample B-1 Test Data

Effective Stress (kPa)	e theoretical	ΔH (cm)	Δe	e	i	K (cm/s)	e backcalc.
0.5	1.57	0.00	0	1.57	1.18	1.90E-06	1.30
2.0		0.10	0.035	1.54	1.15	1.40E-06	1.26
4.0		0.33	0.115	1.46	1.27	9.20E-07	1.19
10.0		0.79	0.275	1.30	1.44	2.70E-07	1.04
20.0		1.24	0.431	1.14	1.1	3.10E-06	0.89
50.0		1.50	0.522	1.05	n/a *	n/a *	**0.80**

* Unable to test permeability due to blocked flow path.

BEFORE CONSOLIDATION

Initial solids content = 53.6%
Frozen sample height = 9.09 cm
Frozen sample diameter = 10.10 cm
Initial sample weight = 975.3 g
Thawed sample height = 7.40 cm (with 0.5 kPa seating load)
Thaw strain = 18.6%
Thawed solids content = 64.8%

AFTER CONSOLIDATION

Final sample height = 5.5 cm (measured)
Final solids content = 74.77%
Bitumen content = 7.76% (dry basis)
Gss = 2.38 (bitumen + mineral solids)
Final void ratio = 0.80

Undrained Shear Strength:
Peak = 12.3 kPa
Residual = 5.0 kPa

OSLO Field Sample G-1 Test Data

Effective Stress (kPa)	e theoretical	ΔH (cm)	Δe	e	i	K (cm/s)	e backcalc.
0.5	2.19	0.00	0	2.19	0.75, 0.42	3.60E-02	2.10
2.0		0.12	0.047	2.15	0.79	2.80E-02	2.05
4.0		0.34	0.134	2.06	0.77	9.70E-03	1.96
10.0		1.76	0.694	1.50	1.86	2.00E-07	1.38
20.0		2.09	0.824	1.37	1.83	1.20E-07	1.25
50.0		2.40	0.946	1.25	n/a *	n/a *	**1.13**

* Unable to test permeability due to blocked flow path.

BEFORE CONSOLIDATION

Initial solids content = 32.9%
Frozen sample height = 15.47 cm
Frozen sample diameter = 10.08 cm
Initial sample weight = 1406.1 g
Thawed sample height = 8.10 cm (with 0.5 kPa seating load)
Thaw strain = 47.6%
Thawed solids content = 54.2%

AFTER CONSOLIDATION

Final sample height = 5.25 cm (measured)
Final solids content = 68.82%
Bitumen content = 4.44% (dry basis)
Gss = 2.48 (bitumen + mineral solids)
Final void ratio = 1.13

Undrained Shear Strength:
Peak = 2.6 kPa
Residual = 1.1 kPa

OSLO Field Sample 10-A Test Data

Effective Stress (kPa)	e theoretical	ΔH (cm)	Δe	e	i	K (cm/s)	e backcalc.
0.5	3.92	0.00	0	3.92	0.78, 1.2	2.40E-02	2.51
2.0		0.43	0.411	3.51	0.95	2.60E-04	2.23
4.0		0.78	0.745	3.17	0.92	1.20E-05	2.00
10.0		1.29	1.232	2.69	0.73	1.20E-07	1.66
20.0		1.60	1.528	2.39	1.41	5.80E-08	1.45
50.0		1.85	1.767	2.15	n/a *	n/a *	1.29

* Unable to test permeability due to air bubble blocking flow path.

BEFORE CONSOLIDATION

Initial solids content = 30.4% (assumed)
Frozen sample height = 7.04 cm
Frozen sample diameter = 10.11 cm
Initial sample weight = 690.7 g
Thawed sample height = 5.15 cm (with 0.5 kPa seating load)
Thaw strain = 26.8%
Thawed solids content = 50.5%

AFTER CONSOLIDATION

Final sample height = 3.45 cm (measured)
Final solids content = 66.60%
Bitumen content = 2.08% (dry basis)
Gss = 2.57 (bitumen + mineral solids)
Final void ratio = 1.29

Undrained Shear Strength:
Peak = 3.95 kPa
Residual = 1.4 kPa

OSLO Field Sample 10-B (sand/tails interface) Test Data

Effective Stress (kPa)	e theoretical	ΔH (cm)	Δe	e	i	K (cm/s)	e backcalc.
0.5	2.45	0.00	0	2.45	0.92	4.20E-04	2.65
2.0		0.03	0.055	2.39	0.93	4.30E-04	2.59
4.0		0.12	0.221	2.23	0.94	2.10E-04	2.42
10.0		0.31	0.572	1.88	0.96	1.20E-05	2.06
20.0		0.45	0.830	1.62	1.03	1.00E-06	1.79
50.0		0.75	1.383	1.07	n/a *	n/a *	**1.22**

* Unable to test permeability due to inverted baffle blocking flow path.

BEFORE CONSOLIDATION

Initial solids content = 30.4% (assumed)
Frozen sample height = 9.46 cm
Frozen sample diameter = 10.10 cm
Initial sample weight = 1164.1 g
Thawed sample height = 7.60 cm (with 0.5 kPa seating load)
Thaw strain = 19.7%
Thawed solids content = 49.2%

initial void ratio= 5.8790054
Measured Ht of Sludge= 3.73 cm

AFTER CONSOLIDATION

Final sample height = 6.9 cm (measured)
Final solids content = 67.76%
Bitumen content = 2.08% (dry basis)
Gss = 2.57 (bitumen + mineral solids)
Final void ratio = 1.22

Assumed to be similar to 10-A.

OSLO Field Sample 2-A (sand/tails interface) Test Data

Effective Stress (kPa)	e theoretical	ΔH (cm)	Δe	e	i	K (cm/s)	e backcalc.
0.5	2.18	0.00	0	2.18	0.96	1.10E-04	3.35
2.0		0.04	0.024	2.16	0.97	8.40E-05	3.24
4.0		0.15	0.088	2.09	1.05	2.50E-05	2.97
10.0		0.58	0.342	1.84	1.29	1.40E-06	1.89
20.0		0.86	0.507	1.67	n/a	n/a*	1.19
50.0		-	-	-	-	-	-

* Unable to test permeability.

BEFORE CONSOLIDATION

Initial solids content = 30.4% (assumed)
Frozen sample height = 7.43 cm
Frozen sample diameter = 10.10 cm
Initial sample weight = 836.2 g
Thawed sample height = 5.40 cm (with 0.5 kPa seating load)
Thaw strain = 27.3%
Thawed solids content = 42.4%

initial void ratio= 5.6354409
Estimated Ht of Sludge= 3.9 cm

AFTER CONSOLIDATION

Final sample height = 4.4 cm (measured)
Final solids content = 67.50%
Bitumen content = 5.12% (dry basis)
Gss = 2.46 (bitumen + mineral solids)
Final void ratio = 1.19

OSLO Field Sample 12-A (sand/tails interface) Test Data

Effective Stress (kPa)	e theoretical	ΔH (cm)	Δe	e	i	K (cm/s)	e backcalc.
0.5	3.48	0.00	0	3.48	0.83	1.70E-03	4.75
2.0		0.60	0.895	2.58	0.92	7.20E-05	3.57
4.0		0.77	1.149	2.33	0.99	1.00E-05	3.23
10.0		1.06	1.581	1.89	1.06	9.60E-07	2.66
20.0		1.28	1.910	1.57	1.09	8.10E-07	2.22
50.0		1.58	2.357	1.12	1.21	1.40E-06	1.63
100.0		1.81	2.700	0.78	1.21	1.60E-06	1.17

BEFORE CONSOLIDATION

Initial solids content = 30.4% (assumed)
Frozen sample height = 13.80 cm
Frozen sample diameter = 10.10 cm
Initial sample weight = 1763.6 g
Thawed sample height = 12.30 cm (with 0.5 kPa seating load)
Thaw strain = 10.9%
Thawed solids content = 34.4%

initial void ratio= 5.7131974
Measured Ht of Sludge= 4.5 cm

AFTER CONSOLIDATION

Final sample height = 10.4 cm (measured)
Final solids content = 68.00%
Bitumen content = 4.10% (dry basis)
Gss = 2.50 (bitumen + mineral solids)
Final void ratio = 1.17

Appendix B

FREEZING AND THAWING MODELS

Researchers at the US Cold Regions Research and Engineering Laboratory (CRREL) have been conducting a pilot scale study on freeze-thaw dewatering of sewage sludges (Martel, 1988). As part of the research, simple models have been developed to predict the freezing and thawing depths of sewage sludge placed in specially designed freeze-thaw beds. These models are used here to estimate freeze-thaw dewatering design thicknesses for fine tails placed at Fort McMurray.

Figure A.1 shows the temperature profile and total winter freezing depth relationship (D_F) used in the freezing model. The model assumes that individual layers, with thickness H_F and at 0° C, are placed on top of previously frozen material also assumed to be at 0° C. Freezing takes place from the top to bottom as latent heat is lost to the atmosphere due to convection .

The CRREL thawing model has been modified (Figure A.2) to allow for two way heat flow (upward convection and downward conduction). The thaw model assumes that water is decanted as thaw proceeds so that the thaw depth is maximized. An alternate warm water cap can be included in the thaw model for predicting thaw depths using warm waste water at the surface as a heat source.

The models presented in Figures A.1 and A.2 require thermal parameters (K_{TT}, K_{FT}, L, h_c) as input values. Johansen (1975) has derived empirical relationships for estimating the thermal conductivity of soils. The saturated thermal conductivity is assumed to be constant in the unfrozen and frozen states and changes from one state to the other as a step function. The Johansen (1975) equation for saturated thermal conductivity is:

$$K_{sat} = K_{soil}^{(1-n))} K_{water}^{n}$$

where: K_{sat} = saturated thermal conductivity

K_{soil} = thermal conductivity of soil solids

K_{water} = thermal conductivity of water or ice

n = porosity

Frozen and unfrozen thermal conductivity values for fine tails at 30% solids (G_s=2.5; K_{soil}=2 W/m°C) are calculated as 2.2 and 0.7 W/m°C respectively using the above relationship.

The volumetric latent heat (L) is directly related to the moisture content of the soil through the following expression:

$$L = L' \gamma_D \omega$$

where: L' = latent heat of water
γ_D = dry density
ω = moisture content

The volumetric latent heat for 30% solids fine tails is 265 kJ/m^3°C.

The convection coefficient (h_c) is a parameter measuring the rate of heat flow at the surface of the freezing/thawing tails. Actual back calculated values of 20 W/m^2 were estimated from thermal studies of heat loss along the tailings beach at the Syncrude site (CANMET, 1991) and this value is assumed in the calculations that follow. The convection coefficient is very sensitive to micro-climatic conditions such as wind speed and relative humidity and additional site specific measurements are required.

REFERENCES

Johansen, C., 1975. "Thermal conductivity of soils" PhD Thesis, University of Trondheim, Norway. (Available as CRREL Draft Translation 637, 1977).

Martel, C.J., 1988. "Development and Design of Sludge Freezing Beds " USA Cold Regions Research and Engineering Laboratory, CRREL Report 88-20.

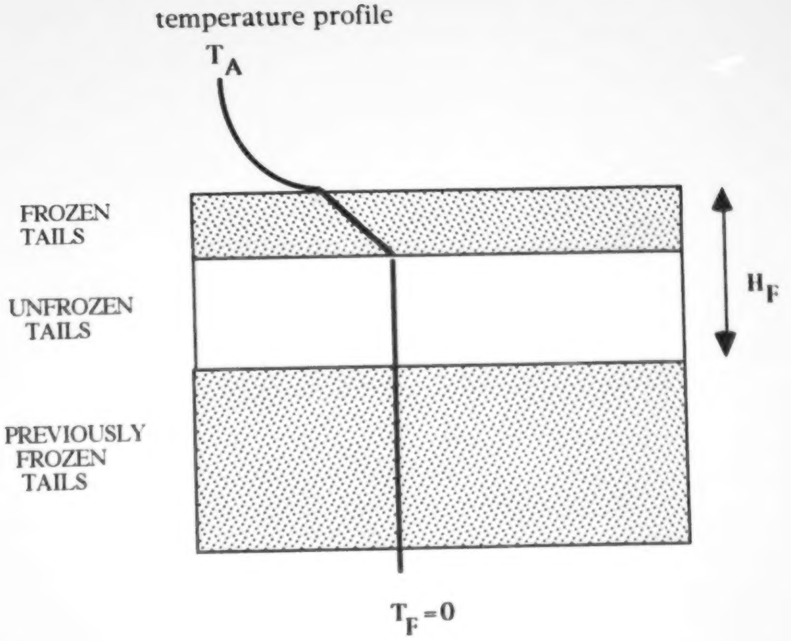

$$D_F = \frac{P_F T_A}{L\left(\frac{1}{h_c} + \frac{H_F}{2K_{FT}} \right)}$$

WHERE: D_F = total winter freezing depth

P_F = freezing period

T_A = average ambient temperature during freezing

L = latent heat

h_c = convection coefficient

H_F = thickness of freezing placement layer

K_{FT} = thermal conductivity of the frozen tails

Figure A.1 Freezing Model

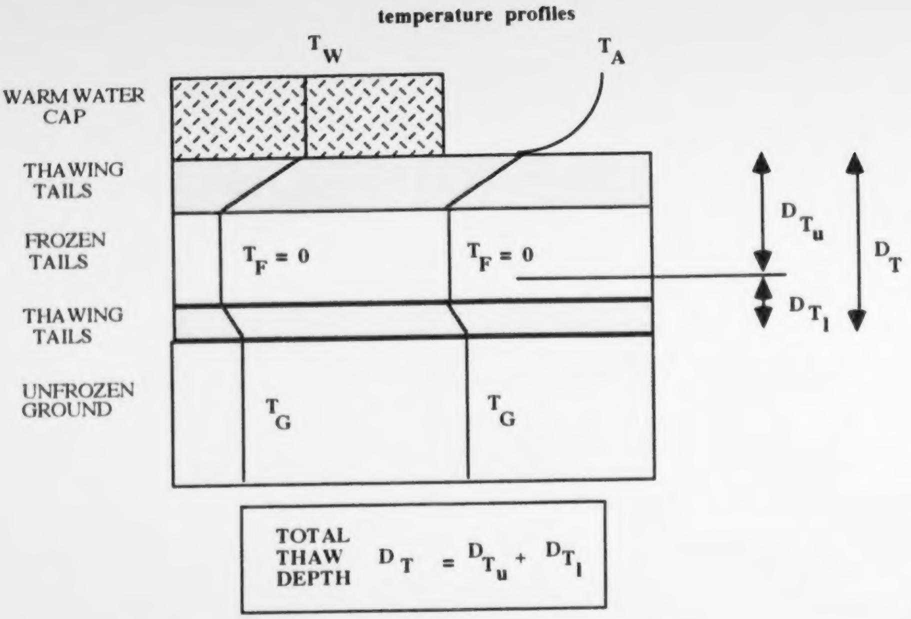

NO WATER CAP (decant water drained during thaw):

$$D_{T_U} = \sqrt{\left(\frac{K_{TT}}{h_c(1-\theta)}\right)^2 + \frac{2K_{TT}P_T\left(T_A + {}^{\alpha I}\!/_{h_c}\right)}{L(1-\theta)}} - \frac{K_{TT}}{h_c(1-\theta)} \qquad D_{T_L} = \sqrt{\frac{2P_T T_G K_{TT}}{L(1-\theta)}}$$

WARM WATER CAP (to enhance thaw):

$$D_{T_U} = \sqrt{\frac{2P_T T_W K_{TT}}{L(1-\theta)}}$$

K_{TT} = thawed tailings thermal conductivity

L = latent heat of fusion

h_c = heat transfer coefficient

θ = thaw strain

P_T = thawing period

T_A = ambient air temperature

T_G = *subsurface* ground temperature

T_W = water cap temperature

α = solar absorptance of fine tails

I = average solar insolation during thaw

Figure A.2 Thawing Model

Appendix C

MINE WASTE ROCK TRIAXIAL TEST METHODOLOGY AND RESULTS

Triaxial tests were carried out with 101mm (4 inch) diameter triaxial cells. Pore pressures, axial diplacement, volume change measurement, and axial loads were measured and recorded with a computerized data acquisition system. Some comments on sample preparation, testing procedures, and void ratio determinations follows:

SAMPLE PREPARATION- The samples were prepared in the sample mold in a moist state by loosely tamping several lifts (4 to 5 layers) until the mold was filled. The coarse angular test materials punctured the conventional thin (0.25 mm) latex membranes normally used for triaxial testing and it was necessary to use a double membrane system which incorporated a thicker (0.75 mm) outer neoprene membrane.

TEST PROCEDURE- The sample was installed in the cell at 20 kPa vacuum pressure, the cell was filled with water, and a cell pressure of 20 kPa was applied (the 20 kPa vacuum pressure was turned off simultaneously) . Saturation was first carried out by percolating de-aired water through the cell for about 30 minutes at the 20 kPa cell pressure. Then the cell pressure was increased to 50 kPa while percolation continued for about another 30 minutes. A B-test was then carried out under a 50 kPa effective stress level with back pressures of 250 to 350 kPa. The test sample was considered to be sufficiently saturated at B values of greater than 0.97. Following saturation the sample was consolidated isotropically until the desired consolidation pressure was achieved. Volume change during consolidation was measured with a rolling diaphragm double acting piston system. Following consolidation the drainage ports were closed and undrained shearing was carried out under constant cell pressure and at a constant axial strain rate of 0.2 mm/minute.

VOID RATIO DETERMINATIONS- The initial void ratio was measured from the initial sample geometry (at 20 kPa vacuum pressure), the initial moisture content (determined from a cut of the test material), the bulk specific gravity (lump or rock fragment density), and the dry weight determined after the test was complete. As the bulk specific gravity was used for the initial void ratio determination the measured void ratio is more correctly termed the bulk void ratio which is a measure of void space between individual particles not including the inter-particle void space. The initial void ratio determined in this fahion should be considered to be accurate to about 0.01 void ratio units.

Volume change during saturation was significant and, for most of the tests was estimated by assuming isotropic consolidation and calculating the volume change during saturation as:

$$\Delta V/V_0=3\Delta h_A/h_0$$

Where: $\Delta V/V_0$=volumetric strain
$\Delta h_A/h_0$=axial strain

Due to the large volume changes during saturation this assumption was questioned and some checks were made by placing a radial tape around the sample at the mid height and measuring radial displacements during saturation. In this fashion the change in the radial geometry during saturation couild be estimated and thus the volume change during saturation calculated from both the axial and radial displacements as:

$$\Delta V/V_0=1+r_f^2/r_0^2(\Delta h_A/h_0-1)$$

Where: r_f =final radius
r_0=initial radius

TRIAXIAL TEST SATURATION
VOLUME CHANGE RELATIONSHIPS

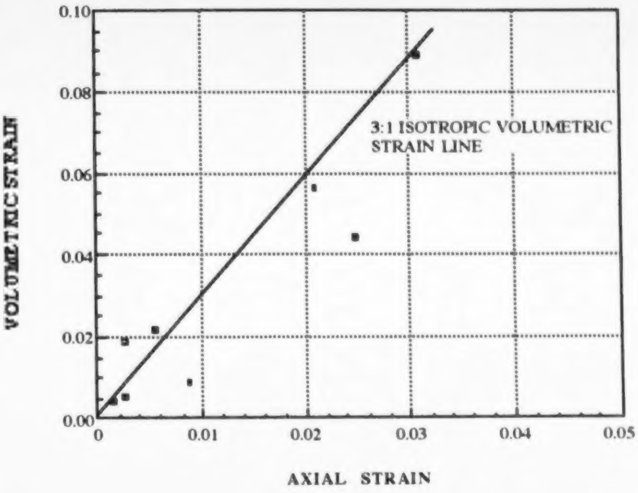

The above figure shows the volumetric strain versus axial strain relationship for the few tests where radial strain measurements were carried out. The graph shows that the 3:1 ratio is a good fit for most of the data points checked but that there are two points which lie closer to a 2:1 line. For these points the volume changes during saturation would have been over estimated by using a 3:1 isotropic assumption. All the tests did not incorporate radial strain measurements. Tests that did not incorporate volume change measurements and exhibited anomalously low void ratios (calculated using a 3:1 assumption) at steady state were checked by re-calculating the void ratio based on final moisture content.

Another imporatant factor affecting void ratio calculations is membrane penetration. The volume change during consolidation can be overestimated due to the membrane penetrating pore spaces on the sample periphery. Membrane penetration effects are more pronounced with coarser materials. However the thick membrane and widely graded material limited membrane penetration. Membrane penetration measurements showed that most of the penetration occurred during the first 100 kPa of confining strerss application and that the volume difference due to membrane penetration was less than 2%. This small volume difference was considered to be insignificant and corrections due to memebrane penetration were not made.

FORDING TRIAXIAL TEST RESULTS

	ID	INIT E	INIT MC	CONS E	P'-C	Q-C	P-PK	Q-PK	P'-SS	Q-SS
0	JAN 4	0.58700	7.1000	0.47900	50.000	0.0000	27.000	20.000	13.000	11.000
1	JAN 7	0.55600	6.6000	0.41800	100.00	0.0000	55.000	46.000	31.000	29.000
2	JAN 12	0.51000	8.1000	0.38600	200.00	0.0000	110.00	125.00	50.000	80.000
3	JAN 20	0.56400	8.2000	0.35800	300.00	0.0000	140.00	165.00	100.00	150.00
4	JAN 27	0.50400	6.4000	0.29800	500.00	0.0000	220.00	275.00	180.00	265.00
5	FEB 10	0.59800	6.7000	0.30900	500.00	0.0000	260.00	280.00	190.00	260.00

QUINTETTE TRIAXIAL TEST RESULTS

	ID	INIT E	INIT MC	CONS E	P'-C	Q-C	P-PK	Q-PK	P'-SS	Q-SS
0	FEB 25	0.58400	9.5000	0.35000	100.00	0.0000	50.000	52.000	31.000	45.000
1	MARCH 4	0.58700	8.0000	0.31700	200.00	0.0000	80.000	120.00	80.000	120.00
2	MARCH5	0.52100	6.7000	0.24200	500.00	0.0000	190.00	280.00	190.00	280.00
3	MARCH8	0.52500	8.3000	0.36000	100.00	0.0000	60.000	60.000	36.000	50.000
4	MARCH9	0.57300	7.5000	0.38000	50.000	0.0000	24.000	21.000	12.000	12.000
5	MARCH15	0.57600		0.34000	150.00	0.0000	75.000	78.000	48.000	64.000
6	MAY5	0.50700	6.6000	0.36500	100.00	0.0000	45.000	45.000	20.000	25.000

GREENHILLS TRIAXIAL TEST RESULTS

	ID	INIT E	INIT MC	E1	P'-C	Q-C	P-PK	Q-PK	P'-SS	Q-SS
0	MARCH 23	0.54300	13.800	0.30300	200.00	0.0000	90.000	125.00	90.000	125.00
1	MARCH24	0.59700	15.000	0.40900	90.000	0.0000	40.000	44.000	25.000	37.000
2	MARCH29	0.63300	12.700	0.30400	200.00	0.0000	90.000	115.00	90.000	115.00
3	APRIL 1	0.62600	13.700	0.28300	350.00	0.0000	150.00	200.00	150.00	200.00
4	APRIL6	0.66200	14.500	0.24000	500.00	0.0000	230.00	300.00	230.00	300.00
5	APRIL11	0.61200	9.4000	0.45800	50.000	0.0000	25.000	24.000	12.000	16.000

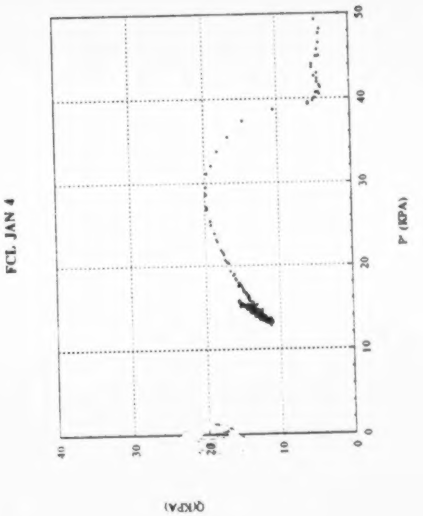
FCL JAN 4
Q(KPA)
P' (KPA)
0
10
20
30
40
50

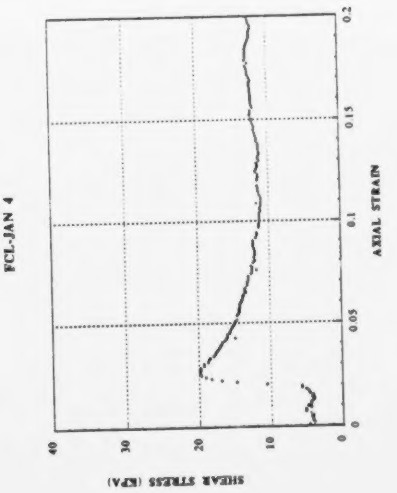
FCL-JAN 4
SHEAR STRESS (KPA)
AXIAL STRAIN
0
10
20
30
40
0.05
0.1
0.15
0.2

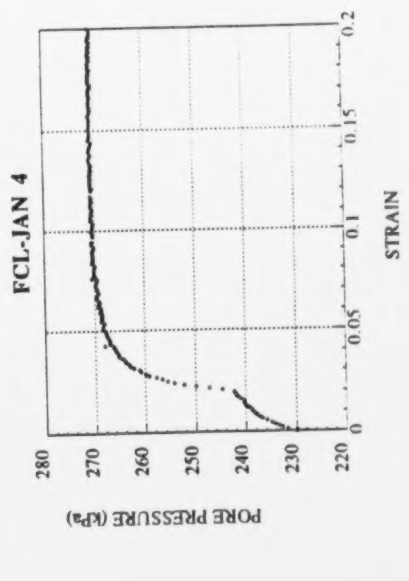
FCL-JAN 4
PORE PRESSURE (kPa)
STRAIN
220
230
240
250
260
270
280
0
0.05
0.1
0.15
0.2

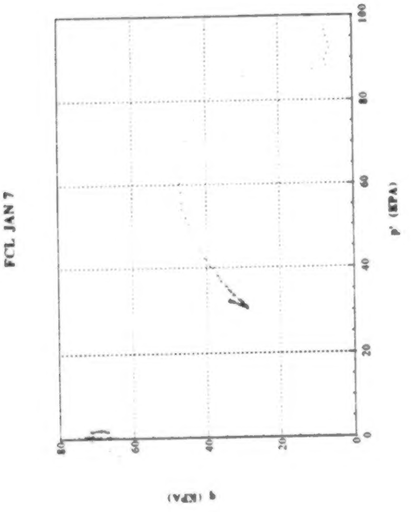
FCL JAN 7
q (KPA)
p' (KPA)
0
20
40
60
80
100

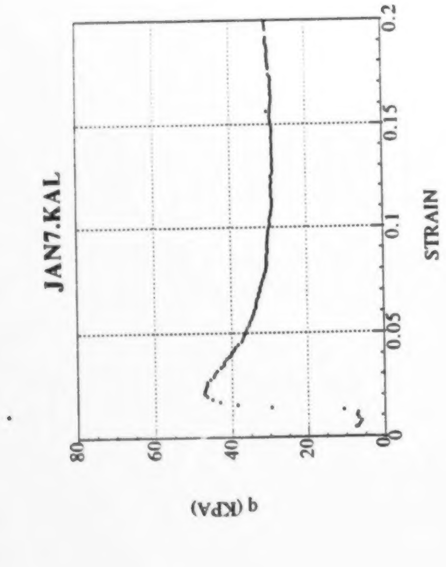
JAN7.KAL
q (KPA)
STRAIN
0
20
40
60
80
0.05
0.1
0.15
0.2

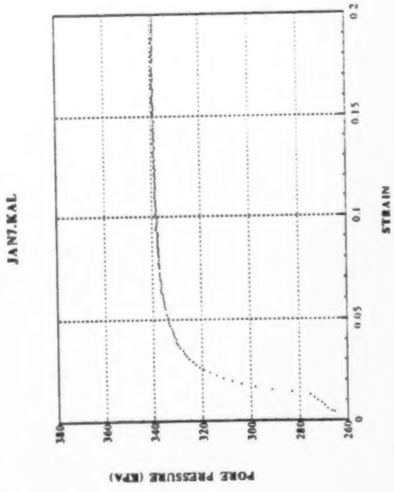
JAN7.KAL
PORE PRESSURE (KPA)
STRAIN
260
280
300
320
340
360
380
0
0.05
0.1
0.15
0.2

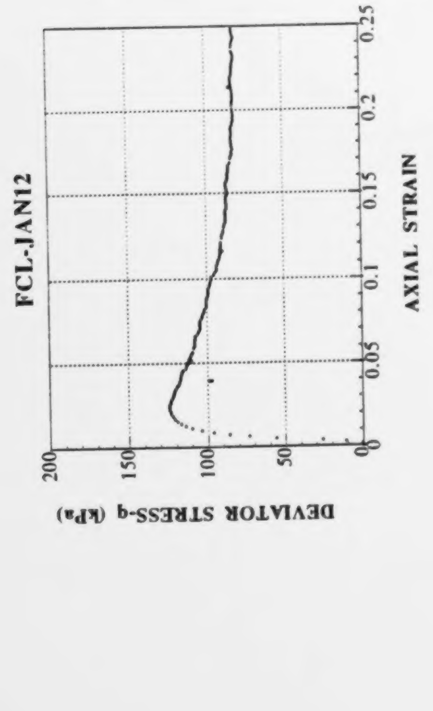
FCL-JAN12
DEVIATOR STRESS-q (kPa)
200
150
100
50
0
AXIAL STRAIN
0
0.05
0.1
0.15
0.2
0.25

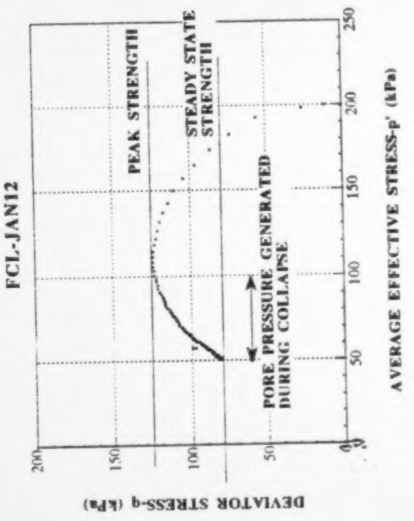
FCL-JAN12
DEVIATOR STRESS-q (kPa)
200
150
100
50
0
PEAK STRENGTH
STEADY STATE STRENGTH
PORE PRESSURE GENERATED DURING COLLAPSE
AVERAGE EFFECTIVE STRESS-p' (kPa)
0
50
100
150
200
250

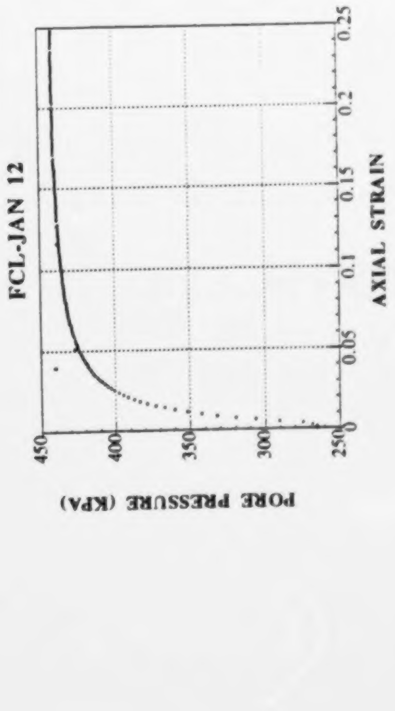
FCL-JAN 12
PORE PRESSURE (KPA)
450
400
350
300
250
AXIAL STRAIN
0
0.05
0.1
0.15
0.2
0.25

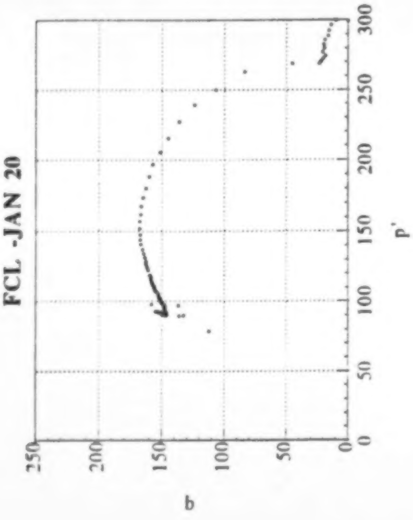
FCL -JAN 20
q
p'
0
50
100
150
200
250
300

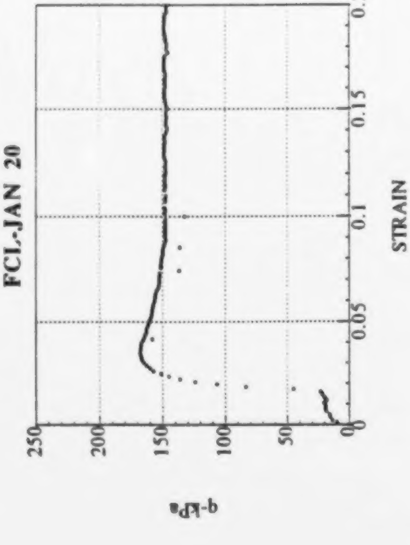
FCL-JAN 20
q-kPa
STRAIN
0
50
100
150
200
250
0.05
0.1
0.15
0.2

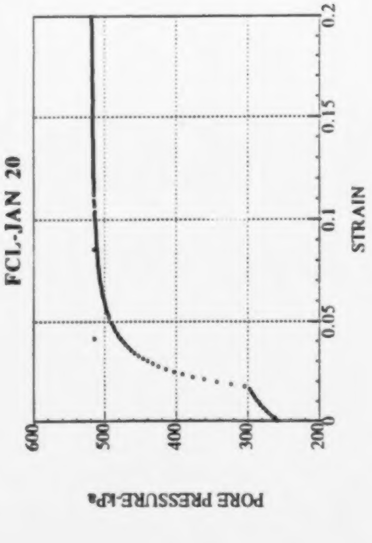
FCL-JAN 20
PORE PRESSURE-kPa
STRAIN
200
300
400
500
600
0
0.05
0.1
0.15
0.2

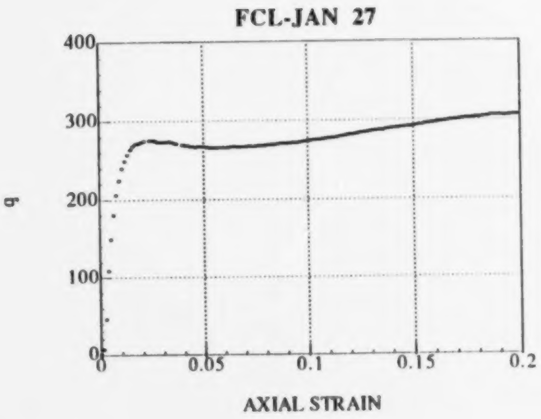
FCL-JAN 27
q
400
300
200
100
0
0
0.05
0.1
0.15
0.2
AXIAL STRAIN

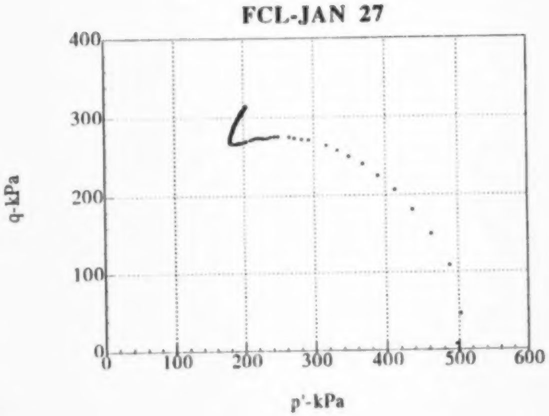
FCL-JAN 27
q-kPa
400
300
200
100
0
0
100
200
300
400
500
600
p'-kPa

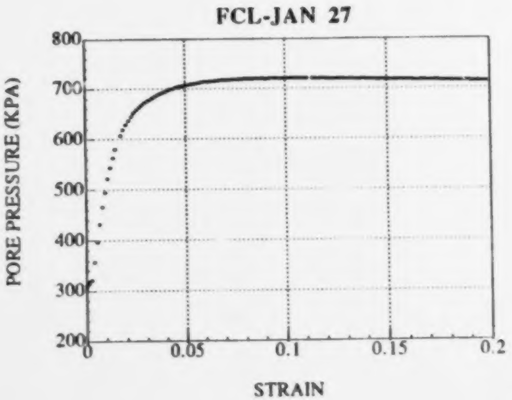
FCL-JAN 27
PORE PRESSURE (KPA)
800
700
600
500
400
300
200
0
0.05
0.1
0.15
0.2
STRAIN

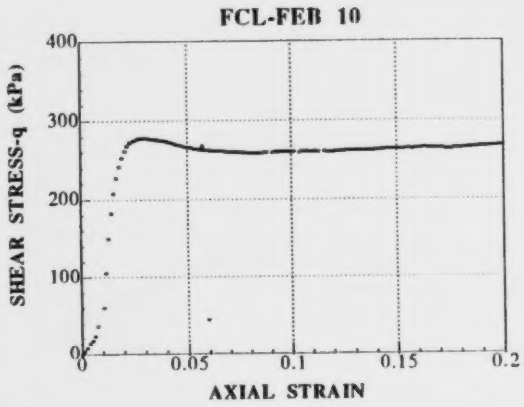
FCL-FEB 10
SHEAR STRESS-q (kPa)
400
300
200
100
0
0
0.05
0.1
0.15
0.2
AXIAL STRAIN

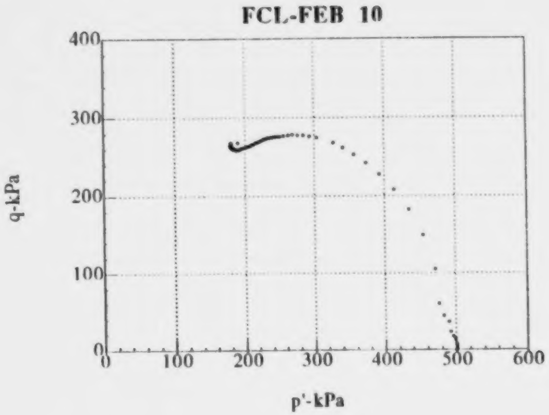
FCL-FEB 10
q-kPa
400
300
200
100
0
0
100
200
300
400
500
600
p'-kPa

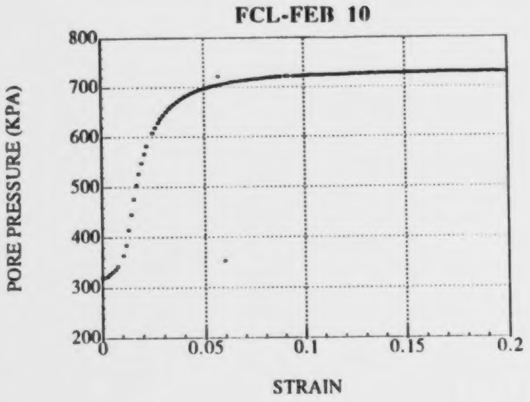
FCL-FEB 10
PORE PRESSURE (KPA)
800
700
600
500
400
300
200
0
0.05
0.1
0.15
0.2
STRAIN

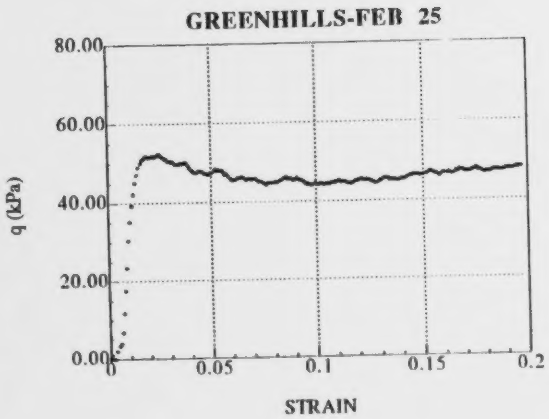
GREENHILLS-FEB 25
q (kPa)
80.00
60.00
40.00
20.00
0.00
0
0.05
0.1
0.15
0.2
STRAIN

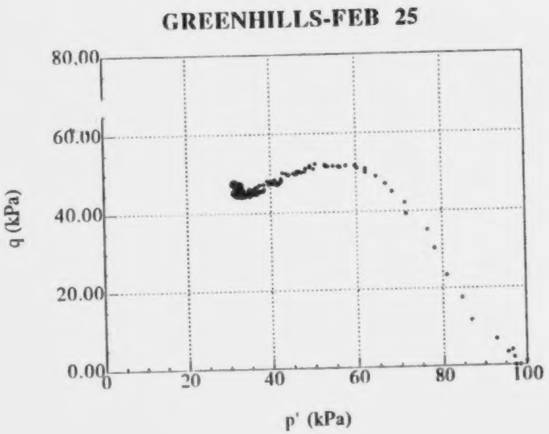
GREENHILLS-FEB 25
q (kPa)
80.00
60.00
40.00
20.00
0.00
0
20
40
60
80
100
p' (kPa)

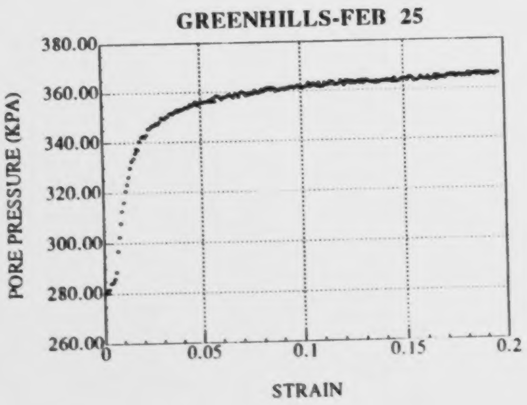
GREENHILLS-FEB 25
PORE PRESSURE (KPA)
380.00
360.00
340.00
320.00
300.00
280.00
260.00
0
0.05
0.1
0.15
0.2
STRAIN

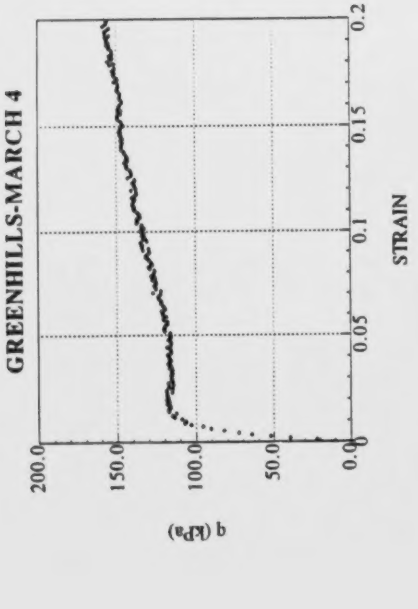
GREENHILLS-MARCH 4
q (kPa)
200.0
150.0
100.0
50.0
0.0
0
0.05
0.1
0.15
0.2
STRAIN

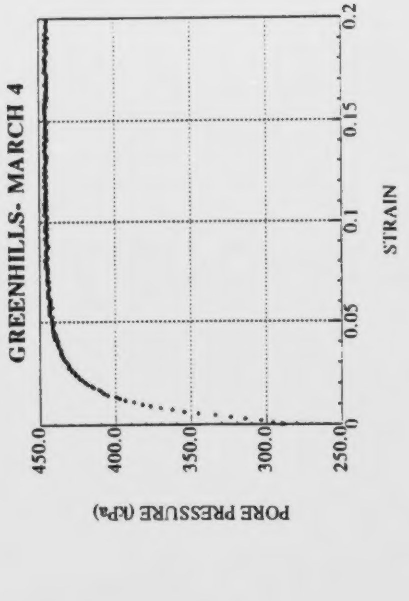
GREENHILLS- MARCH 4
PORE PRESSURE (kPa)
450.0
400.0
350.0
300.0
250.0
0
0.05
0.1
0.15
0.2
STRAIN

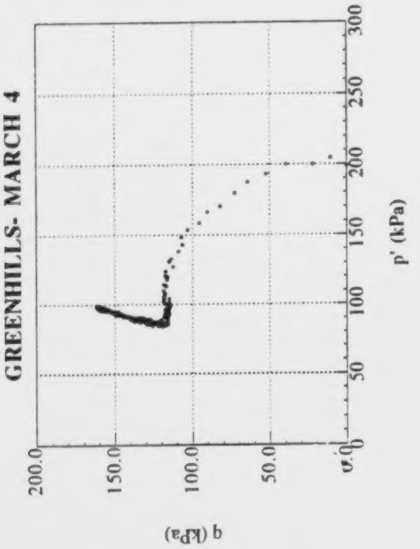
GREENHILLS- MARCH 4
q (kPa)
200.0
150.0
100.0
50.0
0.0
0
50
100
150
200
250
300
p' (kPa)

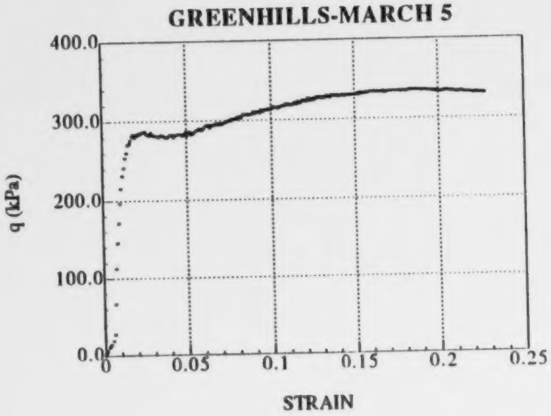
GREENHILLS-MARCH 5
q (kPa)
400.0
300.0
200.0
100.0
0.0
0
0.05
0.1
0.15
0.2
0.25
STRAIN

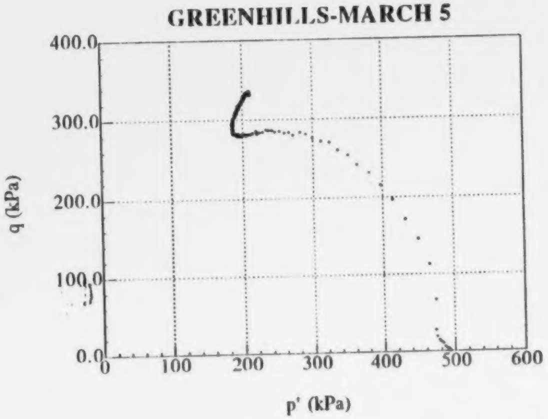
GREENHILLS-MARCH 5
q (kPa)
400.0
300.0
200.0
100.0
0.0
0
100
200
300
400
500
600
p' (kPa)

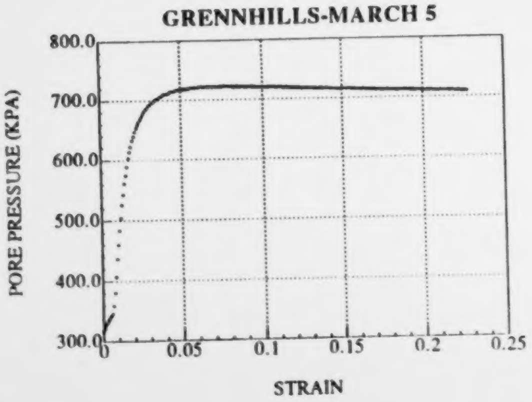
GRENNHILLS-MARCH 5
PORE PRESSURE (KPA)
800.0
700.0
600.0
500.0
400.0
300.0
0
0.05
0.1
0.15
0.2
0.25
STRAIN

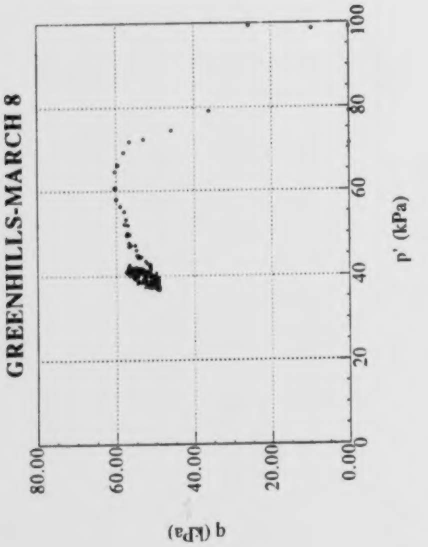
GREENHILLS-MARCH 8
q (kPa)
80.00
60.00
40.00
20.00
0.00
0
20
40
60
80
100
p' (kPa)

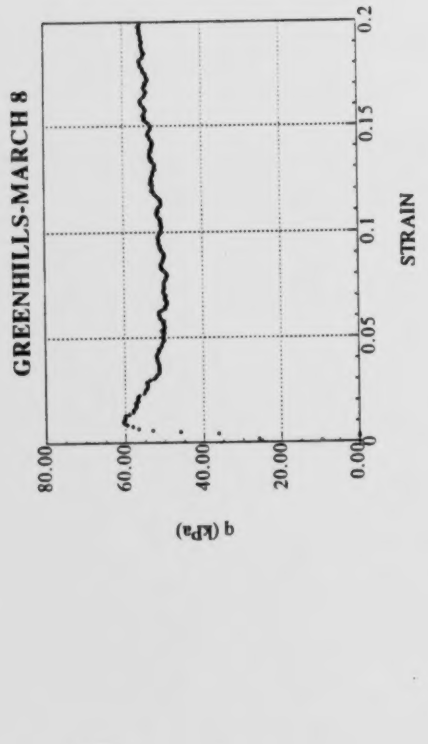
GREENHILLS-MARCH 8
q (kPa)
80.00
60.00
40.00
20.00
0.00
0
0.05
0.1
0.15
0.2
STRAIN

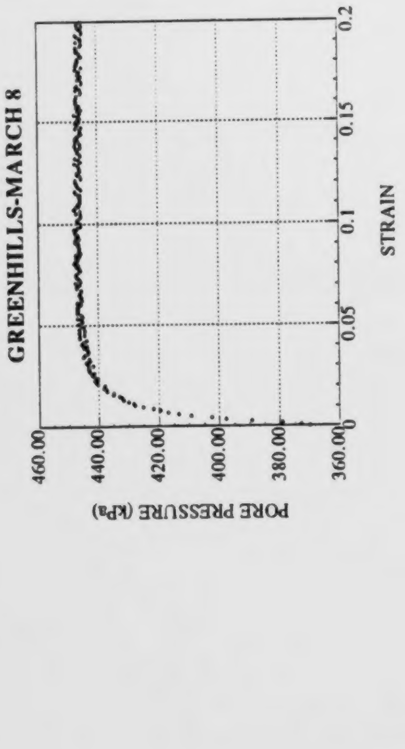
GREENHILLS-MARCH 8
PORE PRESSURE (kPa)
460.00
440.00
420.00
400.00
380.00
360.00
0
0.05
0.1
0.15
0.2
STRAIN

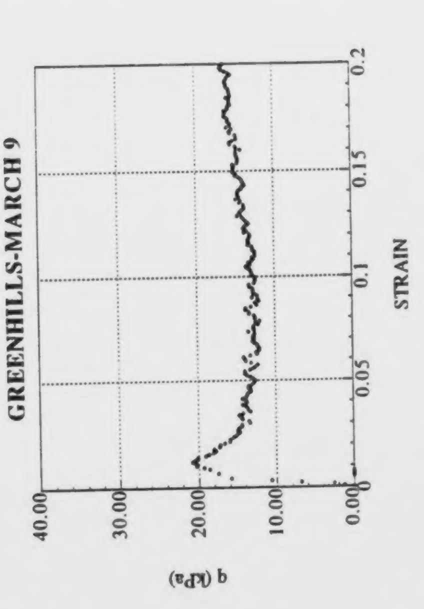
GREENHILLS-MARCH 9
q (kPa)
40.00
30.00
20.00
10.00
0.00
0
0.05
0.1
0.15
0.2
STRAIN

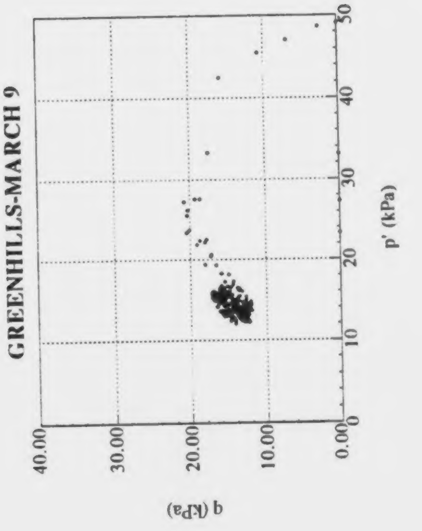
GREENHILLS-MARCH 9
q (kPa)
40.00
30.00
20.00
10.00
0.00
0
10
20
30
40
50
p' (kPa)

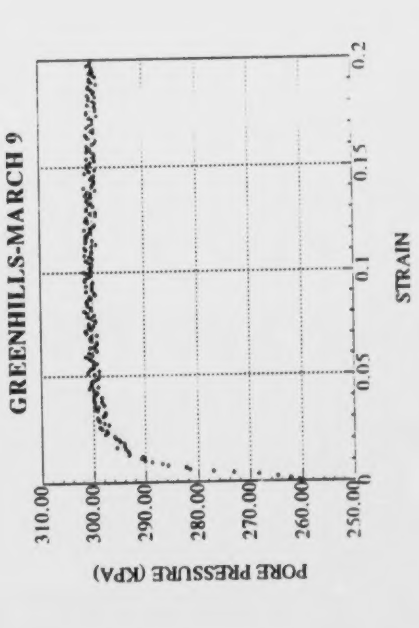
GREENHILLS-MARCH 9
PORE PRESSURE (KPA)
310.00
300.00
290.00
280.00
270.00
260.00
250.00
0
0.05
0.1
0.15
0.2
STRAIN

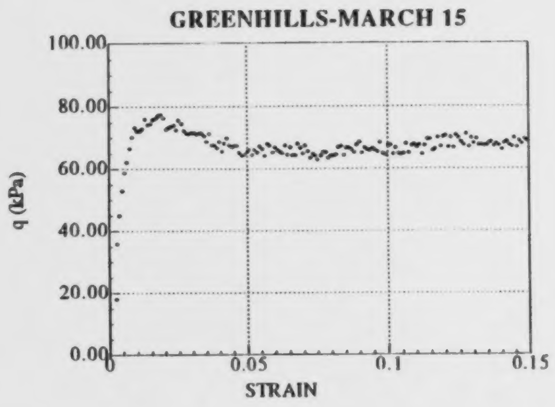
GREENHILLS-MARCH 15
q (kPa)
100.00
80.00
60.00
40.00
20.00
0.00
0
0.05
0.1
0.15
STRAIN

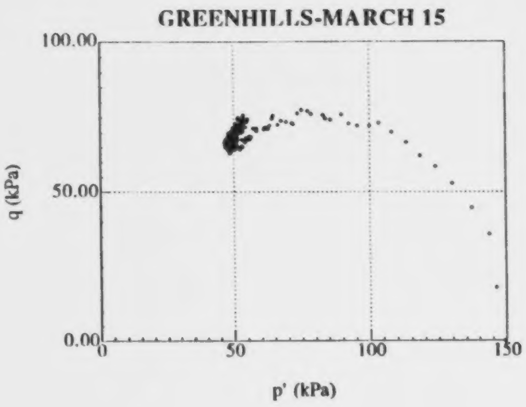
GREENHILLS-MARCH 15
q (kPa)
100.00
50.00
0.00
0
50
100
150
p' (kPa)

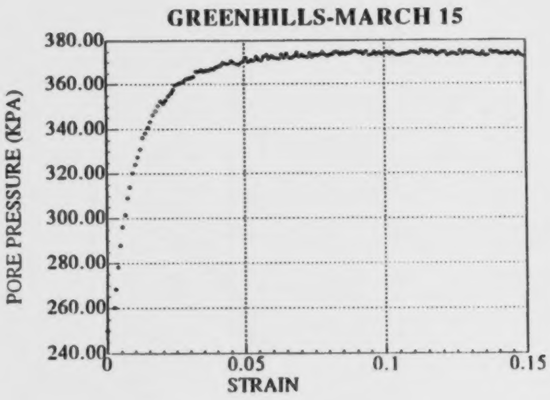
GREENHILLS-MARCH 15
PORE PRESSURE (KPA)
380.00
360.00
340.00
320.00
300.00
280.00
260.00
240.00
0
0.05
0.1
0.15
STRAIN

QCL-MARCH 23

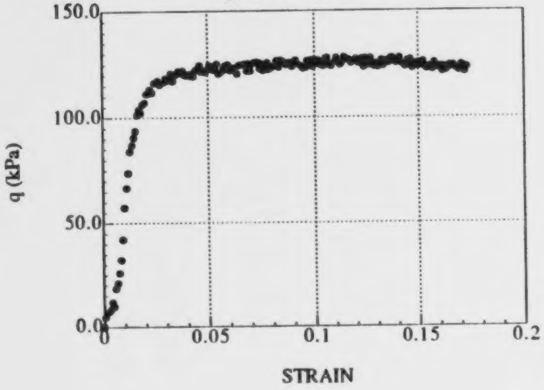

QCL-MARCH 23

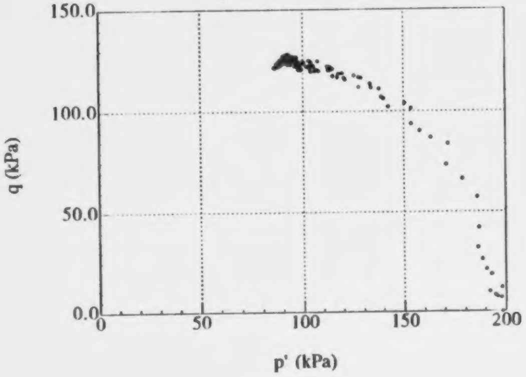

QCL-MARCH 23

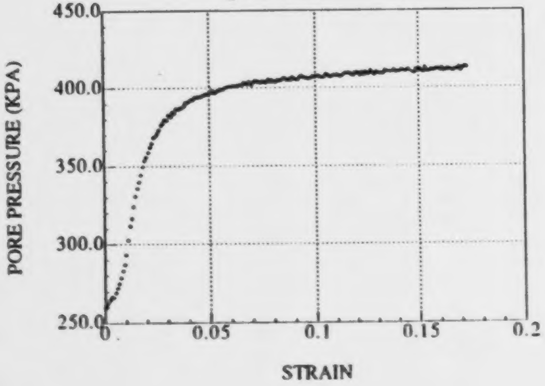

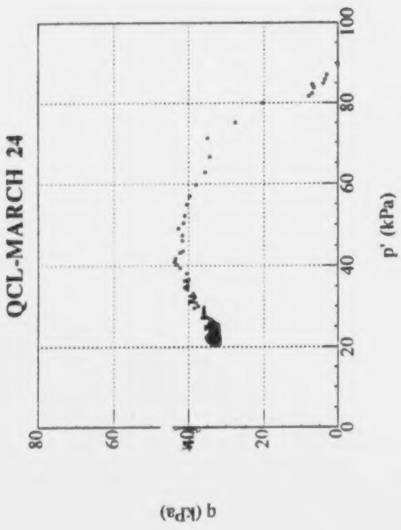
QCL-MARCH 24

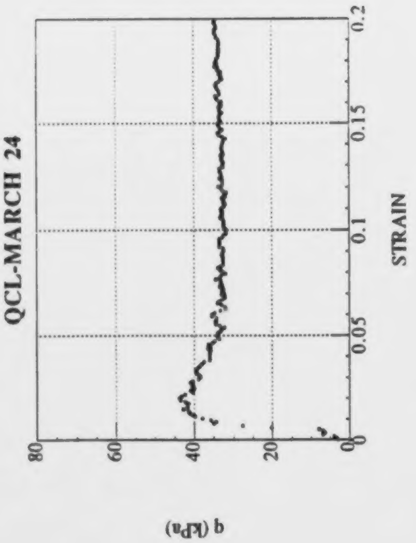
QCL-MARCH 24

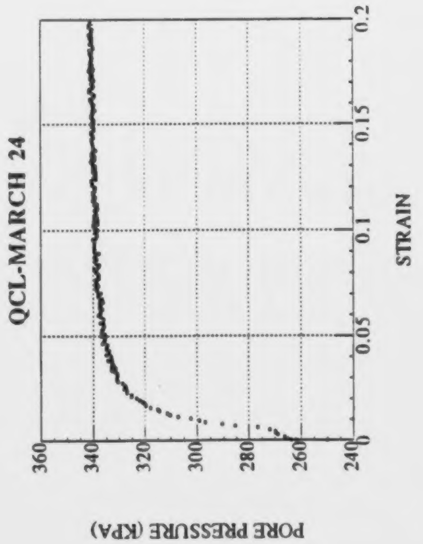
QCL-MARCH 24

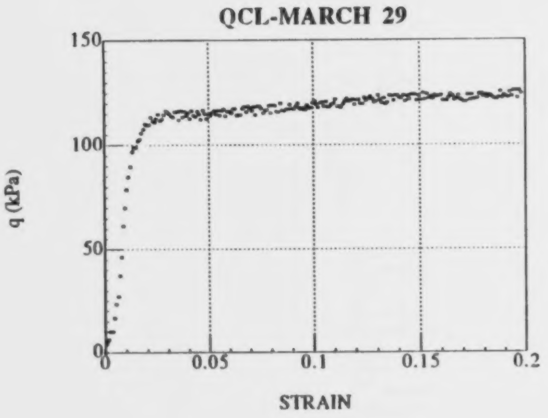
QCL-MARCH 29
q (kPa)
150
100
50
0
0
0.05
0.1
0.15
0.2
STRAIN

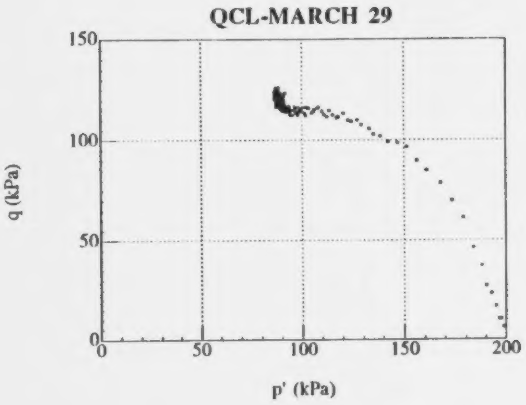
QCL-MARCH 29
q (kPa)
150
100
50
0
0
50
100
150
200
p' (kPa)

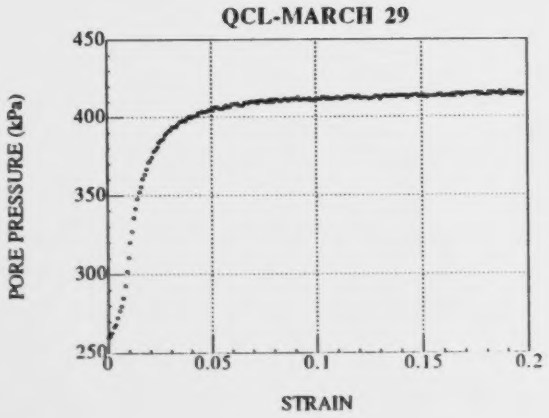
QCL-MARCH 29
PORE PRESSURE (kPa)
450
400
350
300
250
0
0.05
0.1
0.15
0.2
STRAIN

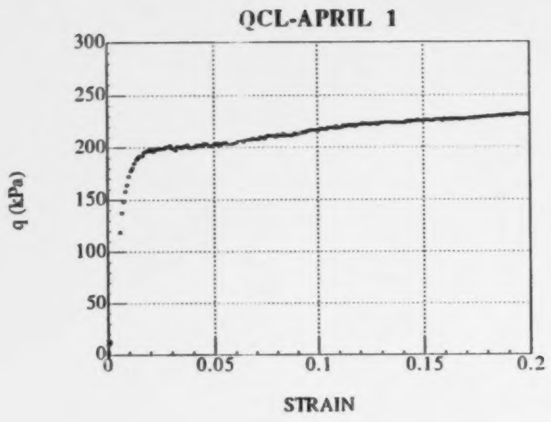
QCL-APRIL 1
q (kPa)
300
250
200
150
100
50
0
0
0.05
0.1
0.15
0.2
STRAIN

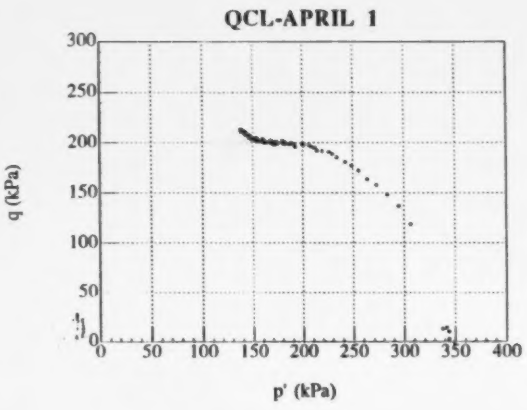
QCL-APRIL 1
q (kPa)
300
250
200
150
100
50
0
0
50
100
150
200
250
300
350
400
p' (kPa)

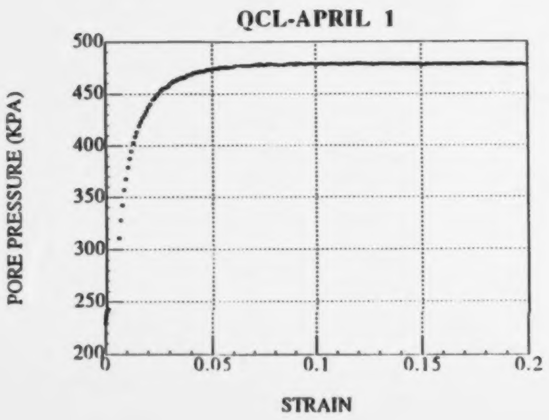
QCL-APRIL 1
PORE PRESSURE (KPA)
500
450
400
350
300
250
200
0
0.05
0.1
0.15
0.2
STRAIN

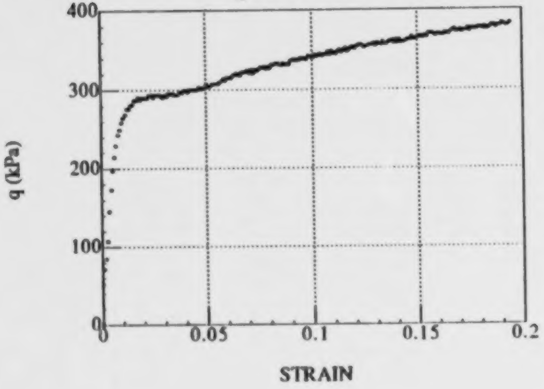
QCL-APRIL 6

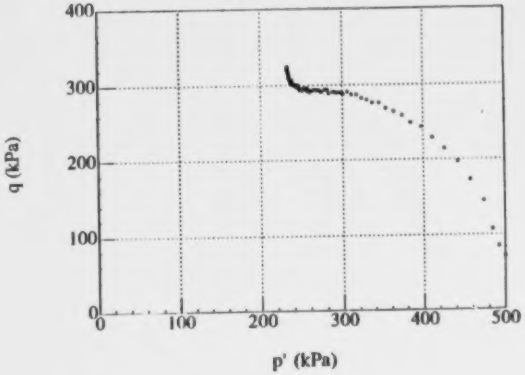
QCL-APRIL 6

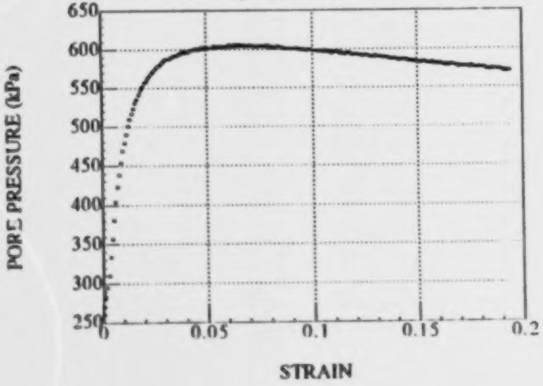
QCL-APRIL 6

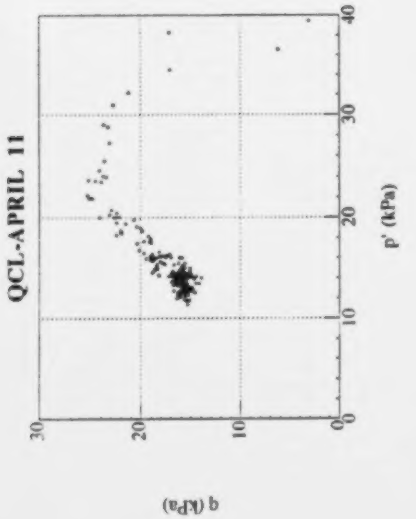
QCL-APRIL 11
q (kPa)
p' (kPa)
0
10
20
30
40

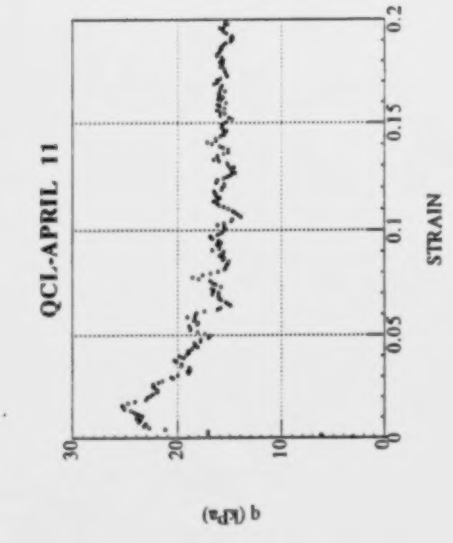
QCL-APRIL 11
q (kPa)
STRAIN
0
10
20
30
0.05
0.1
0.15
0.2

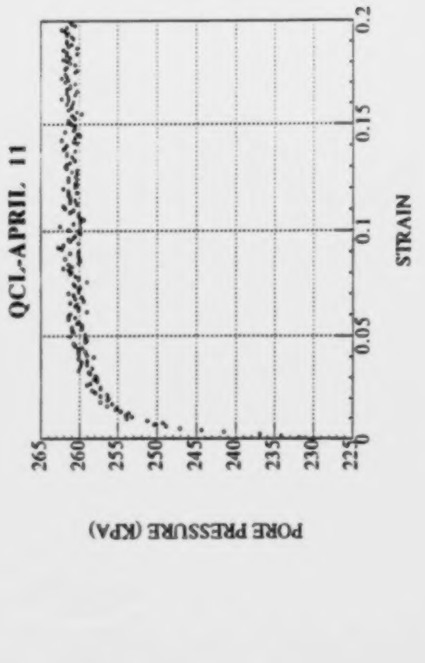
QCL-APRIL 11
PORE PRESSURE (KPA)
STRAIN
225
230
235
240
245
250
255
260
265
0
0.05
0.1
0.15
0.2